The chromatin organizer Satb1 regulates the differentiation into $CD4^+$ T_H subsets and is essential for the development of T_H17 cells

Dissertation
zur
Erlangung des Doktorgrades (Dr. rer. nat.)
der
Mathematisch-Naturwissenschaftlichen Fakultät
der
Rheinischen Friedrich-Wilhelms-Universität Bonn

vorgelegt von

Maren Christin Köhne
aus Datteln, Deutschland

Bonn, Juli 2020

Angefertigt mit Genehmigung der Mathematisch-Naturwissenschaftlichen Fakultät der Rheinischen Friedrich-Wilhelms-Universität Bonn

1. Gutachter: PD Dr. med. Marc D. Beyer

2. Gutachter: Prof. Dr. med. Joachim L. Schultze

Tag der Promotion: 2.3.2021

Erscheinungsjahr: 2021

Table of Content

List of Figures

List of Tables

Abbreviations

Table 1: List of abbreviations

Abbreviation	Definition
APCs	Antigen-presenting cells
2DG	2-Desoxy-D-glucose
4-OH tamoxifen	(Z) 4-hydroxytamoxifen
Ahr	Aryl hydrocarbon receptor
ANOVA	Analysis of variance
ATAC	Assay for transposase-accessible chromatin
AZ	Reference number (Aktenzeichen)
Batf	Basic leucine zipper ATF-like transcription factor
Bcl-6	B cell lymphoma 6
Blimp1	B lymphocyte-induced maturation protein-1
CD	Cluster of differentiation
cDNA	Complementary DNA
CFA	Complete Freund's adjuvant
cLN	Cervical lymph nodes
CLPs	Common lymphoid progenitors
CNS	Central nervous system
CO_2	Carbon dioxide
Cre	Causes recombination
CreERT2	Causes recombination mutant estrogen receptor 2
d	Day
DMEM	Dulbecco's modified Eagle's medium
DN	Double negative
DNA	Desoxyribose nucleic acid
DP	Double positive
Dusp	Dual specificity phosphatase
EAE	Experimental autoimmune encephalomyelitis
ECAR	Extracellular acidification rates
EDTA	Ethylenediaminetetraacetic acid
eGFP	Enhanced green fluorescent protein
EtOH	Ethanol

FACS	Fluorescence activated cell sorting
Fas	Fas cell surface death receptor
FCCP	Carbonyl cyanide 4-(trifluoromethoxy)phenylhydrazone
FCS	Fetal calf serum
fl	Floxed/Flanked by lox sites
frt	Recombination sites for Flp recombinase
Foxp3	Forkhead-box-protein P3
g	Gravitational force
Gata3	GATA-binding protein 3
GM-CSF	Granulocyte macrophage-colony stimulating factor
h	Hour(s)
HBSS	Hanks' balanced salt solution
HCl	Hydrochloric acid
HEPES	4-(2-hydroxyethyl)-1-piperazineethanesulfonic acid
HRP	Horseradish peroxidase
HSCs	Hematopoietic stem cells
IFN-γ	Interferon-gamma
IgG/IgM/IgE	Immunoglobulin G/M/E
Ikzf4	IKAROS family zinc finger 4
IL	Interleukin
IMDM	Iscove's modified Dulbecco's medium
i.p.	intraperitoneally
IRF	Interferon regulatory factor
iTreg cells	Induced Treg cells
KI	Knock-in
Ki-67	Kiel 67
KO	Knock out
LN	Lymph nodes
loxP	Locus of crossing (x) over, P1
Ly6G	Lymphocyte antigen 6 complex, locus G
Mac3	Macrophage-3 antigen (CD107b)
MACS	Magnetic activated cell sorting
MFI	Mean fluorescent intensity

MgCl	Magnesium chloride
MHC	Major histocompatibility complex
min	Minutes
mLN	Mesenteric lymph nodes
MOG	Myelin oligodendrocyte glycoprotein
nd	Not detected
NaCl	Sodium chloride
NaOH	Sodium hydroxide
Nfat	Nuclear factor of activated T cells
NIH	National Institutes of Health
ns	Not significant
OCR	Oxygen consumption rate
PAGE	Polyacrylamide gel electrophoresis
PAMPs	Pathogen-associated molecular patterns
PBS	Dulbecco's phosphate buffered saline
PBST	Dulbecco's phosphate buffered saline with tween
PCR	Polymerase chain reaction
PD-1	Programmed cell death protein 1
PFA	Paraformaldehyde
pH	Power of hydrogen
PMA	Phorbol 12-myristate 13-acetate
pStat	Phosphorylated Stat
Pten	Phosphatase and tensin homolog
pTreg cells	Peripheral Treg cells
qRT-PCR	Semi quantitative real time polymerase chain reaction
Rag	Recombination activating 1
RBCL	Red blood cell lysis
RFP	Red fluorescent protein
rh	Recombinant human
RIPA buffer	Radioimmunoprecipitation assay buffer
rm	Recombinant murine
RNA/mRNA	Ribonucleic acid/messenger ribonucleic acid
Rorc	Retinoic acid receptor-related orphan receptor C

RORγt	Retinoic acid receptor-related orphan receptor-γt
rpm	Revolutions per minutes
RPMI	Roswell Park Memorial Institute medium
RT	Room temperature
Runx	Runt-related transcription factor
Satb1	Special AT-rich sequence-binding protein 1
sc	Spinal cord
SDS	Sodium dodecyl sulfate
SEM	Standard error of the mean
Seq	Sequencing
SI	Small intestine
Socs	Suppressor of cytokine signaling
SP	Single positive
Stat	Signal transducer and activator of transcription
STOP	Stop cassette
TAPS	N-[Tris(hydroxymethyl)methyl]-3-aminopropanesulfonic acid
T-bet	T-box expressed in T cells
Tbx21	T-box transcription factor 21
Tconv cells	Conventional T cells
TCR	T cell receptor
T_{FH} cells	Follicular T_H cells
TGF-β	Transforming growth factor-beta
T_H cells	T helper cells
TLR	Toll like receptor
Tn5	Transposase 5
TNF-α	Tumor necrosis factor-alpha
Treg cells	Regulatory T cells
tTreg cells	Thymus-derived Treg cells
V(D)J	Variable, (diversity), joining
V/V	Volume/Volume
w/o	Without
w/V	Weight/Volume
WT	Wildtype

Summary

$CD4^+$ T cells play a critical role in host defense and tissue homeostasis. Upon encountering their specific antigen, naive $CD4^+$ T cells can differentiate into the effector T helper (T_H) subsets T_H1, T_H2, T_H9, T_H17 and regulatory T cells (Treg), which fulfill various functions. T cell dysfunction is associated with increased susceptibility to pathogen infections, autoimmune diseases as well as cancer formation. Therefore, it is critical to identify the common underlying mechanisms governing T cell differentiation and to establish new approaches to influence their differentiation in disease settings. Special AT-rich sequence-binding protein 1 (Satb1) is a nuclear matrix protein regulating gene expression by organizing the chromatin structure and recruiting chromatin modifying factors to their target gene loci. Thereby, Satb1 plays an important role in the development of T cells. However, its role in T_H subsets has not been studied in detail.

In this thesis, analysis of the impact of Satb1 on T_H cell differentiation *in vitro* revealed that Satb1 is a critical player in the naive $CD4^+$ T cell differentiation process. Expression of Satb1 is important for the differentiation of T_H9 and T_H17 cells, while its downregulation accelerates the differentiation of T_H1 and iTreg cells. In addition, aberrant Satb1 expression diminishes the generation of T_H2 cells.

Especially the differentiation of T_H17 cells is affected by the loss of Satb1 *in vitro*, an observation which was also mirrored *in vivo* both during homeostasis and in T_H17 cell-driven disease settings. In both the experimental autoimmune encephalomyelitis (EAE) and the adoptive transfer colitis model, mice are protected from disease development when Satb1 is deleted in $CD4^+$ T cells due to diminished development of T_H17 cells.

Further analysis revealed that Satb1 is important during the early stages of T_H17 cell development by orchestrating expression of the T_H17 cell gene network. In addition, Satb1 expression improves T_H17 cell function upon restimulation and is required for reprogramming T_H1 cells into T_H17 cells.

Characterization of the transcriptional program and chromatin accessibility of Satb1-deficient naive $CD4^+$ T cells indicated an altered activation state already in naive $CD4^+$ T cells. One dysregulated gene locus in Satb1-deficient naive $CD4^+$ T cells is *Il2*. Satb1 is essential for inhibiting IL-2 expression by preventing access to the genomic *Il2* locus and thus preventing pre-activation of naive $CD4^+$ T cells.

During the early steps of T_H17 cell development, loss of Satb1 results in increased IL-2 signaling indicated by the phosphorylation of Stat5, an upregulation of CD25 as well as a

reduction in the expression of the IL-6 receptor. Strikingly, blocking IL-2 signaling in Satb1-deficient $CD4^+$ T cells restores T_H17 cell development, indicating that Satb1 regulates the generation of T_H17 cells through inhibiting IL-2 signaling.

Taken together, Satb1 is an important pioneer factor in T_H cell differentiation. Satb1 is critical for the differentiation of T_H17 cells through epigenetic programming of naive $CD4^+$ T cells as well as through chromatin organization during the early stages of T_H17 cell development by preventing accessibility of the genomic *Il2* locus. Thus, Satb1 might be a promising novel therapeutic target for the treatment of T_H17 cell-driven autoimmune diseases.

Zusammenfassung

$CD4^+$ T Zellen spielen eine wichtige Rolle in der Immunabwehr. Sie sind entscheidend bei der Bekämpfung von Infektion oder aber auch in der Aufrechterhaltung der Homöostase in Geweben, in denen wir in engen Kontakt mit fremden Mikroorganismen stehen, wie zum Beispiel der Haut oder dem Darm. Abhängig von der gegebenen Situation können sich naive $CD4^+$ T Zellen bei Aktivierung in die verschiedenen T Helfer (T_H) Subtypen T_H1, T_H2, T_H9, T_H17 und regulatorische T (Treg) Zellen differenzieren, die jeweils unterschiedliche Funktionen ausführen. Dies ermöglicht dem Immunsystem, sich gezielt an die Umgebung anzupassen, um einen optimal Schutz zu gewährleisten. Allerding gehen viele Krankheiten wie zum Beispiel Tumore oder Autoimmunerkrankungen mit einer gestörten Differenzierung von T_H Zellen einher. Deswegen ist es wichtig, diese Mechanismen genauer zu entschlüsseln und zu verstehen, um bei einer Fehlregulation mögliche Therapieansätze zu entwickeln. In den letzten Jahren ist bekannt geworden, dass das Protein special AT-rich sequence-binding protein 1 (Satb1) eine wichtige Rolle in der Entwicklung von T Zellen hat. Satb1 ist ein nukleäres Protein, das wichtig bei der Organisation der Chromatinstruktur ist und die Transkription von Genen direkt oder indirekt durch epigenetische Modifizierungen regulieren kann. Die Funktion von Satb1 in der Differenzierung von T_H Zellen ist nur teilweise bekannt und weitergehende Analysen sind noch notwendig, um ein besseres Verständnis der Funktion von Satb1 zu bekommen.

In dieser Arbeit konnten *in vitro* Analysen zeigen, dass Satb1 eine wichtige Rolle bei der Differenzierung von T_H1, T_H2, T_H9, T_H17 und regulatorischen T (Treg) Zellen hat. Während die Expression von Satb1 für die Entstehung von T_H9 und T_H17 Zellen entscheidend ist, begünstigt die Herunterregulation des Proteins die Entstehung von T_H1 und iTreg Zellen. Außerdem ist eine koordinierte Regulation von Satb1 notwendig, um die Entwicklung von T_H2 Zellen zu ermöglichen.

Der Einfluss von Satb1 war sowohl *in vitro* als auch *in vivo* besonders stark in der Entwicklung von T_H17 zu sehen und zeigte sich *in vivo* sowohl unter homöostatischen Bedingungen als auch in verschiedenen Krankheitsmodellen. Sowohl im adaptiven Transfer-Colitis Modell als auch in der experimentellen autoimmunen Enzephalomyelitis (EAE), beides Krankheitsmodelle die mit der Aktivität von T_H17 Zellen assoziiert sind, wird die Entwicklung der Krankheit unterbunden, wenn Satb1 in $CD4^+$ T Zellen nicht exprimiert werden kann. Für ihre Entstehung benötigen sowohl nicht-pathogene aber auch besonders pathogene T_H17 Zellen Satb1.

Satb1 ist vor allem am Beginn der T_H17 Differenzierung wichtig und ermöglicht es, ein T_H17 spezifisches Gen-Netzwerk aufzubauen. Außerdem ist Satb1 wichtig bei der Reaktivierung von T_H17 Zellen und bei der Reprogrammierung von T_H1 Zellen zu T_H17 Zellen.
Eine genauere Charakterisierung von naiven $CD4^+$ T Zellen, in denen artifiziell die Satb1 Expression unterbunden wurde, zeigt bereits eine Umstrukturierung des Chromatins und der Genexpression in naiven Zellen, sodass der Aktivierungsstatus der Zelle verändert wird. Auffällig ist hier zum Beispiel eine Veränderung des *Il2* Genlokus. So konnte gezeigt werden, dass Satb1 wichtig für die Repression von IL-2 in naive $CD4^+$ T Zellen ist.
In den frühen Entwicklungsstadien von T_H17 Zellen führt der Verlust von Satb1 zu einer erhöhten Phosphorylierung von Stat5, einer verstärkten Expression von CD25 sowie einer verminderten Anwesenheit des IL-6 Rezeptors an der Zelloberfläche, alles bekannte Phänomene bei einer Aktivierung des IL-2 Signalwegs. Wird dieser Signalweg unterbunden, konnte die Entwicklung von T_H17 Zellen in Satb1-defizienten $CD4^+$ T Zellen *in vitro* wiederhergestellt werden. Dies verdeutlicht, dass Satb1 die Differenzierung von T_H17 Zellen durch die Repression von IL-2 ermöglicht.

Zusammenfassend konnte gezeigt werden, dass Satb1 eine entscheidende Funktion bei der Differenzierung von T_H Zellen innehat. Satb1 ist essentiell für die Differenzierung von T_H17 Zellen durch die Regulierung der Chromatinstruktur und der Transkription in naiven $CD4^+$ T Zellen sowie in den frühen Entwicklungsstadien der T_H17 Zellen selbst. Satb1 ist für die verminderte Zugänglichkeit des *Il2* Genlokus in naiven $CD4^+$ T Zellen verantwortlich und ermöglicht so die Differenzierung von T_H17 Zellen, bei denen IL-2 in der frühen Entwicklungsphase einen nachteiligen Effekt ausübt. Satb1 könnte somit eine mögliche neue Ansatzstelle für therapeutische Maßnahmen darstellen und die Manipulation von Satb1 könnte für die Behandlung von T_H17 induzierten Autoimmunerkrankungen zielführend sein.

1. Introduction

1.1. The immune system

The immune system is the host defense system that protects the body against invading pathogens and clears occurring infections. In vertebrates, it encompasses the interplay of several structures like barrier cells, leukocytes, tissue resident immune cells but also humoral factors like the complement system and antibodies as well as small signaling molecules like chemokines and cytokines (Parkin and Cohen, 2001).

This network is classically divided into two parts, the innate and the adaptive immune system. The innate immune system acts as a first line of defense and enables an immediate response against invaders. Elements of the innate immune system such as phagocytes, the complement system and others recognize conserved patterns like pathogen-associated molecular patterns (PAMPs), which are present on microbes and absent in eukaryotic cells (Mogensen, 2009; Ricklin et al., 2010). Binding of PAMPs by pathogen recognition receptor is followed by activation, resulting in an effector phase and the elimination of the infection. However, PAMPs are invariant among different classes of pathogens and consequently the innate immune response, initiated by these microbial molecules and structures, is not specific but directed against a general pathogen class (Medzhitov and Janeway, 2000).

In contrast, the adaptive immune system, which becomes activated by the innate immune system, enables a pathogen-specific immune response. Antigen-presenting cells (APCs), mainly dendritic cells, activate B and T lymphocytes by migrating from the site of infection to the secondary lymphatic organs and processing and presenting pathogen-specific antigens on major histocompatibility complex (MHC) I or II molecules while additionally upregulating co-stimulatory molecules and secreting cytokines (Guermonprez et al., 2002). Only specific lymphocytes recognize this particular antigen, become activated and subsequently undergo clonal expansion (Schenten and Medzhitov, 2011). While B lymphocytes are responsible for antigen-specific antibody secretion, T lymphocytes act via direct cellular interactions or effector cytokine release (Schenten and Medzhitov, 2011).

T lymphocytes can be divided into different subclasses. The two major subsets are (1) cluster of differentiation (CD) 8^+ cytotoxic T cells and (2) $CD4^+$ T helper (T_H) cells. Both subsets are classically further characterized by their expression of the αβ T cell receptor (TCR) and CD3 complex (Bosselut, 2004).

Cytotoxic $CD8^+$ T cells recognize foreign antigens presented on MHC class I molecules and subsequently induce cell death of the presenting cells (Barry and Bleackley, 2002). Under

homeostatic conditions, every nucleated eukaryotic cell presents self-antigens on MHC I, however upon intracellular infection also pathogen-specific antigens can be presented, resulting in the demasking of infected cells (Neefjes et al., 2011).

In contrast, $CD4^+$ T_H cells recognize antigens presented on MHC class II molecules, which are primarily expressed by APCs but also by thymic epithelial cells or stroma cells in lymph nodes (LN) (Arudchelvan et al., 2002; Malhotra et al., 2012; Neefjes et al., 2011; Ng et al., 2012). Upon activation, $CD4^+$ T_H cells can enhance both the innate and adaptive immune responses especially by producing a variety of different cytokines (Strutt et al., 2011).

Thus, the innate and adaptive immune system strongly interact with each other. APCs are essential to initiate an adaptive immune response and additionally elements of both innate and adaptive immune system can foster each other for instance by secreting cytokines (Jain and Pasare, 2017; Shanker, 2010).

Furthermore, both the innate and the adaptive immune system are linked to memory. However, especially the adaptive immune system is important for a long-term and specific immunological memory formation and thus for protection against secondary infections (Netea et al., 2019).

1.2. $CD4^+$ T cell-mediated immunity

1.2.1. $CD4^+$ T cell development

Most immune cells derive from hematopoietic stem cells (HSCs), the common progenitor cells of both innate and adaptive immune cells (Sawai et al., 2016). In the bone marrow, HSCs can differentiate into myeloid progenitor cells or common lymphoid progenitors (CLPs) which give rise to the myeloid or lymphatic lineage, respectively (Haas et al., 2018). CLPs can develop into pre-thymic progenitors, which further differentiate into thymus-settling progenitors (TSP) and migrate into the thymus where they undergo T cell development (Zlotoff and Bhandoola, 2011). In the thymus, they can give rise to double negative (DN) thymocytes followed by a series of differentiation steps (DN1-4) for the classical development of αβ T cells (Germain, 2002). During this differentiation process, thymocytes mature and the rearrangement of the TCR β chain occurs. Upon successful rearrangement and presentation, the expression of CD4 and CD8 is initiated. In these double positive (DP) thymocytes the rearrangement of the TCR α chain is initiated (Germain, 2002). Somatic rearrangement of TCR α and β gene loci with the help of Rag proteins enables expression of a unique TCR. Thus, a pool of T lymphocytes develops which differs completely in their TCR repertoire. Subsequently, cells undergo positive selection, in which

only T lymphocytes survive which bind MHC I or MHC II molecules in complex with presented self-peptides with sufficient strength to induce a survival signal (Moran and Hogquist, 2012). According to the MHC class binding and TCR signaling strength, DP cells differentiate into single positive (SP) $CD8^+$ or SP $CD4^+$ T cells (Germain, 2002). Furthermore, both at the DP but also at the SP stage thymocytes, which strongly react to self-antigens, undergo cell death, a process known as negative selection (Germain, 2002). After undergoing both positive and negative selection, SP cells emigrate from the thymus to secondary lymphatic organs like LN and spleen or circulate both in blood and lymph (Tomura et al., 2010). Here, mature $CD8^+$ or $CD4^+$ T cells stay in their naive state until recognition of their cognate antigen in complex with MHC molecules, co-stimulation and stimulating cytokines which will result in their further activation (Pennock et al., 2013).

However, not only classical $CD4^+$ T cells, in the periphery also termed conventional $CD4^+$ T cells (Tconv cells), but also a second class of $CD4^+$ cells can emigrate from the thymus. These cells show a high affinity for self-antigens and are termed regulatory T cells (Treg cells). Thymus-derived $CD4^+$ Treg (tTreg) cells, also called natural Treg cells, can develop from DP or immature SP $CD4^+$ thymocytes (Lee and Hsieh, 2009). These cells recognize self-antigens, however binding was not strong enough to induce cell death by negative selection (Hsieh et al., 2012). Hence, selection of tTreg cells is part of an agonist selection (Oh-hora et al., 2013). The development of tTreg cells is restricted and intraclonal competitions limit the development to a small clonal size (Bautista et al., 2009; Leung et al., 2009). Treg cells negatively control pro-inflammatory immune responses and thus tTreg cells are important mediators of self-tolerance (Perry and Hsieh, 2016). Emigrating tTreg cells stay in a resting phase and circulate through lymph and blood or migrate to secondary lymphatic organs (Pohar et al., 2018). Here, $CD8^+$ T cells, $CD4^+$ Tconv cells as well as tTreg cells can become activated by APCs and Tconv cells further undergo peripheral $CD4^+$ T cell differentiation (an overview of $CD4^+$ T cell development is shown in Figure 1).

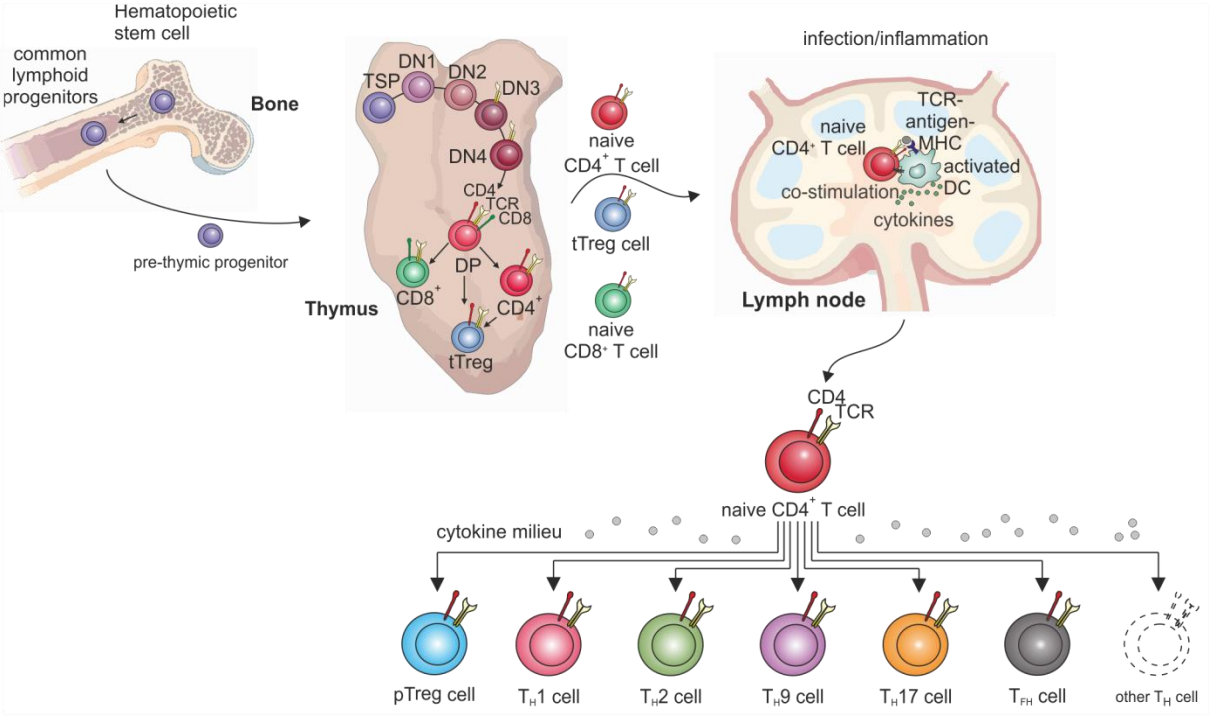

Figure 1: CD4$^+$ T cell development.
Overview of the development of classical αβ thymocytes. Hematopoietic stem cells in the bone marrow give rise to common lymphoid progenitors, which further differentiate into pre-thymic progenitors and migrate into the thymus as thymic-settling progenitors (TSP). Here, serial differentiation steps of double negative (DN) cells occur, which subsequently develop into double positive (DP) cells. Next, positive and negative selection as well as agonist selection takes place and thymocytes finally develop into mature single positive naive CD4$^+$ T cells, thymus-derived CD4$^+$ Treg (tTreg) cells as well as CD8$^+$ naive T cells. Maturate cells emigrate from the thymus into the blood and lymph as well as to lymphatic organs like lymph nodes. Upon activation, naive CD4$^+$ T cells can differentiate into effector T helper (T_H) cells like T_H1, T_H2, T_H9, T_H17, peripheral Treg (pTreg) cells and follicular T_H (T_{FH}) cells. CD, cluster of differentiation; MHC, major histocompatibility complex; TCR, T cell receptor.

1.2.2. Peripheral CD4$^+$ T cell differentiation

Naive CD4$^+$ T cells are mature CD4$^+$ T cells, which did not encounter their specific antigen yet. In the mouse, naive CD4$^+$ T cells are classically defined by a high expression of CD62L in absence of CD25 and low expression of CD44 (Swain et al., 1996). CD62L, also called L-selectin, is important for homing of lymphocytes to lymphatic organs, while in contrast the cell adhesion molecule CD44 plays a role in the migration into inflamed tissue as well as in the formation of an effector T cell response and memory (Baaten et al., 2010). Upon TCR binding to an antigen presented on MHC II in the presence of co-stimulatory molecules and cytokines, naive CD4$^+$ T cells become activated, undergo proliferation, also called clonal expansion, and differentiate into effector CD4$^+$ T cells (Corthay, 2006). Effector T cells upregulate CD44 as well as CD25, the α chain of the IL-2 receptor (Swain et al., 1996).

Effector $CD4^+$ T cells can be subdivided into different $CD4^+$ T_H subtypes (Figure 2). Depending on the surrounding microenvironment, $CD4^+$ T cells can gain different effector functions, which allow for the optimal immune defense in response to the invading pathogens (Swain et al., 2012). Cytokines present during the activation process can activate different Jak-Stat signaling pathways, which are important for establishing lineage-specific gene networks (Villarino et al., 2017).

T_H1 cells differentiate in presence of IL-12 and IFN-γ, which activates Stat4 and Stat1 respectively, resulting among others in the expression of the lineage transcription factor T-bet. T_H1 cells are important for activating macrophages by secreting IFN-γ and TNF-α. Hereby, they especially foster defense against intracellular pathogens, which persist in phagocytic cells (Zhu et al., 2010).

On the other hand, T_H2 cells are generated in an IL-4-rich environment. IL-4 induces Stat6 signaling, which subsequently promotes for instance the expression of the lineage-defining transcription factor Gata3. T_H2 cells additionally secrete IL-4 as a positive feedback-loop but also secrete IL-5 and IL-13, resulting in the recruitment and activation of innate immune cells like eosinophils, mast cells and basophils. In this way, T_H2 cells strengthen the immune response against helminth parasites (Walker and McKenzie, 2018).

In contrast, the presence of IL-2 and especially TGF-β1 in addition to IL-4 enables the differentiation into T_H9 cells instead of T_H2 cells. Just like in T_H2 cells, IL-4 signaling promotes Stat6 activation, while IL-2 induces Stat5 activation, resulting in a specialized gene network formation. T_H9 cells help to overcome parasite infections by secretion of the effector cytokines IL-9, thus promoting a mast cell response (Li et al., 2017).

T_H17 cells are important for eradicating extracellular pathogens. T_H17 cells differentiate in the presence of IL-6 and TGF-β1. IL-6 signaling results in the activation of Stat3, which initiates the T_H17 cell gene network, for instance by upregulating the expression of the transcription factor RORγt. The subsequent secretion of IL-17 and IL-22, among others, promotes immune responses of epithelial and stromal cells, resulting in the recruitment of neutrophils as well as in the production of antimicrobial peptides (Korn et al., 2009).

Furthermore, naive $CD4^+$ T cells can differentiate into follicular T_H cells (T_{FH} cells). T_{FH} cells are important for establishing an efficient B cell response. They differentiate in the presence of IL-6 and IL-21, which, in a manner similar to the activation of T_H17 cells, enables the activation of Stat3. A classical transcription factor, which is linked to effector function of T_{FH} cells, is Bcl-6. Activating Bcl-6 signaling allows T_{FH} cells to migrate to and stay in the B cell follicle and germinal centers (Wu et al., 2018). T_{FH} cells are important for the development

and function of germinal centers and thus promote the maturation of B cells (Crotty, 2014). Furthermore, they are important for high affinity humoral responses, IgG class switch and memory formation (Crotty, 2014).

Not only T_{FH} cells but also T_H1 and T_H2 cells help to establish an efficient antibody response. Secreted effector cytokines, such as IL-4 and IFN-γ, can promote an Ig class switch, which allows an optimal antibody production adapted to the corresponding type of infection (Hasbold et al., 1999).

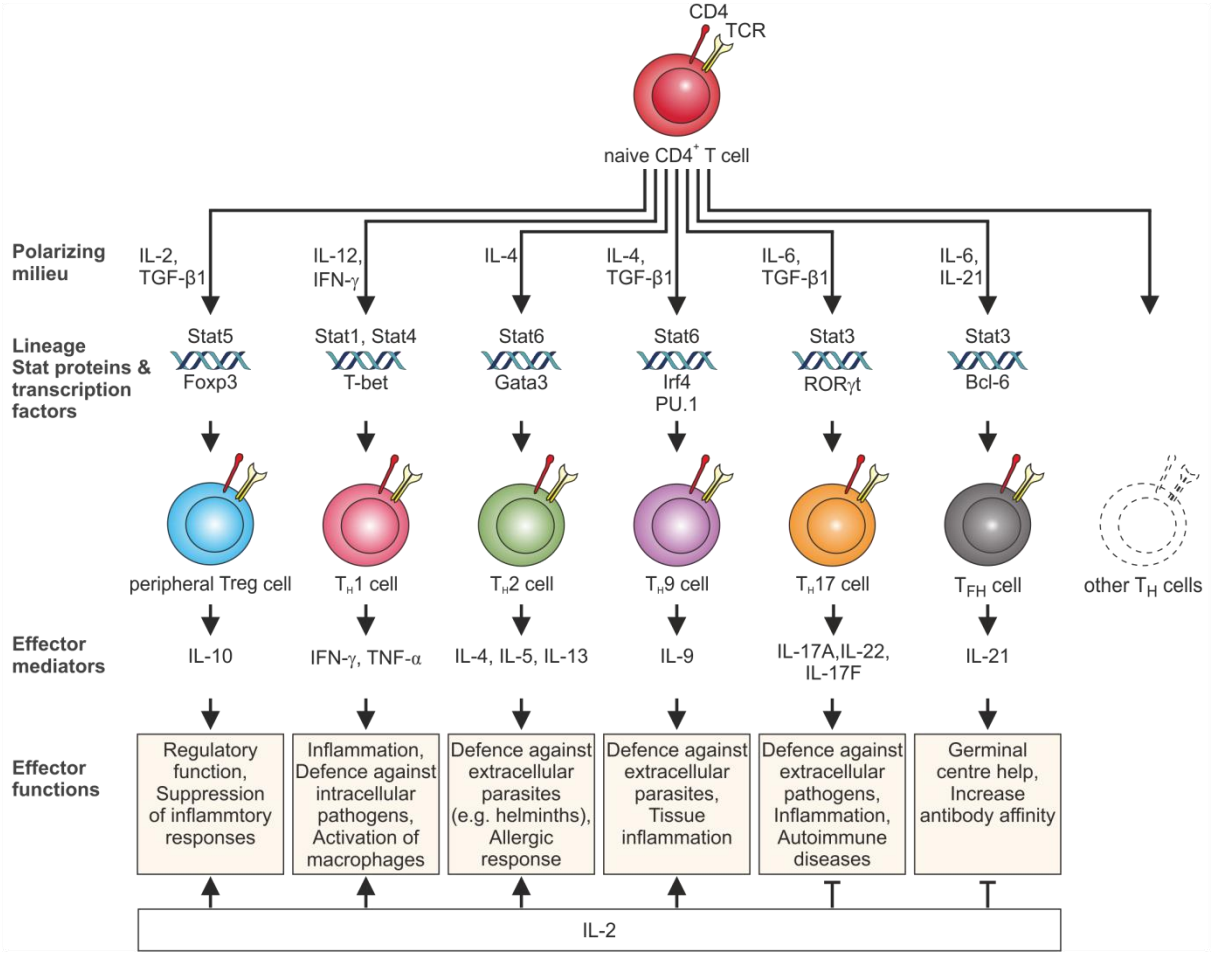

Figure 2: Peripheral CD4$^+$ T cell differentiation.
Upon activation, naive CD4$^+$ T cells can differentiate into various T_H effector cells. Fate decision is determined by the cytokines present in the microenvironment (polarizing milieu). Naive CD4$^+$ T cells can differentiate into peripheral Treg, T_H1, T_H2, T_H9, T_H17 and T_{FH} cells. Each effector group can be characterized by their transcription factor network, specific cytokine release (effector mediators) and their respective effector mediators and function. Bcl-6, B cell lymphoma 6; CD, cluster of differentiation; Foxp3, Forkhead box P3; Gata3, GATA-binding protein 3; IFN-γ, interferon-gamma; IL, interleukin; Irf4, interferon regulatory factor 4; RORγt, retinoic acid receptor-related orphan receptor-γt; Stat, Signal transducer and activator of transcription; T-bet, T-box expressed in T cells; TCR, T cell receptor; T_{FH}, T follicular helper; T_H, T helper; TGF-β1, transforming growth factor-beta 1; TNF-α, tumor necrosis factor-alpha. Figure is modified from Swain et al., 2012 and Dupage and Bluestone, 2016.

In contrast to T_H1, T_H2, T_H9, T_H17 and T_{FH} cells, which together comprise the pro-inflammatory T_H subtypes, naive $CD4^+$ T cell can also differentiate into an anti-inflammatory effector subtype. Treg cells do not only develop in the thymus, but also can differentiate in the periphery, subsequently called peripheral Treg (pTreg) cells. Differentiation of pTreg cells takes place in the presence of TGF-β1 and IL-2. IL-2 allows the activation of Stat5 signaling and thus subsequently enables the expression of the key lineage factor Foxp3 (Owen and Farrar, 2017). The generation of this class of suppressive cells is important to avoid an over-activation of the immune system and thus prevents the development of autoimmunity. Especially in barrier organs like the gut, pTreg cells are important to circumvent immunity against commensal microbes, allergens and food antigens (Josefowicz et al., 2012). Both, pTreg but also tTreg cells express the inhibitory cytokine IL-10, but also regulate immunity by metabolic disruption and cytolysis of effector T cells. Furthermore, they also reduce the differentiation of pro-inflammatory effector cell by inhibiting dendritic cell function (Vignali et al., 2008).

Moreover, the existence of further T_H subtypes has been proposed like T_H22 cells, which like T_H17 cells express IL-22 and, to a lower extent, RORγt but in contrast to T_H17 cells express T-bet and do not secrete IL-17 (Plank et al., 2017). In line with this, plasticity between different subtypes is highly discussed. Dependent on the microenvironment, T_H cells can be reprogrammed into a different T_H subset or can gain intermediate features, resulting in a combined phenotype of different subsets (DuPage and Bluestone, 2016). Thus, the differentiation of $CD4^+$ T cells is not restricted to the classical T_H subsets or terminal, but $CD4^+$ T cell differentiation is a rather flexible system.

For $CD4^+$ T cell plasticity, cytokines und subsequently Stat signaling play an important role. The different Stat proteins regulate the expression of lineage-defining transcription factors and the formation of gene network (Villarino et al., 2017). Stat proteins can share the same DNA binding sites and thus can compete for the regulation of shared genes. Stat3 and Stat5 for instance can both bind to *Il17a*, however while Stat3 induces *Il17a* expression Stat5 represses it (Yang et al., 2011). Furthermore, upon activation, Stat proteins can form heterodimers or tetramers built out of different Stat proteins. These complexes can target different genes and thus influence differentiation (Peters et al., 2015; Villarino et al., 2015). Stat proteins are involved in epigenetic chromatin modification by recruiting histone modifying enzymes and thus can affect thousands of genomic loci (DuPage and Bluestone, 2016; O'Shea et al., 2011; Villarino et al., 2015). In line with this, Stat proteins induce remodeling of the enhancer landscape of $CD4^+$ T cells and thus direct lineage specification

(Vahedi et al., 2012). Hence, the composition of cytokines present during an immune reaction influences the activation of different Stat proteins, which subsequently compete or assist each other, and the balance of Stat proteins allows for the formation of different gene networks.

Although T_H subsets are often linked to only one lineage-defining transcription factor, the specific effector programs are controlled by a dynamic, tightly regulated gene network (Ciofani et al., 2012; Henriksson et al., 2019; Kaplan, 2017; Pedicini et al., 2010; Placek et al., 2009; Shih et al., 2014; Wu et al., 2018; Yosef et al., 2013). Transcription factors in these networks can be shared between T_H subsets, while others antagonize each other and their interplay further shapes the transition of $CD4^+$ T cells (Apetoh et al., 2010; Brown et al., 2015; Huber and Lohoff, 2014; Wang et al., 2014a; Wu et al., 2018).

Furthermore, direction and plasticity of $CD4^+$ T cells can be controlled by the strength of TCR binding as well as by changes in the cellular metabolism. Present nutrients, the metabolic program of the cell, generated metabolic products as well as the extracellular oxygen level can all influence and regulate the effector program of $CD4^+$ T cells (DuPage and Bluestone, 2016).

Thus, multiple components play a role in the differentiation and dynamic of $CD4^+$ T cells, which allows them to be shaped depending on the initial activation and further functionally adapted in response to changes in the microenvironment. However, although new mechanisms driving the differentiation of $CD4^+$ T cells were identified in the last years, the complex networks orchestrating these processes are not yet fully understood and further studies are needed to unravel the master regulators and branching points in these dynamic processes. This is especially necessary, as the plasticity of $CD4^+$ T cells on the one hand helps to better adapt to pathogens and consequently leads to an efficient elimination of the infections, but on the other hand can also foster autoimmunity and cancer progression by skewing inflammatory and suppressive $CD4^+$ T cells in a pathogenic environment (Ivanova and Orekhov, 2015).

1.2.3. T_H17 cells

As described above, T_H17 cells are pro-inflammatory $CD4^+$ T cells which help in the defense against extracellular pathogens. Under homeostatic conditions, T_H17 cells together with Treg cells especially play a role in tissue homeostasis of barrier organs. Here, T_H17 cells prevent the invasion of commensal microbiota and support epithelial cells in their barrier function, while pTreg cells dampen an overreaction of T_H17 cells and other immune cells as well as support tolerance against the microflora (Eisenstein and Williams, 2009). Interestingly, pTreg cells and T_H17 cells share the same intermediate precursor, further underlining the flexible

adaption to microenvironmental conditions and requirements (Zhou et al., 2008). Both cell types require TGF-β1 for their differentiation, however the amount of TGF-β1 and the presence of other cytokines like IL-2, retinoic acid, IL-6 and IL-23 direct the subsequent differentiation and effector program (Brown et al., 2015; Mangan et al., 2006; Veldhoen et al., 2006; Zhou et al., 2008). Furthermore, the cellular metabolism can influence the balance of T_H17/Treg cells. For instance, while T_H17 cells are dependent on glycolysis, Treg cells rely on fatty acid oxidation (Sun et al., 2017).

In the last years, T_H17 cells were linked to several autoimmune diseases like multiple sclerosis, atherosclerosis, psoriasis, inflammatory bowel diseases and others (Zambrano-Zaragoza et al., 2014). Furthermore, it has been shown that IL-23 signaling and the resulting TGF-β3 expression are critical for the development of pathogenic features and the subsequent development of T_H17 cell-driven diseases (Langrish et al., 2005; Lee et al., 2012). Thus, T_H17 cells can be further subdivided into non-pathogenic and pathogenic T_H17 cells (Figure 3). While non-pathogenic T_H17 cells, which are induced in presence of TGF-β1 and IL-6, are

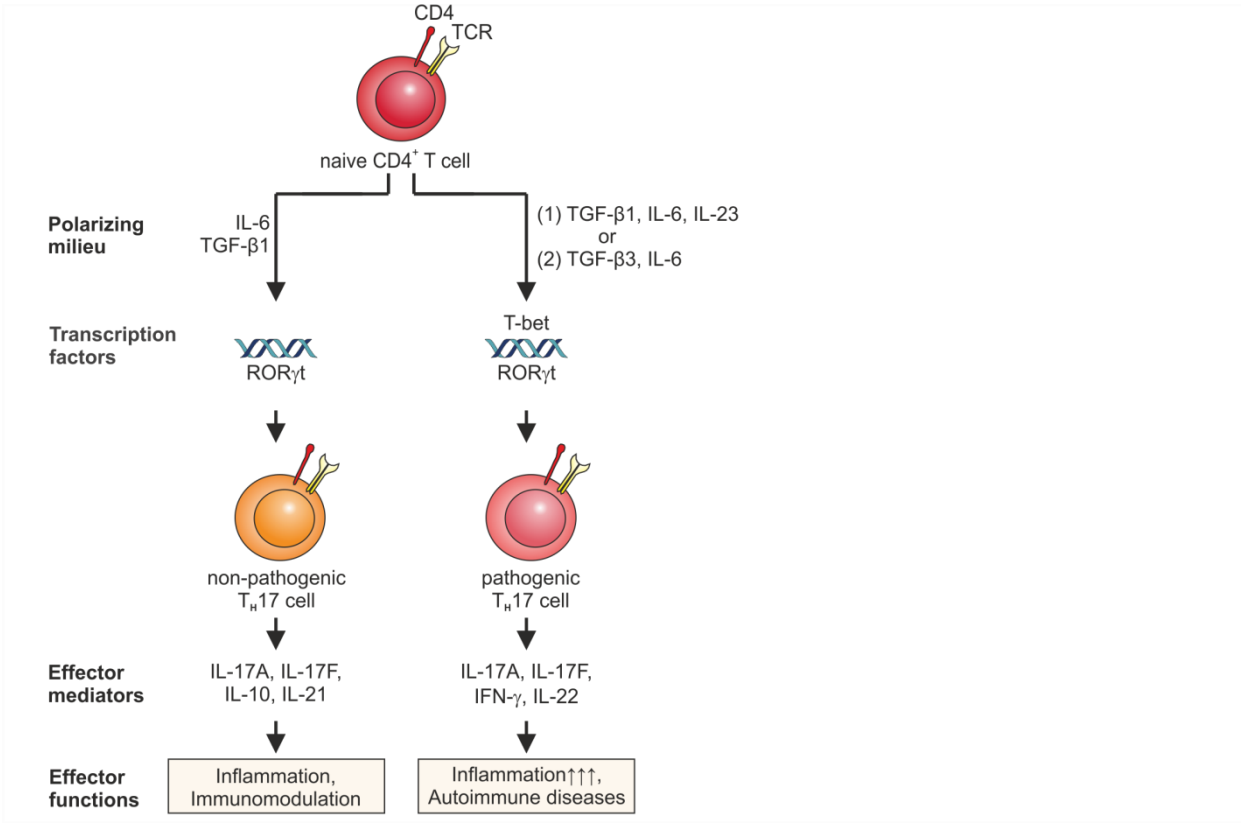

Figure 3: T_H17 cells can be subdivided into non-pathogenic and pathogenic T_H17 cells.
Dependent on the T_H17 cell-polarizing milieu, naive $CD4^+$ T cells can differentiate into non-pathogenic or pathogenic T_H17 cells, which express different effector cytokines and exhibit different effector functions. CD, cluster of differentiation; IFN-γ, interferon-gamma; IL, interleukin; RORγt, retinoic acid receptor-related orphan receptor-γt; T-bet, T-box expressed in T cells; TCR, T cell receptor; T_H, T helper; TGF-β, transforming growth factor-beta.

responsible for tissue homeostasis, pathogenic T_H17 cells develop for instance in presence of (1) TGF-β1, IL-6 and IL-23 or (2) TGF-β3 and IL-6 and subsequently drive inflammation and can cause autoimmune diseases (Lee et al., 2012).

In the last years, the molecular signature of non-pathogenic and pathogenic T_H17 cells was furthers characterized to understand the phenotypes of T_H17 cells and the underlying mechanisms contributing to their respective development. A general T_H17 cell regulatory gene network was defined, showing that in addition to RORγt other transcription factors like Runx1, Fas, Batf, Irf4, c-Maf and Ahr also play an important role in the differentiation of T_H17 cells, while for instance Sp4 and Ikzf4 negatively regulate T_H17 cell differentiation (Ciofani et al., 2012; Yosef et al., 2013). Furthermore, it was shown that Stat3 regulates the expression of most of these genes (Durant et al., 2010). During the development of pathogenic T_H17 cells, this gene network is modified and while for instance Ahr and c-Maf become downregulated, the transcription factors T-bet and Runx are upregulated (Lee et al., 2012; Wang et al., 2014a). Thus, pathogenic T_H17 cells develop T_H1 cell characteristics, often associated with an upregulation of IFN-γ next to or instead of IL-17a (Hirota et al., 2011; Lee et al., 2009; Wang et al., 2014a).

Furthermore, the expression of the IL-23 receptor and GM-CSF are linked to T_H17 cell pathogenicity (Codarri et al., 2011; El-Behi et al., 2011; McGeachy et al., 2009), while CD5L expression limits pathogenic features (Gaublomme et al., 2015; Wang et al., 2015).

Although in the last years new insights about the molecular mechanisms were gained how T_H17 cells are generated, the complete molecular network governing their generation has not been fully determined. Thus, to better understand the differentiation process of T_H17 cells and to elucidate strategies to interfere and manipulate these processes in T_H17 cell-driven diseases further studies are needed.

1.3. IL-2 signaling

The cytokine IL-2 is responsible for the growth of activated T cells. While survival of naive and memory $CD4^+$ T cells is highly dependent on IL-7, IL-2 signaling is important for an effector T cell response and cell proliferation (Katzman et al., 2011). Activation of the TCR in the presence of co-stimulatory cytokines typically results in expression of IL-2. IL-2 signaling, in turn, leads to the activation of Stat5 and the expression of the IL-2 receptor α chain (CD25), which is one of the three subunits of the IL-2 receptor (Malek, 2008). The induction of its own high affinity receptor, as a positive feedback loop, allows the activation of several pathways like the Janus kinase – Stat pathway, the phosphoinositide 3 kinase – Akt pathway and the mitogen-activated protein kinase pathway, resulting in an initial activation of

naive T cells and transition into the effector phase (Malek, 2008). Additionally, IL-2 signaling triggers an auto-inhibitory feedback loop via Blimp-1, which prevents activation-induced cell death (Martins et al., 2008).

IL-2 is further important in thymic T cell development both during the selection process of Tconv cells and during the development of tTreg cells. Mice deficient for IL-2 signaling suffer from severe systemic autoimmune diseases, resulting in an early death of these animals induced by the lack of proper Treg cell development (Furtado et al., 2002; Sadlack et al., 1995; Willerford et al., 1995). Treg cells are incapable of producing IL-2, however they are dependent on IL-2 signaling and they consistently express CD25, resulting in the removal of IL-2 from the microenvironment (Létourneau et al., 2009). Metabolic disruption like IL-2 deprivation in IL-2 low environments inhibits Tconv cells and represents one of the immunosuppressive mechanisms exerted by Treg cells (Vignali et al., 2008).

IL-2 signaling does not only influence the development of Treg cells but it also has an impact on the differentiation of the other T_H subsets (Boyman and Sprent, 2012; Liao et al., 2013) (Figure 2). While IL-2 is essential for the differentiation of tTreg and pTreg cells, it diminishes T_H17 cell differentiation (Fujimura et al., 2013; Laurence et al., 2007). IL-2 signaling results in a reduced expression of the IL-6 receptor α chain and the IL-6 signal transducer gp130 (Liao et al., 2011). Furthermore, IL-2-induced activation of Stat5 diminishes IL-17A expression through the competition of Stat5 and Stat3 for binding sites at the *Il17a* gene locus (Yang et al., 2011). In addition, Stat5 signaling promotes T-bet expression, which not only reduces the differentiation of non-pathogenic T_H17 cells but also fosters the differentiation of T_H1 cells (Liao et al., 2011). Next to its induction of T-bet expression, IL-2 signaling also upregulates the expression of IL-12 receptor β2, which further supports the generation of T_H1 cells (Liao et al., 2011). Additionally, IL-2 also promotes the differentiation of T_H2 cells by Stat5-induced upregulation of the IL-4 receptor α and the T_H2 cell-associated cytokines IL-4, IL-5 and IL-13 (Liao et al., 2008). Furthermore, IL-2 signaling is critical for the development of T_H9 cells through its regulation of IL-9 production and inhibition of Bcl6 expression (Liao et al., 2014). In contrast, IL-2-induced suppression of Bcl6 reduces the development of T_{FH} cells, which is further abated by IL-2-induced upregulation of Blimp-1, which additionally suppresses the differentiation of T_{FH} cells (Johnston et al., 2012). Thus, while IL-2 is essential for the development of Treg cells and supports the differentiation of T_H1, T_H2 and T_H9 cells, it diminishes the development of T_H17 and T_{FH} cells.

Moreover, the duration and the strength of the IL-2 signal also impacts the influence of IL-2 on the differentiation process of the respective T_H subset (Boyman and Sprent, 2012). For instance, the expression level of CD25 can control differentiation. While cells which upregulate CD25 upon TCR stimulation easily develop into effector cells, cells expressing only low levels of CD25 preferentially give rise to T_{FH} cells and central memory cells (Choi et al., 2011; Pepper et al., 2011). Furthermore, DiToro et al. showed that the strength of the TCR signal also influences IL-2 expression and that IL-2-expressing cells do not respond to IL-2 but rather deliver the cytokine to cells, which themselves do not produce IL-2 but express CD25 (DiToro et al., 2018).

The expression of IL-2 itself in T cells is tightly regulated. Several regulatory elements upstream of the *Il2* gene have been identified and differential binding of transcription factors to these elements can result in increased or repressed expression of *Il2*. Upon TCR stimulation and CD28 co-stimulation, especially nuclear factor of activated T cells (Nfat), activator protein 1 and nuclear factor-kappa B play an important role in *Il2* transcription (Liao et al., 2013), while for instance CAMP responsive element binding protein, Blimp-1 and c-Maf can diminish *Il2* expression (Gabryšová et al., 2018; Liao et al., 2013). Furthermore, Ets2 restrains *Il2* expression in naive $CD4^+$ T cells and Pten prevents *Il2* upregulation in the early phase of T_H17 cell differentiation (Kim et al., 2017; Panagoulias et al., 2016). In addition, it has been shown that Satb1 can regulate IL-2 and CD25 expression (Alvarez et al., 2000; Kumar et al., 2005; Pavan Kumar et al., 2006; Yasui et al., 2002).

Nevertheless, the complete mechanism of IL-2 regulation is not determined yet and more knowledge needs to be obtained to understand the transcriptional control and the resulting outcome during T_H cell differentiation.

1.4. The genome organizer Satb1

Satb1 is a chromatin organizer and transcription factor, which has an essential role in the development and function of lymphocytes, the brain as well as during the development of cancer (Alvarez et al., 2000; Naik and Galande, 2019).

Structurally, Satb1 consists of a nuclear localization signal, a ubiquitin-like domain, a nuclear matrix binding domain, as well as multiple DNA binding domains (Dickinson et al., 1997; Seo et al., 2005; Wang et al., 2012, 2014b; Yamasaki et al., 2007). These DNA binding domains include a CUT repeat-like (CUTL) domain, two CUT domains (CUT1 and CUT2) as well as a homeodomain which together enable Satb1 binding to specific base-unpairing regions (BURs), which are especially found in AT-rich matrix attachment regions (MAR)

(Dickinson et al., 1997; Wang et al., 2014b). Furthermore, the ubiquitin-like domain allows tetramerization of Satb1, which is essential for DNA binding (Wang et al., 2012, 2014b).

Satb1 can regulate gene expression via multiple mechanisms (Shannon, 2003). Satb1 can attach BURs to the nuclear matrix, resulting in a three-dimensional organization of the DNA. Thus, Satb1 is involved in the formation of high-ordered chromatin loop structures and builds a cage-like chromatin network (Cai et al., 2003). In this way, Satb1 can bring distant gene elements close together and thus allows long range interactions (Gong et al., 2011; Yang et al., 2015b).

Next to its role in chromatin organization, Satb1 regulates gene expression on an epigenetic level via recruitment of chromatin modifying factors to their target gene loci. Satb1 serves as a landing platform for various interaction partners, especially chromatin remodeling enzymes, and thus regulates gene expression over long distances (Yasui et al., 2002). Dependent on its posttranscriptional modifications, Satb1 can interact with histone acetyltransferases or histone deacetylases, resulting in epigenetic modifications of the respective DNA loci (Pavan Kumar et al., 2006). While phosphorylation of Satb1 leads to a global transcriptional downregulation, acetylation of Satb1 results in an upregulation of gene expression (Pavan Kumar et al., 2006; Purbey et al., 2009).

Thus, Satb1 is involved in the configuration of nuclear chromatin as well as in the formation of the epigenetic landscape and thereby regulates expression of multiple genes.

Next to phosphorylation and acetylation, Satb1 can also be sumoylated, which is linked to caspase-induced Satb1 cleavage (Galande et al., 2001; Tan et al., 2008, 2010). Cleavage of Satb1 occurs during apoptosis in Jurkat T cells, however further studies indicate also a functional role for the cleavage products independent of cell death (Tan et al., 2010, unpublished data by Daniel Sommer).

In the last years, the functional role of Satb1 was studied in more detail by generating Satb1-deficient cell lines and mouse models. Satb1-null mice die three weeks after birth due to neurological defects (Alvarez et al., 2000) and it could be shown that Satb1 is important during postnatal brain development by mediating neuronal plasticity (Balamotis et al., 2012). Furthermore, Satb1 is a risk factor for Parkinson's disease and expression of Satb1 in dopaminergic neurons is important to prevent cellular senescence and an inflammatory response in the brain (Chang et al., 2017; Riessland et al., 2019). Additionally, Satb1 is involved in the early phase of erythropoiesis as well as in the development of the epidermis (Fessing et al., 2011; Wen et al., 2005). Furthermore, Satb1 is important for the development of conventional dendritic cells and ensures proper MHC II expression (Tesone et al., 2016).

Next, to its role in cell development, Satb1 plays an important role in X-chromosomal inactivation and the base excision repair mechanism (Agrelo et al., 2009; Kaur et al., 2016). Aberrant expression of Satb1 is linked to progression and aggressiveness of several cancer types (Naik and Galande, 2019). High expression of Satb1 is associated with poor prognosis of liver, lung or breast cancer due to transcriptional activation of tumor oncogenes and repression of tumor suppressor genes (Naik and Galande, 2019). However, in tumors like cutaneous skin melanoma or pancreatic adenocarcinoma, lower expression of Satb1 is linked to poor prognosis (Naik and Galande, 2019). Thus, proper Satb1 expression is essential for cellular homeostasis and studying its role in cancer formation and treatment might help to find new therapeutic approaches.

Under homeostatic conditions besides the high expression of Satb1 in the CNS, Satb1 is predominantly expressed in thymocytes and in the last years it has become clear that Satb1 plays a critical role during lymphocyte development and differentiation (Ahlfors et al., 2010; Akiba et al., 2018; Alvarez et al., 2000; Beyer et al., 2011; Cai et al., 2006; Ciofani et al., 2012; Dickinson et al., 1992; Doi et al., 2018; Gottimukkala et al., 2016; Hao et al., 2015; Kakugawa et al., 2017; Kitagawa et al., 2017; Kondo et al., 2016; Notani et al., 2010; Nüssing et al., 2019; Satoh et al., 2013; Stephen et al., 2017; Tanaka et al., 2017; Yasuda et al., 2019).

1.4.1. The role of Satb1 in T cell development

In the last years, the role of Satb1 in T cell development was further investigated, which revealed that Satb1 is critical in multiple steps during the development and differentiation of T cells (Figure 4).

Satb1 is required for adult HCSs self-renewal as well as lymphopoiesis (Doi et al., 2018). HSCs can be subdivided into $Satb1^+$ as well as $Satb1^-$ cells. Satb1 expression, however, is not indicative of the maturation stage of HSCs and both subpopulation are still interconvertible (Doi et al., 2018). While $Satb1^-$ cells predominantly give rise to progenitors of the myeloid lineage, expression of Satb1 in HSCs fosters lymphoid lineage development (Doi et al., 2018; Satoh et al., 2013). Thus, Satb1 has a critical role during the lymphoid lineage decision. In line with this, Satb1-null mice exhibit a reduced size of the thymus and contain fewer thymocytes (Alvarez et al., 2000).

Analysis of the expression profile of *Satb1* during thymopoiesis revealed an increased expression of *Satb1* especially during the double positive stage, as well as a high expression in immature $CD4^+$ SP cells and tTreg precursor cells (Gottimukkala et al., 2016; Kitagawa et al., 2017; Kondo et al., 2016). Deletion of Satb1 results in a block of thymopoiesis at the DP stage as cells cannot further differentiate into SP $CD4^+$ or $CD8^+$ T cells (Alvarez et al., 2000;

Kondo et al., 2016; Satoh et al., 2013; Sommer, 2018). In the DP cells, Satb1 facilitates *Rag1* and *Rag2* expression and thus plays a role in the TCRα rearrangement, which is required for subsequent selection (Hao et al., 2015). Furthermore, Kakugawa et al. showed that Satb1 is required for SP lineage decision by regulating expression of the lineage-specifying genes Runx, CD8, Thpok and CD4 (Kakugawa et al., 2017). While Runx orchestrates the differentiation into SP $CD8^+$ T cells, Thpok expression mediates the lineage decision into $CD4^+$ T_H cell (Taniuchi, 2009). Satb1 is important for Thpok expression in thymocytes after positive selection but not in the terminally committed $CD4^+$ T cells (Kakugawa et al., 2017). In addition, downregulation of Satb1 in thymocytes using a heterozygous deletion of Satb1 in combination with transgenic expression of a Satb1-antisense oligo results in a reduced development of $CD8^+$ T cells in mice (Nie et al., 2005).

Furthermore, Satb1 controls the development of tTreg cells, which arise from immature $CD4^+$ SP thymocytes or to a lower extent from DP thymocytes (Kitagawa et al., 2017; Lee

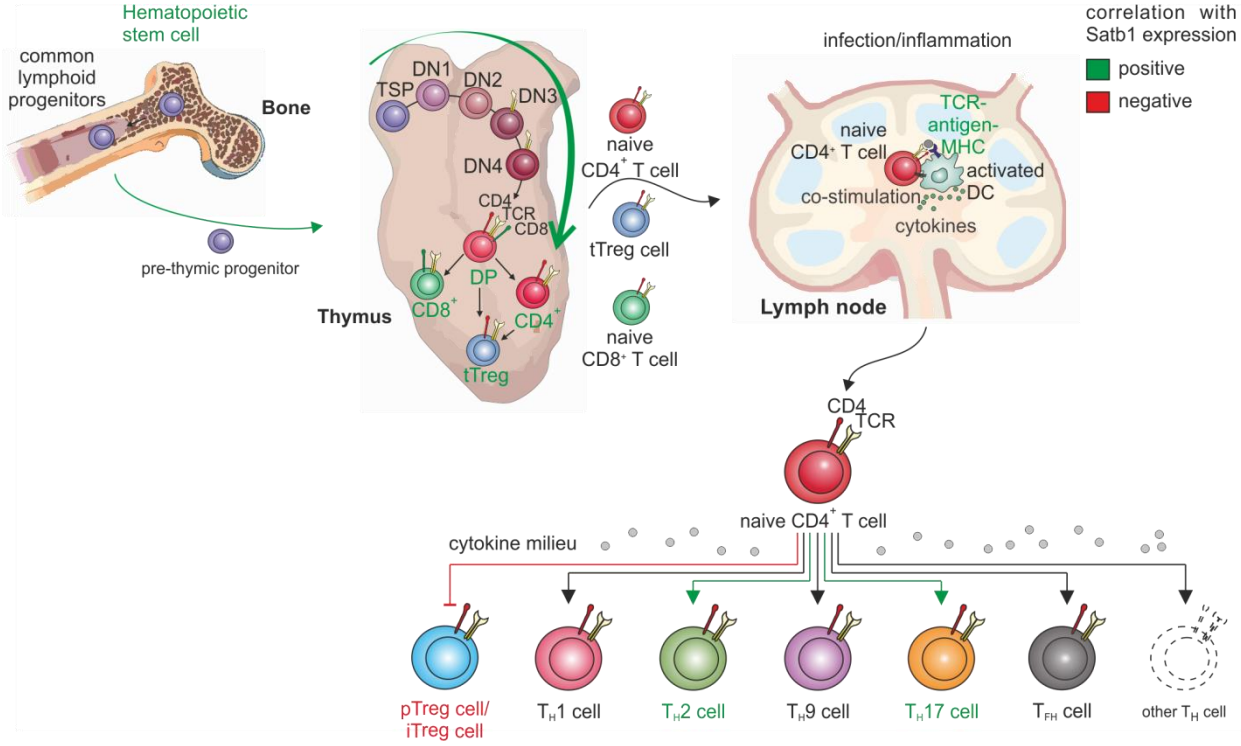

Figure 4: Satb1 governs the development of T cells.
Overview of the role of Satb1 during the development of classical $CD4^+$ αβ T cells. Expression of Satb1 is important for the lymphoid lineage decision as well as for thymopoiesis. In peripheral effector T cells, Satb1 expression is differently regulated and further studies are needed to fully understand the role of Satb1 for lineage decision and function. CD, cluster of differentiation; CLP, common lymphoid progenitors; DP, double positive cells; MHC, major histocompatibility complex; Satb1, special AT-rich sequence-binding protein 1; tTreg, thymus-derived Treg cell; TCR, T cell receptor; T_H, T helper; TSP, thymus-settling progenitors.

and Hsieh, 2009). The commitment of tTreg precursor cells relies on the activation of Treg cell-specific super-enhancers (Kitagawa et al., 2017). Satb1 is required for the activation of these super-enhancers and thus a Satb1 deficiency results in an impaired development of tTreg cells, which causes autoimmune diseases and IgE hyperproduction in adult mice (Kitagawa et al., 2017; Kondo et al., 2016; Tanaka et al., 2017).

All in all, Satb1 has an essential role for thymocyte development, starting at the stage of HSCs favoring maturation into the lymphoid lineage, governing TCRα rearranging, orchestrating tTreg cell development as well as fine-tuning $CD4^+$/$CD8^+$ linage decision. By changing the chromatin configuration and modulating epigenetic modifications, Satb1 can act as an activator or a transcriptional repressor of the respective gene loci (Alvarez et al., 2000; Kakugawa et al., 2017; Kitagawa et al., 2017). A global analysis of thymocytes revealed that Satb1 regulates around 2% of all tested genes during thymopoiesis especially via repression (Alvarez et al., 2000).

In recent years, the role of Satb1 in peripheral $CD4^+$ T cells has been further investigated. Satb1 represses IL-7 receptor α expression, which indicates a role for Satb1 in the homeostasis of naive T cells (Alvarez et al., 2000). In peripheral naive T cells, Satb1 expression is lower compared to DP or immature SP $CD4^+$ T cells during thymic T cell development (Kondo et al., 2016; Nüssing et al., 2019; Yasuda et al., 2019). However, TCR stimulation results in an upregulation of Satb1 (Akiba et al., 2018; Beyer et al., 2011; Gottimukkala et al., 2016; Stephen et al., 2017). Furthermore, Satb1 can associate with Nfat, indicating a role of Satb1 during T cell activation (Gabriel et al., 2016). In line with this, Satb1 is linked to the regulation of IL-2 in Jurkat cells, a well-known Nfat target gene (Kumar et al., 2005; Liao et al., 2013; Pavan Kumar et al., 2006). In addition, Satb1 is known to play a role in IL-2 receptor signaling by regulating CD25 expression (Alvarez et al., 2000; Kumar et al., 2005). Furthermore, Satb1 restrains PD-1 expression and thus decreases T cell exhaustion upon TCR stimulation (Nüssing et al., 2019; Stephen et al., 2017).

Next to its role during T cell activation, Satb1 is associated with the development of different T_H subtypes. Originally, Satb1 was linked to the differentiation of T_H2 cells, since Satb1 is upregulated by IL-4 and was higher expressed in T_H2 cells compared to T_H1 cells (Lund et al., 2003, 2005). In line with this, Satb1 is positively regulated by Stat6 signaling (Ahlfors et al., 2010; Jargosch et al., 2016). Furthermore, Satb1 is upregulated via Gata3 in thymocytes indicating also a role for Satb1 in T_H2 cells (Gottimukkala et al., 2016). Moreover, Satb1 is involved in the regulation of T_H2 cell cytokines like IL-4, IL-5 and IL-13 by binding and

rearranging the T_H2 cell-associated cytokine locus as well as inducing Gata3 expression (Ahlfors et al., 2010; Cai et al., 2006; Notani et al., 2010).

In contrast to T_H2 cells and tTreg cells, Satb1 is downregulated in Treg cells in the periphery (Beyer et al., 2011). Inhibition of Satb1 expression in Treg cells is mediated by Foxp3 as well as Foxp3-regulated miRNAs (Beyer et al., 2011). In addition, it has been shown that Stat5 reduces Satb1 expression in T cell lymphomas via regulation of microRNA 155 (Fredholm et al., 2018). Furthermore, TGF-β1 inhibits Satb1 expression in the tumor microenvironment (Stephen et al., 2017). This further suggests a role for TGF-β1 and Stat5 in the regulation of Satb1 expression in Treg cells. Loss of Satb1 expression fosters the development of pTreg cells and Satb1 overexpression studies showed that downregulation of Satb1 is required for the suppressive function of Treg cells and for the maintenance of a Treg cell phenotype (Beyer et al., 2011; Kitagawa et al., 2017; Sommer, 2018; Wang et al., 2017). Thus, Satb1 exhibits a dual role in the development of Treg cells. While its expression is mandatory at the early stages of tTreg cell development in the thymus, Satb1 is downregulated during pTreg cell development from naive CD4+ T cells in the periphery. Once the cellular identity has been established, downregulation of Satb1 is important to maintain and mediate Treg cell function.

During the preparation of this thesis, further studies revealed a role of Satb1 in the development of T_H17 cells. *In silico* predictions indicated that Satb1 is required for T_H17 cells (Ciofani et al., 2012; Yosef et al., 2013). Analysis of Satb1 expression in *in vitro* differentiated T_H cells, showed an upregulation of *Satb1* in T_H17 cells (Yasuda et al., 2019). Furthermore, knock-down and knock-out studies showed that Satb1 is essential for the development of T_H17 cells both *in vitro* but also *in vivo* (Akiba et al., 2018; Ciofani et al., 2012; Sommer, 2018; Yasuda et al., 2019). Deletion of Satb1 in all hematopoietic cells as well as a deletion specifically in T cells prevents the T_H17 cell-induced autoimmune disease experimental autoimmune encephalomyelitis (EAE), the mouse model for multiple sclerosis (Akiba et al., 2018; Yasuda et al., 2019). In addition, deletion of Satb1 in pre-formed T_H17 cells results in a reduced development of EAE (Yasuda et al., 2019). In line with this, single nucleotide polymorphisms in the Satb1 locus were associated with multiple sclerosis (Beecham et al., 2013). In addition, it could be shown that Satb1 is important for the development of pathogenic T_H17 cells due to the regulation of GM-CSF as well as PD-1 (Yasuda et al., 2019).

Not much is known about the role of Satb1 in T_{FH} cells. A recent study demonstrated that *Satb1* is downregulated in T_{FH} cells in comparison to Treg cells (Georgiev et al., 2018). This

indicates that suppression of Satb1 expression could be an important step for the development of T_{FH} cells.
Thus, Satb1 seems to play a role not only during early T cell development but also in the differentiation and function of peripheral T_H cells.

1.5. Aim of this thesis

Satb1 plays an essential role in development and differentiation of $CD4^+$ T cells. Especially its role in thymopoiesis was intensely studied during the last decade as the loss of Satb1 results in a block of thymocyte development (Alvarez et al., 2000). Additionally, it has become clear that Satb1 has a major impact on peripheral immune homeostasis (Kondo et al., 2016). Recent studies revealed an important role for Satb1 in T_H subtype decision and function (Akiba et al., 2018; Beyer et al., 2011; Cai et al., 2006; Kitagawa et al., 2017; Yasuda et al., 2019). Nevertheless, a comprehensive study analyzing the role of Satb1 in all T_H subsets is missing.

The aim of this thesis was to study the role of Satb1 in peripheral T cells. The impact of Satb1 on naive $CD4^+$ T cells as well as on the differentiation into T_H subsets was investigated. To avoid manipulation of Satb1 expression during thymopoiesis, conditional mouse lines were used. $Satb1^{fl/fl}$ as well as R26-STOP-Satb1 mice were generated by Daniel Sommer during his Ph.D. thesis and allowed spatiotemporal deletion or overexpression of Satb1, when crossing to specific Cre lines (Sommer, 2018).

To more closely analyze the role of Satb1 in the early phase of T_H cell differentiation, epigenetic as well as transcriptional profiling of Satb1-deficient naive $CD4^+$ T cells was performed. Here, the focus was set on the role of Satb1 in T_H17 cells, which are one of the major players in autoimmune disease. As the incidence and prevalence of autoimmune diseases have been on the rise over the last years (Bach, 2002), it is important to identify new target genes which can be used to manipulate pathogenic T cell differentiation and find potential mechanisms to interfere with the development of autoimmune diseases.
Since Satb1 is downregulated in pTreg cells, which exhibit a reciprocal relationship to T_H17 cells, an important role of Satb1 in the development of T_H17 cell is likely.
Thus, the aim of this thesis was to elucidate whether, when and how Satb1 influences T_H17 cell differentiation and T_H17 cell-driven autoimmune diseases.

2. Materials

2.1. Equipment

Table 2: List of equipment used

Equipment	Supplier
2200 TapeStation	Agilent Technologies
4200 TapeStation	Agilent Technologies
Analysis Scale MS104S and EL2001	Mettler Toledo
ARE Heating Magnetic Stirrer	Velp Scientifica
BD High Throughput Sampler	BD Biosciences
Centrifuge 5415R	Eppendorf GmbH
Centrifuge 5424R	Eppendorf GmbH
Centrifuge 5810R	Eppendorf GmbH
Centrifuge Mikro-200R	Hettich
ChemiDoc MP	Bio-Rad Laboratories
CO_2 Incubator	Thermo Fisher Scientific
CryoStar NX70	Thermo Fisher Scientific
Dissecting instruments	Everhards GmbH
DynaMag-2	Thermo Fisher Scientific
Feeding Needle, 22G, 37 mm	AgnTho's AB
Flow cytometer / cell sorter FACS Aria III	BD Biosciences
Flow cytometer FACS Celesta	BD Biosciences
Flow cytometer FACS LSR II	BD Biosciences
Flow cytometer FACSymphony A5	BD Biosciences
Fluorescent Microscope BZ-9000	Keyence
FLUOstar Omega	BMG Labtech
Heraeus Megafuge 40	Thermo Fisher Scientific
HiSeq 1500	Illumina
Isoflurane Vapor 19.3.	DRÄGER
Leica EG1150	Leica Biosystems
Leica TP1020	Leica Biosystems
Magnet MACS Multi Stand	Miltenyi Biotec
Maxi safe 2020	Thermo Fisher Scientific

Microplate reader Infinite M200	Tecan Austria GmbH
Mini-Protean Electrophoresis System	Bio-Rad Laboratories
MiniStar silverline	VWR
Model 50 Sonic Dismembrator	Thermo Fisher Scientific
Multipette M4	Eppendorf GmbH
Neubauer counting chamber	Superior Marienfeld
Pharmacia Pump P-1	Pharmacia
pH-meter S20-SevenEasy	Mettler Toledo
Pipette Controller Accu-Jet Plus	Brand GmbH
Pipette, Eppendorf Research plus set, single and multichannel	Eppendorf GmbH
PowerPac HC Power Supply	Bio-Rad Laboratories
QuadroMACS Separator (LS)	Miltenyi Biotec
Real-time PCR system LightCycler 480	Roche Diagnostics GmbH
Roller Mixer SRT9D	Stuart
Seahorse XFe96 Analyzer	Agilent Technologies
Shaking incubator	Stuart
Spectrophotometer NanoDrop 800	Thermo Fisher Scientific
Spectrophotometer NanoDrop 2000	Thermo Fisher Scientific
Sprout centrifuge	Heathrow Scientific
Sterile work bench	BDK
Thermocycler Biometra TAdvanced	Biometra
Thermocycler Biometra Trio	Biometra
Thermocycler T3000	Biometra
Thermomixer comfort	Eppendorf GmbH
Vaporizer	VetEquip
Vortex Mixer	Velp Scientifica
Water bath	Memmert GmbH

2.2. Disposables

Table 3: List of disposables used

Disposables	**Supplier**
20 gauge, 1 ½ needle	VWR
22 gauge, 1 ½ needle	VWR

27 gauge, ¾ needle	VWR
96-well LightCycler Platte and sealing foil	Sarstedt
BD Luer-Lok 1 ml syringe	VWR
Biopsy embedding cassettes	Roth
CELLSTAR Cell Culture Dishes, 10 cm	Greiner Bio-one
Cell strainer (70 or 100 µm)	Greiner Bio-one, Falcon, Sarstedt
CryoStar NX50 and NX70 Accessories	Thermo Fisher Scientific
Disposable culture tube, Soda-lime-glass	Duran Group
Falcon tubes, 15 ml	Sarstedt
Falcon tubes, 50 ml	Sarstedt
Flow cytometry tubes, 5ml	Sarstedt
Laboratory brushes	VWR
MACS LS columns	Miltenyi Biotec
Nitrocellulose-membrane Hybond-C Extra	GE healthcare
Omnican-F	Braun
Omnifix-F	Braun
PCR reaction tubes, 0.2 ml	Eppendorf GmbH
Pipette tips (10, 200 & 1,000 µl)	Sarstedt
Polystyrene Round Bottom tube, 5ml	Falcon
Pre-Separation Filters	Miltenyi Biotec
Reaction tubes, 0.5-2.0 ml	Eppendorf GmbH
Reagent reservoirs, 50 ml	Carl Roth
Seahorse XF96 Cell Culture Microplates	Agilent Technologies
Seahorse XF96 Sensor Cartridges	Agilent Technologies
Serological pipettes (2, 5, 10 & 25 ml)	Sarstedt
Staining dishes	Neolab Migge GmbH
Staining dish inserts	Neolab Migge GmbH
Stirrup-shaped blades, type 210	Carl Roth
Superfrost microscope slides	Carl Roth
Syringe (2, 5, 10 and 50 ml)	Braun
Tissue Culture-Plate, 6-well, suspension, flat	Sarstedt
Tissue Culture-Plate, 24-well, suspension, flat	Sarstedt

Tissue Culture-Plate, 48-well, suspension, flat	Sarstedt
Tissue Culture-Plate, 96-well, suspension, flat	Sarstedt
Tissue Culture-Plate, 96-well, suspension, round	Sarstedt
Three-way stopcock, Discofix C	VWR
Tissue processing/embedding cassettes	Merck
Ultra Disposable Microtome Blades	Thermo Fisher Scientific
Whatman Qualitative Filter Papers	GE Healthcare

2.3. Chemicals and Reagents

Table 4: List of reagents used

Reagent	Supplier
2-Desoxy-D-glucose (2DG)	Merck
6-Formylindolo(3,2-b)carbazole (FICZ)	Enzo Life Sciences
AccuCount Fluorescent Particles	Spherotech GmbH
Acetic acid	Carl Roth
Acrylamide/Bis Solution 29:1 (30%)	Bio-Rad Laboratories
Adjuvant, Complete H37 Ra	BD
Ammonium chloride	Merck
Ammonium persulfate	Merck
Antimycin A	Merck
BD Cytometer Setup and Tracking Beads	BD Biosciences
BD FACS Accudrop Beads	BD Biosciences
BD FACS Flow	BD Biosciences
Bovine serum albumin	Merck
Brefeldin A	Thermo Fisher Scientific
Brilliant Stain Buffer Plus	BD Biosciences
Carbonyl cyanide 4-(trifluoromethoxy) phenylhydrazone (FCCP)	Merck
Cell Proliferation Dye eFluor 670	Thermo Fisher Scientific
Cell Stimulation Cocktail	Thermo Fisher Scientific
Chloroform	AppliChem GmbH
Complete mini Protease Inhibitor cocktail tablets	Merck
CountBright Absolute Counting Beads	Thermo Fisher Scientific
Crystal violet	Merck

Deoxynucleotide triphosphates	Thermo Fisher Scientific
Dimethyl sulfoxide	Merck
Dithiothreitol	Thermo Fisher Scientific
Dulbecco's modified Eagle medium (DMEM)	PAA Laboratories GmbH
Dulbecco's Phosphate buffered saline (PBS) (1x)	Merck
Dulbecco's Phosphate buffered saline (PBS) (10x)	VWR
Embedding and mounting media, Entellan	VWR
Enhanced chemiluminescence Western Blotting reagents	Merck
Ethanol	Roth
Ethylenediaminetetraacetic acid (EDTA)	Merck
Fetal calf serum (FCS)	Merck
Forane (Isoflurane)	Baxter
Glucose	Thermo Fisher Scientific
GlutaMAX (100x)	Thermo Fisher Scientific
Glycine	Merck
Hanks' Balanced Salt Solution (HBSS) without calcium and magnesium	Thermo Fisher Scientific
HEPES	Merck
IGEPAL-CA -630	Merck
Iscove's modified Dulbecco's medium (IMDM) with L-glutamine	Thermo Fisher Scientific
Isopropanol	AppliChem GmbH
Ketamine (10%)	Medistar
L-glutamine	Thermo Fisher Scientific
Laemmli buffer for SDS-PAGE (10x)	SERVA Electrophoresis GmbH
Lithiumcarbonat	Carl Roth
Luxol Fast Blue, solvent blue 38, practical grade	Schubert und Weiss
Magnesium chloride (MgCl)	Thermo Fisher Scientific
Methanol	Carl Roth
MOG p35-55	Biotrend GmbH
Monensin	Thermo Fisher Scientific
Mouse T-Activator CD3/CD28 Dynabeads	Thermo Fisher Scientific

M. tuberculosis H37 Ra, desiccated	BD
N,N-Dimethylformamide (DMF)	Merck
N,N,N′,N′-Tetramethylethylenediamine (TEMED)	AppliChem GmbH
N-[Tris(hydroxymethyl)methyl]-3-aminopropanesulfonic acid (TAPS)	Merck
Non-essential amino-acids (100x)	Thermo Fisher Scientific
Nuclear fast red solution	Merck
NuPAGE LDS Sample Buffer (4x)	Thermo Fisher Scientific
NuPAGE Sample Reducing Agent (10x)	Thermo Fisher Scientific
OCT embedding cryoembedding Matrix	Thermo Fisher Scientific
Oligomycin	Merck
Olive oil	Merck
OneComp beads	Thermo Fisher Scientific
Paraformaldehyde (PFA) powder	Merck
Paraplast	Carl Roth
Penicillin/Streptomycin	Thermo Fisher Scientific
Percoll	VWR
Permeabilization Buffer (10x)	Thermo Fisher Scientific
Pertussis toxin from Bordetella pertussis	Merck
Pierce 16% Formaldehyde (w/v), Methanol-free	Thermo Fisher Scientific
Poly-L-lysine hydrobromide	Merck
Potassium hydrogen carbonate	Merck
QIAzol	Qiagen
Rotenone	Merck
RPMI cell culture medium (1640)	Thermo Fisher Scientific
Sodium dodecyl sulfate (SDS) solution (10%)	Thermo Fisher Scientific, AppliChem GmbH
Seahorse XF Calibrant solution	Agilent Technologies
Seahorse XF RPMI Medium pH 7.4	Agilent Technologies
SeeBlue Plus 2 standard	Thermo Fisher Scientific
Skim Milk powder	Merck
Sodium chloride (NaCl)	Merck
Sodium deoxycholate	Merck

Sodium hydroxide (NaOH)	Merck
Sodium pyruvate	Thermo Fisher Scientific
Solidofix Cryo spray	Carl Roth
Sucrose	MP Biomedicals
Tamoxifen	Merck
Tris	AppliChem GmbH
Tris-HCl	AppliChem GmbH
Triton-X 100	AppliChem GmbH
Trypan blue solution	Merck
Tween 20	AppliChem GmbH
UltraComp beads	Thermo Fisher Scientific
UltraPure DNase/RNase-Free Distilled Water	Thermo Fisher Scientific
Universal ProbeLibrary Set	Merck
Xylazine (2%)	Bayer Vital GmbH
Xylol	Carl Roth
(Z)-4-hydroxytamoxifen (4-OH tamoxifen)	Merck
β-Mercaptoethanol	AppliChem GmbH

2.4. Buffers and media

Table 5: List of buffers and media and their components

Buffer	**Component**
ATAC-seq lysis buffer	10 mM Tris-HCl, pH 7.4 10 mM NaCl 3 mM $MgCl_2$ 0.1% (V/V) IGEPAL CA-630 in H_2O
Cristal violet solution	0.05% (w/V) Crystal violet in H_2O
Ethanol (70%)	70% Ethanol in H_2O
Ethanol (80%)	80% Ethanol in H_2O
Ethanol (96%)	96% Ethanol in H_2O

FACS buffer	0.5% (w/V) Bovine serum albumin in PBS
Intestinal wash buffer I	5 mM Dithiothreitol 2% FCS 100 U/ml Penicillin 100 µg/ml Streptomycin in HBSS
Intestinal wash buffer II	5 mM EDTA 2% FCS 100 U/ml Penicillin 100 µg/ml Streptomycin in HBSS
Intestinal wash buffer III	10 mM HEPES 100 U/ml Penicillin 100 µg/ml Streptomycin in HBSS
Laemmli running buffer (1x)	1x 10x Laemmli Running Buffer in H_2O
Lithiumcarbonat solution	0.05% (w/V) Lithiumcarbonat in H_2O
Luxol fast blue solution	0.95% (w/V) Solvent blue 38 90% Ethanol 0.47% Acetic acid in H_2O
MACS buffer	0.5% (w/V) Bovine serum albumin 2 mM EDTA in PBS
Methanol (90%)	90% Methanol in H_2O
PBST	0.1% (V/V) Tween-20 in PBS
Permeabilization buffer (1x)	1x 10x Permeabilization buffer in H_2O

PFA w/o methanol (3%)	18.75% (V/V) Pierce 16% Formaldehyde, methanol-free in PBS
PFA (4%)	4% (w/V) PFA in PBS, pH adjusted to 6.9
Poly-L-lysine hydrobromide (10%)	10% (w/V) Poly-L-lysine hydrobromide in H_2O
Red blood cell lysis (RBCL) buffer	155 mM Ammonium chloride 10 mM Potassium hydrogen carbonate 0.1 mM EDTA 0.5% (w/V) SDS in H_2O, pH adjusted to 7.2-7.4
RIPA buffer	10 mM Tris HCl, pH 8.0 1 mM EDTA 140 mM NaCl 1% (V/V) Triton-X 100 0.1% (w/V) SDS 0.1% (w/V) sodium deoxycholate in H_2O
Seahorse medium	Seahorse XF RPMI Medium 2 mM L-glutamine 1 mM Sodium pyruvate 10 mM Glucose pH adjusted to 7.4
Seahorse medium w/o glucose	Seahorse XF RPMI Medium 2 mM L-glutamine 1 mM Sodium pyruvate pH adjusted to 7.4
Sucrose (30%)	30% (w/V) Sucrose in PBS
Tagmentation buffer (5x)	10 mM TAPS-NaOH, pH 8.5 5 mM $MgCl_2$ 10% N,N-Dimethylformamide in H_2O

T cell medium	IMDM with L-Glutamine 10% FCS 1% GlutaMAX (100x) 55 µM β-Mercaptoethanol 0.5 mM Sodium pyruvate 1% Non-essential amino-acids (100x) 5 mM HEPES 100 U/ml Penicillin 100 µg/ml Streptomycin
Wet blot buffer (1x)	1x 10x Wet blot buffer 20% Methanol in H_2O
Wet blot buffer (10x)	250 mM Tris Base 1.92 M glycine in H_2O

2.5. Cytokines

Table 6: List of cytokines used

Cytokine	Supplier
rm IL-1β	PeproTech
rh IL-2	Chiron
rm IL-4	ImmunoTools GmbH
rm IL-6	ImmunoTools GmbH
rm IL-12	PeproTech
rh IL-23	PeproTech
rh TGF-ß1	PeproTech
rh TGF-ß3	PeproTech

2.6. Antibodies and tetramers

Table 7: List of antibodies used for flow cytometric analysis

Epitope	Clone	Supplier	Dilution
CD3	17A2	Biolegend	1:200
CD4	RM4-5	Biolegend	1:200
CD11b	M1/70	Biolegend	1:400
CD16/32	93	Biolegend	1:300

CD25	PC61	Biolegend	1:200
CD44	IM7	Biolegend	1:200
CD45	30-F11	Biolegend	1:200
CD62L	MEL-14	Thermo Fisher Scientific	1:200
Foxp3	FJK-16s	Thermo Fisher Scientific	1:100
Gata3	L50-823	BD Biosciences	1:30
GM-CSF	MP1-22E9	Biolegend	1:100
IFN-γ	XMG1.2	Thermo Fisher Scientific	1:200
IL-2	KES6-5H4	Thermo Fisher Scientific	1:100
IL-4	11B11	Thermo Fisher Scientific	1:200
IL-6Rα	D7715A7	Thermo Fisher Scientific	1:200
IL-9	RM9A4	Biolegend	1:200
IL-10	JES5-16E3	Biolegend	1:100
IL-17	eBio17B7	Thermo Fisher Scientific	1:100
Ki-67	SolA15	Thermo Fisher Scientific	1:200
Ly6G	1A8	Thermo Fisher Scientific	1:200
pStat1 (Y701)	4a	BD Biosciences	1:10
pStat3 (Tyr705)	LUVNKLA	Thermo Fisher Scientific	1:20
pStat5 (Y694)	SRBCZX	Thermo Fisher Scientific	1:20
RORγt	AFKJS-9	Thermo Fisher Scientific	1:40
Satb1	14/SATB1	BD Biosciences	1:100

T-bet	eBio4B10	Thermo Fisher Scientific	1:40
TNF-α	MP6-XT22	Biolegend	1:200

Table 8: List of tetramers used

Tetramer	Epitope	Manufacturer
$MOG_{38–49}$/I-A^b	GWYRSPFSRVVH	NIH tetramer core facility
$CLIP_{87-101}$/I-A^b	PVSKMRMATPLLMQA	NIH tetramer core facility

Table 9: List of antibodies used in western blot analysis

Epitope	Clone	Manufacturer	Dilution
Mouse IgG-HRP	GENXA931	Merck	1:5000
Rabbit IgG-HRP	GENA9340	Merck	1:5000
Satb1	EPR3951	Abcam	1:5000
ß-actin	C4	Merck	1:5000

Table 10: List of antibodies used during *in vitro* culture

Epitope	Clone	Manufacturer	Final concentration
anti-INF-γ	R4-6A2	Biolegend	2 µg/ml or 10 µg/ml
anti-IL-2	JES6-1A12	Biolegend	10 µg/ml
anti-IL-4	11B11	Biolegend	2 µg/ml or 10 µg/ml
CD3	145-2C11	Biolegend	0.25 µg/ml or 5 µg/ml
CD25	PC61	Biolegend	10 µg/ml
CD28	37.51	Biolegend	1 µg/ml
Hamster IgG	polyclonal	MP Biomedicals	50 µg/ml

Table 11: List of antibodies used for immunohistochemical staining

Epitope	Clone	Manufacturer	Final concentration
CD3	CD3-12	Bio-Rad Laboratories	1:200
MAC3	M3/84	BD Biosciences	1:200

2.7. Enzymes

Table 12: List of enzymes used

Enzyme	Supplier
Collagenase Type IV	Merck
DNaseI	Merck
DNaseI, grade II	Merck
Liberase Research Grade	Merck
LightCycler 480 Probe Master	Roche Diagnostics GmbH
NEBNext High-Fidelity 2x PCR Master Mix	NEB
Protector RNase Inhibitor	Merck
SuperScript II Reverse Transcriptase	Thermo Fisher Scientific
Tn5 Transposase	In-house, generated by the group of M. Geyer according to Picelli et al., 2014
Transcriptor Reverse Transcriptase	Merck

2.8. Kits

Table 13: List of kits used

Kit	Supplier
Direct-zol-96 RNA	Zymo research
Foxp3/Transcription Factor Staining Buffer Kit	Thermo Fisher Scientific
High Sensitivity DNA Analysis Kit	Agilent Technologies
LIVE/DEAD Fixable Near-Infra Red Dead Cell Stain Kit	Thermo Fisher Scientific
MagniSort Mouse CD4 T cell enrichment Kit	Thermo Fisher Scientific
miRNeasy Micro Kit	Qiagen
Pierce bicinchoninic acid assay (BCA) Protein Assay Kit	Thermo Fisher Scientific
Qiagen MinElute Kit	Qiagen
Transcriptor First Strand cDNA Synthesis Kit	Merck
TruSeq RNA Library Preparation Kit v2	Illumina
TruSeq Rapid SBS Kit	Illumina
TruSeq Rapid Cluster kit	Illumina

2.9. Oligonucleotides

Oligonucleotides were produced as desalted oligonucleotides by either Sigma Aldrich or IDT.

Table 14: List of qRT-PCR primers used

Target	strand	Sequence 5'-3'	Probe #
Ahr	forward	TGCACAAGGAGTGGACGA	27
	reverse	AGGAAGCTGGTCTGGGGTAT	
Batf	forward	AGAAAGCCGACACCCTTCA	85
	reverse	CGGAGAGCTGCGTTCTGT	
Cd25	forward	TGTGCTCACAATGGAGTATAA	4
	reverse	CTCAGGAGGAGGATGCTGAT	
Dusp6	forward	TAGCAGCGACTGGAATGAGA	22
	reverse	CGGCCTGGAACTTACTGAAG	
Ets2	forward	CTGTTCCATCAGCCAGGACT	3
	reverse	TCTGGAGAGTCGTGGTCCTT	
Fas	forward	GCAGACATGCTGTGGATCTG	34
	reverse	TCGGAGATGCTATTAGTACCTTGAG	
Ifng	forward	ATCTGGAGGAACTGGCAAAA	21
	reverse	TTCAAGACTTCAAAGAGTCTGAGGTA	
Ikzf4	forward	TCCACCCCACAGAAGTTTGTA	41
	reverse	GGCATTCACATCATAGGGAAG	
Il1r1	forward	TTGACATAGTGCTTTGGTACAGG	15
	reverse	TCGTATGTCTTTCCATCTGAAGC	
Il2	forward	GCTGTTGATGGACCTACAGGA	15
	reverse	TTCAATTCTGTGGCCTGCTT-	
Il10	forward	CAGAGCCACATGCTCCTAGA	41
	reverse	GTCCAGCTGGTCCTTTGTTT	
Il17a	forward	CAGGGAGAGCTTCATCTGTG	74
	reverse	GCTGAGCTTTGAGGGATGAT	
Il17f	forward	CCCAGGAAGACATACTTAGAAGAAA	46
	reverse	CAACAGTAGCAAAGACTTGACCA	
Il21	forward	GACATTCATCATTGACCTCGTG	27
	reverse	TCACAGGAAGGGCATTTAGC	
Il22	forward	GCAAGCTTGAGGTGTCCAAC	46

	reverse	AGCCGGACATCTGTGTTGTT	
Il23	forward	TCCCTACTAGGACTCAGCCAAC	19
	reverse	AGAACTCAGGCTGGGCATC	
Irf1	forward	CCTGGGTCAGGACTTGGATA	67
	reverse	GAGACTGCTGCTGACGACAC	
Irf4	forward	GGAGTTTCCAGACCCTCAGA	6
	reverse	CTGGCTAGCAGAGGTTCCAC	
Maf	forward	CCTTCCTCTCCCGAATTTTT	33
	reverse	CCACGGAGCATTTAACAAGG	
Pten	forward	AGGCACAAGAGGCCCTAGAT	60
	reverse	CTGACTGGGAATTGTGACTCC	
Rorc	forward	TCCCACATCTCCCACATTG	6
	reverse	TCCCACATCTCCCACATTG	
Runx	forward	CTCCGTGCTACCCACTCACT	77
	reverse	ATGACGGTGACCAGAGTGC	
Satb1	forward	TTAATGCCTCCATTTATGATGAGA	18
	reverse	ACAGCTCACACAGCCATCC	
Socs1	forward	CGTCCTCGTCTTCGTCCTC	45
	reverse	GAAGGTGCGGAAGTGAGTGT	
Socs3	forward	ATTTCGCTTCGGGACTAGC	83
	reverse	AACTTGCTGTGGGTGACCAT	
Sp4	forward	CAGGGAGTTCCAGTAACAATCA	58
	reverse	CAGGAGCTATAGTAGCTTGTTGGA	
Tbx21	forward	CAACCAGCACCAGACAGAGA	19
	reverse	ACAAACATCCTGTAATGGCTTG	
Tgfb1	forward	TGGAGCAACATGTGGAACTC	72
	reverse	CAGCAGCCGGTTACCAAG	
Tnfa	forward	TCTTCTCATTCCTGCTTGTGG	49
	reverse	GGTCTGGGCCATAGAACTGA	
β-actin	forward	CTAAGGCCAACCGTGAAAAG	64
	reverse	ACCAGAGGCATACAGGGACA	

Table 15: List of primers used for ATAC-seq

Name	Sequence 5'-3'
Ad1_noMX	AATGATACGGCGACCACCGAGATCTACACTCGTCGGCAGCGTCAGATGTG
Ad2.1_TAAGGCGA	CAAGCAGAAGACGGCATACGAGATTCGCCTTAGTCTCGTGGGCTCGGAGATGT
Ad2.3_AGGCAGAA	CAAGCAGAAGACGGCATACGAGATTTCTGCCTGTCTCGTGGGCTCGGAGATGT
Ad2.4_TCCTGAGC	CAAGCAGAAGACGGCATACGAGATGCTCAGGAGTCTCGTGGGCTCGGAGATGT
Ad2.8_CAGAGAGG	CAAGCAGAAGACGGCATACGAGATCCTCTCTGGTCTCGTGGGCTCGGAGATGT
Ad2.9_GCTACGCT	CAAGCAGAAGACGGCATACGAGATAGCGTAGCGTCTCGTGGGCTCGGAGATGT
Ad2.10_CGAGGCTG	CAAGCAGAAGACGGCATACGAGATCAGCCTCGGTCTCGTGGGCTCGGAGATGT
Ad2.13_GTCGTGAT	CAAGCAGAAGACGGCATACGAGATATCACGACGTCTCGTGGGCTCGGAGATGT
Ad2.14_ACCACTGT	CAAGCAGAAGACGGCATACGAGATACAGTGGTGTCTCGTGGGCTCGGAGATGT
Ad2.15_TGGATCTG	CAAGCAGAAGACGGCATACGAGATCAGATCCAGTCTCGTGGGCTCGGAGATGT
Ad2.16_CCGTTTGT	CAAGCAGAAGACGGCATACGAGATACAAACGGGTCTCGTGGGCTCGGAGATGT

2.10.Mouse Lines

Table 16: List of mouse lines

Mouse Line	References	Appendix
Wildtype		
$Rag2^{-/-}$	Shinkai, 1992	Figure 66f
R26-STOP-Satb1/CD4-Cre	Lee et al., 2001; Sommer, 2018	Figure 66c,d
R26-STOP-Satb1/CD4-Cre/Foxp3RFP	Lee et al., 2001; Sommer, 2018; Wan and Flavell, 2005	Figure 66c,d,e

Satb1$^{fl/fl}$/ CD4-Cre	Lee et al., 2001; Sommer et al., 2014	Figure 66a,d
Satb1$^{fl/fl}$/CD4-CreERT2	Śledzińska et al., 2013; Sommer et al., 2014	Figure 66a,b

2.11.Software

Table 17: List of software used

Software	Developer
Adobe Illustrator CS5.1	Adobe
Agilent TapeStation Controller Software, A.02.02	Agilent Technologies
CorelDRAW, Version 19.1.0.419	Corel Corporation
BD FACSDiva	BD Biosciences
FlowJo, Version 7.6.5 - 10.6.1	FlowJo, LLC
GraphPad Prism, Version 6-8	Graph Pad Software
i-control 1.12	Tecan
Illumina Sequencing Analysis Viewer 1.8.4	Illumina
Image Lab software. Version5.2.1 built11	Bio-Rad Laboratories
LightCycler 480 Software, Version 1.5.0.39	Idaho Technology, Inc
Mendeley	Mendeley
R, version 3.5.3	R studio
Seahorse Wave Software, version 2.6.0	Agilent Technologies
TapeStation Analysis Software, A02.02	Agilent Technologies

3. Methods

3.1. Mice housing and handling

All animal experiments were approved by the Local Animal Care Commission of North Rhine-Westphalia (AZ 84-02.04.2013.A248 and AZ 84-02.04.2016.A370). Experiments were performed according to the guidelines for laboratory animal care as elucidated by the NIH (NIH, 2011) following German legislations. Mice were housed under specific pathogen-free conditions in the animal facilities of the University of Bonn or of the German Center for Neurodegeneration in Bonn. Mice were crossed to a C57BL/6JRcc background. Unless otherwise denoted, mice were used for experiments between nine weeks and four months of age and cohorts were age and sex matched. For Satb1-overexpressing experiments the following genotypes were used: R26-STOP-Satb1$^{wt/+}$/CD4-Cre$^{wt/+}$, R26-STOP-Satb1$^{+/+}$/CD4-Cre$^{wt/+}$/ Foxp3RFP$^{Y/+}$ or R26-STOP-Satb1$^{+/+}$/CD4-Cre$^{wt/+}$/Foxp3RFP$^{+/+}$ as KI mice or R26-STOP-Satb1$^{wt/+}$/CD4-Cre$^{wt/wt}$, R26-STOP-Satb1$^{+/+}$/CD4-Cre$^{wt/wt}$/Foxp3RFP$^{Y/+}$ and R26-STOP-Satb1$^{+/+}$/CD4-Cre$^{wt/wt}$/ Foxp3RFP$^{+/+}$ as WT control. Unless otherwise denoted Satb1$^{fl/fl}$/CD4-CreERT2$^{wt/+}$ mice were used for conditional deletion of Satb1. Mice were either treated with tamoxifen (KO) or oil as control (WT). In addition the influence of long term deletion of Satb1 was studied in 44-60 weeks old Satb1$^{fl/fl}$/CD4-Cre$^{wt/+}$ mice and Satb1$^{fl/fl}$/CD4-Cre$^{wt/wt}$ as control. Experimental autoimmune encephalomyelitis (EAE) was induced in 14 weeks old female Satb1$^{fl/fl}$/CD4-CreERT2$^{+/wt}$ or Satb1$^{fl/fl}$/CD4-CreERT2$^{wt/wt}$ mice. Both cohorts were treated with tamoxifen. For adoptive transfer colitis male Rag2$^{-/-}$ mice were used.

3.2. Isolation of murine cells

3.2.1. Isolation of cells from the spleen

Mice were sacrificed by cervical dislocation and the spleen was removed. For lymphocyte isolation, the spleen was homogenized in PBS and filtered through a 70 or 100 µm cell strainer. Cells were centrifuged at 400 g for 5 minutes (min) and the cell pellet was resuspended in 1 ml of RBCL buffer. RBCL was performed while shaking gently for 2 min at room temperature (RT). Lysis was stopped with PBS and the cell suspension was filtered through a 70 or 100 µm cell strainer. Subsequently, cells were centrifuged and directly used for subsequent experiments.

For the isolation of myeloid cells, the spleen was cut into small pieces and transferred into a 6-well plate in 3 ml RPMI supplemented with 0.5 mg/ml Collagenase Type IV and 50 µg/ml DNaseI. The digestion was performed at 37°C for 45 min while shaking at 90 rpm. After the

digestion, any remaining fragments were homogenized and the resulting cell suspension was filtered through a 70 or 100 µm cell strainer and centrifuged for 400 g for 5 min. Afterwards, RBLC and subsequent steps were conducted as described above.

3.2.2. Isolation of cells from LN

Mice were sacrificed by cervical dislocation and mesenteric, inguinal, axillary, brachial or cervical LN were isolated according to the experimental setup. LN were homogenized in PBS and filtered through a 70 or 100 µm cell strainer. Cells were centrifuged at 400 g for 5 min, washed once in PBS and used for subsequent experiments.

3.2.3. Isolation of cells from the central nervous system (CNS)

Mice were anesthetized with 100 mg/kg bodyweight ketamine and 20 mg/kg bodyweight xylazine and perfused with 20 ml cold PBS through the left ventricle according to animal license AZ 84-02.04.2016.A370. Cells were isolated form the CNS as described previously (Poppensieker et al., 2012). Brain and spinal cord were excised, cut into small pieces and further homogenized using a 22 gauge needle. The tissue was digested at 37°C in 5 ml DMEM supplemented with 10% FCS and 200 µg/ml Collagenase Type IV for 45 min followed by digestion with 170 µg/ml DNaseI for 45 min while shaking at 90 rpm. The cell suspension was passed through a 100 µm cell strainer and washed once in DMEM. Cells were resuspended in 5 ml 70% percoll, overlayed with 5 ml 30% percoll and centrifuged at 900 g for 20 min at RT with the brake disengaged. Myelin was removed and the cell-containing interphase was collected. Cells were washed once in PBS and used for subsequent experiments.

3.2.4. Isolation of cells from the intestinal lamina propria

Immune cells from the lamina propria were isolated as described previously (Brandstätter et al., 2016). Mice were sacrificed by cervical dislocation and the colon and small intestine (SI) were excised. The intestinal content was flushed out with PBS and fat and Peyer's patches were removed. The intestine was cut open longitudinally, rinsed in PBS and cut into small pieces. Subsequently, the mucosa and epithelial cells were removed. For mucosal removal, the SI or colon were incubated for 20 min at 37°C while shaking at 200 rpm in 20 ml or 10 ml of intestinal wash buffer I, respectively. To remove the epithelial cells, three washes each for 15 min at 37°C, 200 rpm were performed in 15 ml intestinal wash buffer II for the SI or 7.5 ml for the colon. Afterwards, the tissue was washed in 10 ml intestinal wash buffer III for 10 min at 37°C, 200 rpm to remove EDTA and FCS. The tissue was then minced and digested

for 45 min at 37°C under slow rotation in 7 ml intestinal wash buffer III supplemented with 0.2 U/ml Liberase and 200 U/ml DNaseI, grade II. Digestion was stopped with 3.5 ml MACS buffer and the cell suspension was filtered through a 70 µm cell strainer. Cells were washed twice with HBSS containing 2% FCS and immediately used for subsequent experiments.

3.2.5. Magnetic enrichment of $CD4^+$ T cells

$CD4^+$ T cells were enriched by negative selection by magnetic activated cell sorting (MACS) using the MagniSort Mouse CD4 T cell enrichment Kit. Splenocytes and cells from LN were isolated as described above and pooled. Absolute cell numbers were determined using a Neubauer counting chamber and cells were resuspended in 100 µl MACS buffer and 3.4 µl antibody cocktail per $1x10^7$ cells. Cells were incubated for 10 min at RT with an antibody cocktail containing biotinylated antibodies against B cell, $CD8^+$ T cell, myeloid cell, γ/δ T cell, NKT cell and erythroid cell antigens. Next, cells were washed once with MACS buffer, resuspended in 100 µl MACS buffer and 2 µl streptavidin-coated magnetic beads per $1x10^7$ cells and incubated for 5 min at RT. The cell suspension was passed through a 30 µm pre-separation filter and loaded onto a LS column equilibrated with MACS buffer, which was attached to a MACS multi stand magnet and QuadroMACS Separator. The column was washed once with 3 ml of MACS buffer and both flow throughs, which contained the enriched $CD4^+$ T cells, were collected and pooled.

3.3. Antibody staining for flow cytometry and flow cytometric analysis

For all stainings, Fc receptor-blocking reagent, i.e. CD16/CD32-blocking antibodies, was added at a final dilution of 1:300.

3.3.1. Extracellular staining

Cells were stained with antibodies against surface antigens in a round bottom 96-well plate. An antibody cocktail containing fluorochrome-coupled antibodies in a final dilution of 1:50-1:400 each (Table 7) was added to the cells resulting in a final volume of 50 µl. If exclusion of dead cells was required for instance when isolating cells from non-lymphatic organs, near-infra-red fixable dead cell staining dye was added at a final concentration of 1:1000. Furthermore, if brilliant ultraviolet fluorochrome-coupled antibodies were used 10 µl Brilliant Stain Buffer Plus was added according to the manufacturer's protocol. Surface staining was performed at 4°C for 20 min in the dark. Cells were washed with PBS, centrifuged at 400 g for 5 min and either fixed for subsequent intracellular staining,

resuspended in T cell medium for cytokine analysis or resuspended in PBS for direct flow cytometric acquisition.

3.3.2. Sorting of naive and effector $CD4^+$ T cells

For sorting, enriched $CD4^+$ T cells were resuspended in 100 µl PBS per 2.5 x 10^6 cells and surface staining was performed as described above only in a higher final volume. After washing with PBS, cells were resuspended in T cell medium and $CD3^+CD4^+CD44^-CD62L^+CD25^-$ naive T cells and $CD3^+CD4^+CD44^+CD62L^-CD25^-$ effector/memory T cells were sorted using a BD FACS Aria III cell sorter. Only cells with a purity of greater than 98% were used for subsequent experiments.

3.3.3. Intracellular cytokine staining

After surface staining, cells were stimulated for 4 hours at 37°C with cell stimulation cocktail at a final concentration of 1:500 in the presence of Brefeldin A and Monensin both at a final concentration of 1:1000 in T cell medium. As unstimulated controls, some cells were treated with Brefeldin A and Monensin only. Subsequently, cells were washed with PBS, transferred to round bottom 96-well plates and live/dead staining was performed as described above. Cells were washed in PBS and incubated in 200 µl 4% PFA for 10 min on ice in the dark. Cells were centrifuged at 400 g for 5 min and washed twice in 1x permeabilization buffer. After permeabilization, centrifugation was performed at 700 g for 2 min. After washing, cytokine staining was performed in a final volume of 50 µl 1x permeabilization buffer with a final antibody dilution of 1:100-1:200 each (Table 7) for 30 min at RT in the dark. Cells were washed once in 1x permeabilization buffer and once in PBS and either fixed for subsequent transcription factor staining or resuspended in PBS for direct flow cytometric acquisition.

3.3.4. Transcription factor staining

Transcription factor staining was performed in a round bottom 96-well plate using the Foxp3/Transcription Factor Staining Buffer Kit according to the manufacturer's instruction.

3.3.5. MOG tetramer staining

Tetramer staining was conducted prior to surface staining. Cells were transferred to a round bottom 96-well plate and incubated with 20 µg/ml $MOG_{38–49}$/I-A^b fluorochrome-coupled tetramer for three hours at 37°C in 200 µl RPMI supplemented with 10% FCS. Cells were washed with PBS and stained for extracellular antigens and dead cells as described above.

3.3.6. pStat staining

To stain phosphorylated Stat (pStat) proteins, cells were collected directly after sorting of naive $CD4^+$ T cells or after culture in T_H17 cell-skewing conditions. Cells were transferred to FACS tubes and fixed in 1ml 3% methanol-free PFA for 10 min at 37°C in the dark. Cells were incubated for 60 sec on ice and subsequently centrifuged at 1500 rpm for 5 min. PFA was removed completely and cells were permeabilized in 2 ml cold 90% methanol overnight at -20°C. Cells were washed with FACS buffer and transferred to a round bottom 96-well plate and stained with fluorochrome-labeled antibodies against phosphorylated Stat proteins in a final dilution of 1:10-1:20 (Table 7) in 50 µl FACS Buffer for one hour at RT. Cells were washed with FACS buffer and resuspended in PBS for direct flow cytometric acquisition.

3.3.7. Flow cytometric analysis

Samples were acquired on a flow cytometer (BD Celesta, LSR II, Symphony A5 or Aria III), and data were analyzed using Flow Jo versions 7.6.5 to 10.6.1. To analyze cell division, the proliferation modeling tool of Flow Jo version 10.6.1 was used.

3.3.8. Quantification of cell numbers by flow cytometry

Absolute cell numbers were assessed by adding CountBright Absolute Counting Beads or AccuCount Fluorescent Particles to the cell suspension after cell isolation. During flow cytometric analysis, absolute cell numbers were calculated based on the following formula:

$$\text{absolute cell number} = \frac{\text{number of aqcuired cells} * \text{absolute number of beads added}}{\text{number of acquired beads}}$$

3.4. *In vitro* assays

Cells were culture in T cell medium at 37°C and 5% CO_2.

3.4.1. T_H cell differentiation

Differentiation of naive $CD4^+$ T cells into the different T_H subsets was mainly conducted as previously described (Ciofani et al., 2012). One day or at least 5 hours before start of cell cultures, wells of a flat-bottom 96-well plate or flat-bottom 48-well plate were coated with anti-hamster IgG at a final concentration of 50 µg/ml in PBS at 37°C. Wells were washed twice with PBS and $1x10^5$ or $4x10^5$ naive $CD4^+$ T cells were cultivated per well in a 96- or 48-well plate, respectively, in the presence of the following cytokine and antibody cocktails (Table 18):

Table 18: Differentiation cocktails for T_H subtypes

T_H subtypes	**Cytokines and antibodies**
T_H0	0.25 µg/ml CD3 antibodies 1 µg/ml CD28 antibodies 2 µg/ml anti-IL-4 2 µg/ml anti-IFN-γ
T_H1	0.25 µg/ml CD3 antibodies 1 µg/ml CD28 antibodies 2 µg/ml anti-IL-4 10 ng/ml rm IL-12
T_H2	0.25 µg/ml CD3 antibodies 1 µg/ml CD28 antibodies 2 µg/ml anti-IFN-γ 10 ng/ml rmIL-4
T_H9	0.25 µg/ml CD3 antibodies 1 µg/ml CD28 antibodies 2 µg/ml anti-IFN-γ 10 ng/ml rm IL-4 5 ng/ml rh TGF-ß1
T_H17	0.25 µg/ml CD3 antibodies 1 µg/ml CD28 antibodies 2 µg/ml anti-IL-4 2 µg/ml anti-IFN-γ 0.3 ng/ml rh TGF-ß1 20 ng/ml rm IL-6
iTreg	0.25 µg/ml CD3 antibodies 1 µg/ml CD28 antibodies 2 µg/ml anti-IL-4 2 µg/ml anti-IFN-γ 2 ng/ml rh TGF-ß1 100 U/ml rh IL-2

pathogenic T_H17	1 µg/ml CD28 antibodies 2 µg/ml anti-IL-4 2 ng/ml rh TGF-ß3 25 ng/ml rm IL-6 20 ng/ml rh IL-23 20 ng/ml rm IL-1β 300 nM FICZ 100 U/ml rh IL-2

When T_H0, T_H1, T_H2 and T_H9 cells were cultured for more than three days, cells were transferred on day two to a round bottom 96-well plate and rested without TCR stimulation in the presence of IL-2 at a final concentration of 100 U/ml. On day four, T_H0, T_H1, T_H2 and T_H9 cells were transferred to wells pre-coated with anti-hamster IgG and restimulated for one day under the corresponding T_H subset-skewing conditions as described above. T_H17 and iTreg cells were continuously cultured with stimulation until day five.

If cells were differentiated without IgG crosslinking, wells were coated with 5 µg/ml CD3 antibodies at 4°C overnight and soluble CD3 antibodies were not added to the cytokine/antibody cocktail.

For restimulation experiments, T_H17 cells were cultured for five days. Subsequently, cells were transferred to a round bottom 96-well plate for two days in the presence of (Z) 4-hydroxytamoxifen (4-OH tamoxifen) without TCR stimulation and cytokine supplement. On day 7, cells were transferred to wells pre-coated with anti-hamster IgG and restimulated for two days in T_H17 cell-polarizing conditions as described above.

For T_H1-T_H17 cell-skewing experiments, cells were differentiated in CD3 antibody-coated wells under T_H1 cell-polarizing conditions for two days, followed by three days stimulation in presence of a pathogenic T_H17 cell-polarizing cocktail. Cytokine expression was analyzed on day five.

Blocking of IL-2 and IL-2 signaling during T_H17 cell culture was performed as previously described (Fujimura et al., 2013). Cells were cultured in wells coated with CD3 antibodies in the presence of CD28 (1 µg/ml), anti-IL-4 (10 µg/ml) and anti-IFN-γ antibodies (10 µg/ml), TGF-ß1 (5 ng/ml) and rm IL-6 (20 ng/ml) as well as anti-IL-2 (10 µg/ml) and CD25 antibodies (10 µg/ml) for five days.

3.4.2. Tamoxifen treatment

To delete Satb1 *in vitro*, T cells from Satb1$^{fl/fl}$/CD4-CreERT2$^{wt/+}$ animals were treated with 1 µM 4-OH tamoxifen, which was previously solved in EtOH, during the *in vitro* cell culture. As wildtype control, cells were treated with EtOH at the same final concentration.

3.4.3. Analysis of metabolic parameters

Real-time metabolic parameters were measured using a Seahorse XFe96 Analyzer. Prior to metabolic challenges, the Seahorse XF96 sensor cartridge was hydrated in Seahorse XF Calibrant solution overnight at 37°C without controlled CO_2 concentrations. One hour before cell seeding, Seahorse XF96 cell culture microplates were coated with 100 µg/ml poly-L-lysine hydrobromide for one hour at RT. Subsequently, wells were washed with H_2O and air-dried. For characterization of freshly isolated $CD4^+$ T cells, cells were isolated by MACS and $3x10^5$ cells were plated per well, centrifuged at 200 g for one min and overlaid with a final volume of 175 µl Seahorse medium. Cells were incubated at 37°C for one hour without controlled CO_2 concentration. Subsequently, the ports of the sensor cartridge were loaded with CD3 and CD28 antibodies. Cells as well as the sensor cartridge were loaded in the Seahorse XFe96 Analyzer. Basal extracellular acidification rate (ECAR) was assessed four times with each measurement period including three min mixing and 5 min measuring. Subsequently, CD3 antibodies in a final concentration of 3 µg/ml and CD28 antibodies in a final concentration of 1 µg/ml were injected. As control, only Seahorse medium was injected. Upon stimulation, ECAR was measured 19 times.

For the analysis of the metabolic state of T_H17 cells, cells cultured for three days under T_H17 cell-skewing conditions were collected and $1x10^5$ cells were plated per well. Seahorse sensor cartridge calibration and cell culture microplate coating were prepared as described above. Four baseline measurements of the ECAR and the oxygen consumption rate (OCR) were performed prior to metabolic challenges. Measurement was performed as described above. For challenges of mitochondria, cells were stimulated with 1 µM oligomycin followed by stimulation with 4 µM FCCP and a subsequent incubation with a mixture of 0.5 µM rotenone and 0.5 µM antimycin A. During each stimulation period, four measurement cycles were performed. To analyze the response to glucose stimulation, cells were seeded in glucose-free Seahorse medium. After 4 baseline measurements, cells were stimulated with 10 mM glucose, followed by a treatment with 1 µM oligomycin and 100 mM 2DG. During each stimulation period, four measurement cycles were performed. After each Seahorse run, cells were centrifuged at 400 g for 5 min and stored at -20°C.

For normalization, crystal violet staining was performed. Cells were thawed and protein was fixed in 100 µl 4% PFA for 5 min at RT. Samples were centrifuged and incubated in 100 µl 0.05% crystal violet solution for 30 min at RT. Samples were washed twice with H_2O and subsequently air-dried. Samples were resuspended in 200 µl methanol and absorbance was measured at 590 nm using the microplate reader Infinite M200.

3.4.4. Proliferation assays

To analyze T cell proliferation, $CD4^+$ T cells were labeled with 5 µM cell proliferation dye eFluor670 for 10 min at 37°C according to the manufacturer's protocol. The staining was stopped with FCS and cells were rested on ice for 5 min. Cells were washed three times in T cell medium and $1x10^5$ cells per well were stimulated with $0.34x10^5$ mouse T-Activator CD3/CD28 Dynabeads. Beads were previously washed three times in T cell medium. Cells were cultured for three days and eFluor670 dilution, which reflects T cell proliferation, was measured by flow cytometry.

3.5. *In vivo* assays

3.5.1. Tamoxifen administration

Administration of tamoxifen was approved by the relevant authorities under AZ 84-02.04.2013.A248 and AZ 84-02.04.2016.A370. Tamoxifen was dissolved at 55°C in olive oil at a final concentration of 40 mg/ml. To induce Cre-mediated recombination, 8 mg tamoxifen were administered to $Satb1^{fl/fl}$/CD4-$CreERT2^{wt/+}$ animals by oral gavage on day 0 and on day three. For naive or effector/memory T cell isolation, control mice received olive oil instead of tamoxifen. For EAE experiments, female $Satb1^{fl/fl}$/CD4-$CreERT2^{wt/wt}$ animals were used as control and mice received tamoxifen similar to $Satb1^{fl/fl}$/CD4-$CreERT2^{wt/+}$ animals. Mice were either scarified for cell isolation or EAE was induced seven days after initial tamoxifen administration.

3.5.2. Induction of and analysis of EAE

The induction of EAE was approved by the relevant authorities under AZ 84-02.04.2016.A370. EAE was induced by active immunization of mice with myelin oligodendrocyte glycoprotein (MOG) 35-55 peptide (MOG_{35-55}) and complete Freund's adjuvant followed by opening of the blood brain barrier with pertussis toxin as described previously (Poppensieker et al., 2012). MOG_{35-55} was dissolved at a final concentration of 1 µg/µl in PBS with 1% dimethyl sulfoxide and emulsified 1:1 with complete Freund's adjuvant supplemented with 10 mg/ml Mycobacterium tuberculosis H37RA. Mice were

anesthetized with 2.5-3.5% isoflurane and the emulsion with a final amount of 50 µg of MOG_{35-55} was injected subcutaneously at the tail base. Subsequently, mice received 200 ng pertussis toxin diluted in PBS intraperitoneally (i.p.) on day 0 as well as on day two. Clinical scores were assessed daily by summing up the following score points (Table 19):

Table 19: EAE clinical score points

Clinical score points	Disease symptoms
0	no clinical sign
0.5	reduced tail tonicity or right hind limb weakness or left hind limb weakness
1	loss of tail tonicity or right hind limb paralysis or left hind limb paralysis

If one mouse obtained a clinical score of 0.5, soaked food was placed on the cage floor, mice were weighed daily and further monitored twice daily to determine clinical severity.
If mice reached a clinical score above 3, showed great pain or lost more than 20% of their initial bodyweight, they were excluded from the experiment and sacrificed by cervical dislocation. At peak of disease, occurring on day 18, cells were isolated from different tissues as described above or spinal cord was prepared for histological analysis.

3.5.3. Induction and analysis of adoptive transfer colitis

The adoptive transfer colitis model were approved by the relevant authorities under AZ 84-02.04.2013.A248. Satb1-sufficient or -deficient splenic naive $CD4^+$ T cells were isolated and $1x10^6$ naive $CD4^+$ T cells resuspended in PBS were injected i.p. into $Rag2^{-/-}$ mice. As control, $Rag2^{-/-}$ mice were only injected with PBS. To assess for colitis development, mice were weighed three times a week and the behavior of the mice as well as the consistency of feces was monitored. Mice exhibiting symptoms of pain, dehydration or severe weight loss were excluded from the experiment and sacrificed by cervical dislocation. When colitis symptoms manifested, approximately five weeks after naive $CD4^+$ T cell

injection, mice were sacrificed by cervical dislocation and cells were isolated and colon was prepared for histological analysis.

3.6. Transcriptional and epigenetic profiling

3.6.1. RNA isolation

Cell were lysed in QIAzol lysis reagent at RT for 5 min and stored at -80°C. For RNA isolation, 200 µl Chloroform was added per ml of lysis reagent. The sample was vortexed and incubated at RT for three min. Samples were centrifuged at 13000 rpm for 10 min at 4°C and the aqueous phase was collected. RNA was precipitated with isopropanol and incubated at -20°C for two hours. The sample was centrifuged at 13000 rpm for 30 min at 4°C and the pellet was washed twice in 80% ethanol with centrifugation steps at 13000 rpm for 5 min at 4°C. The pellet was dried, resuspended in 15 µl H_2O and incubated at 55°C for 5 min, while slowly shaking. The RNA concentration was measured using either the NanoDrop 800 or the NanoDrop 2000.

For transcriptional studies of T_H1 and T_H17 cell kinetics, RNA was isolated using the Direct-zol-96 RNA Kit according to the manufacturer's protocol.

For RNA-seq analysis, RNA was isolated together with M. Kraut using the miRNeasy Micro Kit according to the manufacturer's protocol.

3.6.2. Complementary DNA (cDNA) synthesis

The Transcriptor First Strand cDNA synthesis Kit was used to synthesize cDNA. In a final volume of 13 µl, 100-120 ng RNA was mixed with 50 pmol oligo(dT) primer and incubated at 65°C for 15 min. Subsequently cDNA synthesis was performed at 55°C for 30 min in the following reaction setup (Table 20):

Table 20: Reverse transcription reaction mix

Reagents	Volume [µl]
5x Reaction Buffer	4
Protector RNase Inhibitor (40 U/µl)	0.5
Deoxynucleotide triphosphates (10 mM)	2
Transcriptor Reverse Transcriptase (20 U/µl)	0.5
Pre-incubated RNA/ oligo(dT) primer mix	13 µl

Reverse transcription was stopped by heat inactivation at 85°C for 5 min.

3.6.3. qRT-PCR reaction and data analysis

For transcriptional analysis by qRT-PCR, cDNA was diluted by a factor of 6 and the reaction mix and PCR program were set up as followed (Table 21-22):

Table 21: qRT-PCR reaction mix

Reagents	Volume [µl]
LightCycler 480 Probe Master	5
Primer Mix (10 µM each)	0.2
Universal ProbeLibrary probe	0.1
cDNA	2-4
H_2O	0.7-2.7

Table 22: qRT-PCR program

Step	T [°C]	t [sec]	#cycles
Pre-Incubation	95	600	1
Amplification	95	10	50
	60	20	
	72	1	
Cooling	20	30	1

To confirm reproducibility, technical replicates were run for each sample.
Expression of the gene of interest was normalized to the expression of ß-actin and calculated using the $2^{-\Delta CT}$ method. Late called crossing points were manually set to 40. Expression values are shown as a relative value as described in the figure legends.

3.6.4. TruSeq RNA Library preparation and sequencing

For transcriptome analysis, RNA library preparation was performed using the TruSeq RNA Library Preparation Kit v2 according to the manufacturer's instruction with the help of M. Kraut. For indexing, barcoding indexes of Set A were used. Indexed cDNA libraries were measured in quality and quantity on Agilent TapeStation 2200 and were normalized and pooled. Sequencing (single read, 75 bp) was performed with the help of Kristian Händler on a HiSeq1500 platform using the TruSeq Rapid SBS Kit and TruSeq Rapid Cluster Kit according to the manufacturer's instruction.

3.6.5. RNA-seq analysis

RNA-seq data were analyzed by Jonas Schulte-Schrepping. Base calling and de-multiplexing was performed using CASAVA version 1.8.2 and fastQC was used for quality control. Subsequently, the reads were aligned to the mm10-based mouse Gencode reference transcriptome vM16 and quantified on gene level using star version 2.7.1a. (Dobin et al., 2013). Gene expression quantifications were imported to R 3.5.3 (2019-03-11) and DESeq2 v1.22.2 was used for downstream analyses (Love et al., 2014). Lowly expressed genes (rowSums > 10) were filtered and variance stabilizing transformation was performed. Subsequently, principle component analysis was conducted on all present genes using the prcomp function (R/stats 3.5.3). Differential expression analysis was performed comparing WT and KO samples without pre-defined fold change threshold and using independent hypothesis weighting (IHW, v1.10.1) (Ignatiadis et al., 2016) as the multiple testing procedure. Genes with an adjusted p-value < 0.05 and a fold change >1.5 were determined as significantly differentially expressed. Functional enrichment analysis using the MSigDB data base (Liberzon et al., 2015) was performed on the DE gene sets using the R package ClusterProfiler v3.10.1 (Yu et al., 2012).

3.6.6. Assay for transposase-accessible chromatin (ATAC)

ATAC-seq was conducted as previously described (Buenrostro et al., 2013; Picelli et al., 2014). Naive $CD4^+$ T cells were isolated as described above, washed in ice cold PBS and 60,000 cells were lysed in 50 µl cold ATAC-seq lysis buffer. Samples were immediately centrifuged at 500 g for 10 min at 4°C and the supernatant was discarded. For the transposition reaction, the nuclei were resuspended in 1 µl Tn5 transposase, 4 µl 5x tagmentation buffer and 15 µl H_2O and incubated for 30 min at 37°C, while slowly shaking. DNA fragments were purified using the Qiagen MinElute Kit according the manufacturer's instructions. Transposed DNA fragments were amplified using following reaction setup (Table 23-24):

Table 23: ATAC-seq PCR reaction

Reagents	**Volume [µl]**
NEBNext High-Fidelity 2x PCR Master Mix	25
Ad1_noMX (25 µM)	2.5
Ad2 [Barcode] (25 µM)	2.5
Transposed DNA	10
H_2O	10

Table 24: ATAC-seq PCR program

Step	T [°C]	t [sec]	#cycles
Pre-Incubation	72	300	1
Pre-Denaturation	98	30	1
Amplification	98	10	12
	63	30	
	72	60	
Cooling	4	hold	1

PCR products were purified using the Qiagen MinElute Kit according the manufacturer's protocol. Quality of the library was controlled and DNA concentration was measured on the Agilent TapeStation 2200 using the High sensitivity D1000 Screen Tape according to the manufacturer's protocol.

3.6.7. ATAC sequencing and analysis

Libraries were sequenced with the help of Kristian Händler (single read, 75 bp) on an Illumina HiSeq1500 using the TruSeq Rapid SBS Kit and TruSeq Rapid Cluster Kit according to the manufacturer's instruction. ATAC-seq data analysis was performed by Jonas Schulte-Schrepping. After quality inspection using FastQC v 0.11.8 (https://www.bioinformatics.babraham.ac.uk/projects/fastqc/), adapter and low-quality sequences were trimmed using trimmomatic v0.36 (Bolger et al., 2014) and reads were aligned to reference mouse genome mm10 using Bowtie2 v2.3.5 (Langmead and Salzberg, 2012). Picard v2.9.2 (http://broadinstitute.github.io/picard/) was used to identify duplicated reads and removal of Tn5 offset was performed using the alignmentSieve functionality of the deepTools suite v3.3.0 (Ramírez et al., 2016). Bam files were sorted and indexed using SAMtools v1.9 (Li et al., 2009). After subsampling the reads for each sample to 5*10^6 reads using Sambamba v0.7.0, normalized bigwig files were produced using deeptools v3.3.0 for genomic visualization of the read coverage. Subsequently, peaks were called with MACS2 v2.1.2 (Zhang et al., 2008). After peak calling, bed files listing narrow peaks were imported to R 3.5.3 and consensus peak regions across all samples were generated with the 'reduce' function of the Bioconductor GenomicRanges package v1.34.0 and reads were counted per sample using the 'summarizeOverlaps' function of the Bioconductor GenomicAlignments package v1.18.1 (Lawrence et al., 2013). Genomic regions on the ENCODE blacklist for mm10 were excluded from the analysis. ChIPseeker v1.18.0 was used to annotate genomic regions (Yu et al., 2015) using the TxDb.Mmusculus.UCSC.mm10.knownGene data base

v3.4.4. Peak regions were filtered for a minimum sum of 10 counts across all samples and a minimum MACS2 detection rate of at least 2 samples per group. After normalization using the Bioconductor DESeq2 package v1.22.2 (Love et al., 2014), variance stabilizing transformation was performed and principle component analysis on all detected peaks was conducted using the prcomp function (R/stats 3.5.3). Subsequently, differentially accessible regions were determined using the DESeq2 (Love et al., 2014) and independent hypothesis weighting using the R package IHW v1.10.1 (Ignatiadis et al., 2016). Regions with an adjusted p-value < 0.1 and a fold change >1.5 were determined as significantly differentially accessible. Functional enrichment analyses were performed on the differentially accessible region sets using the gene ontology (Ashburner et al., 2000; Carbon et al., 2019) and MSigDB (Liberzon et al., 2015) data bases with the R package ClusterProfiler v3.10.1 (Yu et al., 2012).

3.7. Immunohistochemistry

3.7.1. Histological analysis of CNS immune cell infiltration

For histological analysis of immune cell infiltration of the CNS, mice were anaesthetized at peak of disease as described above and mice were perfused with 20 ml cold PBS through the left ventricle followed by perfusion with 20 ml 4% PFA as approved under animal license AZ 84-02.04.2016.A370. The spinal cord was excised and further fixed in 4% PFA for two days. Until further processing, samples were stored in 70% ethanol. Before embedding, the tissue was dehydrated twice in 70% ethanol followed by two dehydration steps in 96% ethanol and three in absolute ethanol. Subsequently, samples were cleared in Xylene three times and twice waxed in heated paraplast. All incubation steps were performed for two hours. Finally, the tissue was embedded in paraplast. Embedded tissues were sent for further histological analysis to the group of Prof. Dr. Tanja Kuhlmann at the University of Münster, Institute for Neuropathology, and sections were prepared and stained as described previously (Ellwardt et al., 2018). Histological analysis was conducted using a BZ-9000 microscope.

3.7.2. Histological analysis of demyelination

For histological analysis of myelin, spinal cords were dissected and fixed in 4% PFA as described above. Subsequently, samples were incubated in 30% sucrose for two days and embedded in cryoembedding matrix. Sections (12 µm) were prepared using the CryoStar NX70 and myelin was visualized using luxol fast blue staining with help of Svenja Bourry. Sections were washed in H_2O for 30 sec and dehydrated in 95% ethanol for 5 min. Subsequently, tissues were stained in luxol fast blue solution overnight at 60°C. Samples were washed in 95% ethanol for one min, followed by washing in H_2O for one min while gently

shaking. Samples were incubated in lithiumcarbonat solution for 10 sec, washed twice in 70% ethanol for 10 sec each and H_2O for one min while gently shaking. Incubation in lithiumcarbonat solution and subsequent washing steps were serially repeated until the contrast of myelin stained and unstained tissue was sufficient. Subsequently, samples were washed in 70% ethanol for one min while gently shaking and nuclear fast red staining was performed for two min. Samples were washed in H_2O for one min, while gently shaking, and dehydrated for two min in 95% ethanol and two min in 100% ethanol. Samples were cleared in Xylene for one min and coverslips were mounted on top with Entellan. Histological analysis was conducted using a BZ-9000 microscope.

3.7.3. Histological analysis of immune cell infiltration in the colon

For histological analysis of the intestine, the colon was cleaned with PBS and the tissue was fixed in 4% PFA. Samples were sent for further analysis to the group of Prof. Dr. Claudia Wickenhauser at the University Hospital of Halle (Saale), Institute of Pathology. The tissue was embedded in paraffin, prepared sections were stained with hematoxylin and eosin and scored to assess disease progression as described previously (ten Hove et al., 2002).

3.8. Immunoblotting

3.8.1. Protein isolation

For protein isolation of naive or effector/memory $CD4^+$ T cells, 10^7 cells were washed twice in ice-cold PBS and lysed on ice for 30 min in 100 µl RIPA buffer supplemented with protease inhibitor. Cell lysates were sonicated on ice three times for 10 sec at 20 V, centrifuged at 1000 g for 10 min at 4°C and the supernatant was kept for further protein analysis.

For the detection of Satb1 in *in vitro* cultured T_H subsets, cells were harvested on day three or five after initial cell differentiation and 10 wells of a 96-well plate were pooled. Protein isolation was performed as described above by Lisa Holsten during her Bachelor Thesis.

Protein concentration was determined using the Pierce bicinchoninic acid assay (BCA) Protein Assay Kit according to the manufacturer's protocol and absorbance was measured with the Infinite M200 multimode microplate reader or FLUOstar Omega.

3.8.2. SDS-polyacrylamide gel electrophoresis (SDS-PAGE)

Per sample, 20 µg proteins were denatured at 70°C for 10 min in the presence of NuPAGE sample reducing agent and NuPAGE LDS sample buffer according to the manufacturer's

instructions. Samples and protein ladder (SeeBlue Plus 2 standard) were loaded on a 4% stacking gel, which was layered on top of a 10% separation gel (Table 25).

Table 25: SDS-PAGE gel composition

Component	4% stacking gel [ml]	10% separation gel [ml]
H_2O	1.83	2.01
1 M Tris-HCl, pH 6.8	0.83	-
1.5 M Tris-HCl, pH 8.8	-	1.25
10% SDS	0.025	0.05
30% Acrylamide	0.42	1.67
10% Ammonium persulfate	0.017	0.017
Tetramethylethylenediamine	0.003	0.007

Samples were run at 80 V for 20 min followed by 130 V for approximately one hour.

3.8.3. Immunoblotting and detection

To blot proteins onto a nitrocellulose membrane, the SDS-PAGE gel was placed on the membrane and both together surrounded by two pieces of filter paper and sponges. Blotting was performed in 1x Wet Blot buffer for two hours at 0.2 A with constant cooling. The membrane was blocked in 5% milk in PBST for one hour at RT. The anti-Satb1 antibody was added in a final dilution of 1:5000 and incubated for one hour at RT, followed by an overnight incubation at 4°C. Subsequently, the blot was washed three times in PBST for 10 min each and incubated with horseradish peroxidase (HRP) coupled Rabbit IgG in a final dilution of 1:5000 in 5% milk in PBST for one hour at RT. The membrane was washed as described above and incubated with enhanced chemiluminescence western blotting reagents according the manufacturer's instructions. The enzymatic reaction catalyzed by the HRP was imaged on a ChemiDoc MP.

For subsequent ß-Actin detection, the blot was wash washed once in PBST, followed by incubation with anti-ß-actin antibody in a final dilution of 1:5000 in 5% milk in PBST for one hour at RT. Subsequent washing steps, secondary HRP-Mouse IgG antibody incubation, HRP reaction and imaging was performed as described above. All incubation steps were conducted under constant rotation or shaking.

3.9. Statistics

All statistical analyses, except for the analyses of sequencing data, were performed with GraphPad Prism. Sequencing data were analyzed in R studio. When analyzing statistical

differences between two groups, two-tailed unpaired Student's t-tests were performed. Statistical differences between three or more groups treated under similar conditions were analyzed by one-way ANOVA with Dunnett's or Tukey's multiple comparison tests. Two-way ANOVA were performed when comparing multiple groups in the context of different conditions. Sidak's or Tukey's multiple comparison tests were performed dependent of the experimental conditions. If the same cells or mice were measured at different time points, repeated measure analysis was performed. P values of less than 0.05 were considered to be significant (ns indicates not significant, $p < 0.05$ = *; $p < 0.01$ = **; $p < 0.001$ = ***). Descriptive statistics, the performed statistical tests as well as the number of samples are stated in the figure legends.

4. Results

4.1. Satb1 expression is tightly regulated during the transition of naive CD4$^+$ T cells into effector CD4$^+$ T cells

CD4$^+$ T cells play an important role in host defense but also in the regulation of immune homeostasis. The differentiation of CD4$^+$ T cells in T helper (T_H) subpopulations with specific functions adjusted to the environmental conditions allows for the maximal host protection.

Previous work indicated that Satb1 is essential in the early development of naive CD4$^+$ T cells (Kakugawa et al., 2017; Kondo et al., 2016) and that Satb1 expression is further upregulated upon TCR activation (Akiba et al., 2018; Beyer et al., 2011; Gottimukkala et al., 2016; Stephen et al., 2017). However, its role during the differentiation of peripheral CD4$^+$ T cells as well as in the memory CD4$^+$ T cells formation is not fully understood.

To determine how Satb1 is expressed and regulated in peripheral CD4$^+$ T cells, the expression of Satb1 in wildtype naive and memory CD4$^+$ T cells as well as during the differentiation of CD4$^+$ T cells *in vitro* was analyzed.

Satb1 was highly expressed in naive CD4$^+$ T cells on mRNA as well as on protein level, while its expression was downregulated in memory CD4$^+$ T cells (Figure 5a-c).

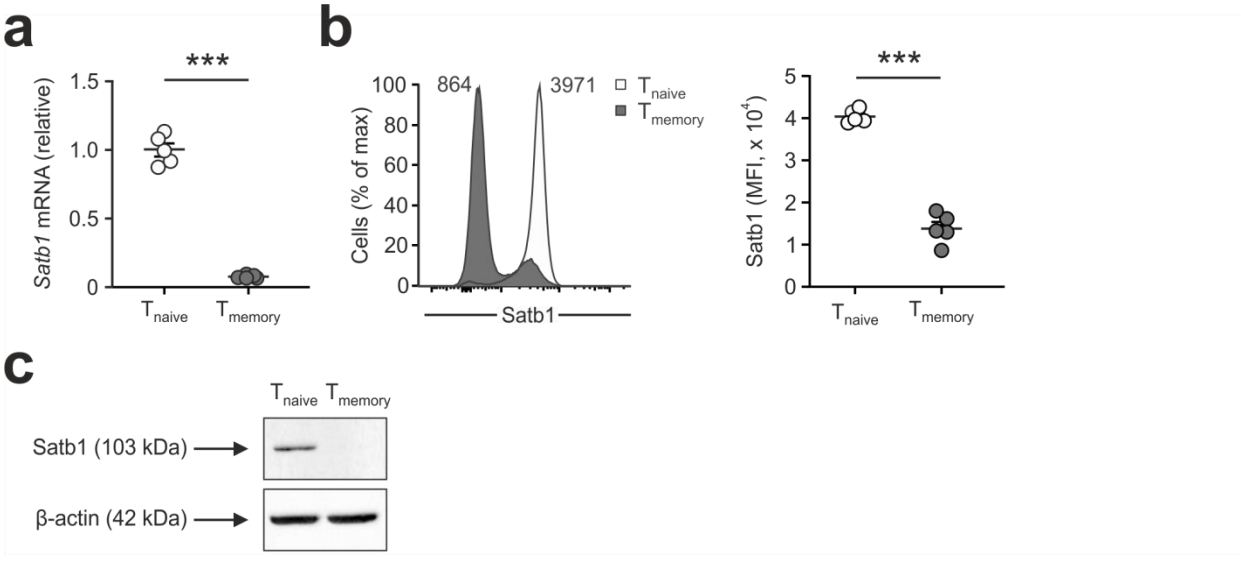

Figure 5: Satb1 is highly expressed in naive CD4$^+$ T cells but downregulated in memory CD4$^+$ T cells.

Wildtype CD4$^+$CD44$^-$CD62L$^+$CD25$^-$ naive T cells and CD4$^+$CD44$^+$CD62L$^-$CD25$^-$ effector/memory T cells were isolated by flow cytometric cell sorting and the expression of Satb1 was determined on mRNA level by qRT-PCR **(a)** and on protein level **(b,c)** by flow cytometry **(b)** and immunoblotting **(c)**. MFI, mean fluorescent intensity. (a,b) n=5, mean ± SEM, unpaired Student's t-test. (b) Data are representative of two independent experiments.

To further analyze the regulation of Satb1 during the differentiation of $CD4^+$ T cells, naive $CD4^+$ T cells were isolated and differentiated *in vitro* into the following $CD4^+$ T cell subsets: T_H1, T_H2, T_H9, T_H17, and iTreg cells. Moreover, *Satb1* mRNA levels were measured at different time points during the differentiation (Figure 6).

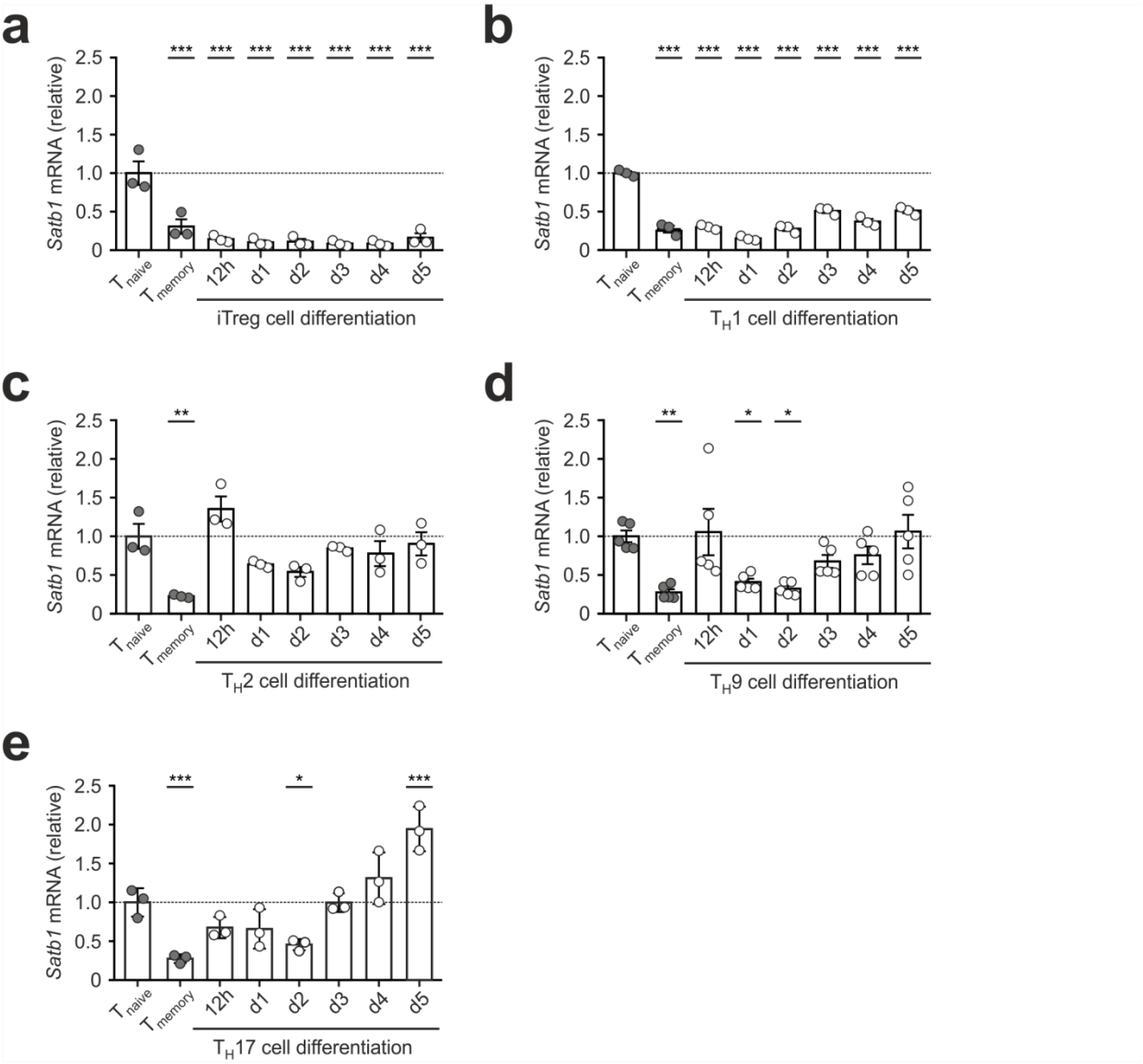

Figure 6: *Satb1* mRNA expression is differently regulated during the differentiation of $CD4^+$ T cells.
Wildtype naive $CD4^+$ T cells and effector/memory $CD4^+$ T cells were isolated by flow cytometric cell sorting and naive $CD4^+$ T cells were differentiated *in vitro* into T helper (T_H) subsets: iTreg cells **(a)**, T_H1 **(b)**, T_H2 **(c)**, T_H9 **(d)** and T_H17 **(e)**. *Satb1* mRNA levels were measured and analyzed relative to the expression of *Satb1* in T_{naive} cells. Data were generated together with Jannis Wißfeld. h, hour; d, day. n=3-5, mean ± SEM, one-way ANOVA with Dunnett's multiple comparison test relative to T_{naive}.

As expected, during the polarization of naive $CD4^+$ T cells towards iTreg cells the expression of *Satb1* was downregulated (Figure 6a). In addition, differentiation of naive $CD4^+$ T cells into T_H1 cells resulted in a downregulation of *Satb1* mRNA (Figure 6b). In contrast, in T_H2

cells and T_H9 cells *Satb1* was not directly downregulated but a downregulation one day after the initiation of differentiation was observed. However, *Satb1* expression was restored by day three, reaching similar *Satb1* mRNA levels on day five as in naive $CD4^+$ T cells (Figure 6c,d). In T_H17 cells, a downregulation of *Satb1* was observed until day two followed by a significant upregulation of *Satb1* resulting in a twofold higher expression of *Satb1* mRNA on day five in comparison to naive $CD4^+$ T cells (Figure 6e).

Next, protein expression of Satb1 during the differentiation into T_H cells was analyzed by flow cytometry and immunoblotting at day three and five after initialization of cell differentiation. Apart from iTreg cells, Satb1 was upregulated on protein level in all $CD4^+$ T_H subsets (Figure 7). On day three of differentiation, Satb1 was especially upregulated in T_H2 and T_H17 cells (Figure 7a,b), while on day five only minor differences between T_H1, T_H2, T_H9 and T_H17 cells were detected (Figure 7c,d).

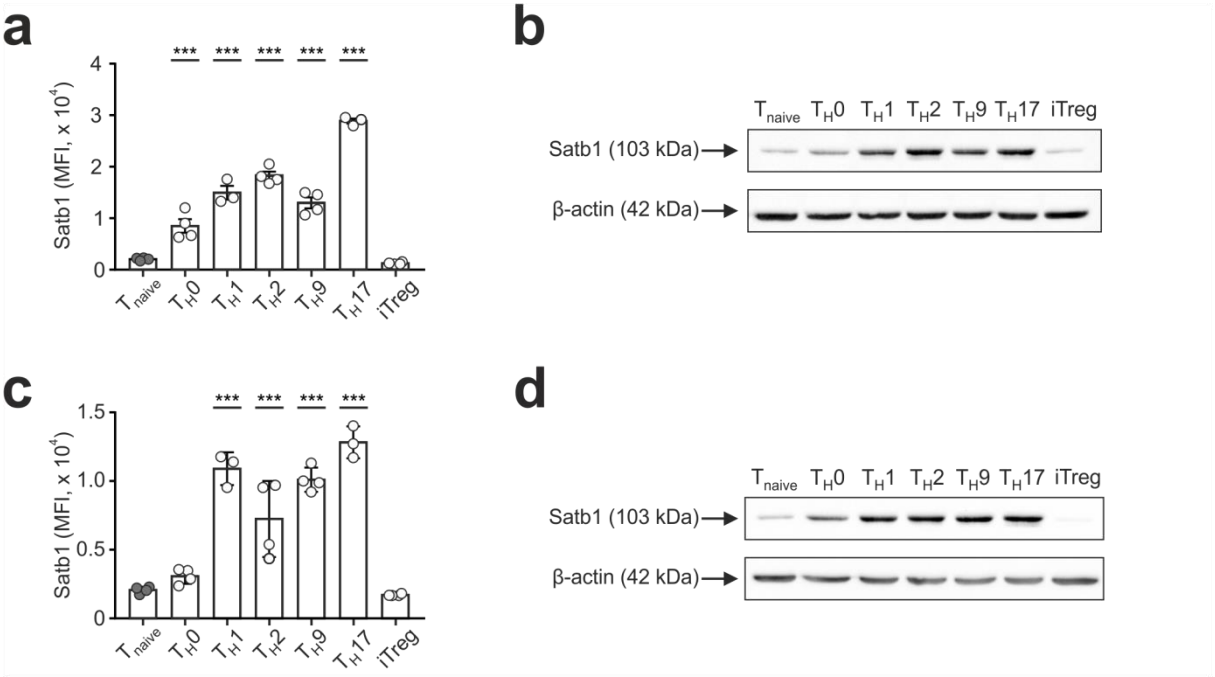

Figure 7: Satb1 is differently regulated in $CD4^+$ T_H subsets.
Wildtype naive $CD4^+$ T cells were isolated by flow cytometric cell sorting and differentiated *in vitro* into T_H0, T_H1, T_H2, T_H9, T_H17 and iTreg cells. Satb1 protein level was determined on day three by flow cytometry **(a)** or immunoblot analysis **(b)** as well as on day five **(c,d)**. Flow cytometry data were generated together with Jannis Wißfeld. n=3-4, mean ± SEM, one-way ANOVA with Dunnett's multiple comparison test relative to T_{naive}.

Taken together, these data demonstrate that Satb1 is differently expressed between naive and memory $CD4^+$ T cells as well as in effector $CD4^+$ T cells. Memory $CD4^+$ T cells and iTreg cells are clearly characterized by a downregulation of Satb1, while T_H17 cells upregulate Satb1 on mRNA and protein level. Thus, Satb1 might be important for lineage decision and function of $CD4^+$ T_H subset and therefore warrants further investigation.

4.2. Satb1 affects the differentiation of naive CD4$^+$ T cells into different T_H subset *in vitro*

To further determine the role of Satb1 during the differentiation of CD4$^+$ T cells, conditional Satb1-deficient as well as conditional Satb1-overexpressing mice were used, which were generated by Daniel Sommer during his Ph.D. thesis (Sommer, 2018).

Satb1$^{fl/fl}$ mice were crossed to CD4-CreERT2 mice, which allowed the deletion of Satb1 in CD4$^+$ T cells upon tamoxifen-induced Cre recombination (Appendix Figure 66a,b) (Śledzińska et al., 2013; Sommer et al., 2014).

Indeed, Satb1 expression was abrogated upon tamoxifen administration both on mRNA (Figure 8a) and protein (Figure 8b) level in naive CD4$^+$ T cells as well as in effector/memory CD4$^+$ T cells (Figure 8c,d). Especially in naive CD4$^+$ T cells, which highly express Satb1 under homeostatic conditions, tamoxifen treatment resulted in a clear depletion of Satb1.

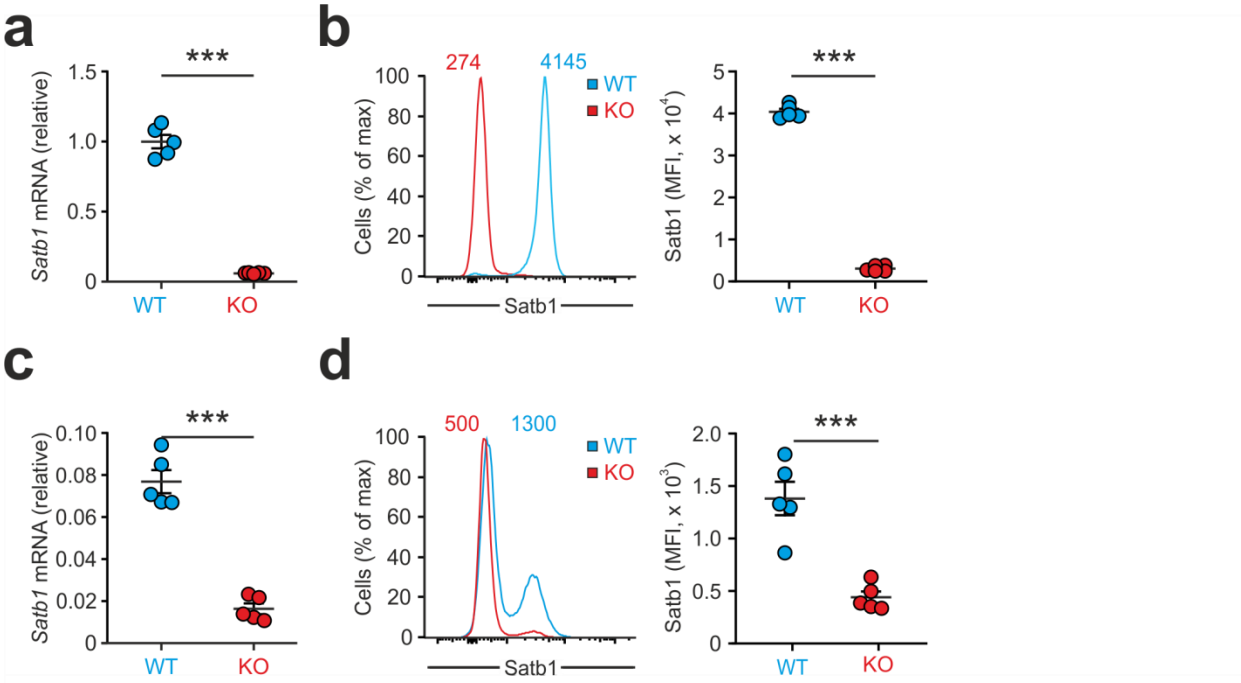

Figure 8: Satb1 is downregulated in naive and effector CD4$^+$ T cells of Satb1$^{fl/fl}$/CD4-CreERT2$^{wt/+}$ mice after tamoxifen administration.
Satb1$^{fl/fl}$/CD4-CreERT2$^{wt/+}$ mice were treated with oil (WT) or tamoxifen (KO) and naive CD4$^+$ T cells and effector/memory CD4$^+$ T cells were isolated by flow cytometric cell sorting. Satb1 expression was analyzed in naive CD4$^+$ T cells on mRNA **(a)** and protein level **(b)** as well as in effector/memory T cells on mRNA **(c)** and protein level **(d)**. (a,c) *Satb1* mRNA levels are shown relative to WT naive T cells. (a-d) n=5, mean ± SEM, unpaired Student's t-test.

In addition, homozygous R26-STOP-Satb1 mice were crossed to CD4-Cre mice to induce the overexpression of Satb1 upon CD4 expression (Appendix Figure 66c,d) (Lee et al., 2001; Sommer, 2018). Furthermore, mice were crossed with Foxp3-RFP mice to allow for the

detection of Foxp3 expression through the simultaneous expression of a fluorescent reporter (Appendix Figure 66e) (Wan and Flavell, 2005).

Analysis of Satb1 expression in $CD4^+$ T cells of R26-STOP-Satb1/CD4-Cre mice revealed an upregulation of Satb1 in naive $CD4^+$ T cells on the protein level although similar mRNA levels were measured (Figure 9a,b). In contrast, in effector/memory $CD4^+$ T cells the expression of Satb1 was increased both on the mRNA and protein level (Figure 9c,d). Thus, in line with the endogenous expression of Satb1 the effect of the overexpression was more pronounced in the effector cell pool. In summary, expression of Satb1 was altered in both naive and effector $CD4^+$ T cells.

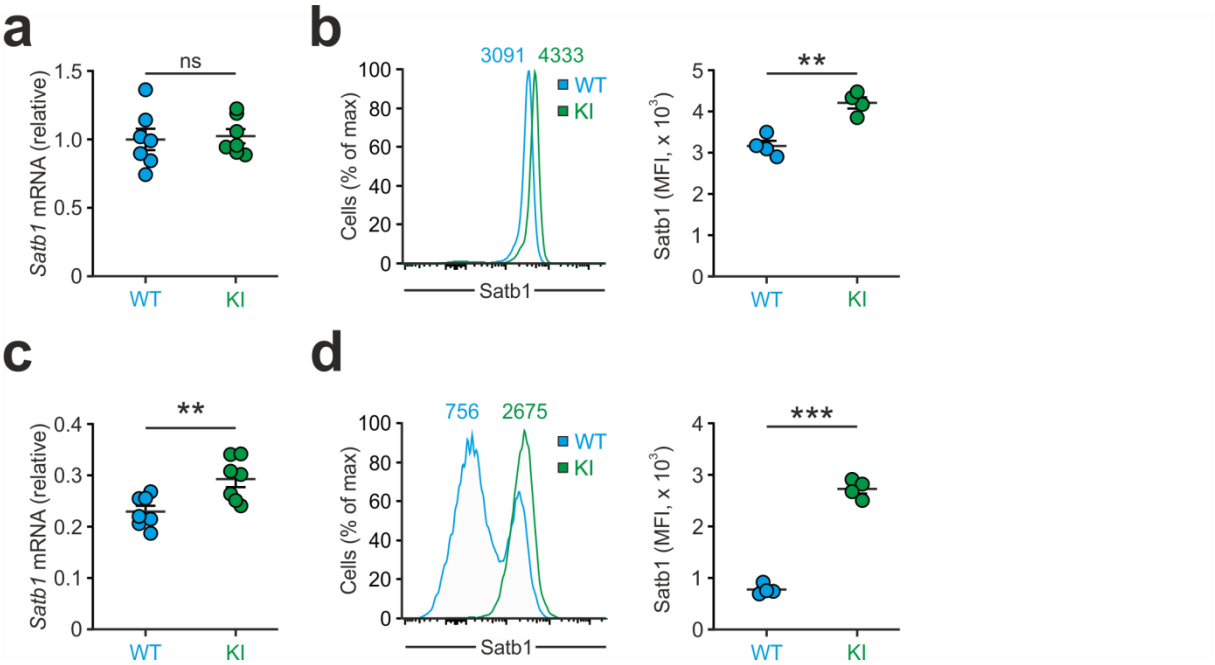

Figure 9: Satb1 is upregulated in naive and effector $CD4^+$ T cells from R26-STOP-Satb1/CD4-Cre mice.

Naive $CD4^+$ T cells and effector/memory $CD4^+$ T cells were isolated from R26-STOP-Satb1 (WT) or R26-STOP-Satb1/CD4-Cre (KI) mice by flow cytometric cell sorting. Satb1 expression was determined on mRNA **(a)** and protein level **(b)** in naive $CD4^+$ T cells as well as in effector/memory T cells **(c, d)**. (a,c) *Satb1* mRNA levels are shown relative to WT naive T cells. n= 7, (b,d) n=4, mean ± SEM, unpaired Student's t-test.

Thus, both the deletion as well as the transgenic overexpression of Satb1 in $CD4^+$ T cells could be validated in the respective mouse lines and allowed to use both mouse lines to further study the functional role of Satb1 in $CD4^+$ T cells.

To analyze to influence of Satb1 during the differentiation of $CD4^+$ T cells, Satb1-wildtyp (WT), -deficient (KO) and -overexpressing (KI) naive $CD4^+$ T cells were isolated and differentiated *in vitro* into the various T_H subsets (Figure 10-15).

4.2.1. T_H1 cell differentiation

Little is known about the role of Satb1 on T_H1 cell development. Downregulation of *Satb1* in wildtype cells during the differentiation of T_H1 cells indicates decreased expression of Satb1 as a consequence of T_H1 cell differentiation (Figure 6b). In line with this, Satb1-deficient naive $CD4^+$ T cells differentiated into T_H1 cells with no significant differences compared to Satb1-sufficient cells at day five (Figure 10a,b). Similar expression levels of IFN-γ as well as

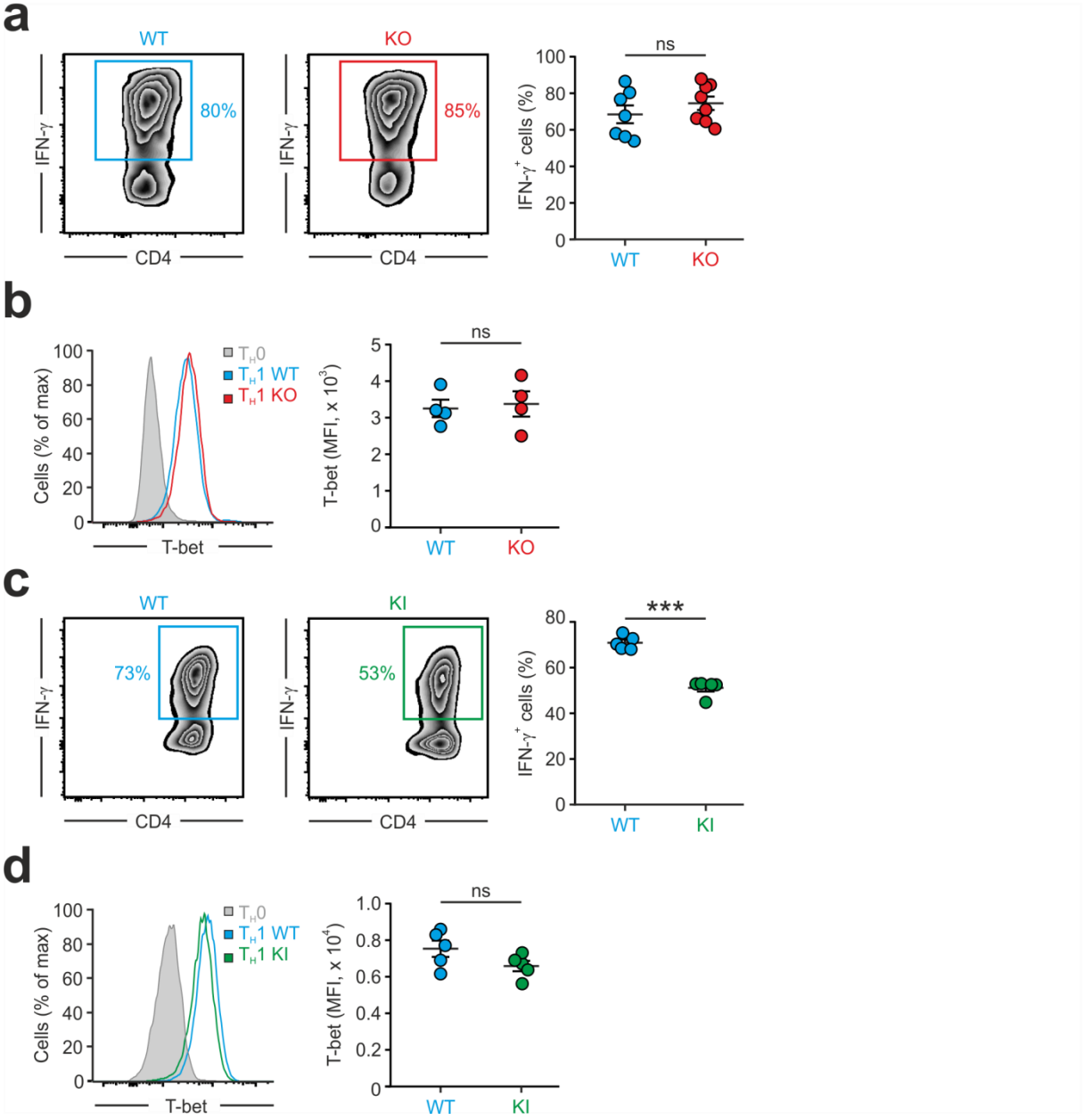

Figure 10: Overexpression of Satb1 diminishes the differentiation of T_H1 cells.
Satb1-wildtype (WT), -deficient (KO) and -overexpressing (KI) naive $CD4^+$ T cells were isolated by flow cytometric cell sorting and differentiated *in vitro* into T_H1 cells. At day five of differentiation, cells were analyzed by flow cytometry. **(a,b)** Analysis of IFN-γ **(a)** and T-bet **(b)** expression in WT and KO cells. **(c,d)** The percentage of IFN-γ^+ cells **(c)** and analysis of T-bet expression **(d)** in WT and KI cells. (a) n=7-8, (b) n=4, (c,d) n=5, mean ± SEM, unpaired Student's t-test. (a) Data were pooled from two independent experiments.

of T-bet, the T_H1 cell-specific transcription factor, were detected (Figure 10a,b). However, when analyzing the differentiation efficiency of Satb1-overexpressing naive T cell into T_H1 cells a significant reduction compared to Satb1 wildtype cells was observed (Figure 10c,d). Fewer IFN-γ^+ cells as well as a slight decrease in T-bet expression were detected when expression of Satb1 was upregulated during the differentiation (Figure 10c,d). This indicates that overexpression of Satb1 diminishes the differentiation of T_H1 cells and suggests that downregulation of Satb1 is a prerequisite for optimal T_H1 cell differentiation.

As *Satb1* expression was downregulated on mRNA level in the early phase of T_H1 cell differentiation in wildtype cells (Figure 6b), it can be hypothesized that downregulation of Satb1 might facilitate the differentiation of T_H1 cells. Thus, deletion of Satb1 already in naive $CD4^+$ T cells might accelerate lineage commitment of T_H1 cells, an effect which might be masked at day five of differentiation. To verify this hypothesis, the differentiation capability of Satb1-deficient cells was analyzed at early time points during the polarization of T_H1 cells. These kinetic studies revealed that both *Ifng* and *Tbx21* (T-bet) mRNA levels were significantly upregulated in Satb1-deficient cells at day one and two of differentiation (Figure 11a,b).

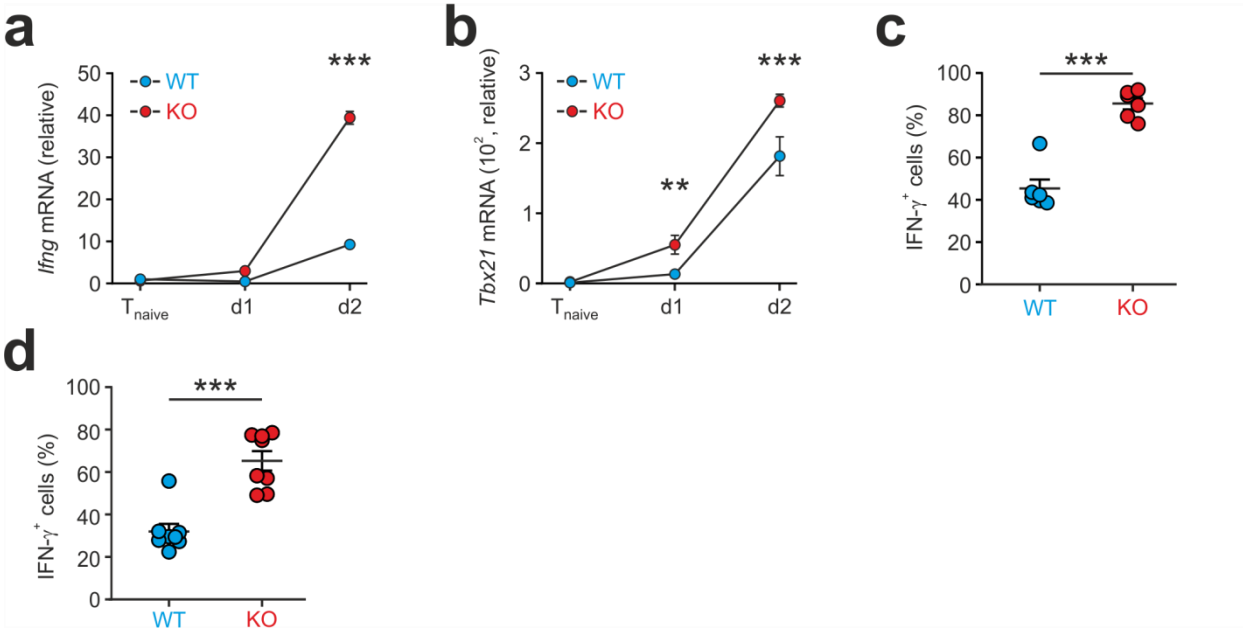

Figure 11: Satb1 deficiency fosters the differentation of T_H1 cells.
Naive $CD4^+$ T cells from Satb1-sufficient (WT) and -deficient $CD4^+$ (KO) mice were isolated by flow cytometric cell sorting and differentiated *in vitro* into T_H1 cells. **(a,b)** mRNA levels of *Ifng* **(a)** and *Tbx21* **(b)** were analyzed by qRT-PCR at different time points during the differentiation into T_H1 cells. **(c)** At day three of differentiation, the percentage of IFN-γ-producing cells was analyzed by flow cytometry. **(d)** Naive $CD4^+$ T cells were differentiated without IgG crosslinking and IFN-γ production was analyzed at day five of T_H1 cell differentiation by flow cytometry. (a,b) n=3, (c) n=6, (d) n=8, mean ± SEM, (a,b) two-way ANOVA with Sidak's multiple comparison test. (c,d) unpaired Student's t-test. Data were pooled from two independent experiments.

Furthermore, contrary to the previous observations at day five, the percentage of IFN-γ^+ cells was significantly increased in Satb1-deficient cells at day three of differentiation (Figure 11c). Besides, it is known that the TCR-signaling strength can influence the differentiation of naive $CD4^+$ T cells, e.g. a strong TCR signaling favors the differentiation of T_H1 cells over T_H2 cells (Morel, 2018). As alternative protocols for T_H1 cell differentiation exist besides using cross-linking IgGs to bind CD3 and CD28 antibodies, the differentiation capacity of Satb1-deficient naive $CD4^+$ T cells into T_H1 cells were tested using plate-bound CD3 antibodies. When cultivating naive $CD4^+$ T cells with plate-bound CD3 antibodies, wildtype naive $CD4^+$ T cells differentiated less efficiently into T_H1 cells compared the CD3 and CD28 crosslinking. However, an increase in T_H1 cell differentiation of Satb1-deficient naive $CD4^+$ T cells was observed at day five of differentiation, indicating that Satb1 downregulation facilitates the differentiation of T_H1 cells under suboptimal differentiation conditions (Figure 11d).

Taken together, these data indicate an inhibitory role of Satb1 during the differentiation of T_H1 cells. Down regulation of Satb1 fosters the differentiation of T_H1 cells, especially in the early steps of the differentiation process as well as under non-ideal differentiation conditions, while an upregulation of Satb1 diminishes T_H1 cell differentiation *in vitro.*

4.2.2. T_H2 cell differentiation

It has been reported that Satb1 plays an important role for the differentiation of T_H2 cells and is important for the coordinated expression of the T_H2 cell-associated cytokine locus (Ahlfors et al., 2010; Cai et al., 2006; Notani et al., 2010). To verify the positive correlation of Satb1 and T_H2 cell differentiation, Satb1-deficient as well as -overexpressing naive $CD4^+$ T cells were differentiated into T_H2 cells *in vitro*. Indeed, a slightly reduced IL-4 expression could be observed in Satb1-deficient cells compared to Satb1-sufficient cells at day five of T_H2 cell differentiation (Figure 12a). Furthermore, impaired differentiation of T_H2 cells was corroborated by a significant reduction in the expression of the T_H2 cell lineage-defining transcription factor Gata3 in Satb1-deficient cells (Figure 12b). Unexpectedly, overexpression of Satb1 also resulted in a reduced IL-4 production (Figure 12c), while Gata3 expression was not significantly altered compared to wildtype cells (Figure 12d).

Thus, this indicates that the levels of Satb1 have to be tightly controlled to allow for T_H2 cell differentiation as any dysregulation of Satb1 diminishes the differentiation of T_H2 cells *in vitro*.

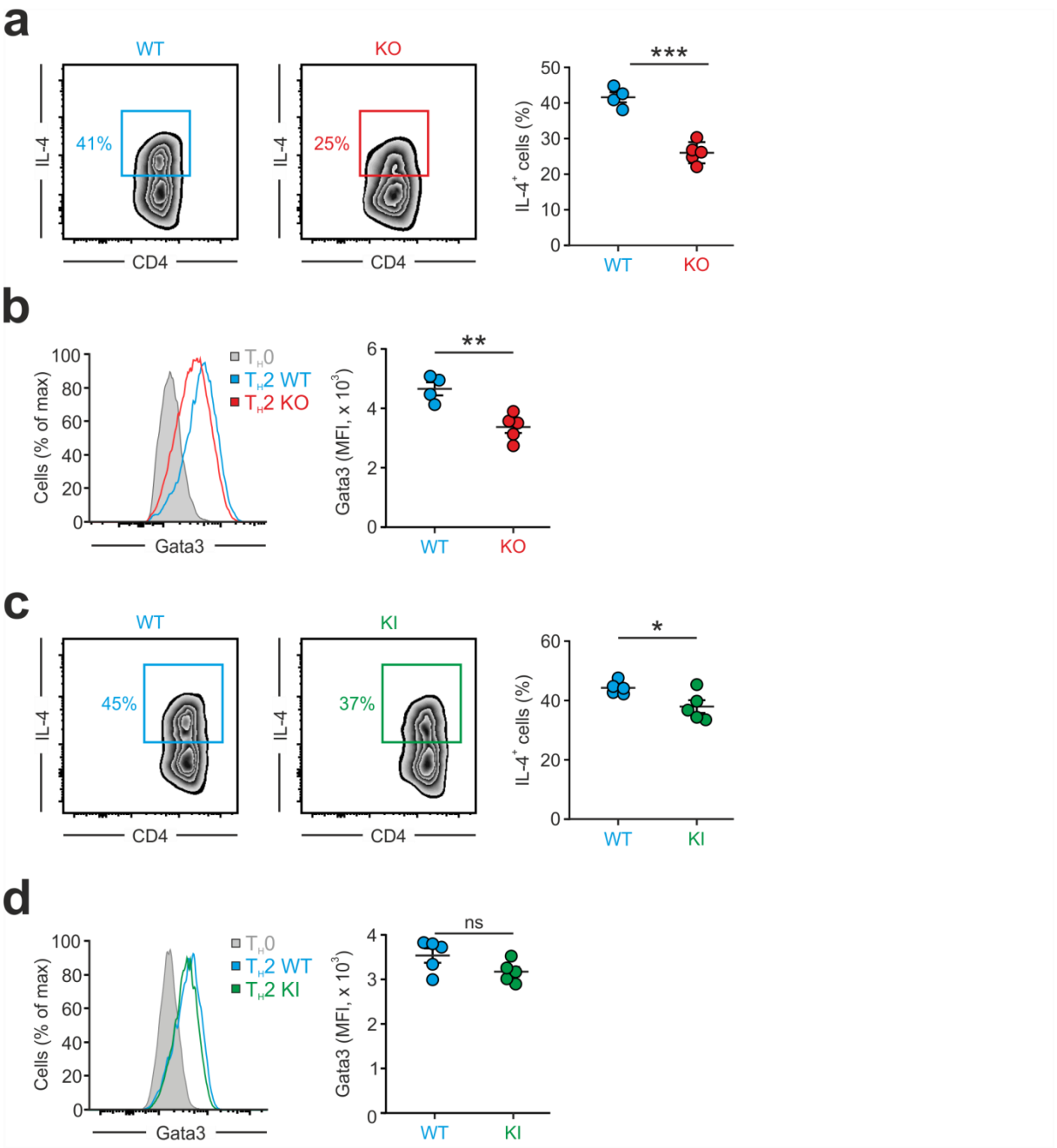

Figure 12: Satb1 disregulation diminishes the differentiation of T_H2 cells.
Satb1-wildtype (WT), -deficient (KO) and -overexpressing (KI) naive $CD4^+$ T cells were isolated by flow cytometric cell sorting and differentiated *in vitro* into T_H2 cells. At day five of differentiation, cells were analyzed by flow cytometry. **(a,b)** Analysis of IL-4 **(a)** and Gata3 **(b)** expression in WT and KO cells. **(c,d)** Percentage of IL-4^+ positive cells **(c)** and analysis of Gata3 expression **(d)** in WT and KI cells. (a,b) n=4-5, (c,d) n=5, mean ± SEM, unpaired Student's t-test.

4.2.3. T_H9 cell differentiation

Next, the effect of Satb1 on the differentiation of T_H9 cells was assessed. Karim et al. observed a correlation of IL-9 and Satb1 expression indicating a role of Satb1 in the differentiation of T_H9 cells (Karim et al., 2017). In line with this, deletion of Satb1 in naive $CD4^+$ T cells resulted in a decreased differentiation capability to T_H9 cells. Fewer IL-9^+ cells

were detected when Satb1 was lacking in $CD4^+$ T cells during the differentiation (Figure 13a). Furthermore, upregulation of Satb1 in $CD4^+$ T cells resulted in an increased differentiation of IL-9-expressing cells underlining a positive regulation of T_H9 cells by Satb1 (Figure 13b). Thus, Satb1 plays an important role for T_H9 cells by fostering their differentiation.

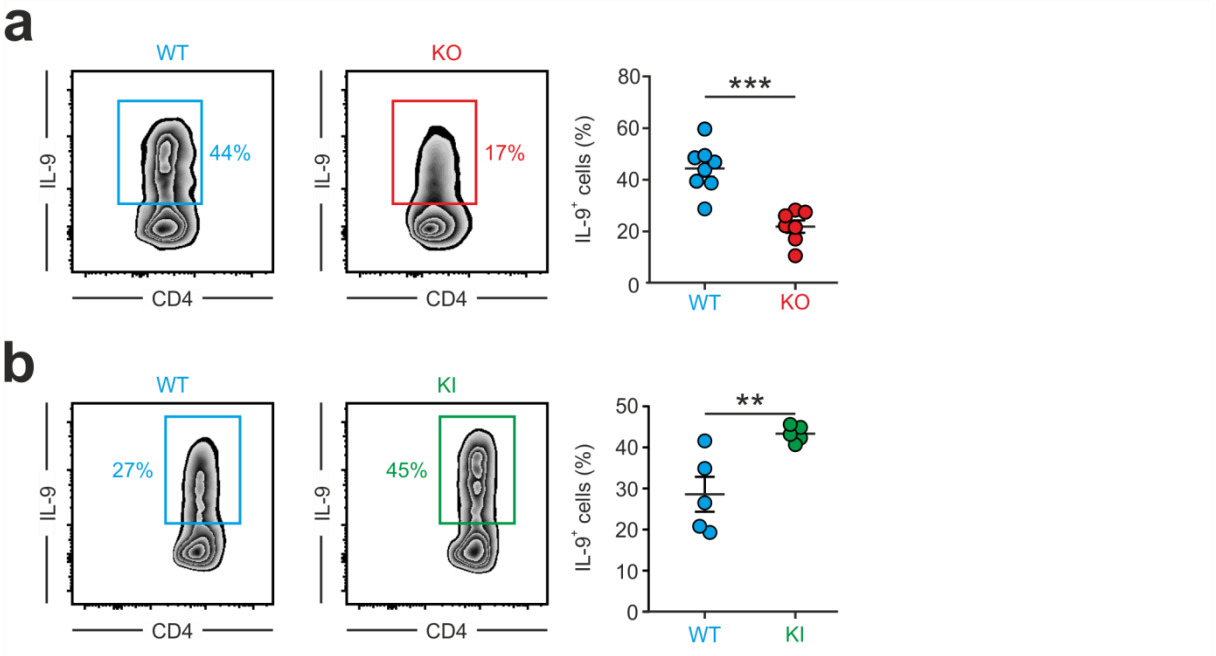

Figure 13: Satb1 expression fosters the differentiation of T_H9 cells.
Satb1-wildtype (WT), -deficient (KO) and -overexpressing (KI) naive $CD4^+$ T cells were isolated by flow cytometric cell sorting and differentiated *in vitro* into T_H9 cells. At day five of differentiation, the percentage of IL-9-producing cells was analyzed by flow cytometry in WT and KO cells **(a)** and WT and KI cells **(b)**. (a) n=7-8, (b) n=5, mean ± SEM, unpaired Student's t-test. Data were pooled from two independent experiments.

4.2.4. T_H17 cell differentiation

Furthermore, the influence of Satb1 on the development of T_H17 cells was analyzed. During the preparation of this thesis it was reported, that Satb1 expression is required for the development of T_H17 cell-driven autoimmune diseases (Akiba et al., 2018; Sommer, 2018; Yasuda et al., 2019). In line with this, deletion of Satb1 resulted in an impaired differentiation of T_H17 cells *in vitro* (Figure 14a,b). Only few IL-17-producing cells could be observed at day five of differentiation (Figure 14a), which was accompanied by a loss of RORγt expression (Figure 14b). Thus, naive $CD4^+$ T cells failed to differentiate into T_H17 cells, when Satb1 was depleted. In contrast, Satb1-overexpressing cells showed an increased differentiation into T_H17 cells. More $IL\text{-}17^+$ cells were observed at day five of *in vitro* culture, when Satb1 was upregulated during T_H17 cell differentiation (Figure 14c). However, RORγt expression in Satb1-overexpressing cells was reduced (Figure 14d). Taken together, these data indicate an essential role of Satb1 in the differentiation of T_H17 cells.

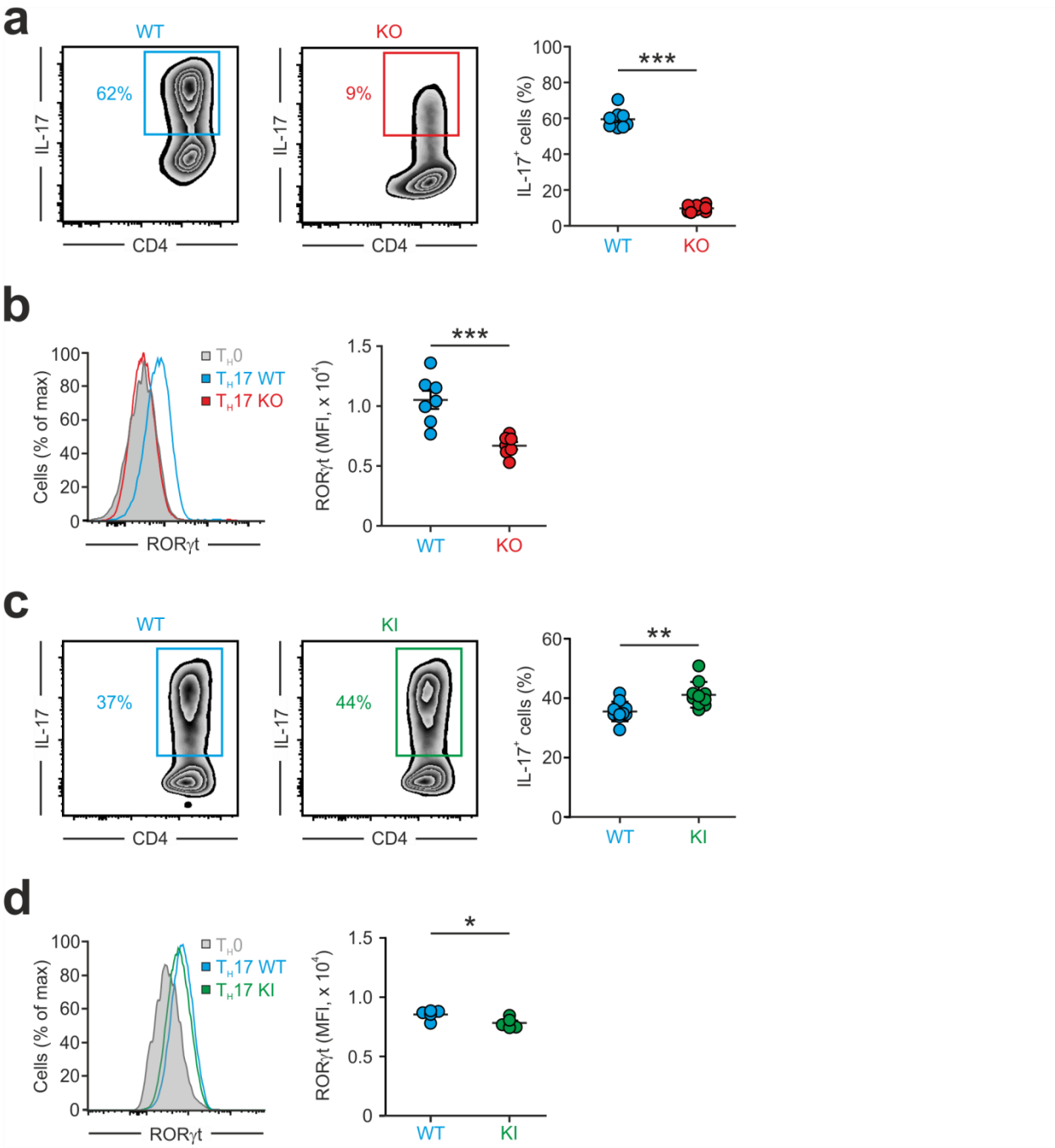

Figure 14: Satb1 is required for the differentiation of T_H17 cells.
Satb1-wildtype, -deficient and -overexpressing naive $CD4^+$ T cells were isolated by flow cytometric cell sorting and *in vitro* differentiated into T_H17 cells. At day five of differentiation, cells were analyzed by flow cytometry. **(a,b)** Analysis of IL-17 **(a)** and RORγt **(b)** expression in WT and KO cells. **(c,d)** The percentage of $IL\text{-}17^+$ cells **(c)** and analysis of RORγt expression **(d)** in WT and KI cells. (a) n=8, (b) n=7 (c) n=10, (d) n =5, mean ± SEM, unpaired Student's t-test. Data were pooled from two to three independent experiments.

4.2.5. iTreg cell differentiation

It is known that Satb1 is downregulated in mature pTreg cells, which is a prerequisite for their suppressive function (Beyer et al., 2011; Kitagawa et al., 2017; Kondo et al., 2016). To determine how Satb1 influences the differentiation process of pTreg cells, wildtype, Satb1-deficient as well as -overexpressing naive $CD4^+$ T cells were differentiated into iTreg cells *in vitro*. Similar Foxp3 expression was observed at day five of differentiation between wildtype and Satb1-deficient $CD4^+$ T cells (Figure 15a). *Satb1* expression was downregulated on mRNA level in the early phase during iTreg cell differentiation in wildtype cells (Figure 6a). Thus, similar as in T_H1 cells, the effect of Satb1 deletion might be masked on day five and it might be necessary to assess the induction of iTreg cell at an earlier time point to faithfully determine the role of Satb1 for iTreg cell differentiation. Indeed, at day three of differentiation, an increase in the percentage of Foxp3-expressing cells was detected when

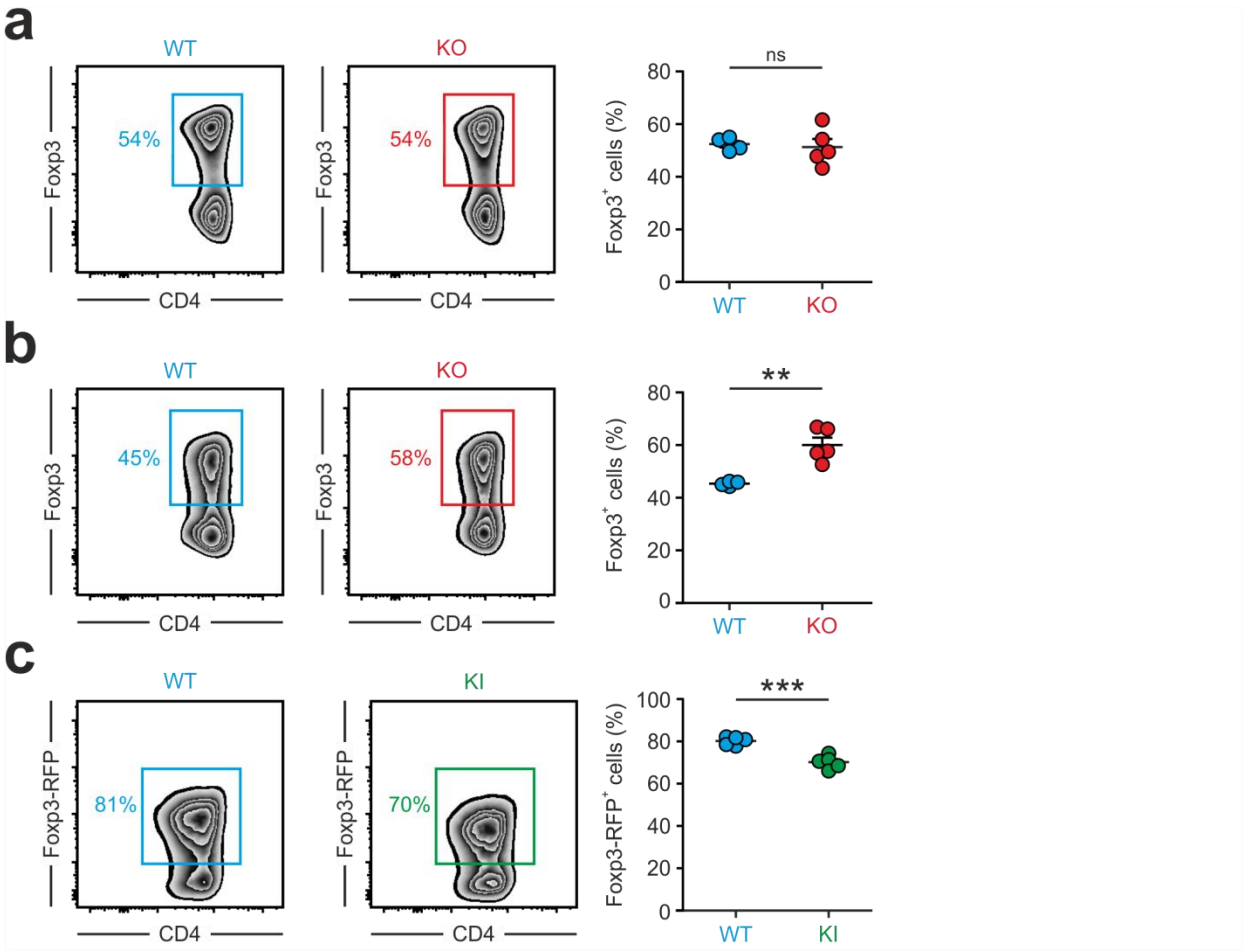

Figure 15: Satb1 impairs the differentiation of iTreg cells.
Satb1-wildtype (WT), -deficient (KO) and -overexpressing (KI) naive T cells were isolated by flow cytometric cell sorting and differentiated *in vitro* into iTreg cells. **(a,b)** The percentage of Foxp3-producing cells was analyzed by flow cytometry in WT and KO cells at day five **(a)** and day three **(b)**. **(c)** Analysis of Foxp3-RFP expression in WT and KI cells at day five was determined by flow cytometry. (a,b) n=4-5, (c) n=5, mean ± SEM, unpaired Student's t-test.

Satb1 was deleted, indicating that the loss of Satb1 facilities the development of iTreg cells (Figure 15b). In line with this, overexpression of Satb1 resulted in a slight reduction in iTreg cell differentiation at three (not shown) and day five (Figure 15c). Thus, downregulation of Satb1 in wildtype cells during iTreg cell differentiation improves the differentiation capability.

Taken together, Satb1 plays an important role in the differentiation of all $CD4^+$ T cell subsets in *vitro*. On the one hand, Satb1 fosters the differentiation of T_H9 and T_H17 cells, while on the other hand loss of Satb1 improves T_H1 and iTreg cell differentiation. In addition a tight regulation of Satb1 is important for the generation of T_H2 cells.

4.3. Satb1 regulates the development of T_H1 and T_H17 cells *in vivo* under homeostatic conditions

As Satb1 regulates the differentiation of naive $CD4^+$ T cells *in vitro*, it is likely that Satb1 also controls the differentiation potential *in vivo*. To verify this, the influence of Satb1 on the composition of the effector pool was assessed under homeostatic conditions. Therefore, heterozygous R26-STOP-Satb1 mice as well as homozygous $Satb1^{fl/fl}$ mice were crossed to CD4-Cre mice and cytokine expression of effector $CD4^+CD44^+$ T cells was determined. As a more pronounced phenotype is expected with age, mice older than 24 weeks were characterized.

When analyzing heterozygous R26-STOP-Satb1/CD4-Cre, a slightly increased development of $CD4^+CD44^+$ effector cells was observed in the spleen (Figure 16a). Within this effector cell pool, cells expressed more IL-17 as well as IFN-γ (Figure 16b,c).

In addition, upon deletion of Satb1 in $CD4^+$ T cells, the development of $CD4^+CD44^+$ effector T cells was significantly increased in the spleen of aged animals (Figure 17a). In line with the findings observed during *in vitro* differentiation, a reduction in the percentage of IL-17-producing cells (Figure 17b) as well as a more pronounced development of IFN-γ-producing cells (Figure 17c) was established within the effector T cell population.

Together, these data indicate a critical role of Satb1 in the differentiation of $CD4^+$ T cells not only *in vitro* but also *in vivo*. Furthermore, the differentiation profile of T_H17 cells was consistent *in vitro* and *in vivo* in both Satb1-overexpressing and -deficient cells, indicating that Satb1 is a key driver of T_H17 cell differentiation. In contrast, the role of Satb1 in T_H1 cells is more ambiguous. While overexpression of Satb1 diminishes the differentiation of T_H1 cells *in vitro*, an increased differentiation was observed *in vivo* both upon deletion and

overexpression of Satb1. To resolve this discrepancy, the role of Satb1 in T_H1 cell development needs to be further characterized.

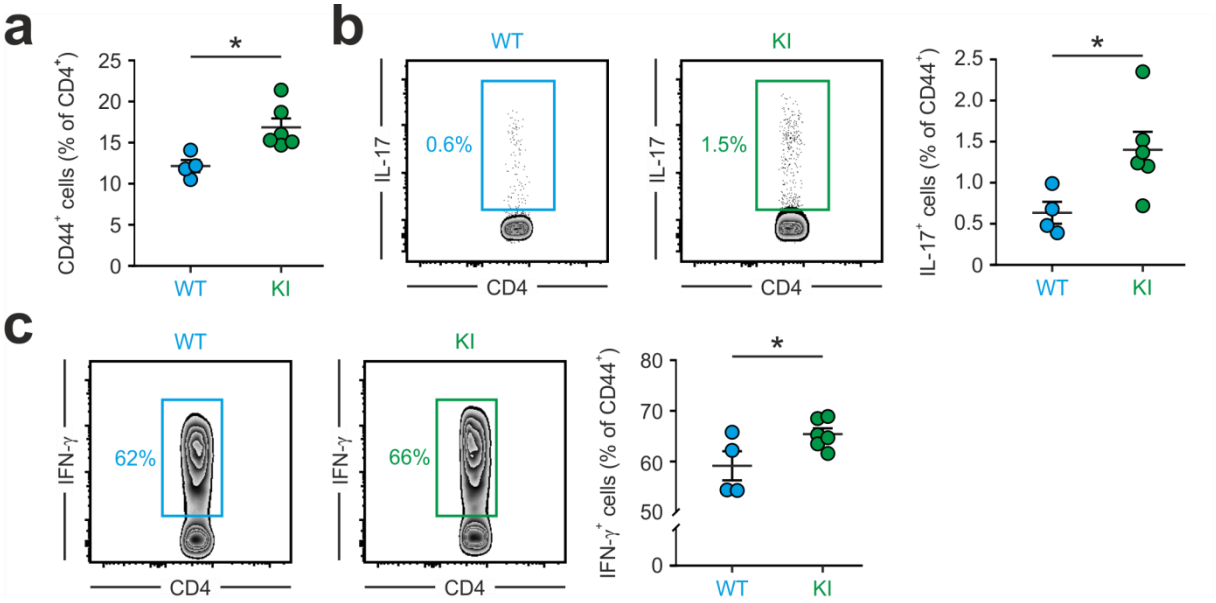

Figure 16: Overexpression of Satb1 in CD4$^+$ T cells results in an increased splenic T_H17 and T_H1 cell differentiation.
Flow cytometric analysis of Satb1-wildtype (WT) and heterozygous Satb1-overexpressing (KI) splenic T cells of middle-aged (27-30 weeks old) mice. **(a)** Quantification of CD44$^+$ effector/memory CD4$^+$ T cells. **(b,c)** Quantification of IL-17-producing **(b)** as well as IFN-γ-producing cells **(c)** within the effector/memory pool. (a-c) n=4-6, mean ± SEM, unpaired Student's t-test.

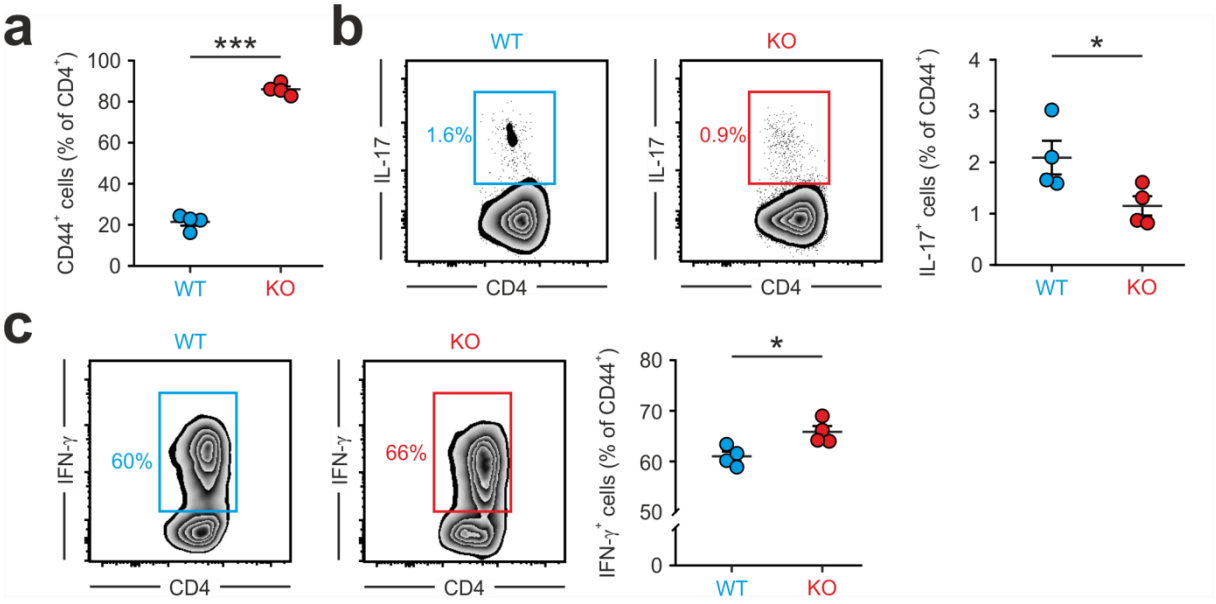

Figure 17: Deletion of Satb1 in CD4$^+$ T cells results in a reduced splenic T_H17 and increased T_H1 cell differentiation.
Flow cytometric analysis of Satb1-sufficient and -deficient splenic T cells of 44-60 weeks old Satb1$^{fl/fl}$/CD4-Cre$^{wt/wt}$ (WT) or Satb1$^{fl/fl}$/CD4-Cre$^{wt/+}$ (KO) mice. **(a)** Quantification of CD44$^+$ effector/memory CD4$^+$ T cells. **(b,c)** Quantification of IL-17-producing **(b)** as well as IFN-γ-producing cells **(c)** within the effector/memory pool. (a-c) n=4, mean ± SEM, unpaired Student's t-test.

4.4. Satb1 is involved in T_H17 cell pathogenicity

So far the data supported that Satb1 appears to be a positive regulator of T_H17 cell differentiation. Since their first description in 2005, it has become clear that T_H17 cells are important in host defense and that dysregulation of T_H17 cells is associated with inflammatory disorders, such as autoimmune diseases (Harrington et al., 2005; Korn et al., 2009; Langrish et al., 2005; Park et al., 2005; Zambrano-Zaragoza et al., 2014). To further decipher the functional impact of Satb1 during the differentiation of $CD4^+$ T cells, the differentiation capability of Satb1-deficient naive $CD4^+$ T cells was addressed under pathogenic conditions *in vivo*. Diseases in which T_H17 cells play an important role are autoimmune diseases, including chronic intestinal bowel diseases like Crohn's disease and ulcerative colitis (Ahern et al., 2010; Annunziato et al., 2007; Leppkes et al., 2009; Yen et al., 2006). In addition to T_H17 cells, T_H1 cells are also linked to chronic intestinal inflammation, while Treg cells are anti-inflammatory and protective (Brand, 2009).

One model for chronic intestinal inflammation is the adoptive transfer colitis model. Here, naive $CD4^+$ T cells are transferred into $Rag2^{-/-}$ recipient mice (Appendix Figure 66f), which do not contain any host B or T cells since they lack the V(D)J recombination activity (Powrie et al., 1993; Shinkai et al., 1992). Injected naive $CD4^+$ T cells become activated by enteric antigens, resulting in the polarization into antigen-specific effector T cells followed by cell expansion and intestinal inflammation (Ostanin et al., 2009). Especially the differentiation into pathogenic T_H17 cells results in disease formation (Ahern et al., 2010).

One advantage of the adoptive transfer colitis model is that the differentiation of naive $CD4^+$ T cells can be studied in a controlled disease setting. The differentiation of T_H17, T_H1 and Treg cells can be investigated and the functional impact of Satb1 in these cells on intestinal diseases can be addressed.

Previous work performed by Daniel Sommer showed that $Rag2^{-/-}$ mice injected with Satb1-deficient naive $CD4^+$ T cells are resistant to colitis development (Sommer, 2018). He observed a reduced proliferation of $CD4^+$ T cells in mesenteric lymph nodes (mLN), the draining LN of the intestine, of $Rag2^{-/-}$ mice injected with Satb1-deficient naive $CD4^+$ T cells and found less IL-17^+IFN-γ^+ pathogenic T_H17 cells in mLN.

In this thesis, $Rag2^{-/-}$ mice injected with Satb1-sufficient or -deficient naive $CD4^+$ T cells were further characterized and the differentiation of naive $CD4^+$ T cells was analyzed at the time point when the experiment had to be terminated (Figure 18a). Indeed, when transferring Satb1-deficient naive $CD4^+$ T cells into $Rag2^{-/-}$ mice, these animals were protected from colitis development. $Rag2^{-/-}$ mice injected with Satb1-deficient naive $CD4^+$ T cells did not

show any disease symptoms, such as weight loss (Figure 18b) or increased cell infiltration and tissue damage of the colon (Figure 18c), in contrast to mice injected with Satb1-sufficient naive $CD4^+$ T cells. Furthermore, enlarged spleens in $Rag2^{-/-}$ mice injected with Satb1-sufficient naive $CD4^+$ T cells were observed, unlike when Satb1-deficient cells were injected, indicating a reduced expansion of Satb1-deficient $CD4^+$ cells (Figure 18d).

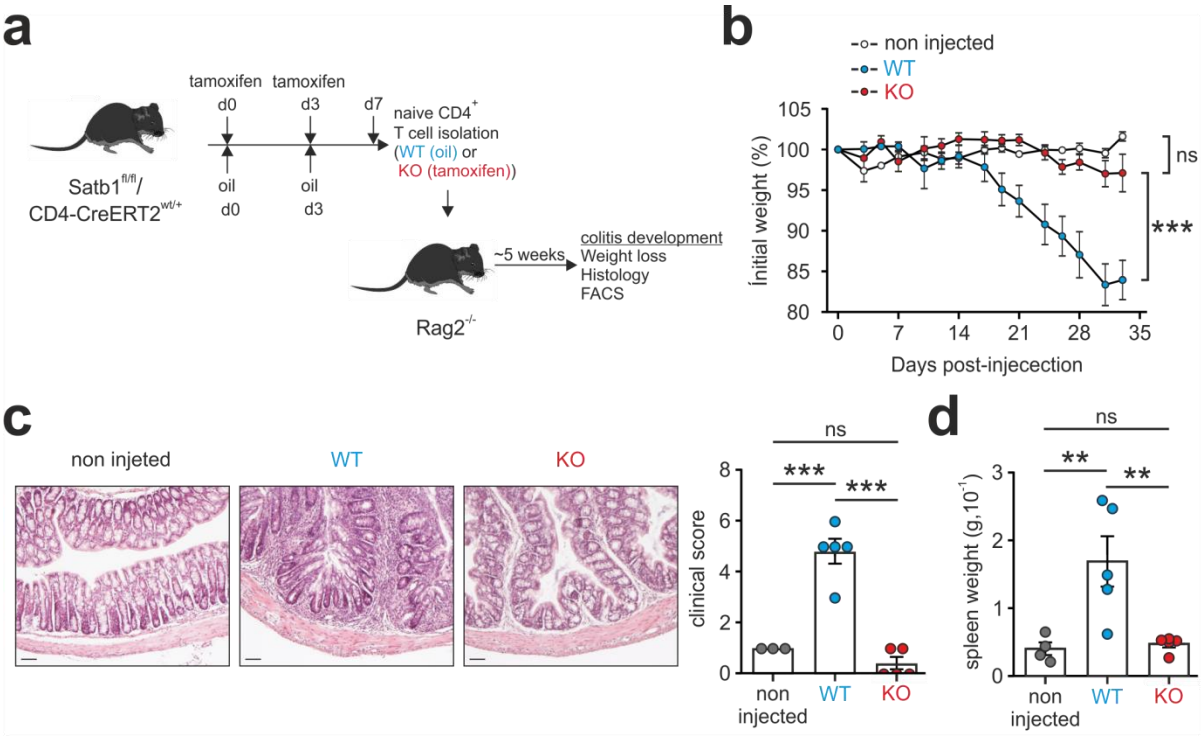

Figure 18: Deletion of Satb1 in $CD4^+$ T cells prevents the development of colitis in the adoptive transfer colitis model.
(a) Schematic overview of the adoptive transfer colitis model. **(b)** Weight curve of $Rag2^{-/-}$ mice injected with Satb1-sufficient or -deficient naive $CD4^+$ T cells. **(c)** Representative hematoxylin and eosin staining of colon section at the time point when the experiment had to be terminated (left) and histological score thereof (right). Histology and corresponding analysis was performed in the Institute for Pathology, University Hospital Halle in collaboration with Prof. Dr. Claudia Wickenhauser. **(d)** Weight of spleens at the time point when the experiment had to be terminated. (b,d) n=4-5, (c) n=3-5, mean ± SEM, (b) two-way repeated measures ANOVA with Tukey's multiple comparison test, (c,d) one-way ANOVA with Tukey's multiple comparison test. (b) Data were shown from one representative experiment, which was repeated at least three times.

Thus, subsequently $CD4^+$ T cell numbers and the expression of the proliferation marker Ki-67 were evaluated. Fewer Satb1-deficient $CD4^+$ T cells were observed in the spleen and mLN of $Rag2^{-/-}$ mice (Figure 19a,b). Additionally, $CD4^+$ cells in the intestine were analyzed and a clearly reduced infiltration of $CD4^+$ T cells both in the colon and small intestine was observed (Figure 19c,d). Furthermore, Satb1-deficient cells showed less expression of the proliferation

marker Ki-67, both in spleen and mLN (Figure 20a,b), indicating an overall reduced proliferation of Satb1-deficient CD4$^+$ T cells in Rag2$^{-/-}$ mice.

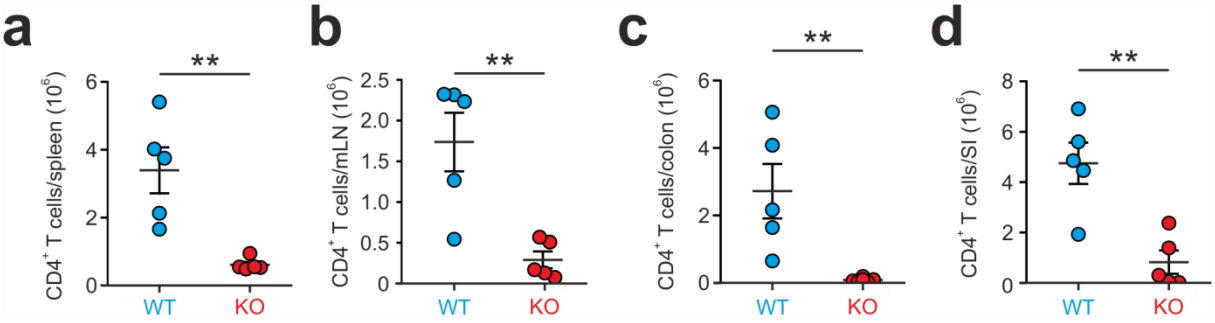

Figure 19: Satb1-deficient CD4$^+$ T cells accumulate less in Rag2$^{-/-}$ mice after transfer.
Quantification of absolute cell numbers of CD4$^+$ T cells in spleen **(a)**, mLN **(b)**, colon **(c)** and small intestine **(d)** by flow cytometry. Rag2$^{-/-}$ mice were either injected with Satb1-sufficient or -deficient naive CD4$^+$ T cells. mLN, mesenteric lymph nodes; SI, small intestine. (a,b,d) n=5, (c) n=5-6, mean ± SEM, unpaired Student's t-test. (a,b) Data are representative of at least three independent experiments.

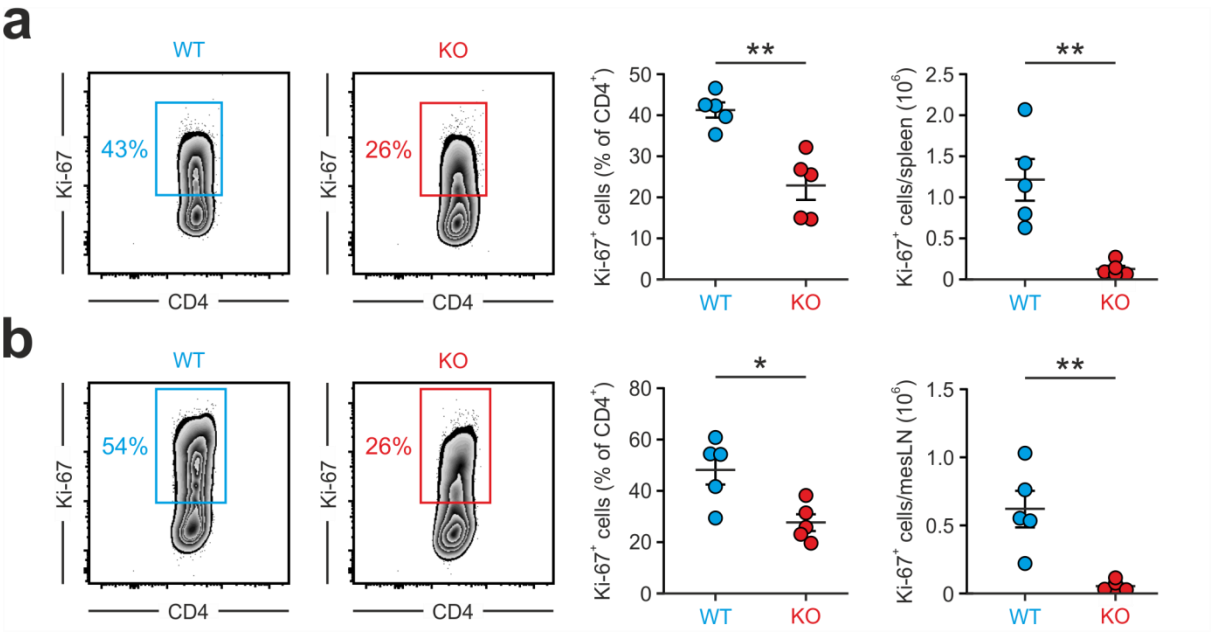

Figure 20: Satb1-deficient CD4$^+$ T cells proliferate less after injection into Rag2$^{-/-}$ mice.
Quantification of Ki-67 expression of CD4$^+$ T cells in spleen **(a)** and mLN **(b)** by flow cytometry. Rag2$^{-/-}$ mice were either injected with Satb1-sufficient or -deficient naive CD4$^+$ T cells. n=5, mean ± SEM, unpaired Student's t-test. Data are representative of at least three independent experiments.

Next, the activation marker CD25 was analyzed. Only a small population of splenic CD4$^+$ T cells in Rag2$^{-/-}$ mice expressed CD25 after injection of either Satb1-sufficient or -deficient naive CD4$^+$ T cells. However, still fewer CD25$^+$ T cells were detected in the spleen when Satb1 was deleted (Figure 21a). In contrast, increased CD25 expression was observed in the mLN in Rag2$^{-/-}$ mice injected with Satb1-sufficient naive CD4$^+$ T cells, which was clearly

reduced when Satb1 was deleted before injection (Figure 21b). Thus, Satb1-deficient CD4$^+$ T cell were less activated than Satb1-sufficient CD4$^+$ T cells, especially in proximity to the site of inflammation.

Taken together, these data indicate that Satb1-deficient CD4$^+$ T cells injected into Rag2$^{-/-}$ mice are less activated and show lower proliferation which resulted in a reduced cell expansion and decreased intestinal infiltration.

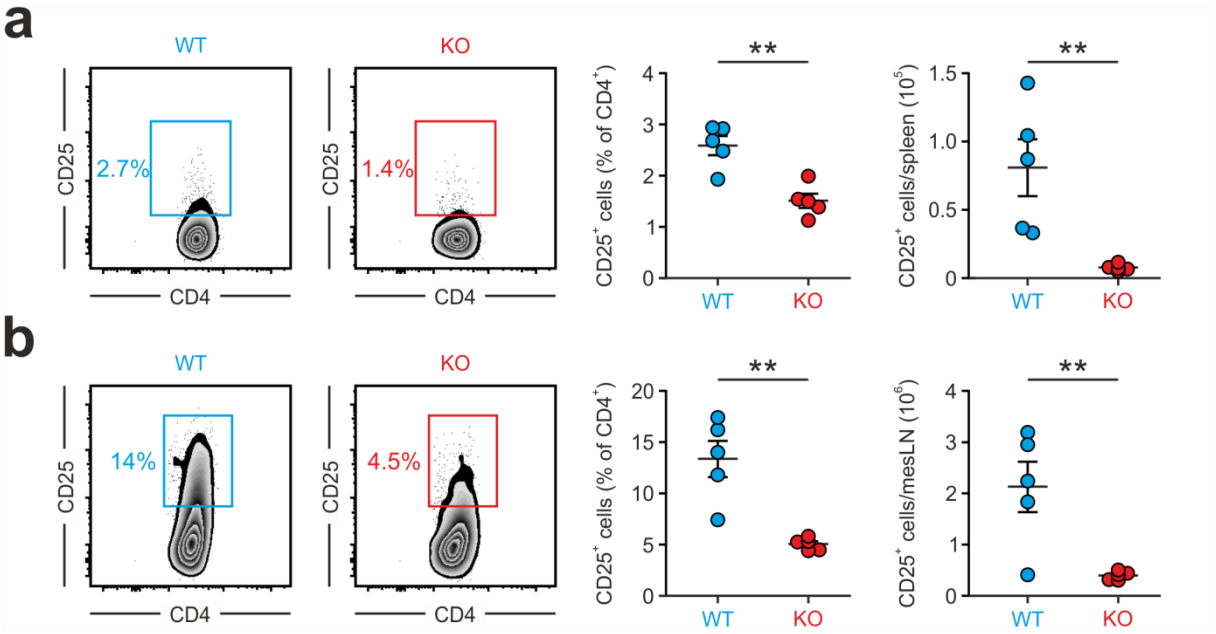

Figure 21: Satb1-deficient CD4$^+$ T cells show reduced CD25 expression when transferred into Rag2$^{-/-}$ mice.

Quantification of CD25 expression in CD4$^+$ T cells in the spleen **(a)** and mLN **(b)** of Rag2$^{-/-}$ mice injected with Satb1-sufficient or -deficient naive CD4$^+$ T cells by flow cytometry. n=5, mean ± SEM, unpaired Student's t-test. Data are representative of at least three independent experiments.

Reduced cell expansion and infiltration can be caused by enhanced differentiation of naive CD4$^+$ T cells into pTreg cells, which might subsequently prevent disease formation, or by intrinsically reduced pathogenic CD4$^+$ T cell differentiation, similarly resulting in a decreased clonal expansion. Moreover, downregulation of Satb1 is known to play an important role for the formation and function of iTreg cells (Beyer et al., 2011) and an increased iTreg cell development was observed early in the *in vitro* differentiation when naive CD4$^+$ T cells lack Satb1 (Figure 15b). To study whether the reduced inflammation in Rag2$^{-/-}$ mice is a consequence of an enhanced pTreg cell differentiation caused by the loss of Satb1, Foxp3 expression was analyzed. Although a slight increase in the percentage of Foxp3-expressing cells was observed in spleen, mLN and colon in Rag2$^{-/-}$ mice injected with Satb1-deficient CD4$^+$ T cells, the total percentages were very low (Figure 22a-c). Furthermore, the total number of Foxp3$^+$CD4$^+$ T cells was reduced in Rag2$^{-/-}$ mice injected with Satb1-deficient

$CD4^+$ T cells (Figure 22a-c). Thus, it is highly unlikely that Treg cells are the key drivers preventing the development of colitis when Satb1-deficient naive $CD4^+$ T cells are transferred.

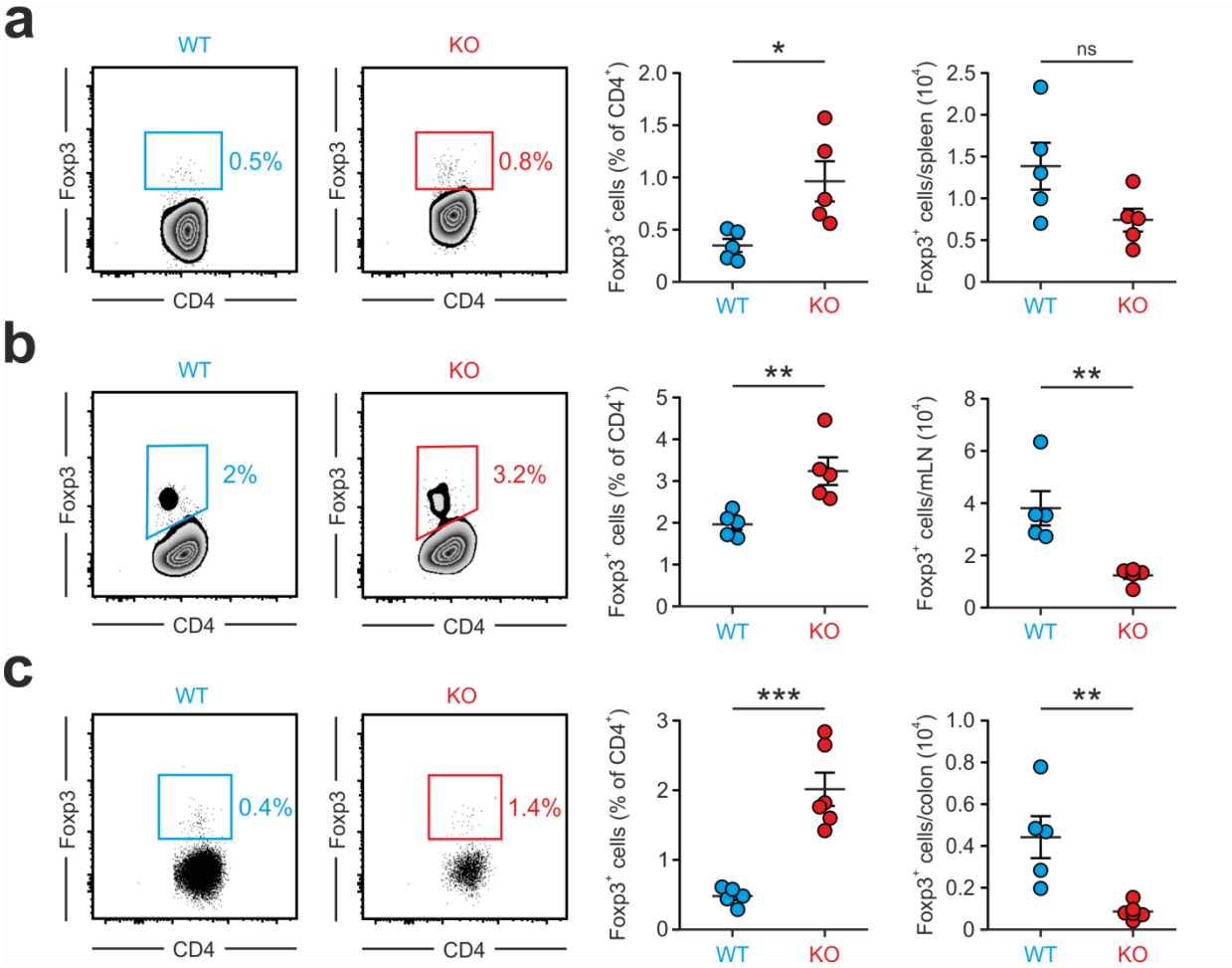

Figure 22: Neglectable induction of pTreg cells in the adoptive transfer colitis model.
Flow cytometric analysis of $Rag2^{-/-}$ mice injected with Satb1-sufficient or -deficient naive $CD4^+$ T cells. The percentage and total numbers of $CD4^+Foxp3^+$ cells was evaluated in the spleen **(a)**, mLN **(b)** and colon **(c)**. (a,b) n=5, (c) n=5-6, mean ± SEM, unpaired Student's t-test. (a,b) Data are representative of at least three independent experiments.

Since neither Satb1-sufficient nor Satb1-deficient naive $CD4^+$ T cells highly differentiation into Treg cells in the $Rag2^{-/-}$ mice, it can be hypothesized that Satb1 might instead influence the differentiation into T_H1 and T_H17 effector cells.

In the last years, T_H17 cells were further subdivided into non-pathogenic as well as pathogenic T_H17 cells (Figure 3) (Lee et al., 2012) and chronic intestinal inflammation was linked in particular to pathogenic T_H17 cells (Ahern et al., 2010). Thus, differentiation of naive $CD4^+$ T cells into non-pathogenic IL-17^+IFN-γ^- and pathogenic IL-17^+IFN-γ^+ T_H17 cells as well as IL-17^-IFN-γ^+ T_H1 cells was studied. Significantly fewer pathogenic IL-17^+IFN-γ^+ as well as non-pathogenic IL-17^+IFN-γ^- T_H17 cells were detected in the spleen

and mLN of $Rag2^{-/-}$ mice injected with Satb1-deficient $CD4^+$ T cells compared to animals injected with Satb1-sufficient T cells $CD4^+$ (Figure 23a,b). In contrast to T_H17 cells, the percentage of IL-17^-IFN-γ^+ T_H1 cells did not differ between $Rag2^{-/-}$ mice injected with Satb1-sufficient or -deficient $CD4^+$ T cells although frequencies were reduced both in spleen and mLN (Figure 23a,b). Interestingly, when the differentiation of T_H17 cells was assessed in the colon, an increased percentage of both IL-17^+IFN-γ^- non-pathogenic and IL-17^+IFN-γ^+ pathogenic T_H17 cells could be detected in animals injected with Satb1-deficent $CD4^+$ T cells, while the percentage of IL-17^-IFN-γ^+ T_H1 cells was reduced (Figure 24a). This result suggests that Satb1 deficiency does not completely prevent the differentiation of T_H17 cells. However, as the total numbers of colon infiltrating $CD4^+$ T cells were dramatically lower in $Rag2^{-/-}$ mice injected with Satb1-deficient cells (Figure 19c), the numbers of T_H17 cells and T_H1 cells in the colon were reduced within these animals as well (Figure 24b). Thus, these data support that Satb1 deficiency reduces pathogenic cell differentiation resulting in a reduced systemic inflammation, which prevents subsequent intestinal inflammation although a residual induction of T_H17 cells in the large intestine was possible.

Indeed, a more detailed characterization of cytokine expression revealed a reduced differentiation into polyfunctional $CD4^+$ T cells in the spleen and mLN when Satb1 is lost (Figure 25a,b). Expression of IFN-γ, IL-17 and TNF-α was analyzed and expression of single or multiple cytokines was determined. Satb1-deficient $CD4^+$ T cells were prone to express none or only a single of these cytokine compared to Satb1-sufficient $CD4^+$ T cells, which polarized into polyfunctional T cells both in spleen and mLN (Figure 25a,b). Furthermore, this analysis could confirm that especially pathogenic IL-17^+IFN-γ^+TNF-α^- and IL-17^+IFN-γ^+TNF-α^+ T_H17 cells did not develop in the spleen and mLN when Satb1-deficient $CD4^+$ T cells were transferred (Figure 25a,b). In contrast, the development of polyfunctional $CD4^+$ T cells was still observed in the colon (Figure 25c). However, due to the reduced cell numbers of pathogenic cells, Satb1-deficient cells were not capable to induce intestinal inflammation.

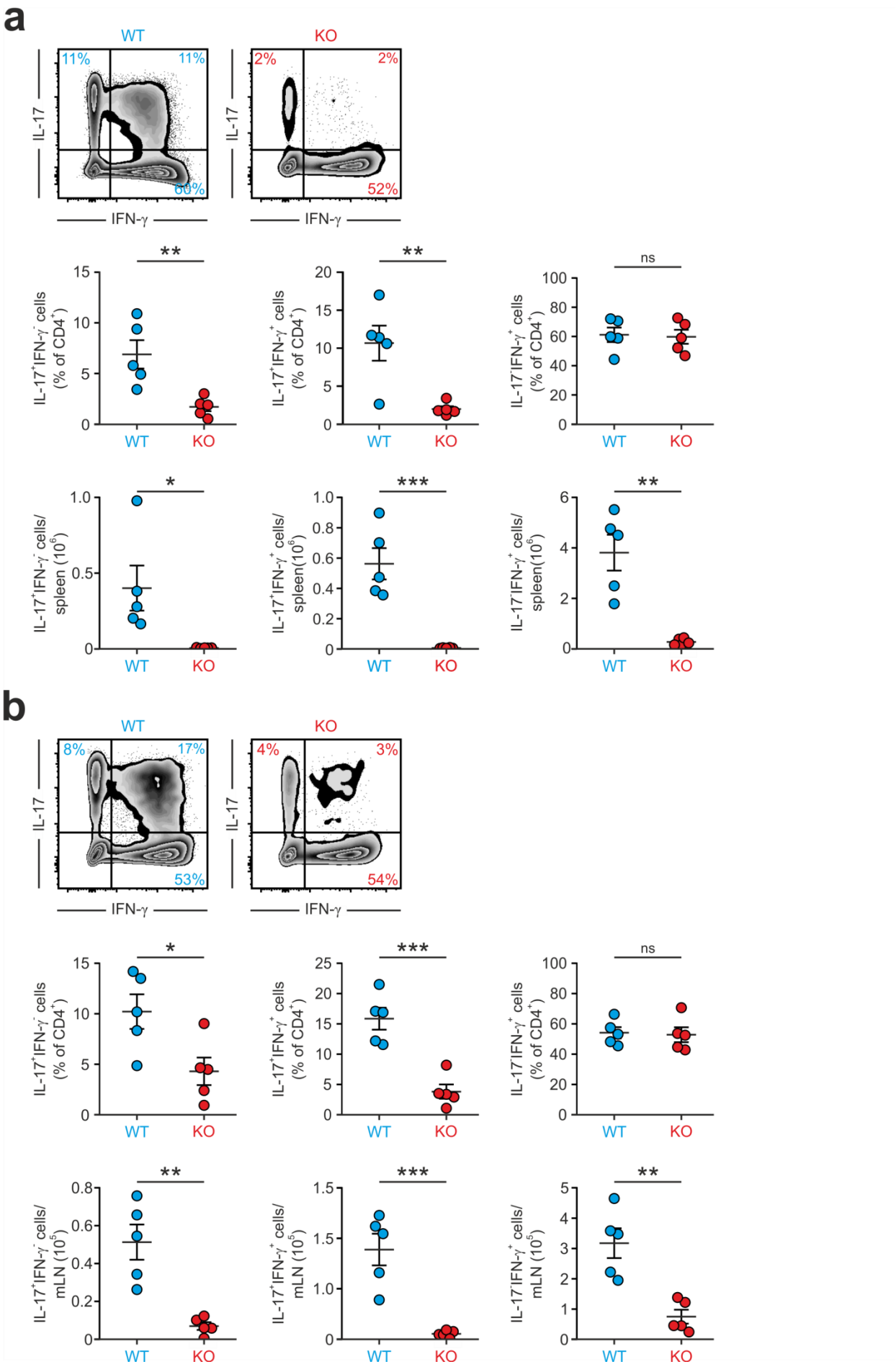
a
WT
KO
11%
11%
66%
2%
2%
52%
IL-17
IFN-γ
IL-17+IFN-γ- cells (% of CD4+)
IL-17+IFN-γ+ cells (% of CD4+)
IL-17-IFN-γ+ cells (% of CD4+)
IL-17+IFN-γ- cells/ spleen (10^6)
IL-17+IFN-γ+ cells/ spleen(10^6)
IL-17-IFN-γ+ cells/ spleen(10^6)
**
*
***
ns
b
8%
17%
53%
4%
3%
54%
IL-17+IFN-γ- cells/ mLN (10^5)
IL-17+IFN-γ+ cells/ mLN (10^5)
IL-17-IFN-γ+ cells/ mLN (10^5)

Figure 23: Satb1-deficient CD4$^+$ T cells fail to differentiate into non-pathogenic and pathogenic T_H17 cells in the adoptive transfer colitis model.
Flow cytometric analysis of Rag2$^{-/-}$ mice injected with Satb1-sufficient or -deficient CD4$^+$ T cells. Quantification of IFN-γ and IL-17 expression in the spleen **(a)** and mLN **(b)**. n=5, mean ± SEM, unpaired Student's t-test. Data are representative of at least three independent experiments.

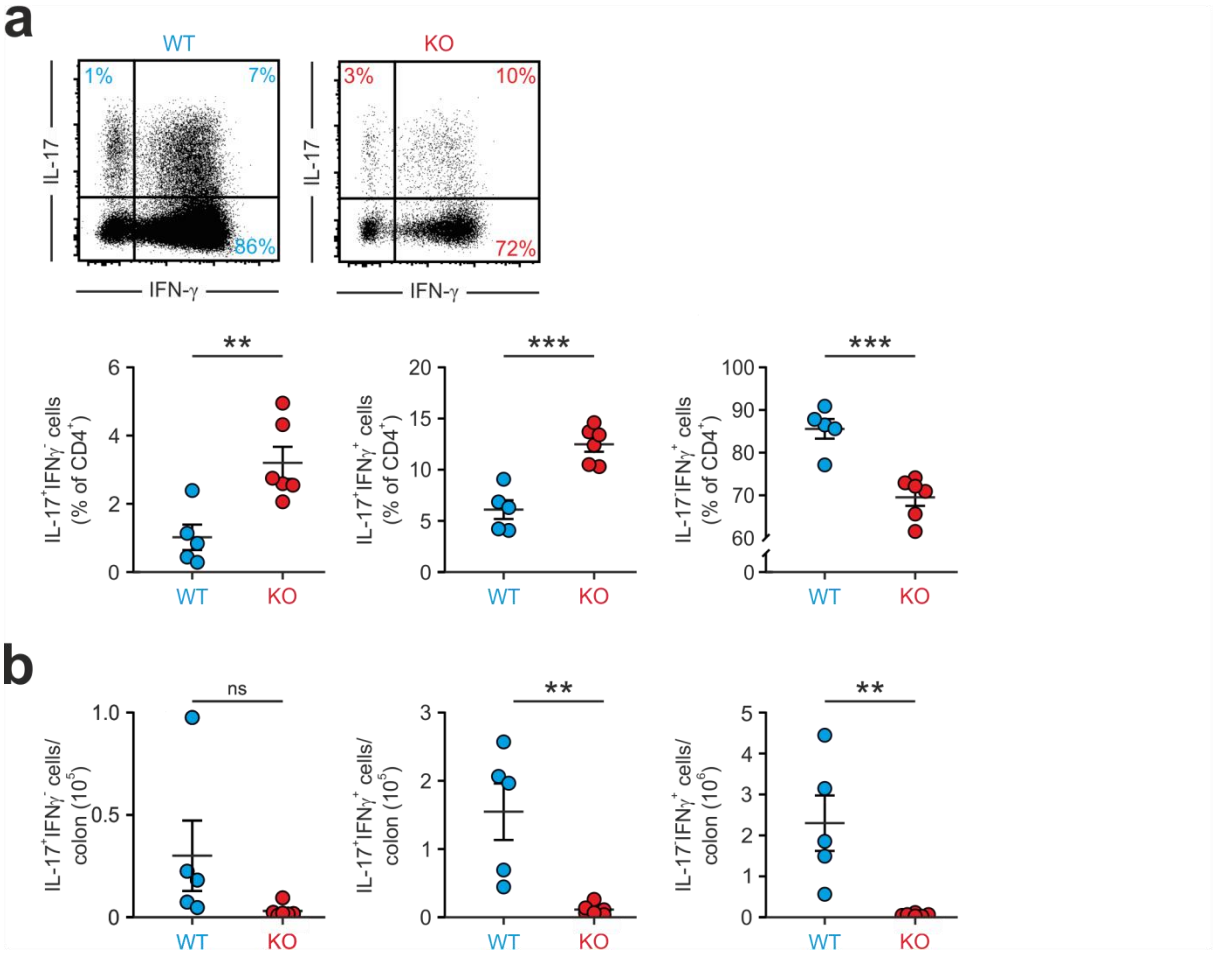

Figure 24: Satb1-deficient CD4$^+$ T cells can differentiate into T_H17 cells in the colon in the adoptive transfer colitis model.
Flow cytometric analysis of Rag2$^{-/-}$ mice injected with Satb1-sufficient or -deficient CD4$^+$ T cells. Quantification of IFN-γ and IL-17 expression in the colon in percentage **(a)** and total numbers **(b)**. n=5-6, mean ± SEM, unpaired Student's t-test.

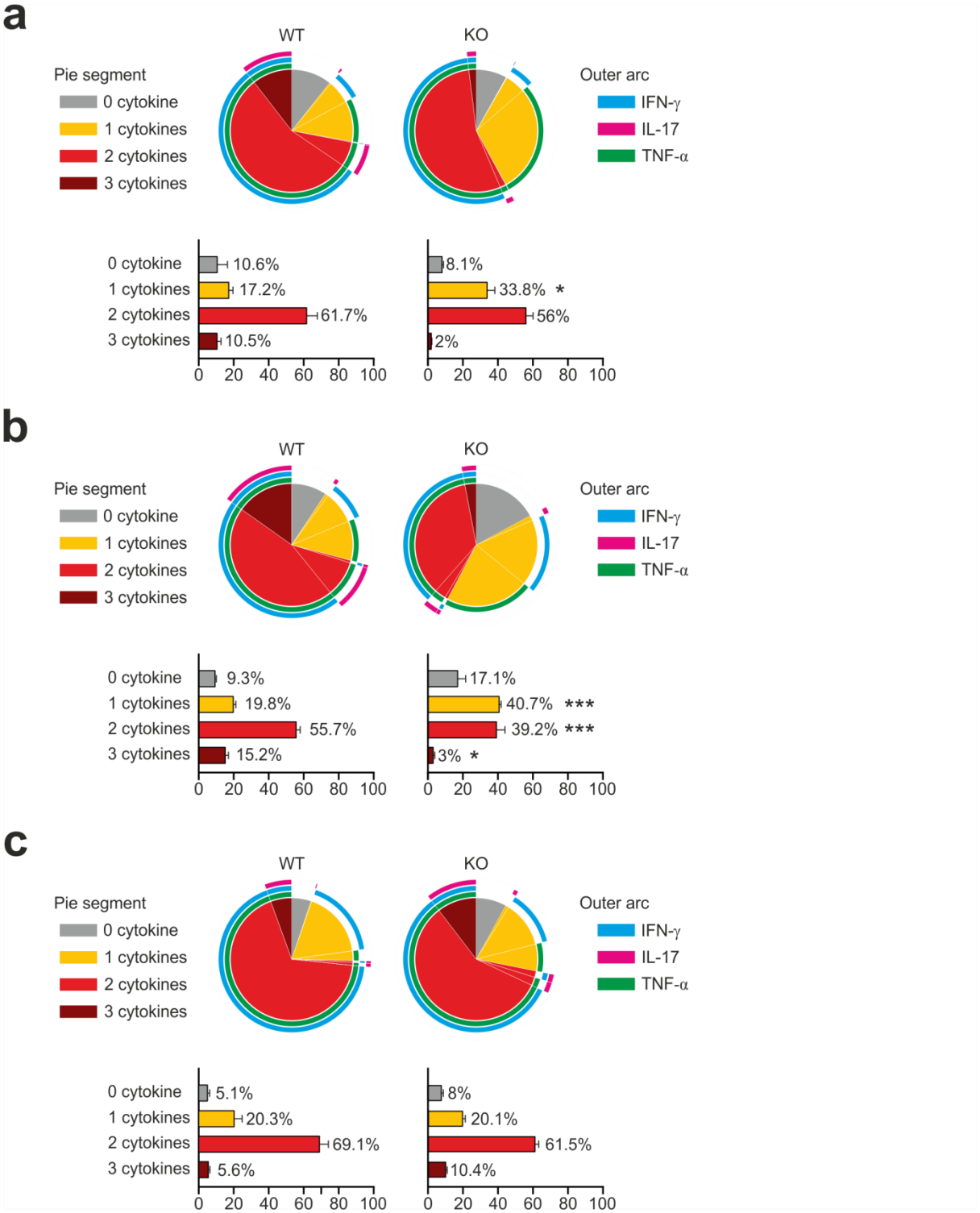

Figure 25: Reduced differentiation of Satb1-deficient naive CD4$^+$ T cells into polyfunctional CD4$^+$ T cells after injection into Rag2$^{-/-}$ mice.

Flow cytometric analysis of Rag2$^{-/-}$ mice injected with Satb1-sufficient or –deficient CD4$^+$ T cells. Quantification of IFN-γ, IL-17 and TNF-α expression in spleen **(a)**, mLN **(b)** and colon **(c)**. Pie segments represent polyfunctional cytokine expression (left key) and the outer arcs indicate the composition of the respective cytokines (right key). (a-b) n=5, (c) n=5-6, mean ± SEM, two-way ANOVA with Sidak's multiple comparison test. (a,b) Data are representative of at least three independent experiments.

Since T_H17 cells are known to recruit myeloid cells and especially neutrophils to sites of inflammation (Gaffen, 2008), their presence in the spleen, mLN as well as in the colon was quantified. Indeed, in $Rag2^{-/-}$ mice injected with Satb1-deficient $CD4^+$ T cells fewer $CD11b^+$ cells (Figure 26a) as well as fewer $Ly6G^+$ neutrophils (Figure 26b) were observed. The reduced recruitment of myeloid cells including neutrophils is consistent with decreased T_H17 cell development and overall reduced inflammation.

In summary, these results indicate that expression of Satb1 in $CD4^+$ T cells in the adoptive transfer colitis model is essential for disease development by intrinsically regulating pathogenic T_H17 cell development.

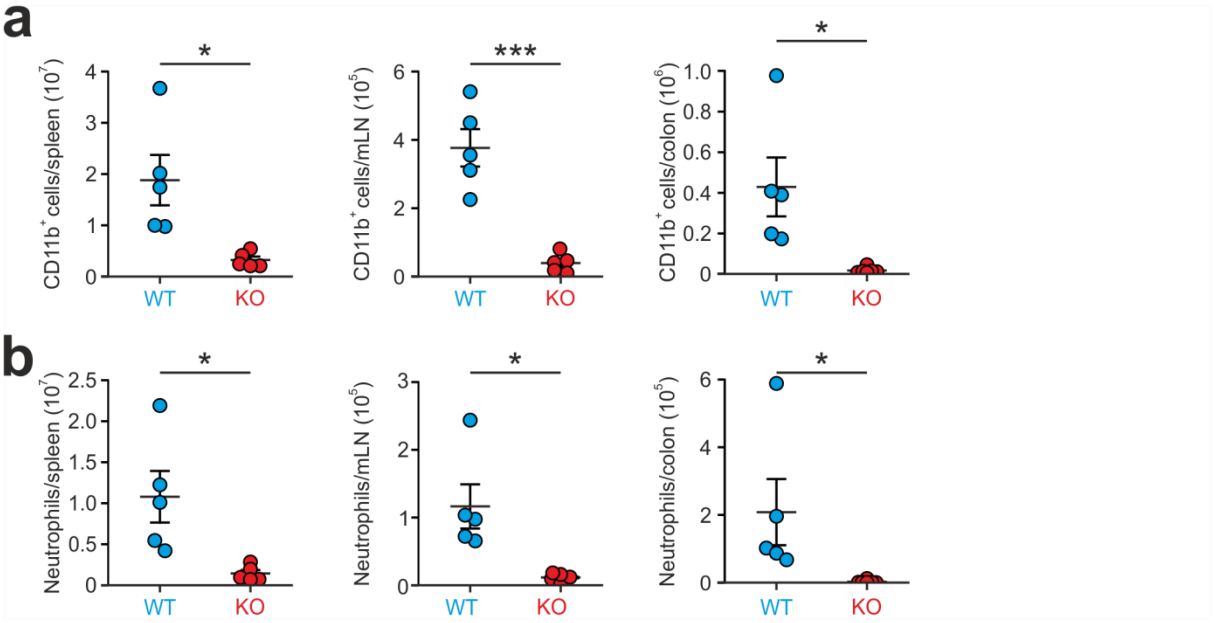

Figure 26: Reduced recruitment of myeloid cells in the adoptive transfer colitis model when Satb1 is deleted in $CD4^+$ T cells.
Quantification of absolute cell numbers of $CD11b^+$ myeloid cells **(a)** and $Ly6G^+$ neutrophils **(b)** in spleen, mLN and colon by flow cytometry. $Rag2^{-/-}$ mice were either injected with Satb1-sufficient or -deficient naive $CD4^+$ T cells. (a-b) n=5-6, mean ± SEM, unpaired Student's t-test**.** Spleen and mLN data are representative of at least three independent experiments.

Strikingly, Satb1 deficiency completely prevents the development of colitis in the adoptive transfer colitis model. To validate whether a loss of Satb1 in $CD4^+$ T cells generally prevents T_H17 cell-dependent disease formation, the impact of Satb1 deficiency was studied in an additional T_H17 cell-driven disease.

Another diseases in which pathogenic T_H17 cells play an important role is the autoimmune disease multiple sclerosis (Hirota et al., 2011; Kebir et al., 2009; Zambrano-Zaragoza et al., 2014). To further analyze the functional role of Satb1 in this disease, further experiments in

the experimental autoimmune encephalomyelitis (EAE) model, the murine model for multiple sclerosis, were performed.

An active immunization was used to cause EAE, in which mice were immunized with complete Freund's adjuvant (CFA) and myelin oligodendrocyte glycoprotein (MOG) 35-55 peptide to induce MOG-specific T cell development (Figure 27a). Furthermore, mice were injected with pertussis toxin to open the blood-brain barrier resulting in an infiltration of immune cells in the central nervous system (CNS) and inflammation as well as demyelination (Miller and Karpus, 2007). To study the development of EAE in relationship to the loss of Satb1, mice were treated with tamoxifen one week and three days before immunization to induce the deletion of Satb1 in $CD4^+$ T cells (Figure 27a). As tamoxifen is known to influence the development of EAE (Bebo et al., 2009), tamoxifen was administered to both $Satb1^{fl/fl}$/CD4-$CreERT2^{wt/wt}$ mice as WT control as well as to $Satb1^{fl/fl}$/CD4-$CreERT2^{wt/+}$ mice.

Interestingly, mice with Satb1-deficient $CD4^+$ T cells failed to develop EAE (Figure 27b,c). While mice with Satb1-sufficient $CD4^+$ T cells exhibited symptoms of paralysis as well as loss of weight, mice with Satb1-deficient $CD4^+$ T cells did not show any disease symptoms and only minimal weight loss subsequent to MOG_{35-55}/CFA immunization and pertussis toxin

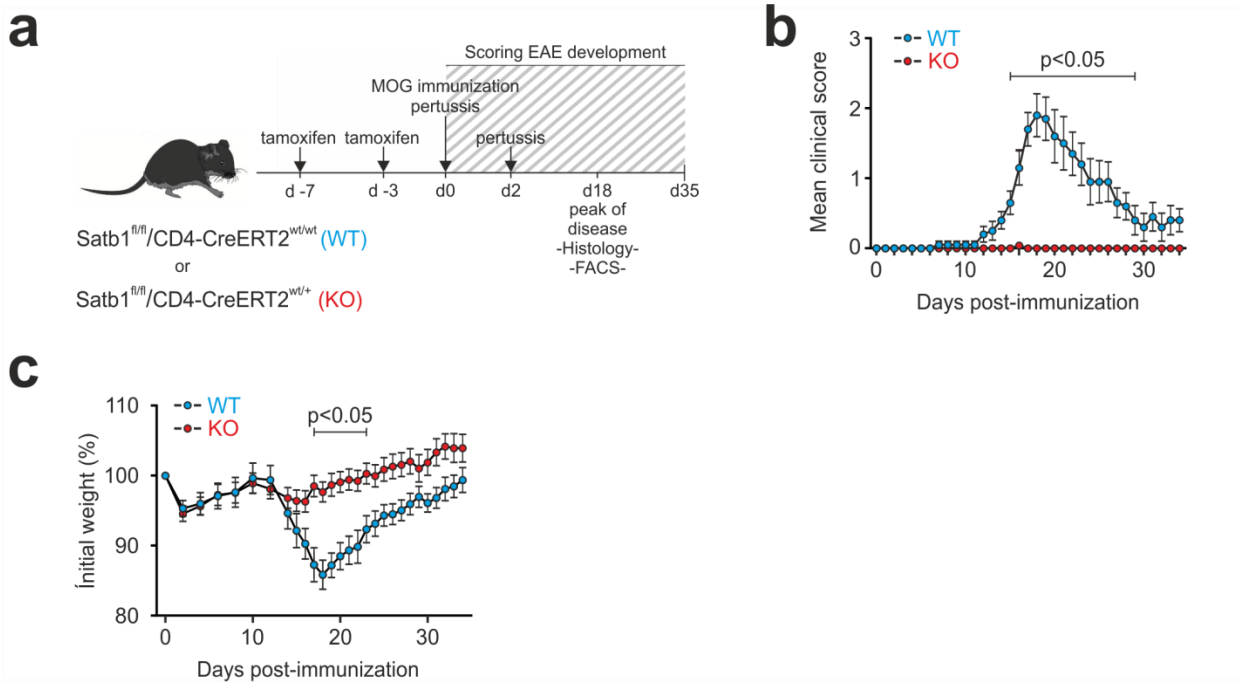

Figure 27: Mice with Satb1-deficient $CD4^+$ T cells fail to develop experimental autoimmune encephalomyelitis (EAE).

(a) Schematic overview of the EAE model. **(b)** Mean clinical score of EAE in mice with Satb1-sufficient or -deficient $CD4^+$ T cells and **(c)** the corresponding weight of these mice. MOG, Myelin oligodendrocyte glycoprotein. (b-c) n=10-12, mean ± SEM, two-way repeated measures ANOVA with Sidak's multiple comparison.

injection (Figure 27b,c). Thus, similar as observed in the adoptive transfer colitis model, disease development was prevented in the EAE model if $CD4^+$ T cells were deficient for Satb1.

Consistently, in mice with Satb1-deficient $CD4^+$ T cells only few immune cells infiltrated the CNS at the peak of disease (Figure 28a-c). An increased infiltration of $CD3^+$ T cells and $MAC3^+$ macrophages was observed in the spinal cord of EAE mice with Satb1-sufficient $CD4^+$ T cells by histological analyses (Figure 28a) as well as an increased infiltration of $CD4^+$ T cells in both the brain and spinal cord by flow cytometry (Figure 28b,c), which was not detectable in mice with Satb1-deficient $CD4^+$ T cells. Furthermore, histological staining of myelin revealed a demyelination after MOG_{35-55}/CFA immunization in EAE mice with Satb1-sufficient $CD4^+$ T cells at the peak of disease, which was barely detectable in animals lacking Satb1 in $CD4^+$ T cells (Figure 28d).

Taken together, these data indicate an essential role for Satb1 in $CD4^+$ T cells during EAE development.

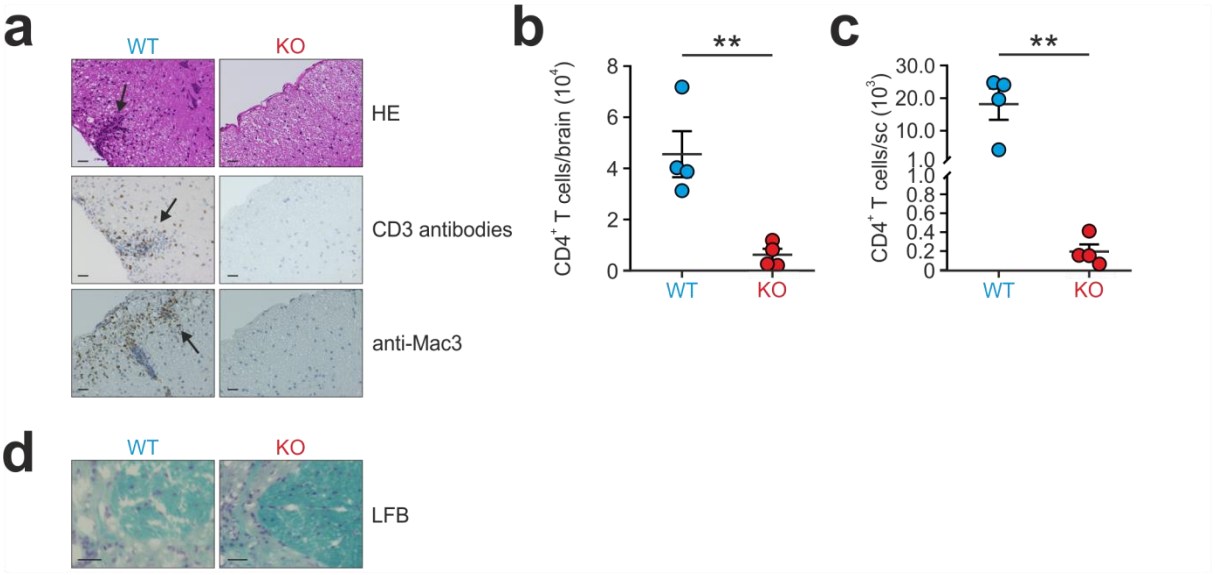

Figure 28: Low infiltration of Satb1-deficient $CD4^+$ T cells in the CNS during EAE.
(a) Representative hematoxylin and eosin (HE) (top), CD3 antibodies (middle) and anti-Mac3 (bottom) staining of spinal cord at the peak of EAE disease. Staining was performed in the Institute for Neuropathology, University of Münster in collaboration with Prof. Dr. Tanja Kuhlmann. **(b,c)** Quantification of absolute cell numbers of $CD4^+$ T cells in the brain **(b)** and in the spinal cord (sc) **(c)** at the peak of disease by flow cytometry. **(d)** Representative myelin staining with luxol fast blue (LFB) of spinal cord at the peak of disease. Staining was performed by Svenja Bourry. (b,c) n=4, mean ± SEM, unpaired Student's t-test.

To further investigate why mice with Satb1-deficient $CD4^+$ T cells are resistant to EAE, the $CD4^+$ T cell compartment and especially the differentiation into T_H cells were analyzed and analogies to the adoptive transfer colitis model were determined.

In cervical lymph nodes (cLN), the draining LN of the brain, similar frequencies of $CD44^+CD62L^-$ effector $CD4^+$ T cells were detected in both animals with Satb1-sufficient or -deficient $CD4^+$ T cells (Figure 29a). Furthermore, there was no significant difference in $CD25^+$ expression between Satb1-sufficient and -deficient $Foxp3^-$ Tconv cells in the cLN at the peak of disease, although a trend toward increased activation upon loss of Satb1 was observed (Figure 29b). In contrast, in the brain and spinal cord Satb1-deficient Tconv cells showed significantly less CD25 expression, and thus were less activated at the site of disease than their wildtype counterparts (Figure 29c,d). Thus, similar to the adoptive transfer colitis model deletion of Satb1 results in a reduced $CD4^+$ T cell infiltration and activation at the site of disease and thus loss of CNS inflammation.

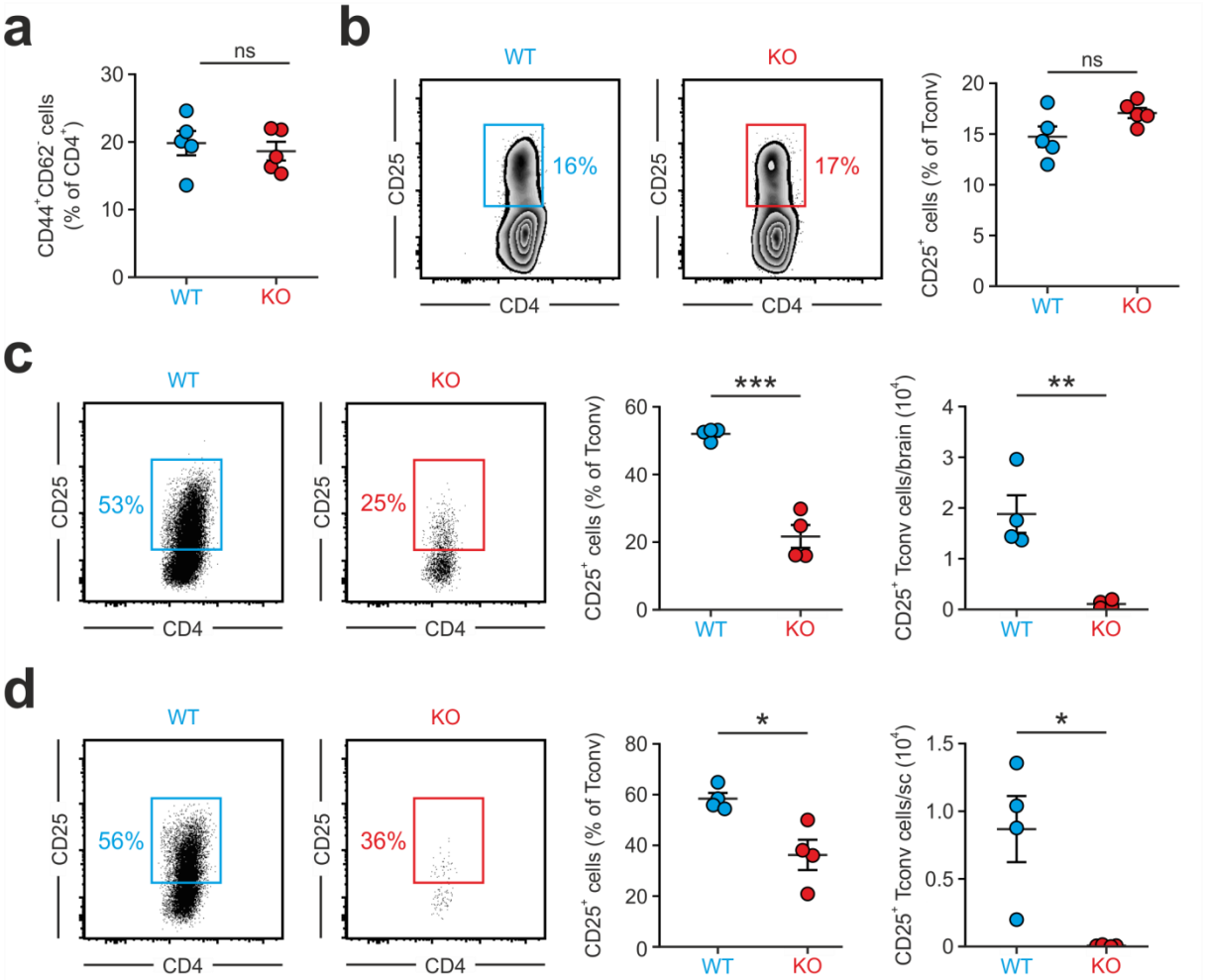

Figure 29: Satb1-deficient $CD4^+$ T cells are less activated in the CNS.
Flow cytometric analysis of EAE mice with Satb1-sufficient or -deficient $CD4^+$ T cells at the peak of disease. **(a)** Quantification of $CD44^+$ effector/memory T cells in the cLN. **(b-d)** Analysis of CD25 expression of Tconv cells in the cLN **(b)**, brain **(c)** and spinal cord **(d)** and quantification of absolute cell numbers. (a,b) n=5, (c,d) n=4, mean ± SEM, unpaired Student's t-test.

Next, the cytokine expression profile of $CD4^+$ T cells was analyzed, both in cLN and CNS at the peak of disease. Similar as in the adoptive transfer colitis model, especially T_H1 as well as T_H17 cells are induced during EAE and contribute to disease pathology with recent data favoring a more T_H17 cell-driven process (Domingues et al., 2010; Duhen et al., 2013; Lee et al., 2012).

When assessing IFN-γ expression, an increased percentage of IFN-γ^+ cells was detected within the effector $CD4^+$ T cell pool in the cLN and brain when Satb1 was deleted (Figure 30a,b). In contrast, no significant difference was observed in the percentage of IFN-γ^+ cells in the spinal cord (Figure 30c). Thus, similar to the *in vitro* and *in vivo* observations under homeostatic conditions, Satb1-deficient $CD4^+$ T cells tend to express slightly more IFN-γ after MOG_{35-55}/CFA immunization. However, although the percentage of IFN-γ-producing

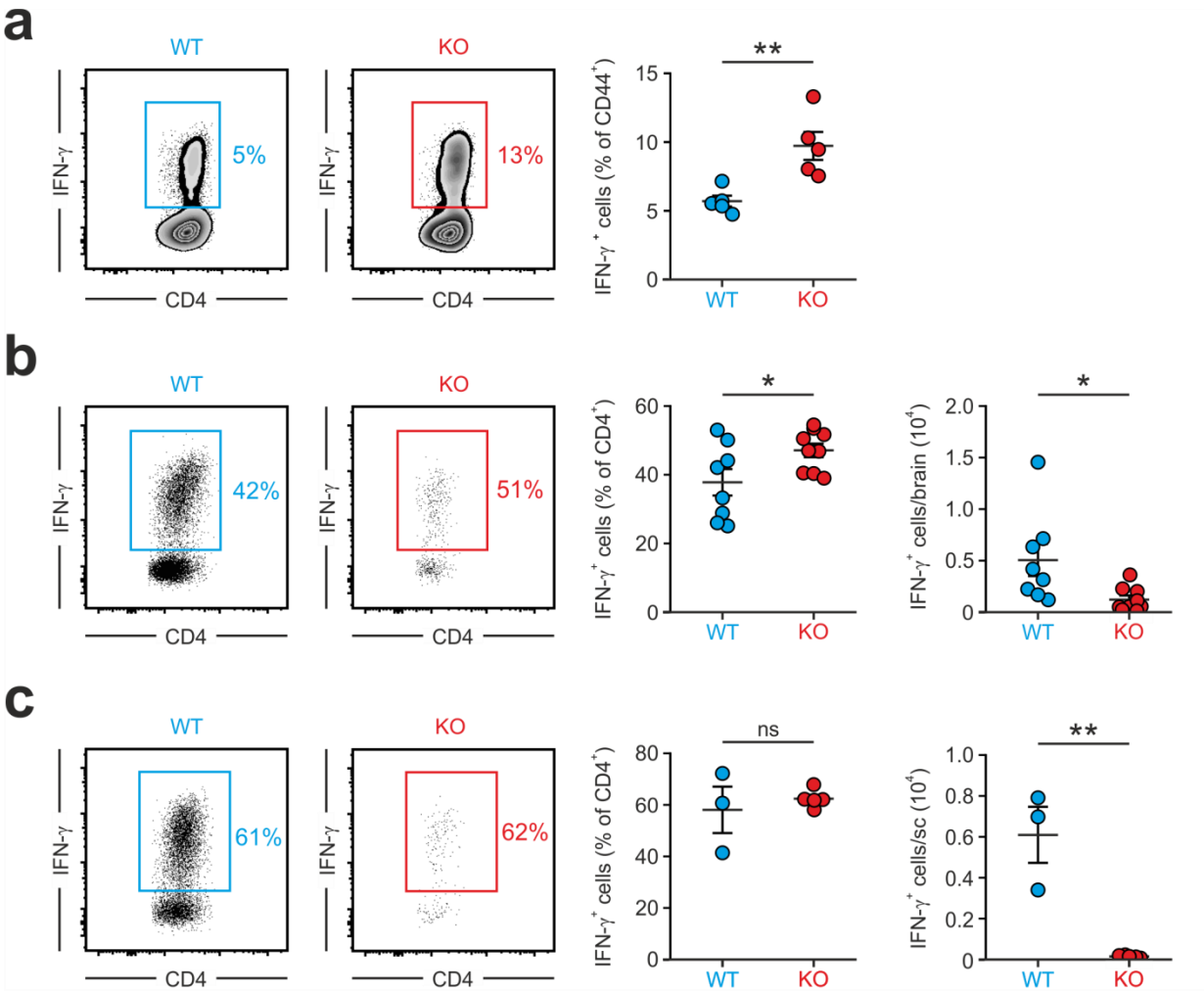

Figure 30: Satb1-deficient $CD4^+$ T cells show similar or increased IFN-γ expression at the peak of EAE disease.

Flow cytometric analysis of EAE mice with Satb1-sufficient or -deficient $CD4^+$ T cells at the peak of disease. Quantification of IFN-γ expression in the cLN **(a)**, brain **(b)** and spinal cord **(c)**. (a) n=5, (b) n=8-9, (c) n=3-5, mean ± SEM, unpaired Student's t-test, (b,c) Data were pooled from two independent experiments.

$CD4^+$ T cells was either unaltered or partly increased when Satb1 was deleted, no disease formation could be observed. This can be explained by the reduced infiltration of Satb1-deficient $CD4^+$ T cells in the CNS, additionally resulting in a reduced number of total IFN-γ-producing Satb1-deficient $CD4^+$ T cells in the brain and spinal cord (Figure 30b,c).

In contrast, when analyzing IL-17 expression, a clear reduction in the percentage of $IL\text{-}17^+$ cells in cLN and brain were detected when Satb1 was lost in $CD4^+$ T cells (Figure 31a,b). Furthermore, a reduced number of IL-17-producing Satb1-deficient $CD4^+$ T cells was detected in the brain (Figure 31b). In line with this, although not statistically different, the percentage of $IL\text{-}17^+$ cells was reduced in the spinal cord of mice with Satb1-deficient $CD4^+$ T cells (Figure 31c). Furthermore, the total number of $IL\text{-}17^+$ cells was clearly reduced in the spinal cord when Satb1 was deleted in $CD4^+$ T cells (Figure 31c).

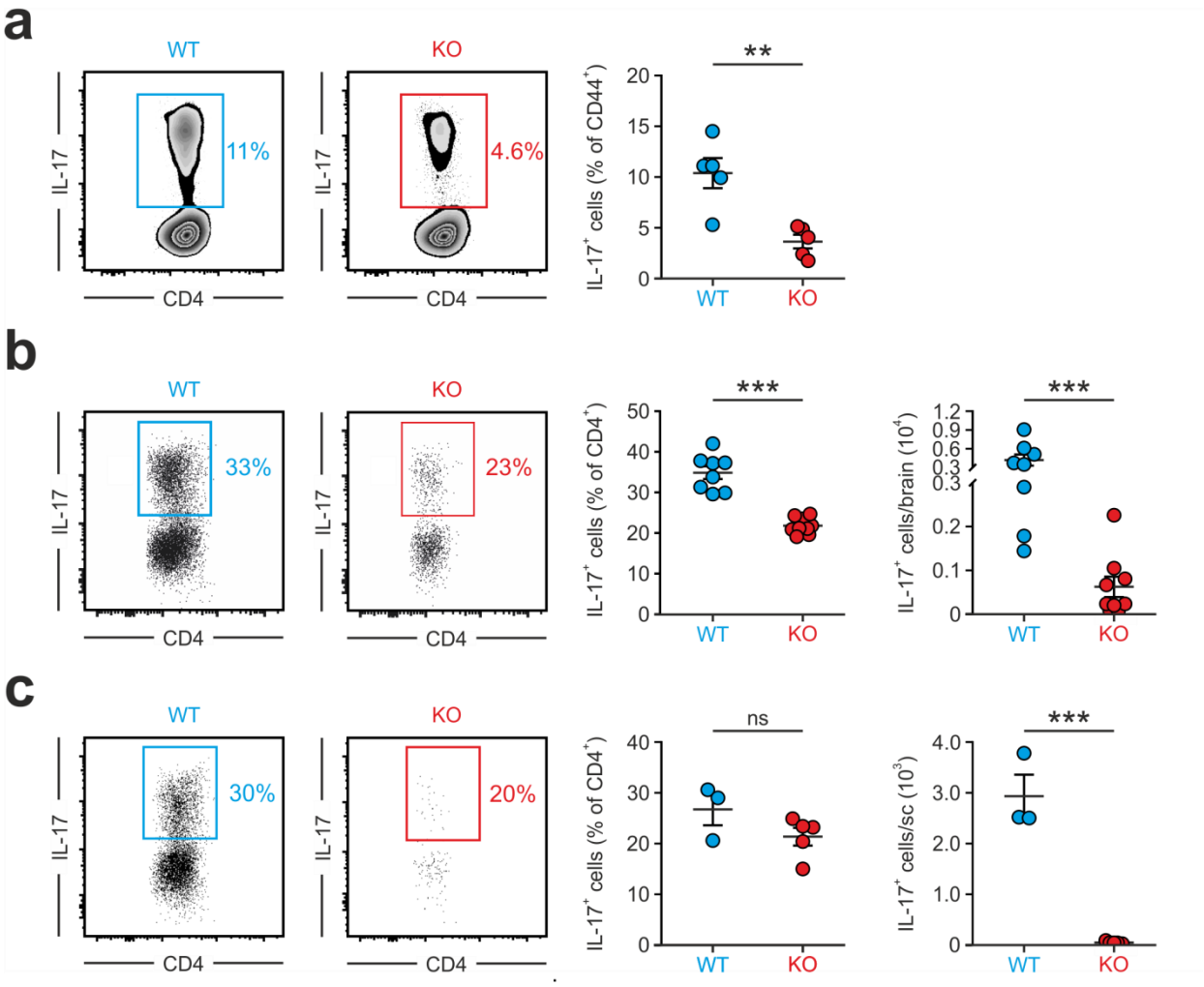

Figure 31: Decreased differentiation of Satb1-deficient $CD4^+$ T cells into T_H17 cells after EAE induction.

Flow cytometric analysis of EAE mice with Satb1-sufficient or -deficient $CD4^+$ T cells at the peak of disease. Quantification of IL-17 expression in the cLN **(a)**, brain **(b)** and spinal cord **(c)**. (a) n=5, (b) n=8-9, (c) n=3-5, mean ± SEM, unpaired Student's t-test, (b,c) Data were pooled from two independent experiments.

Furthermore, fewer RORγt-expressing cells were present in the brain and spinal cord when Satb1 was deleted in $CD4^+$ T cells (Figure 32a,b). Thus, Satb1-deficient $CD4^+$ T cells show a decreased differentiation capability into T_H17 cells.

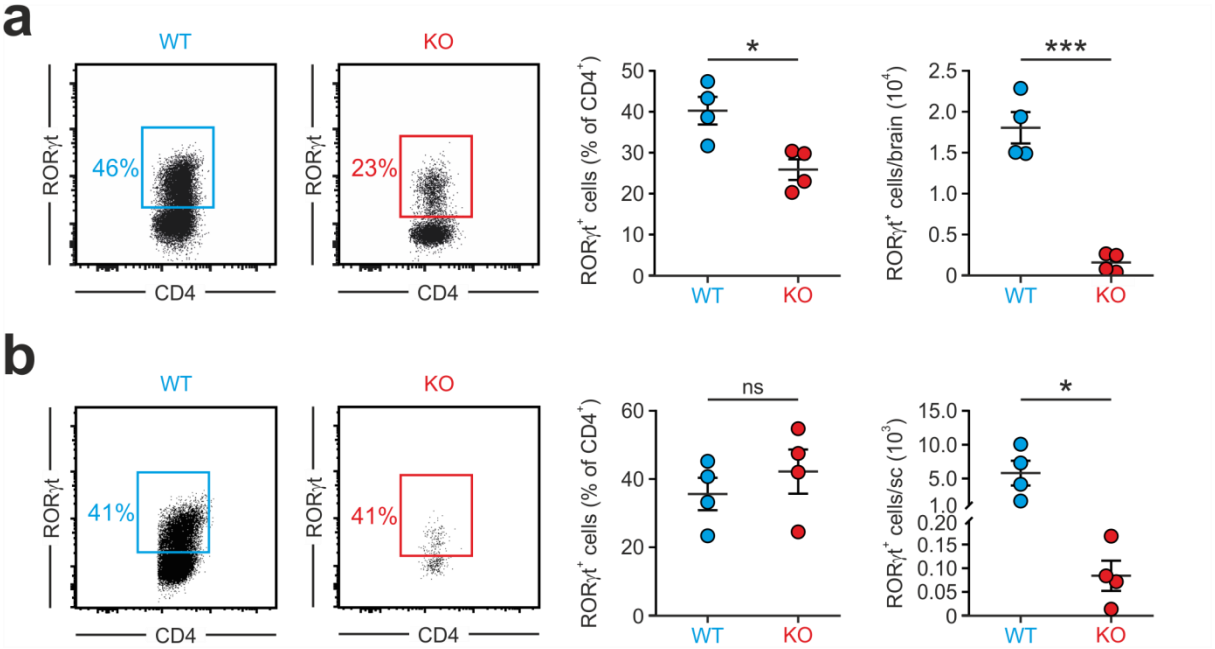

Figure 32: Fewer Satb1-deficient T_H17 cells infiltrate the CNS after EAE induction.
Flow cytometric analysis of EAE mice with Satb1-sufficient or -deficient $CD4^+$ T cells at the peak of disease. Quantification of RORγt-expressing $CD4^+$ T cells in the brain **(a)** and spinal cord **(b)**. (a,b) n=4, mean ± SEM, unpaired Student's t-test.

As both multiple sclerosis and EAE have been previously linked with the development of pathogenic T_H17 cells (van Langelaar et al., 2018; Langrish et al., 2005; Lee et al., 2012), the influence of Satb1 deficiency on the differentiation of pathogenic and non-pathogenic T_H17 cells during EAE was examined in more detail.

In cLN, in general nearly no pathogenic IL-17^+IFN-γ^+ T_H17 cells could be detected, while IL-17^+IFN-γ^- non-pathogenic T_H17 cells were clearly reduced upon deletion of Satb1 (Figure 33). Furthermore, when assessing the $CD4^+$ T cell population in the brain, both T_H17 cell subtypes were decreased in percentages and absolute cell numbers (Figure 34a,b). In contrast, in the spinal cord, only the percentage of IL-17^+IFN-γ^- non-pathogenic T_H17 cells was significantly reduced in mice with Satb1-deficient $CD4^+$ T cells (Figure 34c). Thus, similar to the adoptive transfer colitis were pathogenic T_H17 cells could be observed in the colon, Satb1 deficiency does not completely prevent the differentiation of T_H17 cells in the EAE model. However, in combination with the reduced peripheral T_H17 cell differentiation and the dramatically reduced number of spinal cord infiltrating Satb1-deficient $CD4^+$ T cells the total numbers of non-pathogenic and pathogenic T_H17 cells was clearly decreased in the spinal

cord (Figure 34d). Thus, in line with the adoptive transfer colitis experiment, Satb1 deficiency reduces the differentiation of pathogenic T_H17 cells and prevents subsequent inflammation.

In contrast, IL-17$^-$IFN-γ$^+$ T_H1 cells were increased in percentage in the cLN and brain as already indicated upon analysis of IFN-γ expression (Figure 33, Figure 34a). However, this was not observed in the spinal cord where a similar percentage of IL-17$^-$IFN-γ$^+$ cells was detected (Figure 34c). This further indicates that specifically T_H17 cells drive EAE development instead of T_H1 cells and that Satb1 controls EAE formation by interfering with T_H17 cell differentiation.

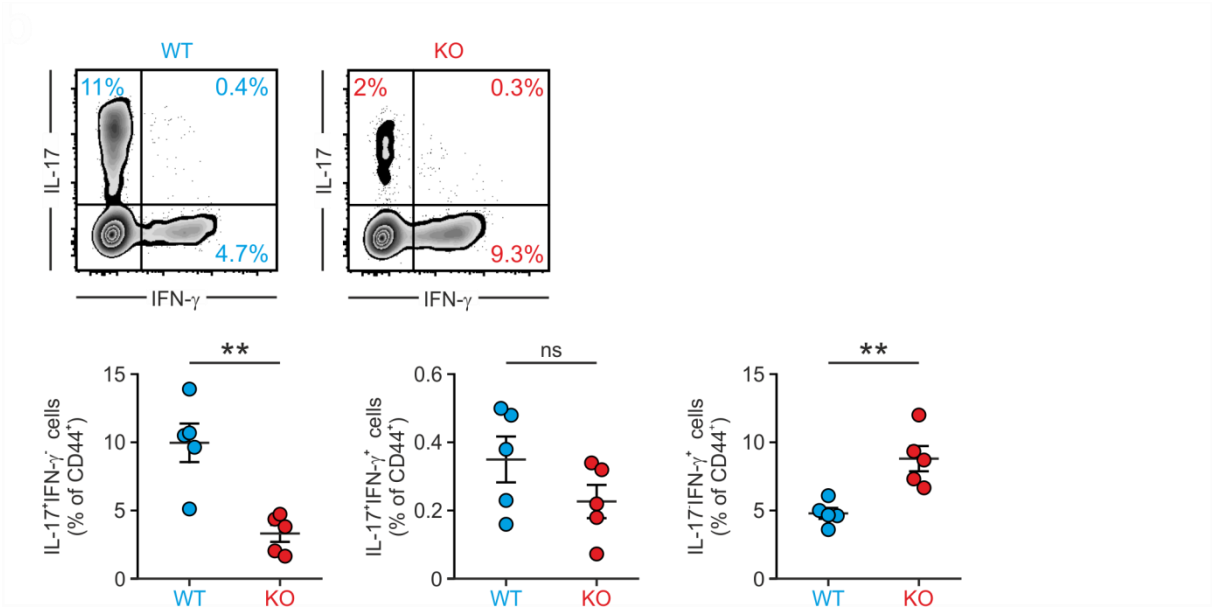

Figure 33: Decreased differentiation of Satb1-deficient CD4$^+$ T cells into non-pathogenic T_H17 cells in cLN after EAE induction.

Flow cytometric analysis of EAE mice with Satb1-sufficient or -deficient CD4$^+$ T cells at the peak of disease. Quantification of IFN-γ and IL-17 expression in the cLN. n=5, mean ± SEM, unpaired Student's t-test.

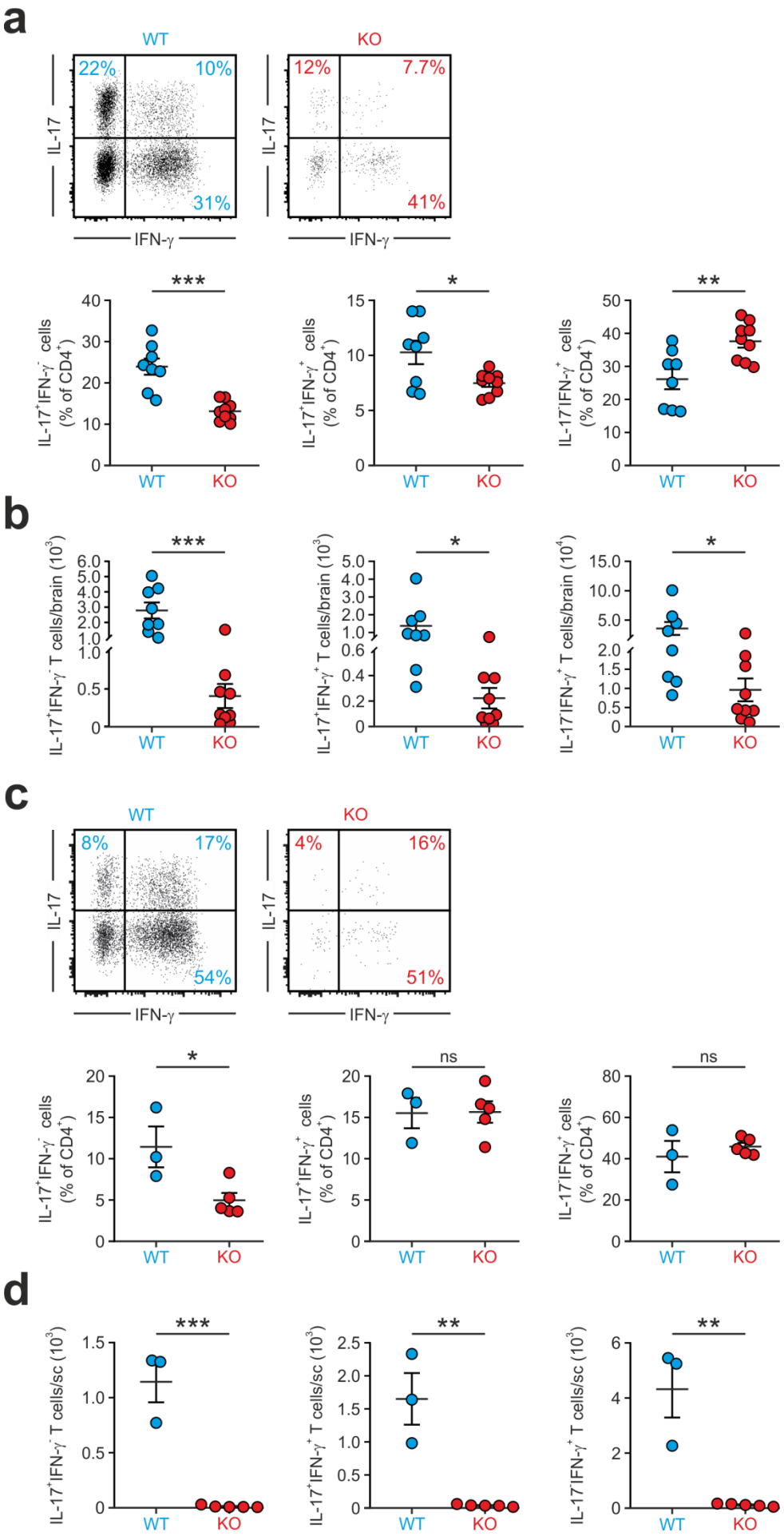
a
WT
KO
22%
10%
31%
12%
7.7%
41%
IL-17
IFN-γ
IL-17+IFN-γ- cells (% of CD4+)
IL-17+IFN-γ+ cells (% of CD4+)
IL-17-IFN-γ+ cells (% of CD4+)
***
*
**
b
IL-17+IFN-γ- T cells/brain (10^3)
IL-17+IFN-γ+ T cells/brain (10^3)
IL-17-IFN-γ+ T cells/brain (10^4)
c
8%
17%
54%
4%
16%
51%
ns
d
IL-17+IFN-γ- T cells/sc (10^3)
IL-17+IFN-γ+ T cells/sc (10^3)
IL-17-IFN-γ+ T cells/sc (10^3)

Figure 34: Decreased infiltration of Satb1-deficient non-pathogenic and pathogenic T_H17 cells in the CNS after EAE induction.
Flow cytometric analysis of EAE mice with Satb1-sufficient or -deficient $CD4^+$ T cells at the peak of disease. **(a,b)** Analysis of IFN-γ and IL-17-expressing $CD4^+$ T cells **(a)** and calculation of absolute cell numbers **(b)** in the brain. **(c,d)** Analysis of IFN-γ and IL-17-expressing $CD4^+$ T cells **(c)** and calculation of absolute cell numbers **(d)** in the spinal cord. (a,b) n=8-9, (c,d) n=3-5, mean ± SEM, unpaired Student's t-test. Data were pooled from two independent experiments.

It has been reported that EAE is driven by MOG-specific $CD4^+$ T cells and especially pathogenic $IL\text{-}17^+IFN\text{-}\gamma^+$ T_H17 cells are known to recognize MOG (Duhen et al., 2013). As fewer pathogenic T_H17 cells were detected, the question arose whether this was accompanied by a reduced expansion of MOG-specific $CD4^+$ T cells if Satb1 is absent.

Thus, $CD4^+$ T cells were stained in addition with a $MOG_{38\text{-}49}/I\text{-}A^b$ peptide–MHC tetramer. This analysis revealed a decreased development of MOG-specific $CD4^+$ T cells in the absence of Satb1 (Figure 35). Significantly fewer $CD4^+$ MOG $Tetramer^+$ T cells were present in the brain of mice with Satb1-deficient $CD4^+$ T cells (Figure 35a) and a similar trend was observed in the spinal cord in percentage and frequency (Figure 35b).

Together, these data indicate a prevention of autoimmunity and the resulting neurodegeneration in the EAE model through an impaired generation of pathogenic cell in the absence of Satb1.

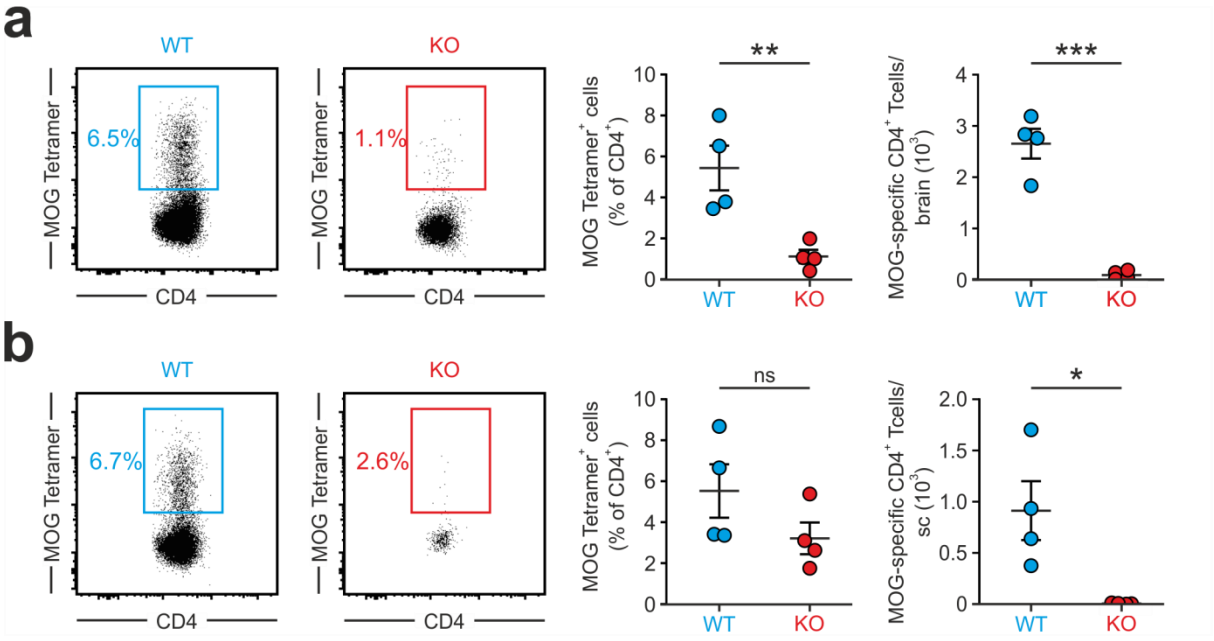

Figure 35: Lower specificity of Satb1-deficient $CD4^+$ T cells for myelin oligodendrocyte glycoprotein (MOG).
Flow cytometric analysis of MOG-specific $CD4^+$ T cells and quantification of absolute cell numbers in the brain **(a)** or spinal cord **(b)** of EAE mice with Satb1-sufficient or -deficient $CD4^+$ T cells at the peak of disease. n=4, mean ± SEM, unpaired Student's t-test.

As discussed above, reduced frequencies of T_H17 cells *in vivo* can be caused by an intrinsic deficiency of T_H17 cell differentiation, or by a Treg cell-induced prevention of autoreactive T_H17 cell expansion, thus by an extrinsic effect. Experiments in the adoptive transfer colitis model indicated that Satb1 has a direct influence on the development of T_H17 cells instead of modulating pathogenic cell development via Treg cells (Figure 22).

To address this question in the EAE model, it was analyzed whether the deletion of Satb1 in $CD4^+$ T cells resulted in an increased percentage of Treg cells in MOG_{35-55}/CFA immunized mice.

However, the percentage of Foxp3-expressing cells was not significantly altered in the cLN, although a trend towards an increased Treg cell development could be observed when Satb1 was deleted (Figure 36a). In contrast, this trend was reversed in the CNS and a reduced percentage and frequency of Treg cells in the brain as well as the spinal cord could be detected (Figure 36b,c). Furthermore, when characterizing Treg cells in more detail, an increased percentage of $CD25^-Foxp^+$ cells was observed both in the cLN and brain (Figure 37a,b). Thus, as described for $Satb1^{fl/fl}$/Thpok-Cre animals (Kitagawa et al., 2017), the absence of Satb1 favor de-repression of Foxp3 in Tconv cells. In contrast, the percentage of $CD25^+Foxp3^+$ Treg cells was unaltered in the cLN and was reduced in the brain (Figure 37a,b).

As it has been shown that in Satb1-deficient animals $CD25^-Foxp^+$ cells do not display Treg cell characteristics besides Foxp3 expression (Kitagawa et al., 2017) and no increase of $CD25^+Foxp^+$ pTreg cells was observed upon EAE induction, these data indicate that the resistance towards EAE development upon deletion of Satb1 in $CD4^+$ T cells is not caused by an enhanced differentiation of Treg cells. In contrast, even a reduced recruitment of Satb1-deficient $CD25^+Foxp^+$ Treg cells was observed in the CNS.

Taken together, Satb1 deficiency in $CD4^+$ T cells intrinsically restrains T_H17 cell differentiation also in an autoimmune disease setting. Protection from EAE is induced by reduced differentiation and expansion of non-pathogenic and especially pathogenic T_H17 cells, resulting in decreased development of MOG-specific T cells, reduced $CD4^+$ T cell infiltration in the CNS and less cell activation at the site of disease.

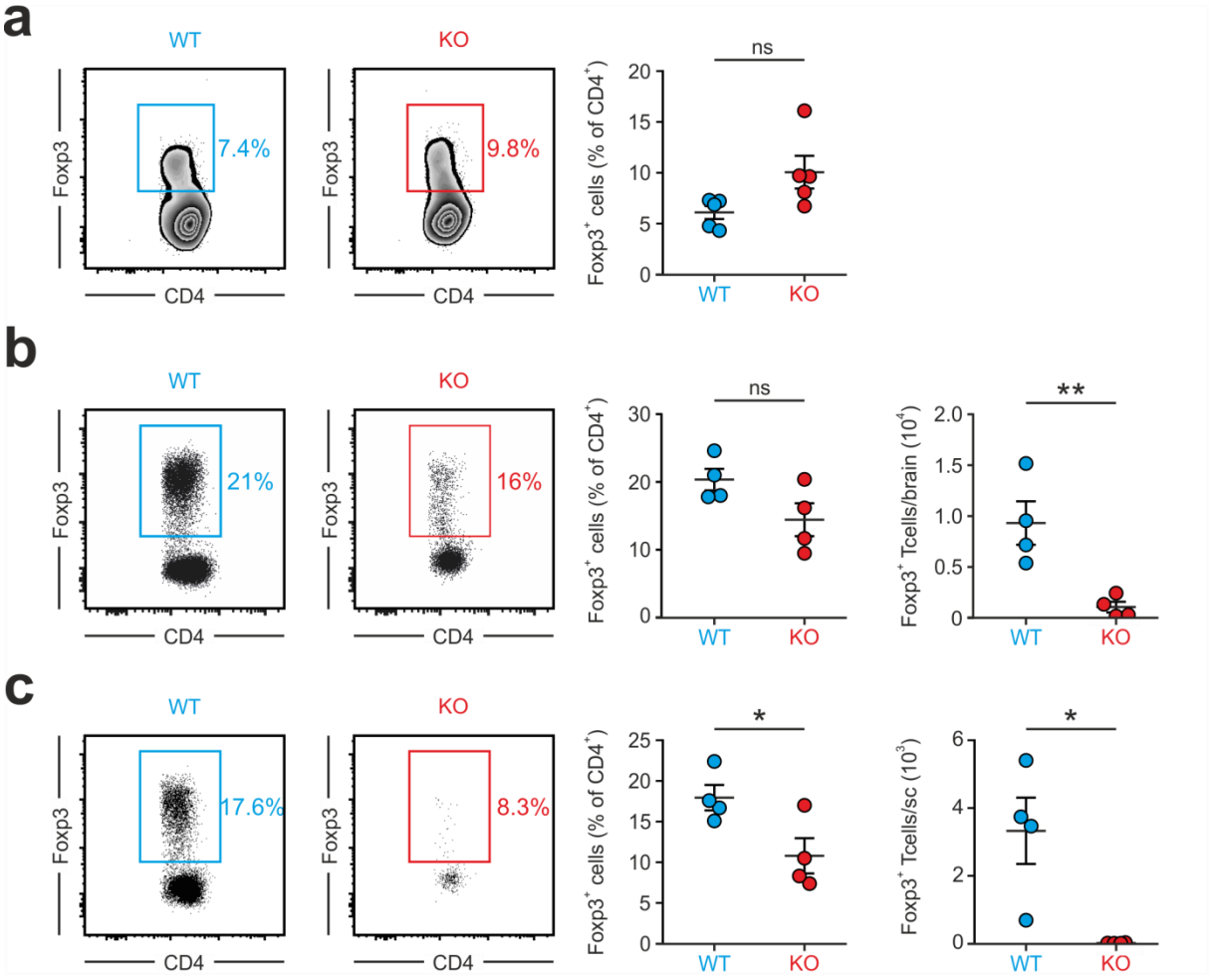

Figure 36: Loss of Satb1 in CD4$^+$ T cells does not result in an increased differentiation of Treg cells in the EAE model.

Flow cytometric analysis of EAE mice with Satb1-sufficient or -deficient CD4$^+$ T cells at the peak of disease. Quantification of Foxp3 expression in cLN **(a)**, brain **(b)** and spinal cord **(c)**. (a) n=5, (b,c) n=4, mean ± SEM, unpaired Student's t-test.

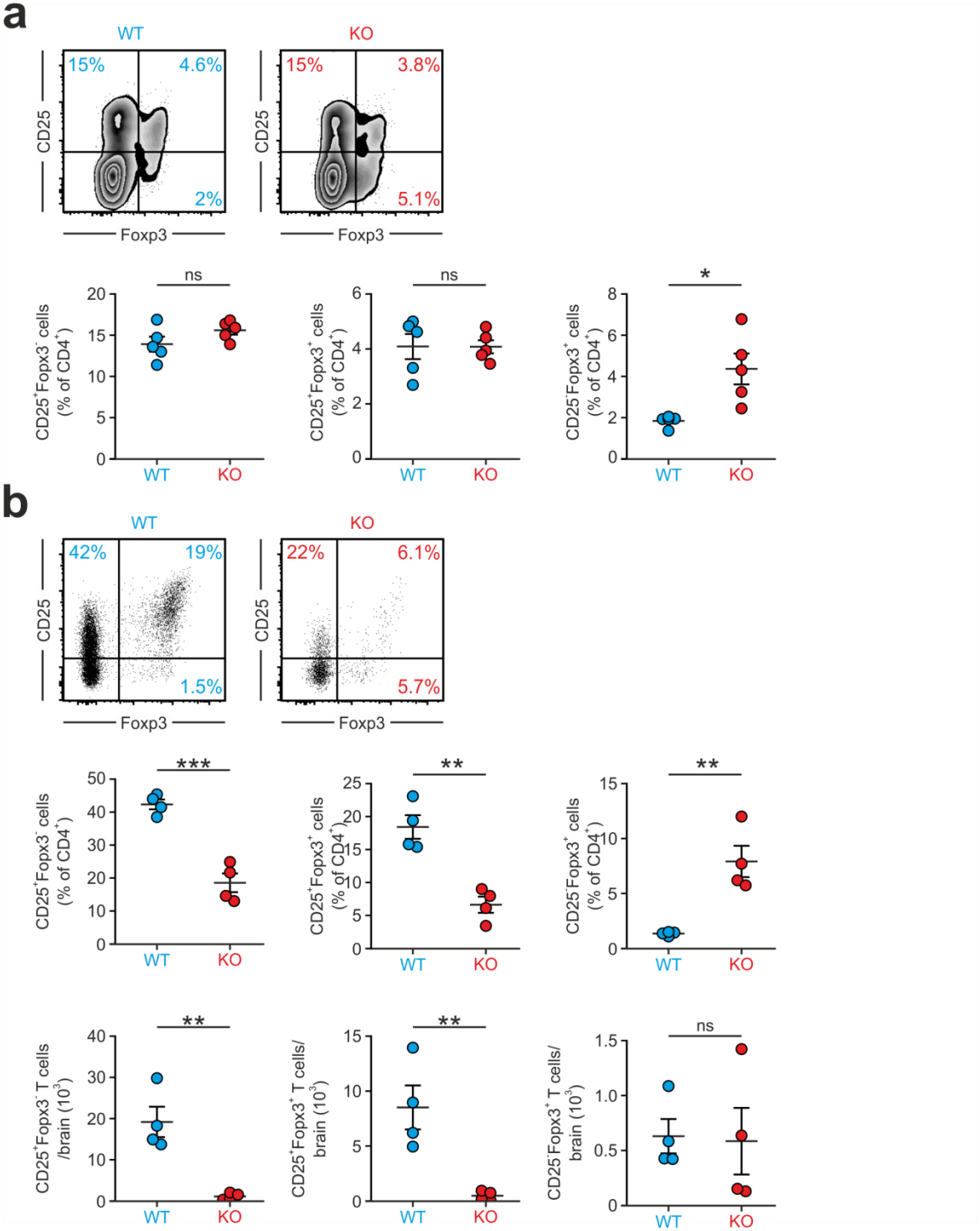

Figure 37: Loss of Satb1 in CD4$^+$ T cells results in a de-repression of Foxp3 in Tconv cells but fails to induce increased CD25$^+$Foxp3$^+$ Treg cell development in EAE.
Flow cytometric analysis of EAE mice with Satb1-sufficient or -deficient CD$^+$ T cells at the peak of disease. Quantification of CD25 and Foxp3 expression in the cLN **(a)** and brain **(b)**. (a) n=5, (b) n=4, mean ± SEM, unpaired Student's t-test.

Thus, it can be concluded that Satb1 is required for the formation of T_H17 cell-driven diseases. In both the EAE and the adoptive transfer colitis model, mice were protected from disease development when Satb1 was deleted in CD4$^+$ T cells. In both disease models, Satb1 expression is essential for the differentiation of naive CD4$^+$ T cells into non-pathogenic and

pathogenic T_H17 cells, thereby regulating inflammation. Furthermore, the formation of T_H1 cells was not or only slightly affected by Satb1 deletion in $CD4^+$ T cells. IFN-γ was produced at high levels by Satb1-sufficient and -deficient $CD4^+$ T cells in both the EAE and the adoptive transfer colitis model. In addition, an increased percentage of IFN-γ production in Satb1-deficient $CD4^+$ T cells present in the brain of EAE mice did not foster disease development, indicating that pathogenic T_H17 but not T_H1 cells are responsible for both EAE and colitis development.

4.5. Characterization of Satb1-deficient cells under T_H17 cell conditions

As Satb1 was important for the development of T_H17 cells during the *in vitro* differentiation process, under homeostatic conditions *in vivo* as well as during disease formation, the question arose how Satb1 regulates T_H17 cell differentiation.

Thus, Satb1-sufficient and -deficient cells differentiated under T_H17 cell-polarizing conditions were further characterized in the *in vitro* differentiation system.

4.5.1. Satb1-deficient naive $CD4^+$ T cells maintained repression of alternative T_H cell fates under T_H17 cell-driving conditions *in vitro*

First, the expression of other T_H subset markers like IFN-γ, IL-4 and IL-10 was analyzed at day three or day five of T_H17 cell differentiation. However, none of these cytokines were expressed in neither Satb1-sufficient nor -deficient cells (Figure 38a,b).

In line with this, also no upregulation of the transcription factors T-bet, Gata3 and Foxp3 corresponding to T_H1, T_H2 and iTreg cells was detected neither at day three nor at day five in Satb1-competent or deficient cells (Figure 39a,b). Thus, Satb1-deficient naive $CD4^+$ T cells do not spontaneously differentiate into other T_H subset under T_H17 cell-polarizing conditions *in vitro*.

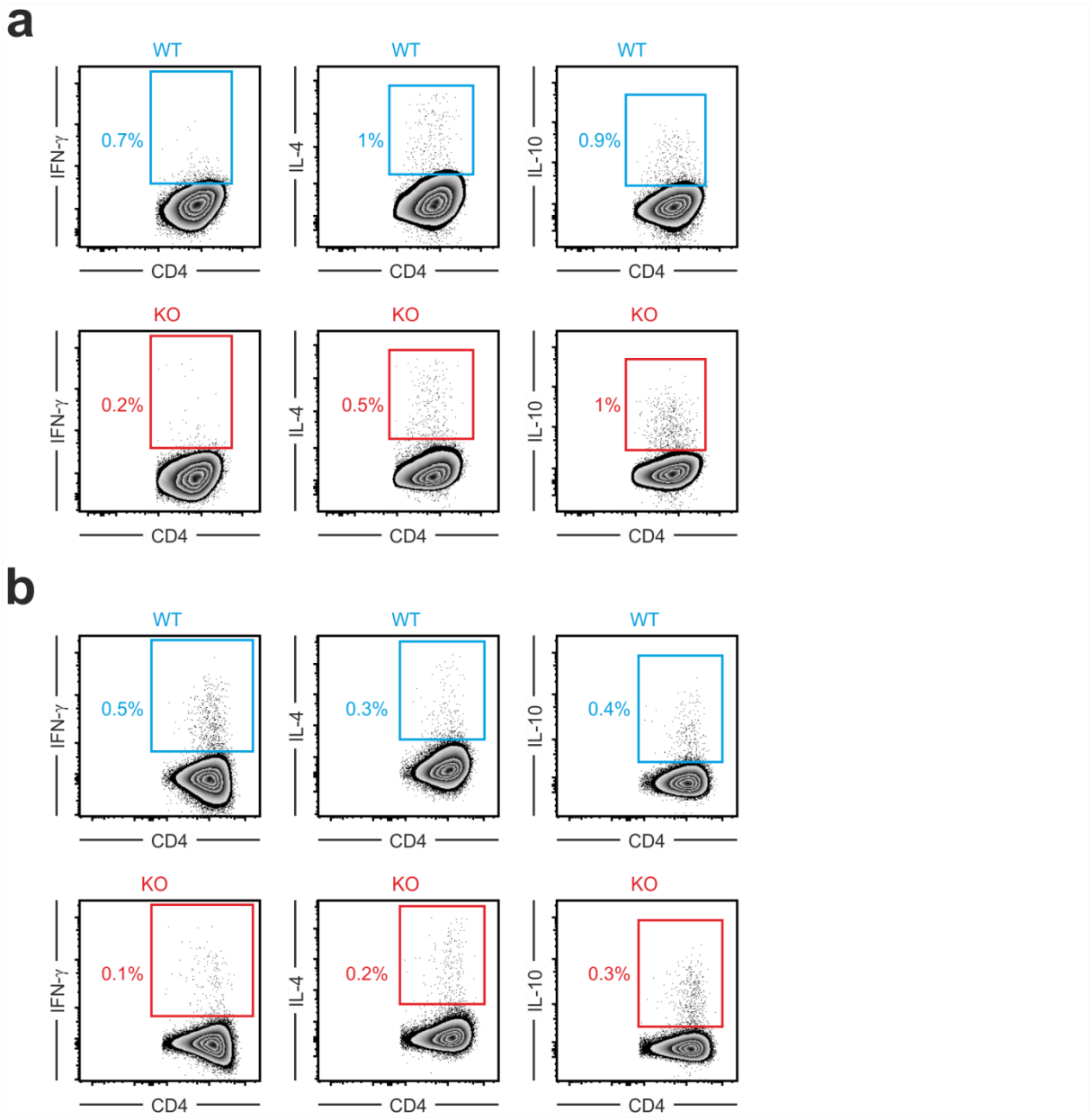

Figure 38: Maintained repression of alternative T_H cell fates in Satb1-deficient $CD4^+$ T cells under T_H17 cell-polarizing conditions *in vitro*.
Satb1-sufficient and -deficient naive $CD4^+$ T cells were isolated by flow cytometric cell sorting and differentiated *in vitro* into T_H17 cells. At day three **(a)** and day five **(b)** of differentiation, expression of IFN-γ, IL-4 and IL-10 was analyzed by flow cytometry. n=4. Representative dot plots are shown.

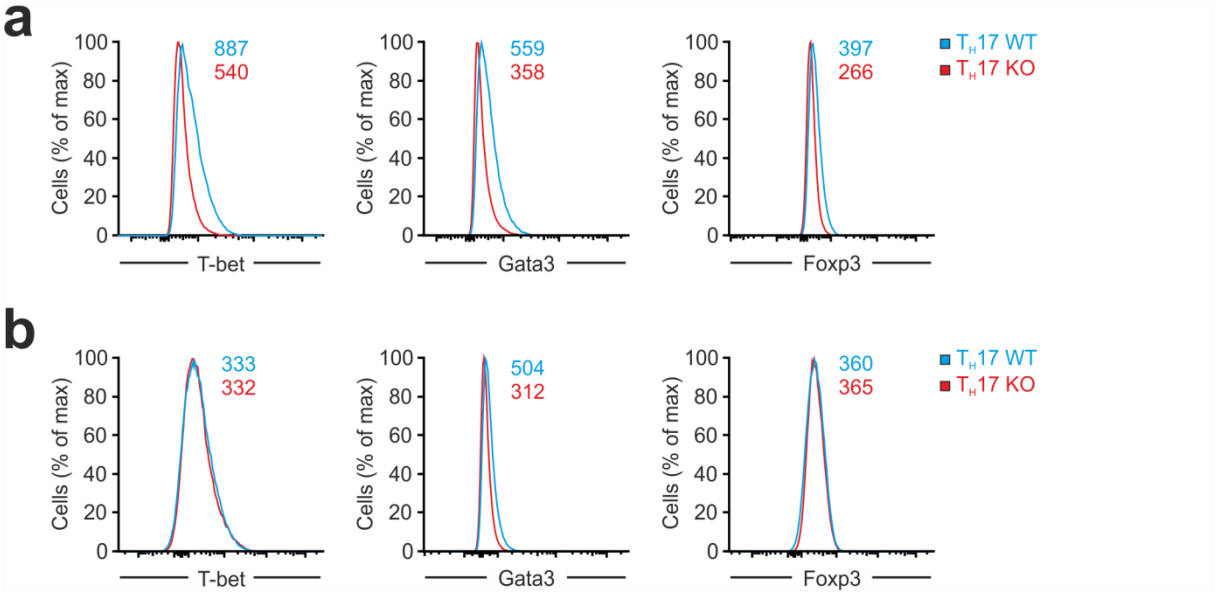

Figure 39: Satb1-deficient naive CD4$^+$ T cells do not differentiate into other T_H subtypes under T_H17 cell-driving conditions *in vitro*.
Satb1-sufficient and -deficient naive CD4$^+$ T cells were isolated by flow cytometric cell sorting and differentiated *in vitro* into T_H17 cells. At day three **(a)** and day five **(b)** of differentiation, expression of T-bet, Gata3 and Foxp3 was analyzed by flow cytometry and the MFI was calculated. n=4. Representative histograms are shown.

4.5.2. Cellular metabolism during T_H17 cell differentiation is mainly unaffected by the deletion of Satb1

Furthermore, the metabolic state and response of Satb1-sufficient and -deficient cells were analyzed. T_H subsets differ in their cellular metabolism and T_H17 cells are highly glycolytic, while T_H1 cells show a slightly reduced glycolytic activity in comparison to T_H17 cells (Gerriets et al., 2015; Michalek et al., 2011). In contrast, Treg cells predominately use oxidation of fatty acids as their energy source (Gerriets et al., 2015; Sun et al., 2017). To examine the basal metabolic phenotype and the cellular respiratory capacity of Satb1-sufficient and -deficient cells, the oxygen consumption rate (OCR) and the extracellular acidification rates (ECAR) were measured in relation to different stimuli at day three of T_H17 cell culture (Figure 40). While the oxygen consumption reflects mitochondrial function and activity, the extracellular acidification is an indicator for glycolytic activity. Interestingly, an overall reduction in basal metabolic activity was detected in Satb1-deficient cells. Both the OCR and the ECAR were reduced in Satb1-deficient cells when cells were transferred to fresh medium in the absence of any stimuli three days after commencement of T_H17 cell differentiation (Figure 40a,b). However, during metabolic challenges, Satb1-sufficient and -deficient cells showed a comparable metabolic response (Figure 40a-c).

Both mitochondrial inhibition and uncoupling (Figure 40a,b) as well as glycolytic interference (Figure 40c) influenced Satb1-sufficient and -deficient cells to a similar extent, indicating that although under homeostatic conditions Satb1-deficient cells are less metabolically active, both Satb1-sufficient and -deficient cells have the same respiratory capacity and do not differ in their metabolic potential three days after initial T_H17 cell differentiation.

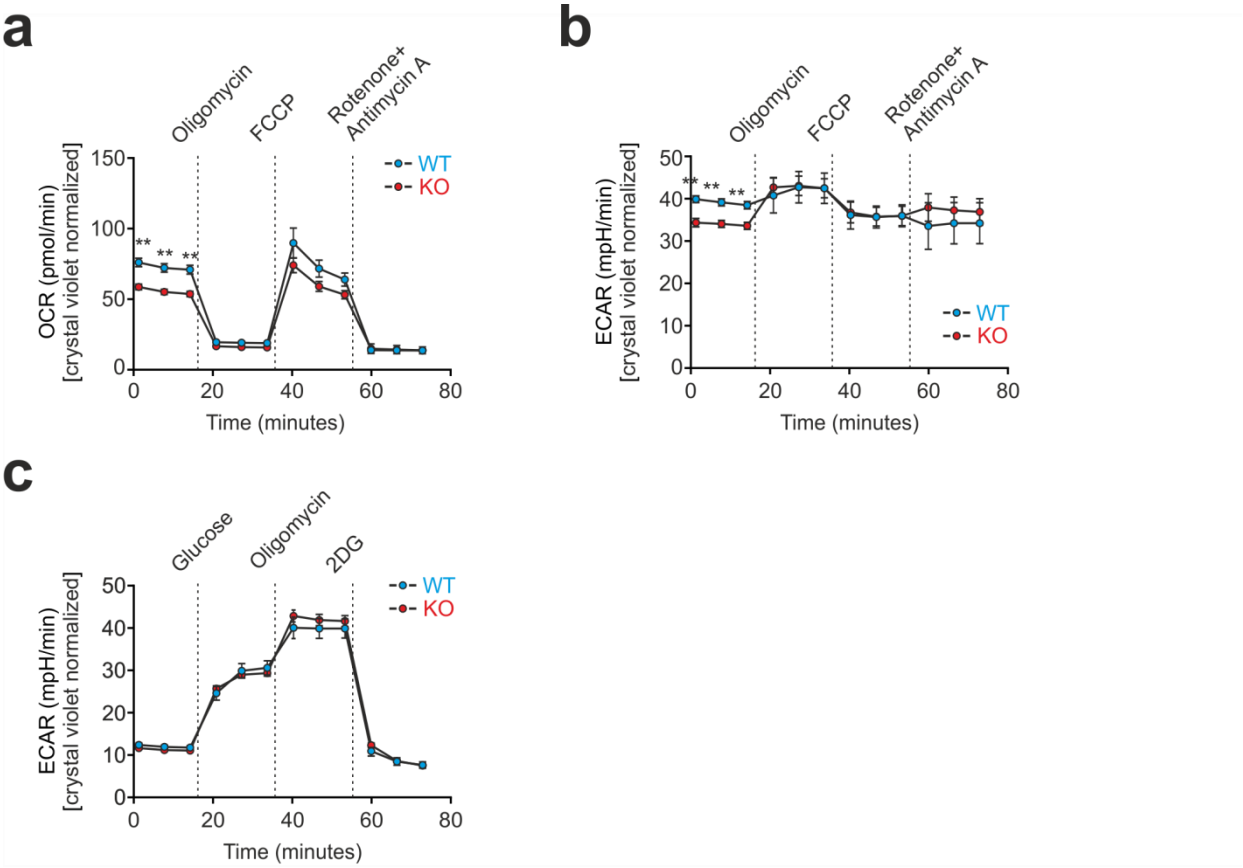

Figure 40: During metabolic challenges, Satb1-sufficient and -deficient CD4$^+$ T cells differentiated under T_H17 cell-driving conditions show similar mitochondrial respiration and glycolysis.

Satb1-sufficient and -deficient naive CD4$^+$ T cells were isolated by flow cytometric cell sorting and differentiated *in vitro* into T_H17 cells. At day three of differentiation, the metabolic state of these cells was analyzed. **(a,b)** Analysis of the basal oxygen consumption rate (OCR) and oxygen consumption upon sequential treatment **(a)** as well as analysis of the basal extracellular acidification rate (ECAR) and changes in the ECAR **(b)** upon treatment with oligomycin, FCCP and rotenone/antimycin A. **(c)** Analysis of the basal ECAR as well as changes in the ECAR upon challenges with glucose, oligomycin and 2DG. Cells were harvested and rested in glucose free medium before stimulation. (a,b) Data (mean ± SEM) were obtained from three WT and three KO animals by repeated measurement, n=13 (WT), n=11 (KO), (c) n=13 (WT), n=10 (KO) of cells from three WT and two KO mice, two-way repeated measures ANOVA with Sidak's multiple comparison test.

4.5.3. Satb1 regulates the expression of GM-CSF

Next, the expression of GM-CSF was measured since Yasuda et al. observed that GM-CSF is downregulated in T_H17 cells at sites of inflammation both in the draining LN and spinal cord in EAE when Satb1 was deleted in IL-17-producing cells (Yasuda et al., 2019).

Indeed, a reduced percentage of GM-CSF$^+$ cells was detected in Satb1-deficient CD4$^+$ T cells at day three and five of *in vitro* T_H17 cell differentiation (Figure 41a,b).

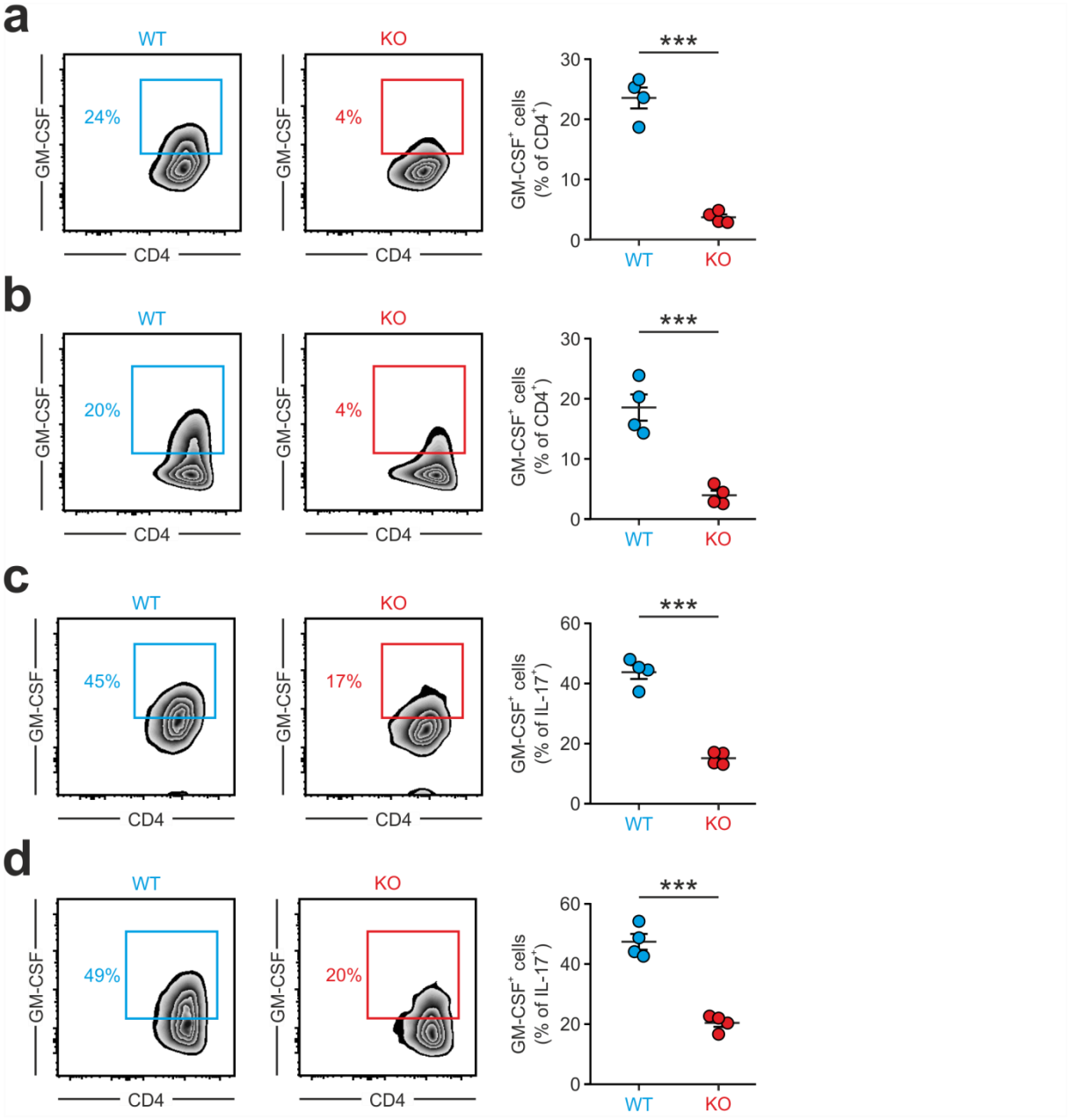

Figure 41: Satb1-deficient CD4$^+$ T cells express less GM-CSF under T_H17 cell-driving conditions.

Satb1-sufficient and -deficient naive CD4$^+$ T cells were isolated by flow cytometric cell sorting and differentiated *in vitro* into T_H17 cells. **(a,b)** Expression of GM-CSF was analyzed by flow cytometry in total CD4$^+$ cells at day three **(a)** and day five **(b)**. **(c,d)** Expression of GM-CSF was analyzed by flow cytometry in IL-17$^+$ cells at day three **(c)** and day five **(d)**. (a-d) n=4, mean ± SEM, unpaired Student's t-test.

Next, to validate whether the loss of GM-CSF expression upon deletion of Satb1 was due to an overall reduction of T_H17 cell differentiation, or whether the loss also affects T_H17 cells itself, GM-CSF expression was analyzed in IL-17^+ cells. Again, also when studying only IL-17^+ cells, fewer GM-CSF^+ cells were observed at day three and five of differentiation when Satb1 was deleted (Figure 41c,d), indicating that indeed Satb1 is important for GM-CSF expression in T_H17 cells.

4.5.4. Satb1-deficient cells fail to develop the T_H17 gene network

For T_H cell fate decision and subset differentiation, a tightly regulated formation of gene networks is required. RORγt is an essential lineage transcription factor for T_H17 cells, however other transcriptions factors and their temporal expression and dynamic interplay are also essential for the proper differentiation and maintenance of T_H17 cells (Ciofani et al., 2012; Yosef et al., 2013). In the last years, factors both positively as well as negatively regulating T_H17 cell differentiation were revealed by gene expression studies as well as functional experiments in murine models (Ciofani et al., 2012; Yosef et al., 2013).

Because of the role of Satb1 as transcription factor and chromatin organizer, Satb1 might influence expression of gene modules associated with T_H17 cell differentiation. In this case, it would be important to understand if Satb1 enables the differentiation of T_H17 cells by promoting expression of genes acting as positive regulators of T_H17 cell differentiation or whether it further decreases expression of suppressive modules and thereby promotes T_H17 cell cytokines and receptor expression.

To address this question, Satb1-sufficient and -deficient naive $CD4^+$ T cells were differentiated into T_H17 cells *in vitro*. Cells were harvested at different time points during the differentiation and expression of genes associated with the differentiation of T_H17 cells were analyzed by qRT-PCR (Figure 42).

As expected, an overall change in gene expression was observed between Satb1-sufficient and -deficient cells. Strikingly, a reduced expression of regulators positively affecting T_H17 cell differentiation was detected in Satb1-deficient $CD4^+$ T cells at early time points during the differentiation process, especially after 12 hours of differentiation. *Irf4*, *Runx* and *Ahr* were expressed at significantly lower levels 12 hours after the start of differentiation and a similar trend was detected for *Rorc* (RORγt) and *Fas*. Furthermore, a similar trend of reduced expression of positive modulators was still detectable at day one of differentiation in Satb1-deficient cells. However, this was not as prominent as after 12 hours as these genes after an initial phase of high expression were downregulated in Satb1-sufficient cells as well. As the complete positive module besides *Batf* was dysregulated early after the initiation of

differentiation, it is conceivable that Satb1 does not influence one specific positive modulator but might rather interfere upstream and thus, in general, allows for the lineage commitment of T_H17 cells. Interestingly, later during T_H17 cell differentiation, most of these genes were upregulated in Satb1-deficient cells compared to Satb1-sufficient cells, which might be explained by some compensatory mechanism while *Rorc* was still expressed at significantly reduced levels in Satb1-deficient $CD4^+$ T cells.

Focusing on the key members of the inhibitory module revealed a significantly higher expression of all inhibitory genes in Satb1-deficient cells at day five of culture with the exception of *Irf1* and *Ikzf4*, which showed a similar expression pattern independent of Satb1. In addition, the upregulation of this mainly suppressing module was evident already at day three or four. However, none of the genes were significantly altered in naive $CD4^+$ T cells or 12 hours after differentiation between Satb1-sufficient and -deficient cells, suggesting that

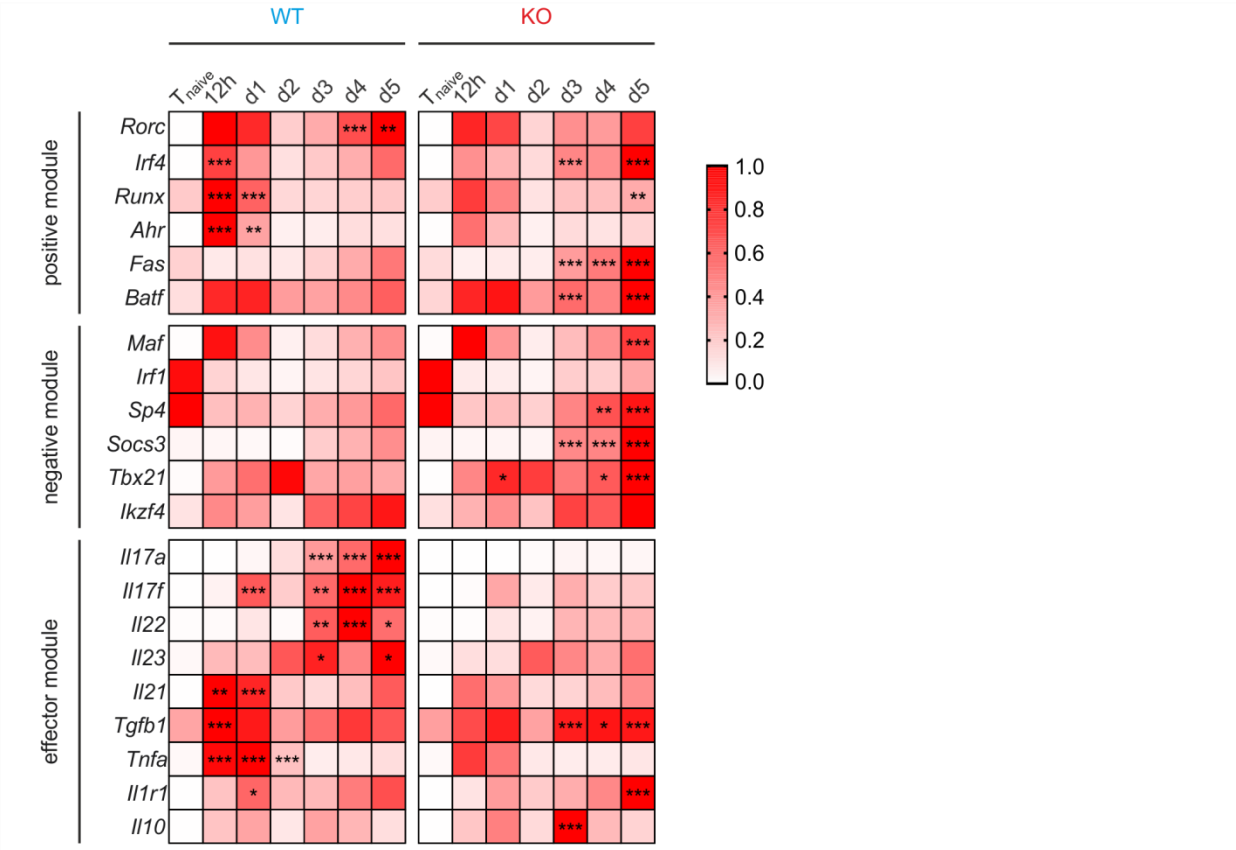

Figure 42: The T_H17 cell gene network is altered in Satb1-deficient $CD4^+$ T cells.
Satb1-sufficient and -deficient naive $CD4^+$ T cells were isolated by flow cytometric cell sorting and differentiated *in vitro* into T_H17 cells. Relative mRNA expression of T_H17 cell network genes is shown before and at different time point during the differentiation. The highest average mean was set to one and the average of the other time points were set into relation separately for each gene. h, hours. n=3-5, two-way ANOVA with Sidak's multiple comparison test. Significant differences in gene expression between WT and KO cells at different time points are shown and illustrated on the higher expressing cells.

these genes will most likely not affect the early events driving T_H17 cell differentiation but rather stabilize the observed difference between Satb1-competent and -deficient cells.

As expected due to the dysregulation of the transcription factor network, when analyzing the effector program of Satb1-sufficient and -deficient cells at different time points during the differentiation, an overall reduction in the expression of cytokines was clearly detectable in Satb1-deficient cells. Consistent with protein data, a reduced expression of *Il17a* mRNA was observed in Satb1-deficient cells and similarly *Il17f* mRNA was expressed at low levels in Satb1-deficient cells. Furthermore, the expression of *Il22* and *Il23*, coding for two other cytokines associated with T_H17 cells (Korn et al., 2009), was reduced in Satb1-deficient cells from day three onwards.

Moreover, *Il21 and Tgfb1* both autocrine T_H17 cell-polarizing cytokines (Gutcher et al., 2011; Wei et al., 2007) were expressed at lower levels in the early phase of differentiation in cells lacking Satb1. However, *Tgfb1* was upregulated in Satb1-deficient cells later on. In addition, similar to *Il21* and *Tgfb1*, the expression of *Tnfa* was significantly reduced in Satb1-deficient cells after the initiation of differentiation, in line with the protein data from Satb1-deficient $CD4^+$ T cells isolated from the adoptive transfer colitis model. Furthermore, *Il1r1*, whose receptor signaling is critical during the commitment of T_H17 cells (Sha and Markovic-Plese, 2011), was expressed at lower levels in Satb1-deficient cells at early stages of differentiation, further explaining their loss of T_H17 cell differentiation.

In contrast to the other effector cytokines, *Il10* was transiently upregulated in Satb1-deficient cells at day three. However, this upregulation of IL-10 could not be confirmed on protein level in Satb1-deficient cells (Figure 38).

Taken together, the analysis of the gene network critical for T_H17 cells and their effector cytokine genes revealed that Satb1 is essential in the early steps of T_H17 cell lineage commitment. Furthermore, loss of Satb1 impacted not only the expression of one specific key downstream gene but rather dysregulated the complete differentiation program and consequently resulted in the disturbance of key effector molecules required for T_H17 cells.

4.6. Satb1 is essential in the early phase of T_H17 cell generation and during restimulation of preformed T_H17 cells

Since the analysis of key transcriptional events indicated a complete lack of the T_H17 cell gene network already in the early phase of differentiation, the time frame in which Satb1 governed the differentiation and commitment of T_H17 cells was assessed in more detail. Therefore, the role of Satb1 was analyzed at different time points during the differentiation

process and the influence of Satb1 on the maintenance and restimulation of T_H17 cells as well as on T_H subset plasticity was determined. To this end, specific deletion of Satb1 in $CD4^+$ T cells was induced *in vitro* instead of inducing Satb1 deficiency *in vivo*.

To analyze the importance of Satb1 during the differentiation process of T_H17 cells, Satb1 was deleted before and at different time point during the differentiation and the percentage of IL-17^+ cells was determined at day five of the T_H17 cell cultures (Figure 43).

These data clearly revealed that Satb1 was especially important in the early phase of differentiation. A significantly reduced T_H17 cell differentiation was observed when Satb1 was deleted before or until day one of differentiation. In addition, the loss of Satb1 on day two resulted in a significant but less dramatic reduction of T_H17 cells. In contrast, the deletion of Satb1 on day three or four did not result in an altered frequency of IL-17^+ cells, indicating that Satb1 is vital in the initiation of the differentiation process but dispensable for the maintenance of T_H17 cells once the commitment towards T_H17 cells has been established.

To address whether Satb1 is also important during the reactivation of resting T_H17 cells, Satb1-sufficient cells were differentiated into T_H17 cells for five days, followed by two days of culture without TCR and cytokine stimulation. During this resting phase the deletion of Satb1 was induced by adding tamoxifen to the cultures. In line with the previously obtained data, the deletion of Satb1 at this stage of T_H17 cell differentiation did not result in a loss of IL-17 expression (Figure 44). However, when these cells were restimulated with CD3 and CD28 antibodies in a T_H17 cell-polarizing milieu, EtOH-treated T_H17 cells showed increased IL-17 expression while IL-17 expression remained constant in Satb1-deficient T_H17 cells (Figure 44). Similar results were obtained when cells were pretreated with either IL-21, IL-2 or IL-23 and IL-1β before restimulation of cells under T_H17 cell conditions (data not shown).

In summary, these data support that although a deletion of Satb1 in pre-committed T_H17 cells does not influence IL-17 expression or the maintenance of the T_H17 cell phenotype *in vitro*, it diminishes their capacity to produce IL-17 when these cells are restimulated in a T_H17 cell supporting milieu. This suggests that Satb1 also affects the function of T_H17 cells upon activation.

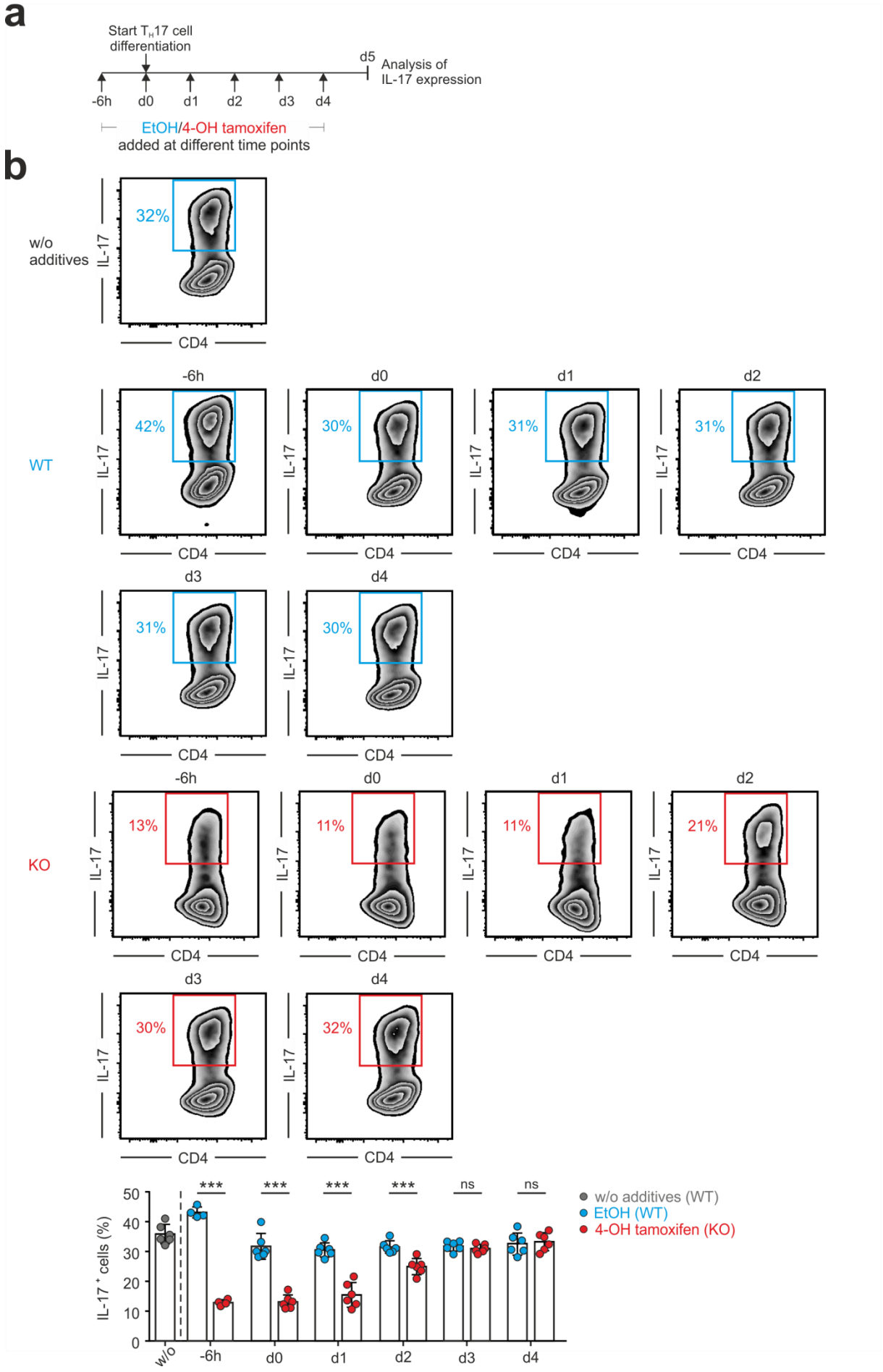
a
Start TH17 cell differentiation
d5
Analysis of IL-17 expression
-6h
d0
d1
d2
d3
d4
EtOH/4-OH tamoxifen added at different time points
b
w/o additives
32%
IL-17
CD4
WT
-6h
d0
d1
d2
42%
30%
31%
31%
d3
d4
31%
30%
KO
13%
11%
11%
21%
30%
32%
IL-17+ cells (%)
50
40
30
20
10
0
***
ns
w/o
-6h
d0
d1
d2
d3
d4
w/o additives (WT)
EtOH (WT)
4-OH tamoxifen (KO)

Figure 43: Satb1 is essential during the initiation of T_H17 cell differentiation.
(a) Schematic overview of the experimental design. Naive $CD4^+$ T cells of untreated $Satb1^{fl/fl}$/CD4-$CreERT2^{wt/+}$ mice were isolated by flow cytometric cell sorting and differentiated *in vitro* into T_H17 cells. At different time points during the differentiation, cells were treated with 4-hydroxytamoxifen (4-OH tamoxifen) to induce the deletion of Satb1 or were treated with ethanol (EtOH) as WT control. **(b)** At day five, the percentage of IL-17-producing cells was analyzed by flow cytometry. w/o, without. n=4-6, mean ± SEM, two-way ANOVA with Sidak's multiple comparison test. Data were pooled from two independent experiments.

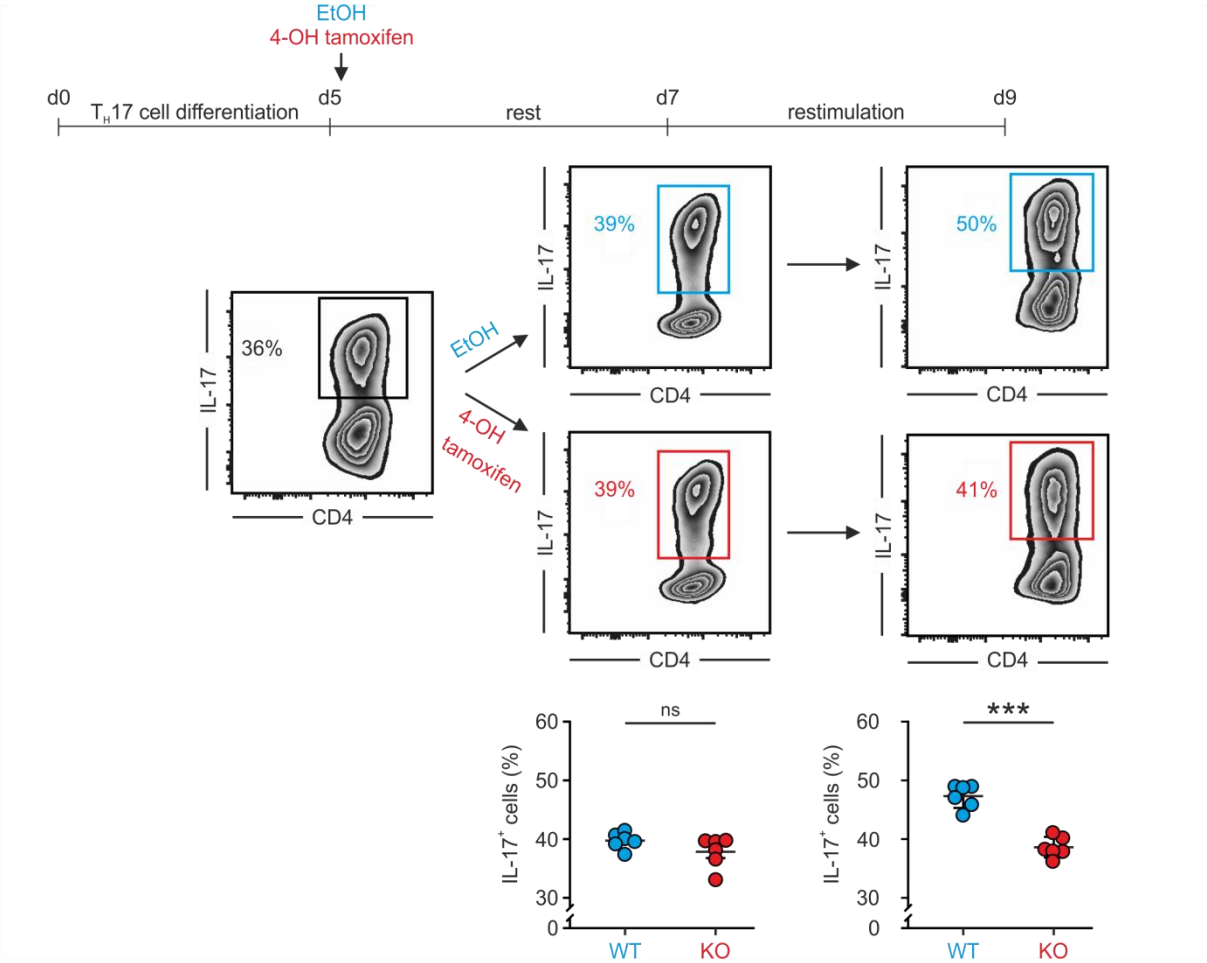

Figure 44: Satb1 is important to increase IL-17 production in restimulated T_H17 cells.
Naive $CD4^+$ T cells from untreated $Satb1^{fl/fl}$/CD4-$CreERT2^{wt/+}$ mice were isolated by flow cytometric cell sorting and differentiated *in vitro* into T_H17 cells. After five days of differentiation, cells were rested for two days and simultaneously treated with 4-hydroxytamoxifen (4-OH tamoxifen) to induce Satb1 deletion or were treated with ethanol (EtOH) as WT control. After two day, on day seven, cells were restimulated with CD3 and CD28 antibodies and T_H17 cell-inducing cytokines for two days (day nine). The percentage of IL-17-producing cells was analyzed by flow cytometry at day five, seven and nine. n=6, mean ± SEM, unpaired Student's t-test.

Next, the role of Satb1 in the polarization or reprogramming of already committed T_H subsets was analyzed. To understand whether Satb1 expression is only important for the differentiation of naive $CD4^+$ T cells into T_H17 cells or if it also regulates T_H cell skewing, Satb1-sufficient and -deficient naive $CD4^+$ T cells were differentiated *in vitro* for two days into T_H1 cells followed by cultivation in pathogenic T_H17 cell-promoting conditions for three additional days. By analyzing IFN-γ and IL-17 expression on day five, reprogramming of T_H1 cells towards T_H17 cells was determined.

While Satb1-sufficient T_H1 cells lost IFN-γ expression and gained the propensity to produce IL-17 as a proxy for a T_H17 cell phenotype, loss of Satb1 completely prevented the reprogramming of T_H1 cells into T_H17 cells (Figure 45).

Thus, Satb1 not only controls the decision process of T_H17 cell differentiation of naive $CD4^+$ T cells but also skewing of T_H1 cells into T_H17 cells.

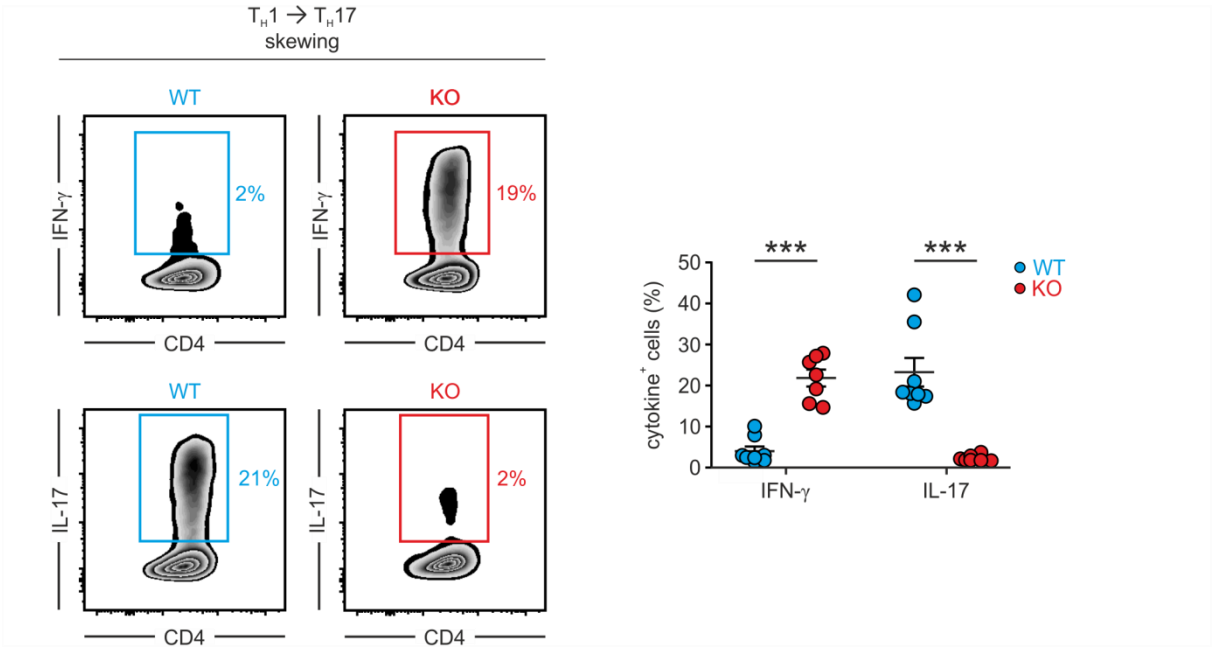

Figure 45: Satb1 is important for the reprogramming of T_H1 cells into T_H17 cells.
Satb1-sufficient and -deficient naive $CD4^+$ T cells were isolated by flow cytometric cell sorting and differentiated *in vitro* into T_H1 cells. At day two of differentiation, cells were restimulated using a pathogenic T_H17 cell-inducing cytokines cocktail. The percentage of $IL\text{-}17^+$ and $IFN\text{-}\gamma^+$ cells was analyzed by flow cytometry at day five. n=7-8, mean ± SEM, multiple t-test. Data were pooled from two independent experiments.

Taken together, these data indicate that Satb1 promotes T_H17 cells at multiple time points during their lifetime. Satb1 is essential early during the differentiation of T_H17 cells but also regulates T_H17 cell function during restimulation and allows for the reprogramming of other T_H subsets into T_H17 cells.

4.7. Satb1 deficiency alters gene expression and chromatin accessibility in naive CD4$^+$ T cells

Since Satb1 is already expressed at high levels in naive CD4$^+$ T cells, the deletion of Satb1 might alter gene expression already in naive CD4$^+$ T cells, subsequently inhibiting the differentiation into T_H17 cells upon activation. To address this, chromatin accessibility and transcriptome profiles in Satb1-sufficient and -deficient naive CD4$^+$ T cells were analyzed.

ATAC-seq revealed changes in the chromatin accessibility between Satb1-sufficient and -deficient naive CD4$^+$ T cells (Figure 46a). Although most genomic regions showed similar accessibility, chromatin rearrangements were observed in 794 differentially accessible regions, of which 678 were accessible in Satb1-deficient but not in Satb1-sufficient naive CD4$^+$ T cells (Figure 46b,c). Thus, one can conclude that Satb1 acts predominantly as a repressor of open chromatin in naive CD4$^+$ T cells as previously suggested based on transcriptome data in other cell types like baby hamster kidney fibroblasts and thymocytes (Alvarez et al., 2000; Kohwi-Shigematsu et al., 1997).

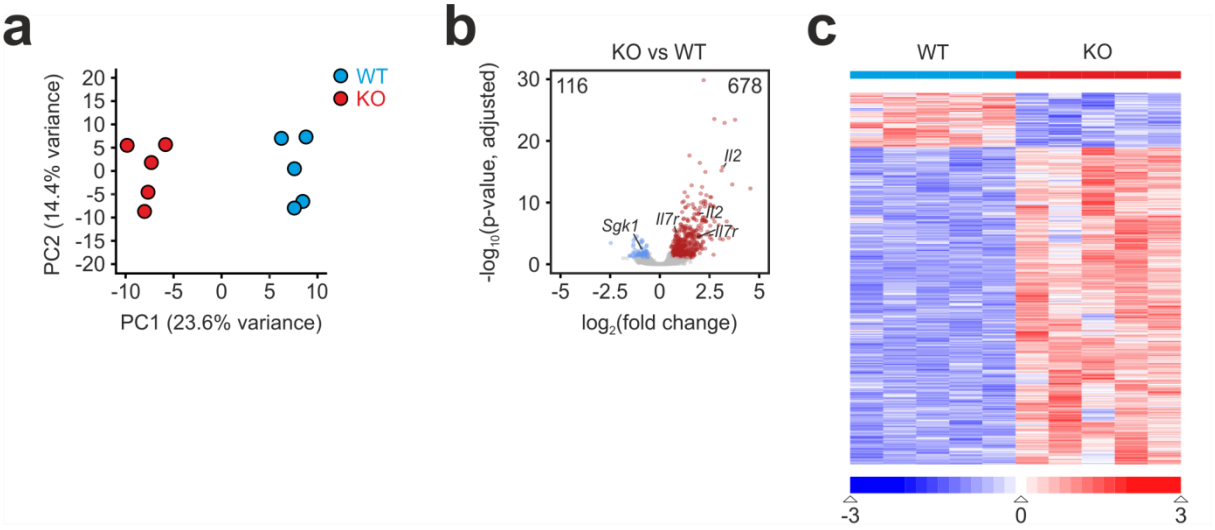

Figure 46: Satb1 acts as a chromatin repressor in naive CD4$^+$ T cells.
Satb1-sufficient and -deficient naive CD4$^+$ T cells were isolated by flow cytometric cell sorting and chromatin accessibility was analyzed using ATAC-seq. **(a)** Principal component analysis (PCA) based on all present accessible regions. **(b)** Changes in accessible regions in Satb1-deficient versus -sufficient naive CD4$^+$ T cells presented as volcano plot. **(c)** Heatmap of differentially accessible regions. (a-c) n=5. Regions with an adjusted p-value < 0.1 and a fold change >1.5 were determined as significantly differentially accessible. Data were analyzed by Jonas Schulte-Schrepping.

Gene ontology enrichment of differentially accessible regions predicted an increased activation and differentiation state of Satb1-deficient naive CD4$^+$ T cells (Figure 47a). Characterization of these T cell activation genes on the transcriptional level revealed a trend towards higher expression in Satb1-deficient naive CD4$^+$ T cell for only a few factors like *Il2*,

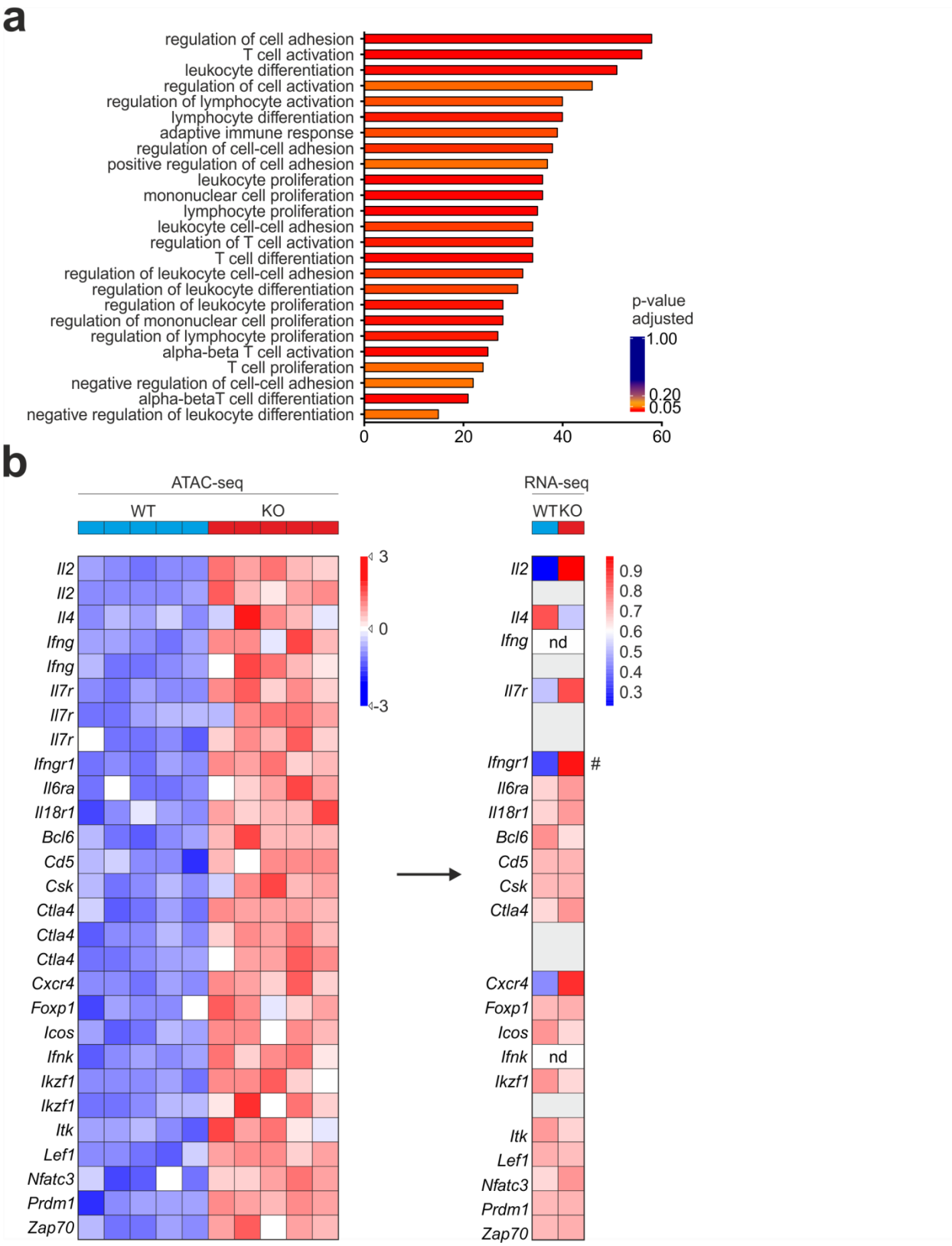

Figure 47: Satb1 retains the inactive state of naive CD4$^+$ T cells.
Bulk RNA-seq and ATAC-seq were performed on Satb1-sufficient and -deficient naive CD4$^+$ T cells. **(a)** Gene ontology enrichment analysis was conducted on differentially accessible regions. **(b)** Heatmap of differentially accessible regions and cumulative transcriptional expression values of selected genes associated with T cell activation and differentiation. #, differentially expressed genes; nd, not detected. ATAC-seq, n=5, RNA-seq, n=4. Data were analyzed by Jonas Schulte-Schrepping.

Il7, *Cxcr4* or *Ifngr1* (Figure 47b). However, altered chromatin accessibility did not result in a general simultaneous differential gene expression of T cell activation genes in naive CD4$^+$ T cells. Nevertheless, it is likely that changed gene accessibility will allow for earlier expression of these factors once T cell activation is induced, suggesting that Satb1-deficent cells are in an alert state which allows them to react earlier to activation signals.

On the transcriptional level, although Satb1-sufficient and -deficient naive CD4$^+$ T cells can be clearly separated by principle component analysis (Figure 48a), only few genes were differentially expressed (Figure 48b,c). In total 91 genes were upregulated and 25 genes were downregulated in Satb1-deficient cells.

Together, this indicates that Satb1 functions as a chromatin organizer and especially as a gene repressor in naive CD4$^+$ T cells. Deletion of Satb1 in naive CD4$^+$ T cells results in a different chromatin profile and provides an optimal genomic framework for cell activation. However, the deletion does not directly mediate enhanced gene transcription in the naive state. Thus, increased chromatin accessibility does not correspond to the initiation of a cellular activation program, but poises cells for optimal activation.

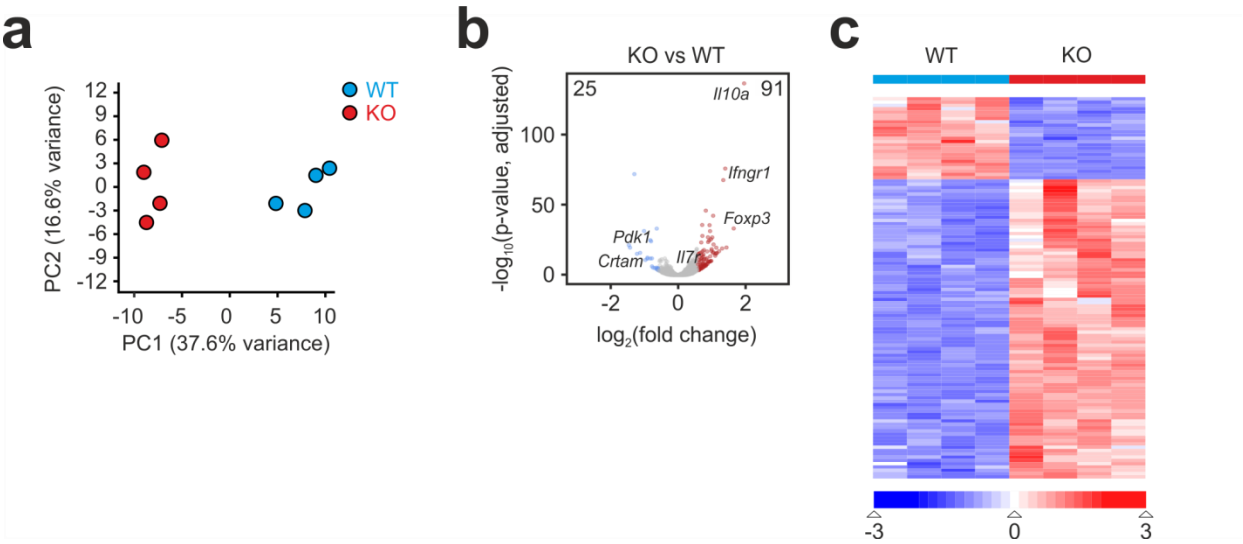

Figure 48: Satb1 influences gene expression in naive CD4$^+$ T cells.
Satb1-sufficient and -deficient naive CD4$^+$ T cells were isolated by flow cytometric cell sorting and transcriptome analysis performed on bulk RNA. **(a)** Principal component analysis (PCA) based on all present expressed genes. **(b)** Changes in gene expression in Satb1-deficient versus -sufficient naive CD4$^+$ T cells presented as volcano plot. **(c)** Heatmap of differentially expressed genes. (a-c) n=4. Genes with an adjusted p-value < 0.05 and a fold change >1.5 were determined as significantly differentially expressed. Data were analyzed by Jonas Schulte-Schrepping.

To further investigate whether the altered chromatin state as well as transcriptional profile of naive $CD4^+$ T cells block T_H17 cell differentiation, genes negatively influencing the generation of T_H17 cells were further characterized. Although, the chromatin landscape and expression profile of most of these genes were unaltered, several T_H17 cell repressor genes, such as *Ets1*, *Gfi1*, *Il2*, *Irf8*, *Maf* and *Sp4*, showed increased chromatin accessibility in Satb1-deficient naive $CD4^+$ T cells (Figure 49). However, in line with the observations for T cell activation genes, mainly chromatin accessibility was altered while gene expression remained nearly unaffected except for *Foxp3* and a clear trend in *Il2*. This further supports the interpretation that loss of Satb1 mainly will shift cells towards a poised state which allows for a more rapid reaction towards stimulatory cues.

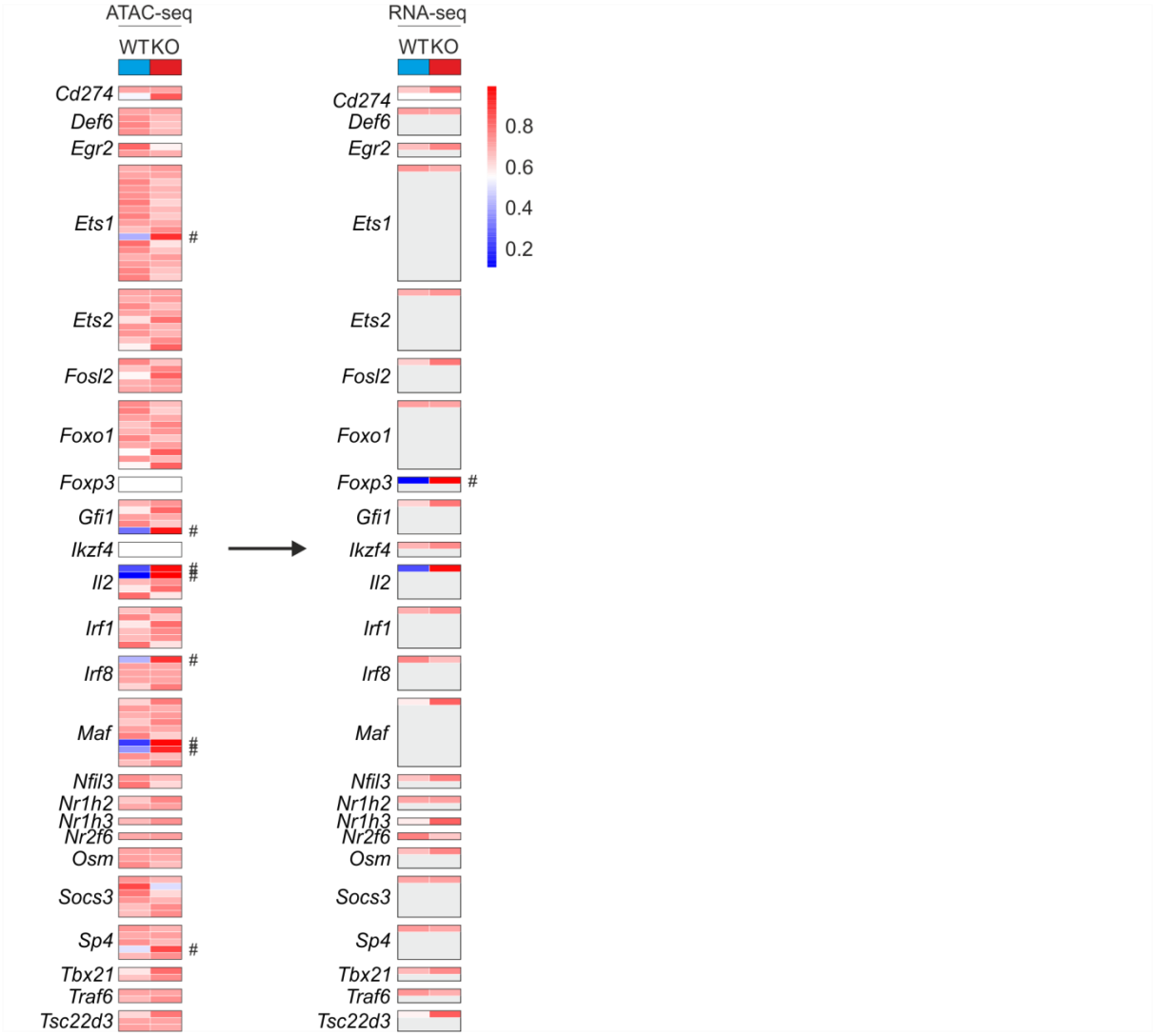

Figure 49: Satb1 rearranges the chromatin of T_H17 cell-regulating genes in naive $CD4^+$ T cells.
Bulk RNA-seq and ATAC-seq was performed on Satb1-sufficient and -deficient naive $CD4^+$ T cells. Cumulative heatmaps of accessible regions and expression values of selected genes negatively regulating T_H17 cell differentiation. #, differential accessible regions or expressed genes. ATAC-seq, n=5, RNA-seq, n=4. Data were analyzed by Jonas Schulte-Schrepping.

One interesting candidate previously reported to be regulated by Satb1 in T lymphoblastoid cell lines and PBMCs (Kumar et al., 2005; Pavan Kumar et al., 2006) is *Il2*. The *Il2* gene locus was more accessible in Satb1-deficient naive CD4$^+$ T cells (Figure 50a) and showed already slightly higher expression in unstimulated cells (Figure 49). In line with this, when characterizing differentially accessible regions and differentially expressed genes upregulated

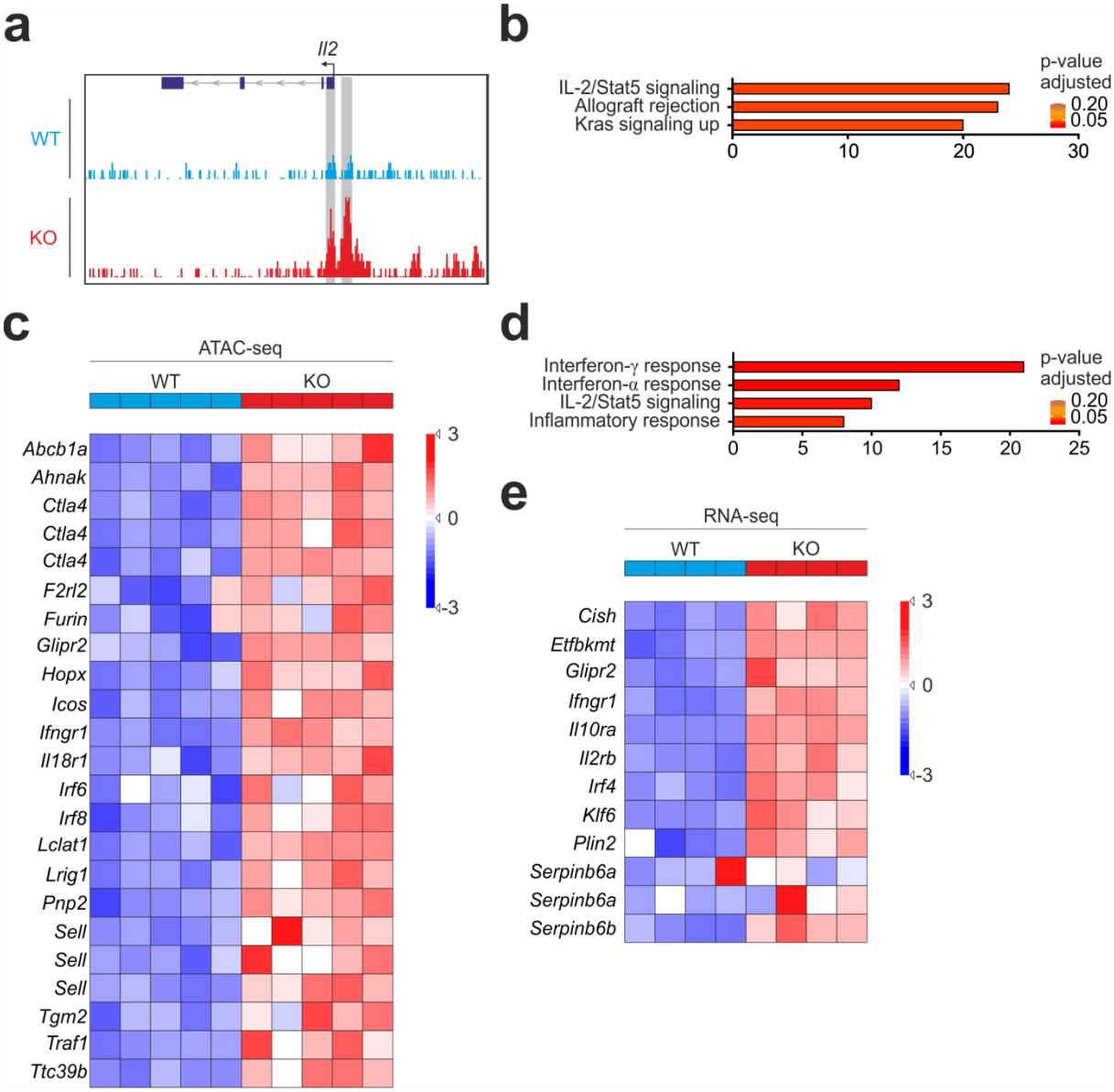

Figure 50: Satb1 suppresses the *Il2* gene locus and IL-2 signaling in naive CD4$^+$ T cells. Bulk RNA-seq and ATAC-seq was performed on Satb1-sufficient and -deficient naive CD4$^+$ T cells. **(a)** ATAC-seq profiles across the *Il2* gene locus. **(b)** Enrichment of hallmark pathways (using MSigDB) in differentially accessible regions upregulated in Satb1-deficient naive CD4$^+$ T cells. **(c)** Heatmap of differentially accessible regions present in the hallmark term IL-2/Stat5 signaling. **(d)** Enrichment of hallmark pathways (using MSigDB) in differentially expressed genes upregulated in Satb1-deficient naive CD4$^+$ T cells. **(e)** Heatmap of differentially expressed genes present in the hallmark term IL-2/Stat5 signaling. (a-c) n=5, (d-e) n=4. Data were analyzed by Jonas Schulte-Schrepping.

in Satb1-deficient cells, an enrichment of genes involved in the IL-2/Stat5 signaling pathway was observed (Figure 50b-e). This finding lead to the hypothesis, that blockade of IL-2 and Stat5 signaling in naive $CD4^+$ T cells and early upon cell activation might be one mechanism how Satb1 controls the differentiation of T_H17 cells, which warrants further investigation.

4.8. Satb1 inhibits IL-2 expression in naive $CD4^+$ T cells

If Satb1-deficient naive $CD4^+$ T cells are in a poised state which allows for rapid T cell activation, TCR stimulation of Satb1-deficient naive $CD4^+$ T cells should result in an increased $CD4^+$ T cell activation. To validate this both Satb1-sufficient and -deficient $CD4^+$ T cells were stimulated with CD3 and CD28 antibodies and their glycolytic activity was analyzed by measuring the ECAR as it has been reported that TCR signaling rapidly induces glycolysis in T cells (Menk et al., 2018). In line with the proposed hypothesis that loss of Satb1 will increase T cell activation, $CD4^+$ T cells showed an increased glycolytic activity upon TCR stimulation when Satb1 is absent in these cells (Figure 51).

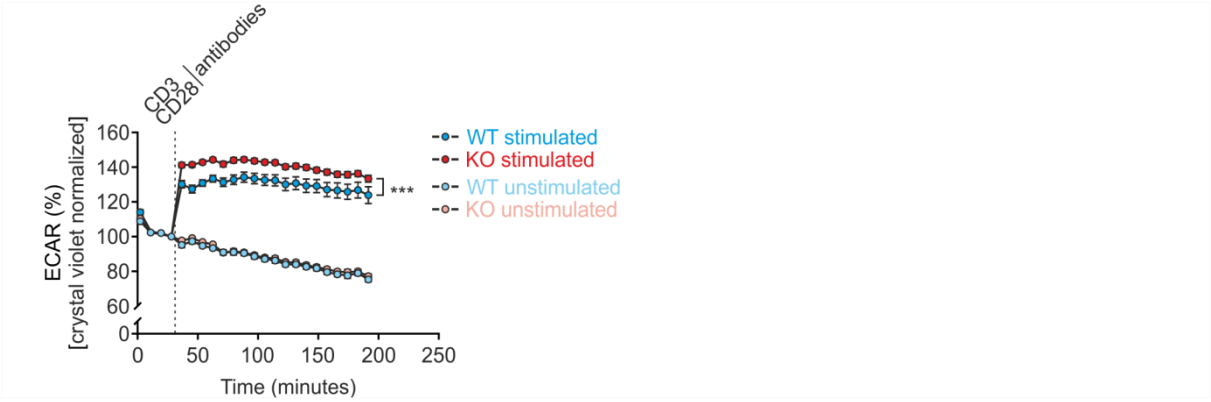

Figure 51: Satb1-deficient naive $CD4^+$ T cells exhibit increased glycolysis after TCR stimulation.
Real-time changes of the ECAR upon CD3 and CD28 antibody stimulation of Satb1-sufficient and -deficient $CD4^+$ T cells enriched by magnetic separation. Data (mean ± SEM) were obtained from three WT and three KO animals by repeated measurement, n=10-13, two-way repeated measures ANOVA with Tukey's multiple comparison test.

When filtering Satb1-regulated genes and looking for genes which are already linked with T cell activation and the modulation of T_H17 cell differentiation one interesting candidate, namely *Il2*, was identified. IL-2 is known to diminish the differentiation of T_H17 cells (Liao et al., 2013). Since the *Il2* gene locus was more accessible in naive $CD4^+$ T cells upon deletion of Satb1 and analysis of RNA-seq data hinted towards higher expression of *Il2* in Satb1-deficient naive $CD4^+$ T cells, the role of Satb1 for *Il2* expression and its subsequent role in the differentiation of T_H17 cells were further investigated.

To verify whether the increased accessibility of the *Il2* gene locus in Satb1-deficient naive CD4$^+$ T cells also results in upregulated gene expression, *Il2* mRNA expression was analyzed by qRT-PCR. Indeed, *Il2* was highly expressed in Satb1-deficient naive CD4$^+$ T cells in the spleen (Figure 52a). Furthermore, short-term stimulation of Satb1-deficient CD4$^+$ T cells with PMA/Ionomycin resulted in increased IL-2 protein expression in naive CD4$^+$ T cells both in cells isolated from the spleen and mLN (Figure 52b,c).

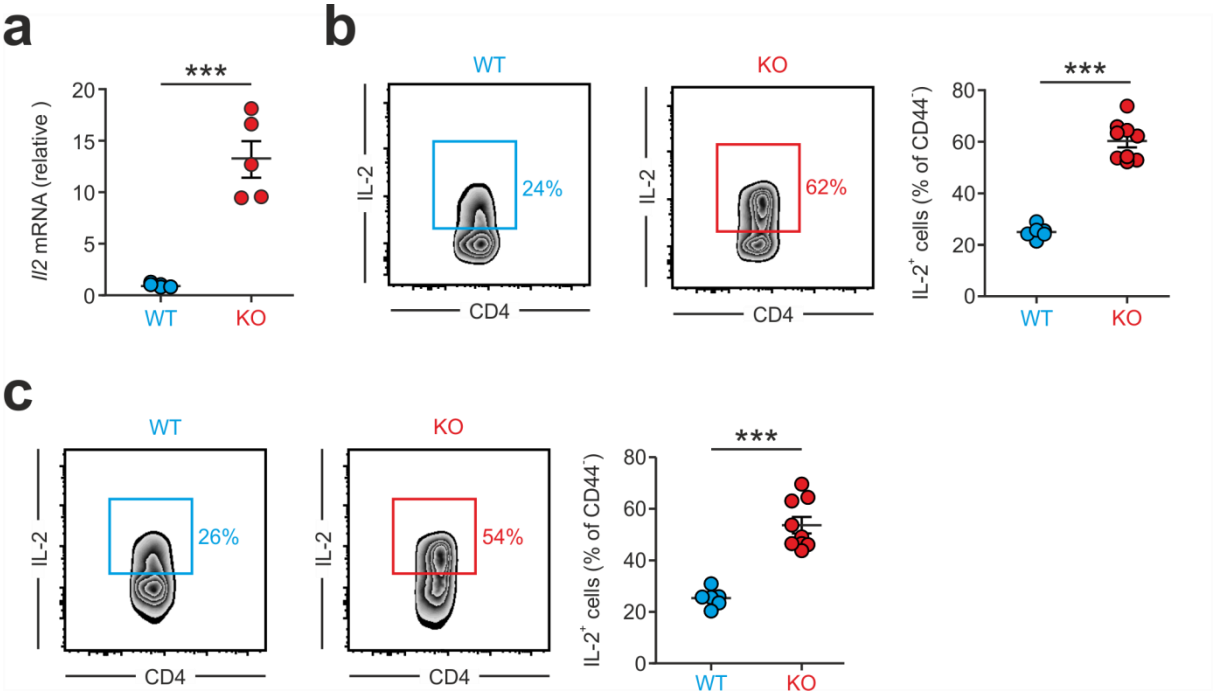

Figure 52: Satb1-deficient naive CD4$^+$ T cells upregulate IL-2 expression.
(a) Analysis of *Il2* mRNA expression in splenic Satb1-sufficient and -deficient naive CD4$^+$ T cells by qRT-PCR. **(b,c)** Quantification of IL-2-producing CD4$^+$CD44$^-$ naive T cells in spleen **(b)** and mLN **(c)** by flow cytometry. (a) n=5, (b,c) n=6-9, mean ± SEM, unpaired Student's t-test.

As IL-2 promotes the proliferation of T cells (Malek, 2008), increased IL-2 secretion of Satb1-deficient cells might result in an enhanced T cell proliferation. Indeed, upon stimulation with beads coated with antibodies against CD3 and CD28 for three days, Satb1-deficient CD4$^+$ T cells exhibited an increased proliferation further supporting that Satb1-deficient cells show an increased IL-2 signaling (Figure 53).

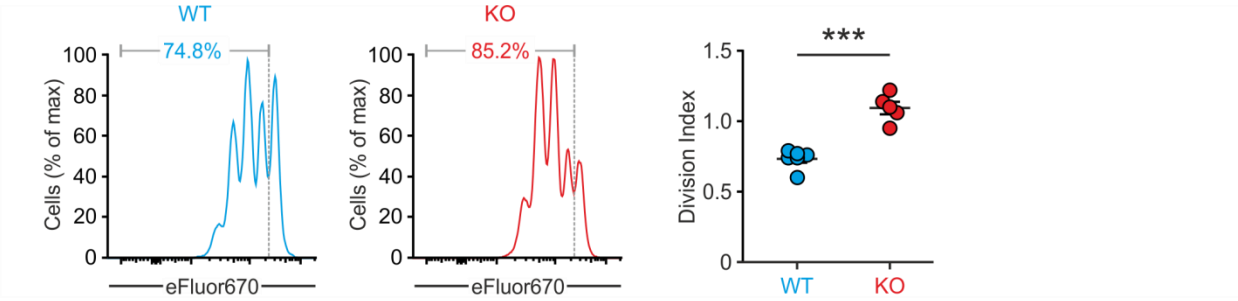

Figure 53: Satb1-deficient cells show an increased proliferation upon TCR stimulation. Satb1-sufficient and -deficient Tconv CD4$^+$ T cells were isolated by flow cytometric cell sorting, stained with the cell proliferation dye eFluor 670 and subsequently stimulated *in vitro* with CD3 and CD28 antibody-coated beads. At day three of stimulation, dilution of the cell proliferation dye was analyzed by flow cytometry. n=5-6, mean ± SEM, unpaired Student's t-test.

As already a spontaneous upregulation of IL-2 was observed seven days after Satb1 deletion in CD4-Cre-ERT2 animals and TCR stimulation resulted in an increased cell proliferation of Satb1-deficient cells, the question arose how prolonged deletion of Satb1 *in vivo* would influence IL-2 expression. Therefore, IL-2 expression was analyzed in aged Satb1$^{fl/fl}$/CD4-Cre mice. Similar to the data from CD4-Cre-ERT2 animals, an increased expression of IL-2 in naive CD4$^+$ T cells was observed (Figure 54a). Furthermore, IL-2 expression was upregulated not only in naive but also in CD44$^+$ effector CD4$^+$ T cells (Figure 54b), resulting in a significantly increased IL-2 expression in Satb1-deficient CD4$^+$ T cells in old animals independent of their differentiation state (Figure 54c). Thus, aged Satb1$^{fl/fl}$/CD4-Cre mice do not only show a reduced T_H17 cell differentiation (Figure 17b) but simultaneously show an upregulation of IL-2 expression.

Taken together, it can be concluded that in Satb1-deficient CD4$^+$ T cells the increased accessibility of the *Il2* gene locus results in an upregulation of IL-2 expression under homeostatic conditions in both young and aged animals.

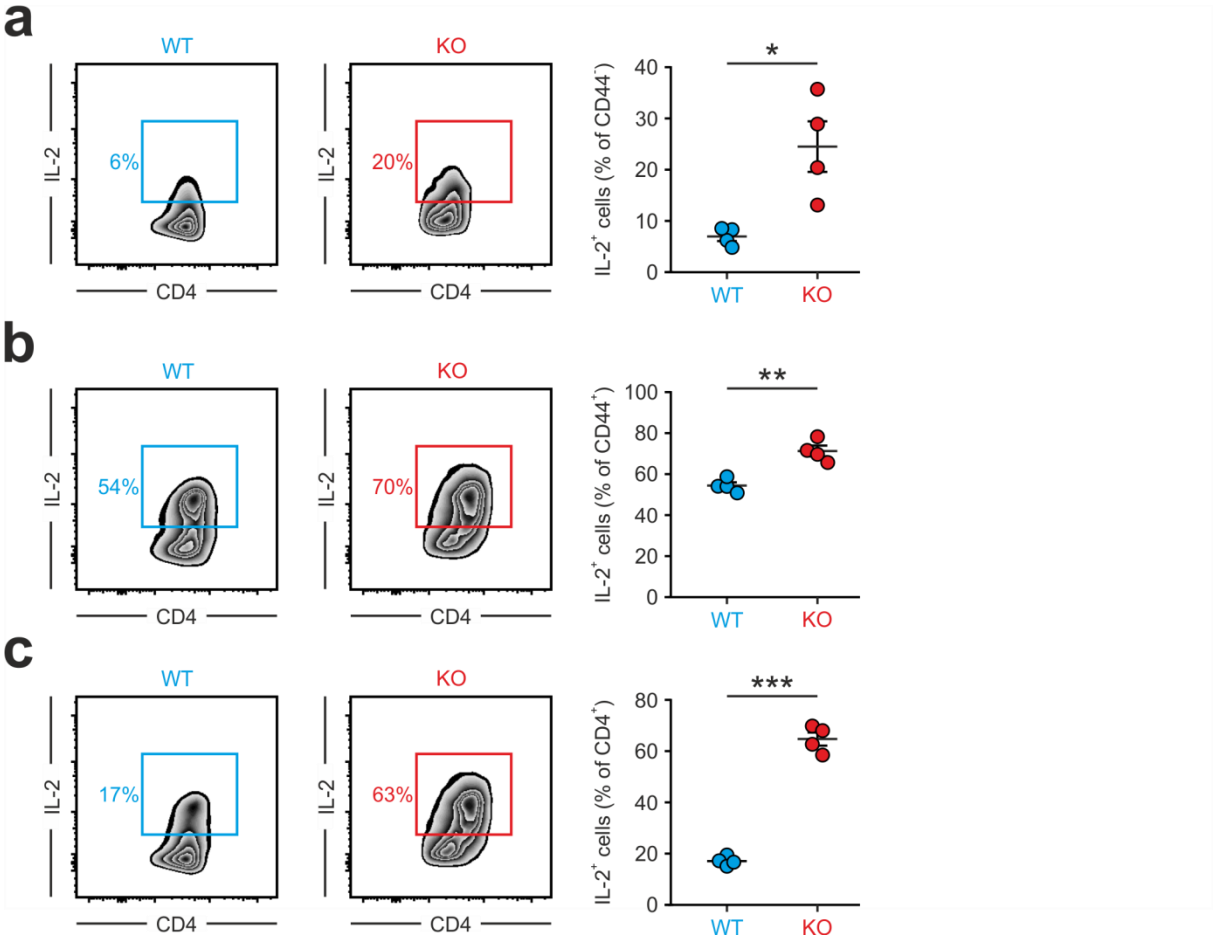

Figure 54: Deletion of Satb1 in CD4$^+$ T cells results in an increased IL-2 expression in aged animals.

Flow cytometric analysis of Satb1-sufficient and -deficient splenic CD4$^+$ T cells of 44-60 weeks old Satb1$^{fl/fl}$/CD4-Cre mice. Quantification of IL-2-producing cells in CD4$^+$CD44$^-$ naive T cells **(a)**, in the CD4$^+$CD44$^+$ effector pool **(b)** as well as in total CD4$^+$ T cells **(c)**. (a-c) n=4, mean ± SEM, unpaired Student's t-test.

As the loss of Satb1 results in the spontaneous expression of IL-2 in Satb1-deficient cells, it is tempting to speculate that overexpression of Satb1 would block IL-2 expression. To test this hypothesis, the influence of overexpression of Satb1 on IL-2 expression was analyzed by flow cytometry. Although IL-2 expression was not altered in naive CD4$^+$ T cells upon PMA/Ionomycin stimulation (Figure 55a), reduced IL-2 expression could be detected in the effector/memory CD4$^+$ T cells if Satb1 is overexpressed (Figure 55b). As Satb1 expression levels are already very high in wildtype naive CD4$^+$ T cells and thus overexpression of Satb1 only showed a gradual increase in Satb1 expression (Figure 9a,b), it is likely that these facts mask any potential changes in the naive CD4$^+$ T cell pool upon short-term stimulation. In contrast expression of Satb1 in wildtype effector/memory CD4$^+$ T cells is significantly lower and thus the overexpression of Satb1 has an actual impact on Satb1 protein levels (Figure 9c,d) allowing for assessing the impact of Satb1 overexpression on the production of IL-2 in effector/memory CD4$^+$ T cells. These results further indicate that Satb1 influences IL-2

expression and plays an important role in preventing unwanted IL-2 expression by altering accessibility of the genomic *Il2* gene locus.

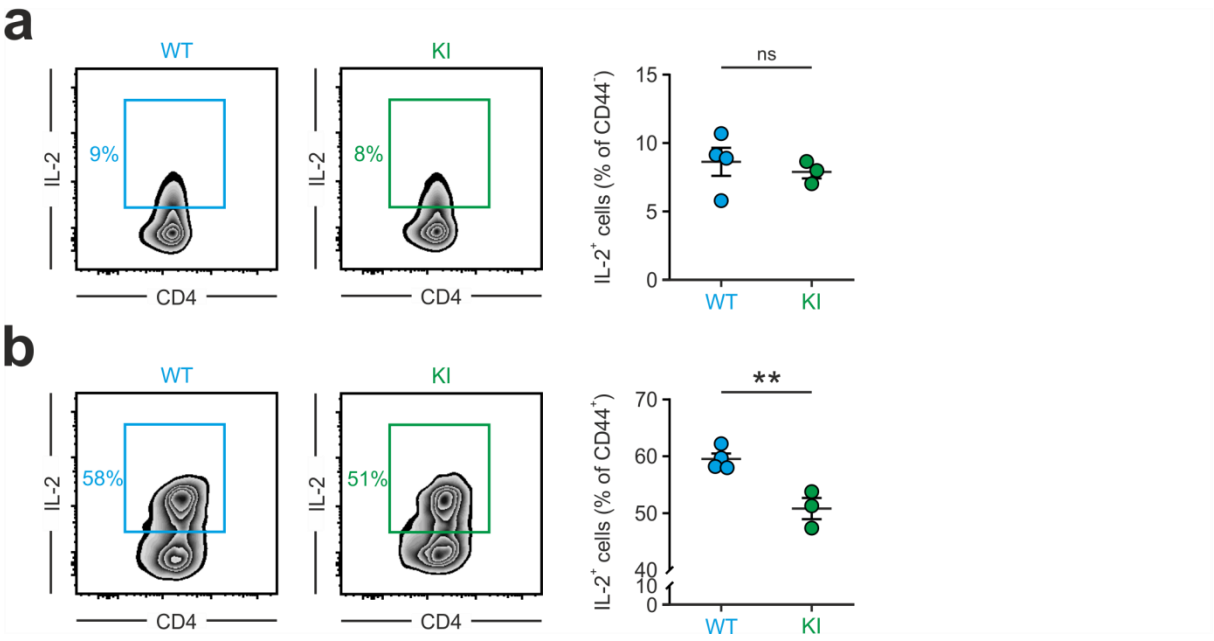

Figure 55: Overexpression of Satb1 in CD4$^+$ T cells results in decreased IL-2 production. Flow cytometric analysis of Satb1-wildtype and -overexpressing splenic T cells of 11-14 weeks old R26-STOP-Satb1 (WT) or homozygous R26-STOP-Satb1/CD4-Cre (KI) mice. Quantification of IL-2-producing cells in CD4$^+$CD44$^-$ naive T cells **(a)** and in the CD4$^+$CD44$^+$ effector pool **(b)**. n=3-4, mean ± SEM, unpaired Student's t-test.

In CD4$^+$ T cells, *Il2* expression is tightly controlled and multiple factors have been identified that can block *Il2* expression (Liao et al., 2013). In the last years, Kim et al. showed that Pten blocks *Il2* expression and that a lack of Pten results in reduced differentiation of T_H17 cells (Kim et al., 2017), similar to what has been observed in this thesis upon deletion of Satb1. Furthermore, Panagoulias et al. showed that in naive CD4$^+$ T cells *Il2* expression is repressed by Ets2 (Panagoulias et al., 2016).

To determine if Satb1 regulates *Il2* expression by Pten or Ets2, the expression of the two IL-2-regulating genes was analyzed in Satb1-sufficient and -deficient naive CD4$^+$ T cells. Expression of both, *Pten* and *Ets2*, was not significantly altered on mRNA level in Satb1-deficient naive CD4$^+$ T cells (Figure 56), indicating that Satb1 blocks *Il2* expression downstream or independently of both regulators.

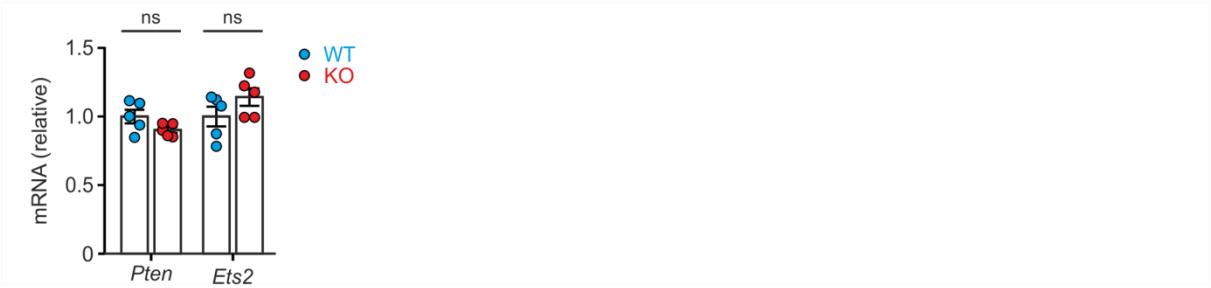

Figure 56: Satb1 inhibits IL-2 expression independent of *Pten* and *Ets2*.
Analysis of *Pten* and *Ets2* mRNA expression in Satb1-sufficient and -deficient naive $CD4^+$ T cells by qRT-PCR. n=5, mean ± SEM, unpaired Student's t-test.

Next, downstream targets of IL-2 in Satb1-sufficient and -deficient naive $CD4^+$ T cells were analyzed to determine if upregulation of *Il2* mRNA expression already increases IL-2 signaling in naive $CD4^+$ T cells without further stimulation. Thus, expression of *Socs1*, *Dusp6* and the IL-2 receptor α chain, *Cd25*, were analyzed (Kovanen et al., 2005). While expression of *Socs1* was not detectable in naive $CD4^+$ T cells independent of Satb1 expression, *Dusp6* mRNA expression was downregulated after deletion of Satb1 (Figure 57a). In contrast, *Cd25* was upregulated in Satb1-deficient naive T cells on mRNA level (Figure 57a). However, the increased mRNA level was not reflected on protein level (Figure 57b). This suggests that the loss of Satb1 might pre-activate and prime naive $CD4^+$ T cells by altering chromatin accessibility but to achieve full IL-2 signaling further activation signals are required.

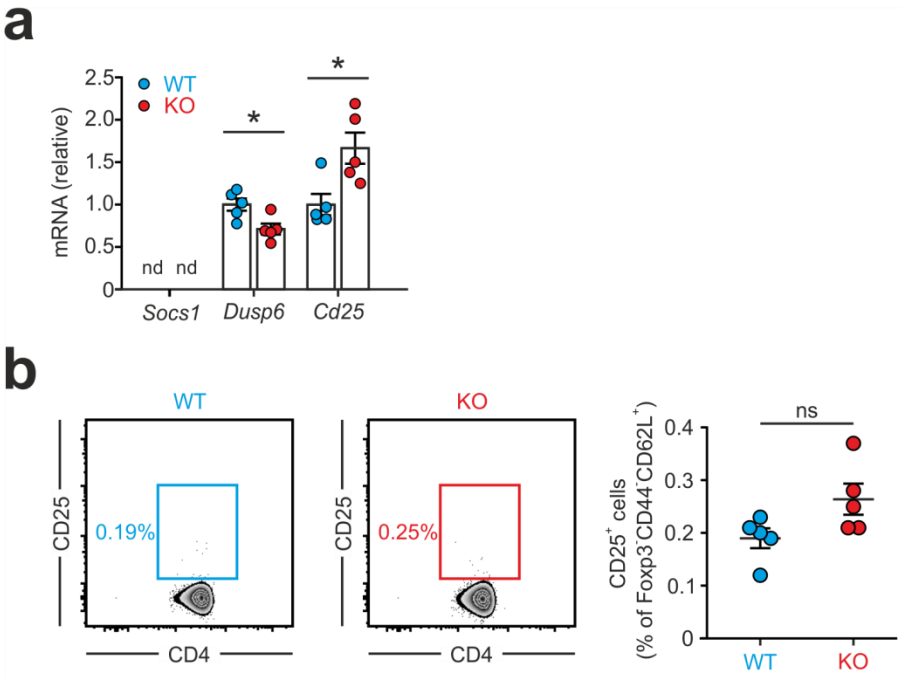

Figure 57: Satb1-deficient naive $CD4^+$ T cells upregulate *Cd25* expression.
(a) mRNA expression of the IL-2-regulated genes *Socs1*, *Dusp6* and *Cd25* in Satb1-sufficient and -deficient naive $CD4^+$ T cells was determined by qRT-PCR. **(b)** The percentage of CD25-expressing $CD4^+Foxp3^-CD44^-CD62L^+$ naive T cells was analyzed by flow cytometry. nd, not detected. n=5, mean ± SEM, unpaired Student's t-test.

4.9. Satb1 regulates T_H17 cell differentiation by controlling the expression of IL-2

Next, it was analyzed whether Satb1 deficiency diminishes T_H17 cell differentiation via IL-2 signaling. IL-2 limits the generation of T_H17 cells through various mechanisms (Liao et al., 2013). On the one hand, IL-2 represses signaling of IL-6, a key T_H17 cell-promoting cytokine. Both IL-6Rα as well as the signal transducer gp130 are downregulated by IL-2 (Liao et al., 2011).

Therefore, it was assessed whether the IL-6R was downregulated in Satb1-deficient cells in T_H17 cell culture. Indeed, reduced IL-6Rα expression in Satb1-deficient cells was observed three days after initiation of T_H17 cell differentiation (Figure 58).

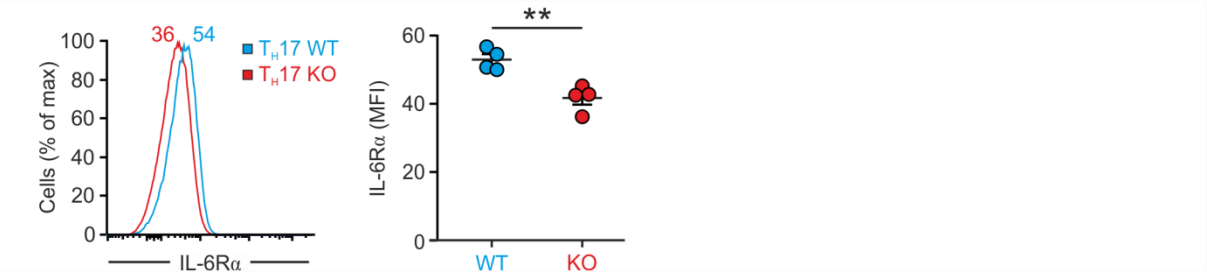

Figure 58: Satb1-deficient CD4$^+$ T cells exhibit a reduced IL-6 receptor (IL-6R) expression under T_H17 cell-driving conditions.
Satb1-sufficient and -deficient naive CD4$^+$ T cells were isolated by flow cytometric cell sorting and differentiated *in vitro* into T_H17 cells. At day three of differentiation, expression of IL-6Rα was analyzed by flow cytometry. n=4, mean ± SEM, unpaired Student's t-test.

On the other hand, IL-2 inhibits T_H17 cell differentiation by activation of Stat5 through phosphorylation (Laurence et al., 2007). Phosphorylated Stat5 attenuates IL-17 expression by reducing binding of phosphorylated Stat3 to the *Il17* gene locus and instead repressing *Il17* transcription (Yang et al., 2011).

To validate differences in the activation of Stat5 between Satb1-sufficient and -deficient CD4$^+$ T cells, the phosphorylation of Stat5 was analyzed at different time points during T_H17 cell differentiation. An increased Stat5 phosphorylation was detectable after 12 hours of differentiation in cells lacking Satb1, which became even more pronounced after 24 and 48 hours (Figure 59).

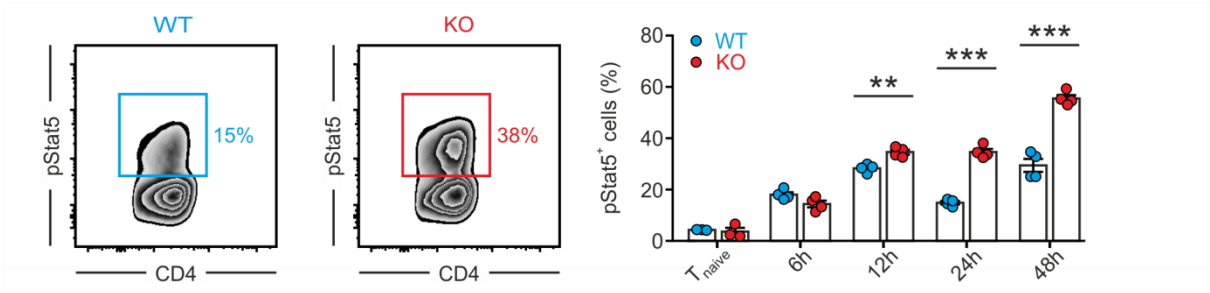

Figure 59: Satb1-deficient CD4$^+$ T cells show an increased Stat5 phosphorylation under T_H17 cell-driving conditions.
Satb1-sufficient and -deficient naive CD4$^+$ T cells were isolated by flow cytometric cell sorting and differentiated *in vitro* into T_H17 cells. At different time points during the differentiation, phosphorylation of Stat5 was analyzed by flow cytometry. Representative dot plots of pStat5 expression after 24 hours (left) and quantification of pStat5 over time (right). h, hour. n=3-4, mean ± SEM, two-way ANOVA with Sidak's multiple comparison test. Data are representative of two independent experiments.

Furthermore, when analyzing CD25 expression, which is induced by IL-2 via activation of Stat5 as a positive feedback loop (Malek, 2008), an increased upregulation of CD25 was observed in Satb1-deficient CD4$^+$ T cells from day one of T_H17 cell differentiation onwards (Figure 60). Thus, phosphorylation of Stat5 was followed by an upregulation of CD25 in Satb1-deficient cells under T_H17 cell-promoting conditions.

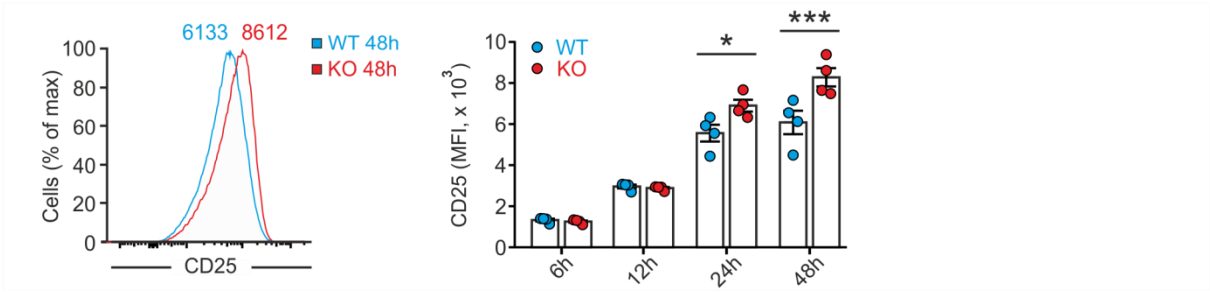

Figure 60: Satb1-deficient CD4$^+$ T cells show an increased expression of CD25 under T_H17 cell-driving conditions.
Satb1-sufficient and -deficient naive CD4$^+$ T cells were isolated by flow cytometric cell sorting and differentiated *in vitro* into T_H17 cells. At different time points during the differentiation, expression of CD25 was analyzed by flow cytometry. Representative histogram of CD25 expression after 48 hours (left) and quantification of CD25 (right). h, hour. n=4, mean ± SEM, two-way ANOVA with Sidak's multiple comparison test. Data are representative of two independent experiments.

In addition, Stat5 signaling promotes T-bet expression (Liao et al., 2011), which was upregulated on mRNA level in Satb1-deficient cells at day one of differentiation (Figure 42), although this was not reflected on the protein level on day three or five of differentiation (Figure 39).

Taken together, reduced expression of IL-6Rα as well as the activation of Stat5 and subsequent induction of CD25 expression are clear evidence of enhanced IL-2 signaling in Satb1-deficient cells under T_H17 cell-driving conditions.

As other members of the Stat family have been described as key determinants of T_H17 cells, the influence of Satb1 on other Stat proteins was further analyzed during T_H17 cell differentiation. Phosphorylation of Stat3 as well as Stat1 was assessed early after initiation of T_H17 cell differentiation, as both events are known as key downstream signals induced by cytokine/cytokine receptor interactions influencing T_H17 cell differentiation (Korn et al., 2009). For instance, IL-6 receptor signaling is important for Stat3 phosphorylation, which subsequently induces the differentiation of T_H17 cells (Yang et al., 2007).

Stat3 phosphorylation was not altered in the first 12 hours after initiation of T_H17 cell differentiation. Both Satb1-sufficient and -deficient cells showed an increase in pStat3 levels, directly after cell activation (Figure 61a). However, after 24 and 48 hours phosphorylation of Stat3 was prolonged in Satb1-deficient cells. Thus, although formation of the central T_H17 gene network was impaired and IL-6Rα was downregulated at day three of T_H17 cell differentiation, phosphorylation of Stat3 was not diminished by Satb1 deficiency but rather maintained after one and two days of differentiation. This might be explained by a compensatory mechanism to allow for T_H17 cell differentiation despite absence of Satb1.

In addition, phosphorylation of Stat1 was analyzed during T_H17 cell differentiation. Similar to phosphorylation of Stat5, the activation of Stat1 counteracts T_H17 cell differentiation (Neufert et al., 2007). Interestingly, an increase in Stat1 phosphorylation was detected 15 min after commencement of differentiation in Satb1-deficient cells (Figure 61b). However, Stat1 activation was lost within six hours after the start of T_H17 cell differentiation independent of Satb1 expression and the downregulation of Stat1 phosphorylation was even more rapid in Satb1-deficient cells. Thus, loss of Satb1 resulted in accelerated Stat1 phosphorylation with a concomitant increased dephosphorylation, indicating that regulation of Stat1 phosphorylation is a possible additional mechanism how Satb1 influences the differentiation of T_H17 cells.

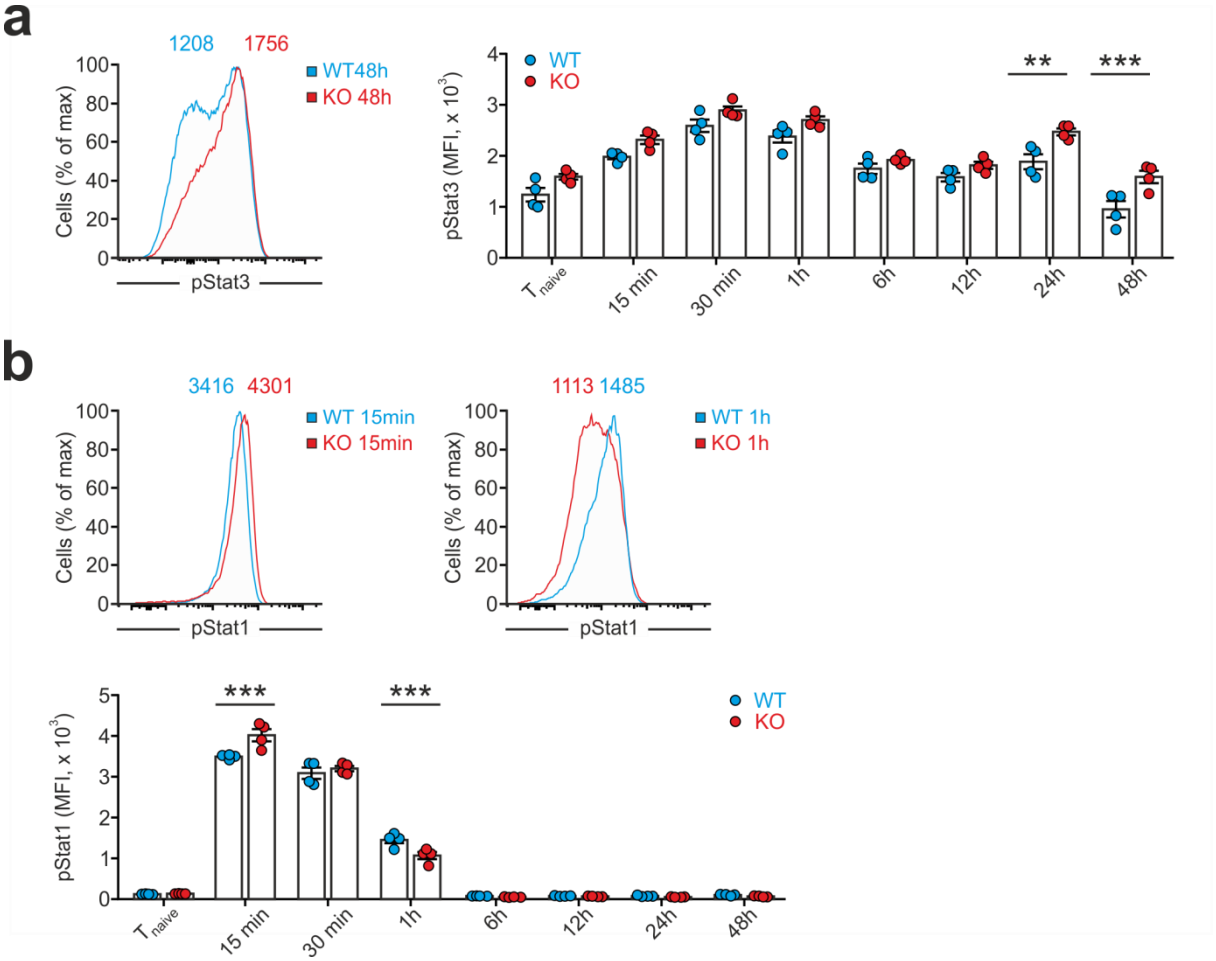

Figure 61: Satb1-deficient CD4$^+$ T cells show increased Stat1 and Stat3 phosphorylation under T_H17 cell-driving conditions.
Satb1-sufficient and -deficient naive CD4$^+$ T cells were isolated by flow cytometric cell sorting and differentiated *in vitro* into T_H17 cells. Phosphorylation of Stat3 **(a)** and Stat1 **(b)** was analyzed by flow cytometry at different time points during the differentiation process. h, hour; min, minutes. n=4, mean ± SEM, two-way ANOVA with Sidak's multiple comparison test.

4.10. Blockage of IL-2 signaling restores T_H17 cell differentiation

Since the loss of Satb1 predominantly resulted in increased IL-2 signaling and IL-2 constrains the differentiation of T_H17 cells, the question arose if a blockage of IL-2 signaling would restore T_H17 cell generation in Satb1-deficient CD4$^+$ naive T cells. Thus, Satb1-sufficient and -deficient CD4$^+$ T cells were differentiated *in vitro* in T_H17 cells in the absence or presence of IL-2 neutralizing and CD25-blocking antibodies and IL-17 expression was analyzed on day five of differentiation. Similar to previously reported data (Fujimura et al., 2013; Laurence et al., 2007), inhibition of IL-2 signaling greatly increased T_H17 cell differentiation in Satb1-sufficient CD4$^+$ T cells (Figure 62). Furthermore, the absence of IL-2 signaling in Satb1-deficient cells restored IL-17 expression to the same level as in

Satb1-sufficient cells, showing that Satb1 regulates the generation of T_H17 cells through inhibiting IL-2 signaling.

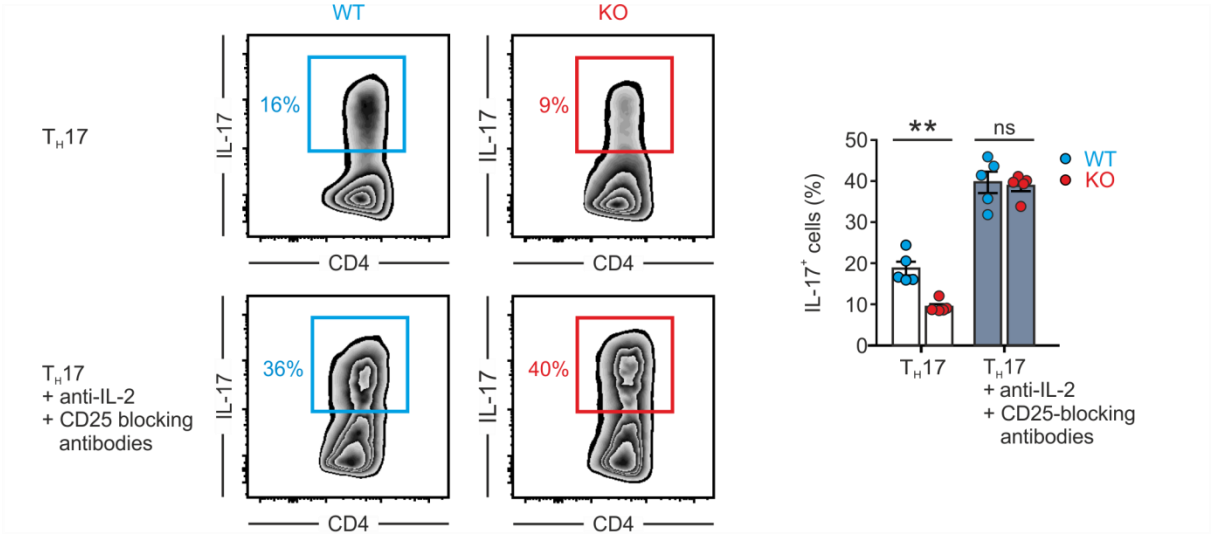

Figure 62: Blockade of IL-2 and CD25 restores T_H17 cell differentiation in Satb1-deficient $CD4^+$ T cells.
Satb1-sufficient and -deficient naive $CD4^+$ T cells were isolated by flow cytometric cell sorting and differentiated *in vitro* into T_H17 cells in absence or presence of anti-IL-2 and CD25-blocking antibodies. At day five of differentiation, expression of IL-17 was analyzed by flow cytometry. n=5, mean ± SEM, two-way ANOVA with Sidak's multiple comparison test.

Taken together, these data show that Satb1 plays an important role in the differentiation of $CD4^+$ T cells. Satb1 is differently regulated in T_H subsets and a dysregulation of Satb1 expression resulted in an altered differentiation capability of naive $CD4^+$ T cells *in vitro*.

Deletion and overexpression of Satb1 in $CD4^+$ T cells revealed that Satb1 expression is supporting the differentiation of T_H2, T_H9 and T_H17 cells. Furthermore, in T_H2 cells a tightly controlled expression of Satb1 is important, as both overexpression and loss of Satb1 expression diminished T_H2 cell differentiation. In contrast, loss of Satb1 accelerated the differentiation of T_H1 and iTreg cells.

Satb1 had a high impact especially for T_H17 cell differentiation. A more detailed look revealed upregulation of Satb1 in T_H17 cells. Deletion of Satb1 in naive $CD4^+$ T cells or in the early phase of T_H17 cell differentiation resulted in greatly diminished T_H17 cell generation *in vitro* but also *in vivo* under homeostatic conditions as well as during T_H17 cell-driven disease formation. One possible explanation for this decreased differentiation of Satb1-deficient cells into T_H17 cells is the dysregulation of the central T_H17 cell gene network. Furthermore, expression of Satb1 was important for the restimulation of T_H17 cells and reprogramming of T_H1 cells into T_H17 cells.

Transcriptional and epigenetic characterization of Satb1-deficient naive $CD4^+$ T cells revealed an increased activation state, which is caused by enhanced chromatin accessibility at the *Il2* gene locus, among others, allowing an upregulation of IL-2 expression. IL-2 signaling in Satb1-deficient cells resulted in an increased phosphorylation of Stat5, augmented expression of CD25 and downregulation of IL-6Rα, all mechanisms known to constrain T_H17 cell differentiation. In line with this, blockade of IL-2 in Satb1-deficient cells restored the differentiation of T_H17 cells.

In summary, Satb1 is important for the generation of T_H17 cells by inhibiting IL-2 expression in naive $CD4^+$ T cells as well as during the early stages of T_H17 cell differentiation. Based on this observation, Satb1 plays a critical role in T_H17 cell biology and consequently in T_H17 cell-driven autoimmune diseases.

5. Discussion

For a comprehensive adaptive immune response, the differentiation of activated naive $CD4^+$ T cell into specialized T_H subsets is essential. Each subset fulfills specified functions and the differentiation into T_H subsets in response to the microenvironment allows for an optimal adjustment to the prevailing conditions. However, dysregulated differentiation of $CD4^+$ T cells is associated with tumorigenesis and autoimmunity (Ivanova and Orekhov, 2015). Thus, it is important to understand the underlying mechanisms which drive lineage decision and to find targeting approaches, how to interfere with and modify the differentiation into T_H cells in a specific manner. For linage commitment, the establishment of a specific gene network is required (Ciofani et al., 2012; Henriksson et al., 2019; Kaplan, 2017; Pedicini et al., 2010; Placek et al., 2009; Shih et al., 2014; Wu et al., 2018; Yosef et al., 2013). Here, especially epigenetic modifications and chromatin reorganization have a crucial role in the set-up of these networks (Avni and Rao, 2000; Murphy and Reiner, 2002; Shih et al., 2014).
Satb1 regulates gene expression by linking chromatin to the nuclear matrix and recruiting chromatin-modifying factors to their target gene loci (Shannon, 2003; Yasui et al., 2002). It is known that Satb1 plays an essential role in the development of T cells, starting from lymphoid lineage determination in HSCs and continuing over several steps during thymopoiesis (Figure 4) (Alvarez et al., 2000; Doi et al., 2018; Hao et al., 2015; Kakugawa et al., 2017; Kitagawa et al., 2017; Nie et al., 2005; Satoh et al., 2013). Furthermore, in recent years it has become clear that Satb1 also influences peripheral T_H cell differentiation. Especially its role in in the differentiation of Treg, T_H2 and T_H17 cells was studied in more detail (Akiba et al., 2018; Beyer et al., 2011; Cai et al., 2006; Ciofani et al., 2012; Kitagawa et al., 2017; Yasuda et al., 2019). However, the exact role of Satb1 for lineage decision and differentiation into T_H cells is still unknown. The aim of this study was to investigate the influence of Satb1 on the differentiation of naive $CD4^+$ T cells into different T_H subsets and to understand the mechanisms how Satb1 governs the differentiation process.

5.1. Satb1 influences the differentiation of naive $CD4^+$ T cells into T_H cells

In this thesis, the expression profile of Satb1 during the differentiation of wildtype $CD4^+$ T cell was analyzed both on mRNA and protein level. Furthermore, the influence of Satb1 on the differentiation potential of naive $CD4^+$ T cells was assessed using Satb1-deficient or overexpressing cells. As most studies so far were performed under conditions where Satb1 was either knocked down or deleted, analyzing Satb1-overexpressing cells gave important insights into the role of Satb1 during the differentiation into T_H subsets. Analyzing the

development of T_H1, T_H2, T_H9, T_H17 as well as iTreg cells in context of Satb1 expression delivered a comprehensive view on the impact of Satb1 on T_H cell differentiation (Figure 63).

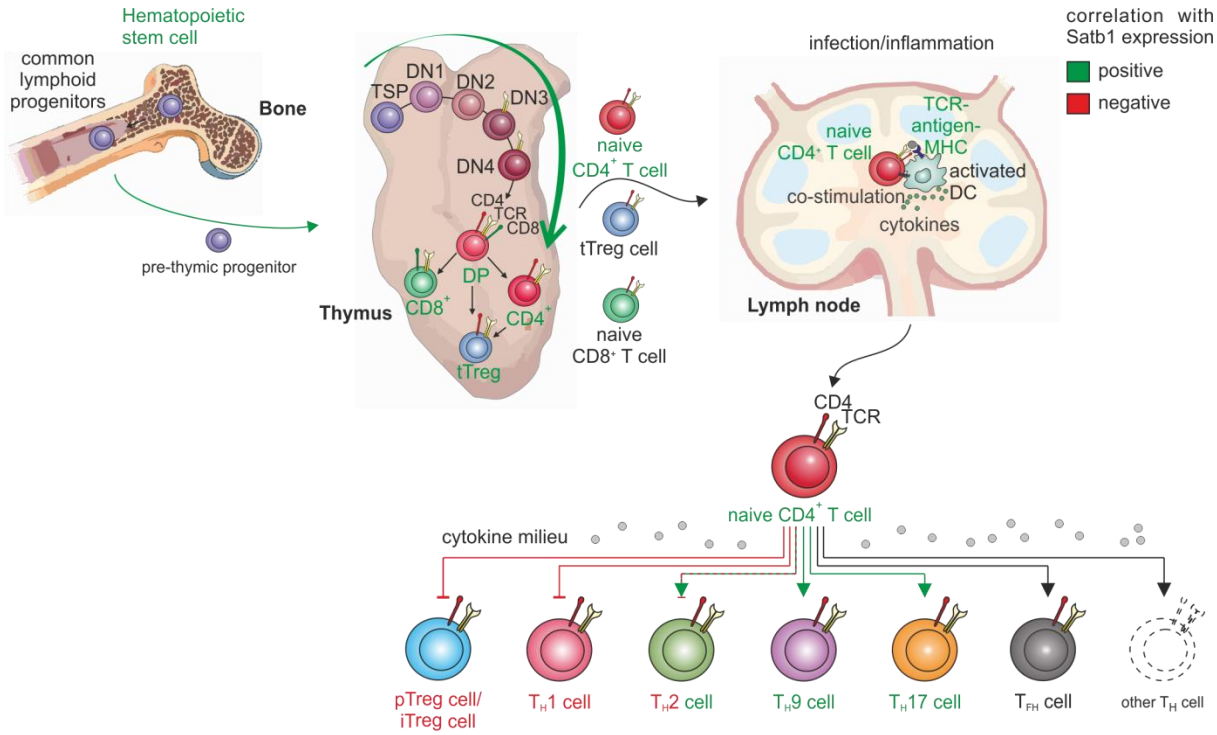

Figure 63: Satb1 influences the development of T cells and peripheral naive CD4$^+$ T cell differentiation.
Current understanding of the influence of Satb1 on the development and differentiation of CD4$^+$ T cells. Satb1 is required for lymphoid lineage decision as well as during thymopoiesis. In peripheral effector T cells, Satb1 is downregulated in pTreg and T_H1 cells, which facilitates lineage commitment into both T_H subsets. In contrast, expression of Satb1 is important for the differentiation into T_H9 and T_H17 cells. In T_H2 cells, a tight regulation of Satb1 is required and aberrant Satb1 expression diminishes T_H2 cell differentiation. CD, cluster of differentiation; CLP, common lymphoid progenitors; DP, double positive cells; MHC, major histocompatibility complex; Satb1, special AT-rich sequence-binding protein 1; tTreg, thymus-derived Treg cell; TCR, T cell receptor; T_H, T helper; TSP, thymus-settling progenitors.

Little was known about the role of Satb1 in the differentiation of T_H1 cells until Lund et al. showed that *Satb1* is downregulated in T_H1 cells in comparison to T_H2 cells (Lund et al., 2003, 2005). In contrast, Yasuda et al. only detected minor differences in *Satb1* mRNA expression in T_H1 cells in comparison to T_H2 cells, but a greater difference when comparing *Satb1* expression between T_H1 and T_H17 cells (Yasuda et al., 2019).

The analysis of Satb1 expression in this thesis revealed a downregulation of *Satb1* during the early steps of T_H1 cell differentiation in comparison to T_H2, T_H17 cells and naive CD4$^+$ T cells as well as a slight reduction in comparison to T_H9 cells. However, independent of the downregulation of *Satb1* mRNA expression an upregulation of Satb1 was observed in T_H1 cells on the protein level on day three and five. This discrepancy between mRNA and

protein expression might be explained by a generally more open chromatin structure upon differentiation and thus better accessibility to Satb1 protein within the nucleus during antibody staining, which would result in increased binding despite lower protein levels. However, preliminary data from our group support an upregulation of Satb1 independent of chromatin accessibility. Upon activation of $CD4^+$ T cells with CD3 and CD28 antibodies for 72 hours, protein levels of Satb1 were increased in the different cellular fractions like cytoskeleton, nuclear matrix and chromatin but also in the cytosol, where e.g. no changes in accessibility was expected upon activation (data not shown). Thus, the observed increase in Satb1 protein cannot be explained by activation-induced better accessibility of Satb1 protein. Nevertheless, these findings need to be further validated as activation of cells can also result in the cleavage of Satb1 (Olson et al., 2003, unpublished data), which might explain increased Satb1 protein in the cytosol. Besides, expression of Satb1 protein was similar in T_H1 and T_H9 cells at day three and five of the differentiation process and only minor changes were observed in comparison to T_H2 cells, although differences in *Satb1* mRNA expression could be detected. As outlined above, this discrepancy between mRNA and protein data cannot be explained by differences in chromatin accessibility upon TCR activation and thus needs to be studied in more detail in the future.

As *Satb1* mRNA as well as protein expression data can only suggest but not formally establish a functional role of Satb1 during T_H cell differentiation, overexpression and knock-out studies were performed. Interestingly, overexpression of Satb1 in naive $CD4^+$ T cells resulted in the downregulation of T_H1 cell development, while deletion of Satb1 fostered the differentiation into T_H1 cells *in vitro*. Increased IFN-γ expression was observed on day three in Satb1-deficient naive $CD4^+$ T cells, an effect which was masked by day five. Besides, a closer inspection of the time-course of *Ifng* and *Tbx21* (T-bet) expression revealed that deletion of Satb1 accelerates lineage commitment into T_H1 cells. This indicates that the downregulation of *Satb1* in wildtype cells facilitates the development of T_H1 cells.

In an approach similar to the one described in this thesis, published during the preparation of this thesis, Yasuda et al. studied the differentiation of Satb1-deficient naive $CD4^+$ T cells *in vitro* using $Satb1^{fl/fl}$/Thpok-Cre mice (Yasuda et al., 2019). In contrast to the results described in this thesis, Yasuda et al. did not observe differences in IFN-γ expression at day three between wildtype and Satb1-deficient cells. However, this might be due to differences in the differentiation protocols. While Yasuda et al. used plate-bound CD3 and soluble CD28 antibodies for stimulation (Yasuda et al., 2019), CD3 and CD28 antibodies cross-linked on immobilized goat anti-mouse IgG antibodies were used in this thesis. This might result in a

different strength of TCR stimulation, which is known to play an essential role in lineage decision by influencing for instance Stat activation (DuPage and Bluestone, 2016). Furthermore, the usage of a different Satb1$^{fl/fl}$ mouse line might additionally explain differences between the studies.

Over the last years several conditionally targeted Satb1 mouse lines have been generated, which differ in the targeted exons. While in one conditional mouse line exons two and three are flanked by loxP sites (Close et al., 2012), in others exons three to five (Skowronska-Krawczyk et al., 2014) or only exon four are flanked (Tesone et al., 2016). Although full protein expression is abrogated in all of these lines, differences might arise as it has been suggested that shorter fragments of the Satb1 protein created by Caspase-dependent cleavage exhibit a functional role (Galande et al., 2001; Gotzmann et al., 2000; Olson et al., 2003; Tan et al., 2008, 2010). Thus, although unlikely, a truncated version of the Satb1 protein with residual function might be translated if exon 2, the first coding exon, is not targeted and only early in-frame stop codons are created. In this thesis, the Satb1$^{fl/fl}$ mouse line generated by Daniel Sommer was used (Sommer et al., 2014). Sommer et al. integrated an inverted gene cassette behind the second exon, which contains the coding sequence for the enhanced green fluorescent protein (eGFP) as well as the 3' untranslated region of Satb1. The endogenous exon 2 together with the integrated gene cassette is flanked by two pairs of different loxP sites facing in opposite directions. When crossing these mice to Cre recombinase-expressing mice, a reversion of the allele is induced and eGFP is expressed instead of Satb1 (Sommer et al., 2014). Thus, in this thesis, the translation of mRNA residuals resulting in a truncated Satb1 protein is excluded.

Furthermore, not only *in vitro* but also *in vivo* differences in the development of T_H1 cells were observed upon deletion of Satb1 underlining the important role of Satb1 in the differentiation of T_H1 cells. In aged Satb1$^{fl/fl}$/CD4-Cre mice an increased differentiation into T_H1 cells in the spleen was detected. In line with this, an increase in the percentage of IFN-γ^+ cells in the brain and cLN was observed in the EAE model when Satb1 was deleted in CD4$^+$ T cells. However, the percentage of IFN-γ-expressing cells was similar between Satb1-sufficient and -deficient CD4$^+$ T cells in the adoptive transfer colitis model at the time point when the experiment had to be terminated. Furthermore, Yasuda et al. did not observe any differences in IFN-γ expression seven days after injection of Satb1-sufficient or -deficient naive CD4$^+$ T cells in Rag2$^{-/-}$ mice (Yasuda et al., 2019). Taken together, first experiments indicate that downregulation of Satb1 fosters T_H1 cell development but this was not consistent over the different experiments and further studies are needed to delineate in more detail how

Satb1 influences the differentiation of T_H1 cells. One possibility to further study the role of Satb1 in T_H1 cells would be disease models with only minor involvement of T_H17 cells to avoid an undue influence of T_H17 cells. Both the EAE model as well as the adoptive transfer colitis model used in this thesis are primarily pathogenic T_H17 cell-driven diseases (Ahern et al., 2010; Hirota et al., 2011; Kebir et al., 2009) and thus are not optimal models to study the differentiation into T_H1 cells *in vivo*. Altered interaction between T_H17 and T_H1 cells due to the loss of T_H17 cell development as well as a conversion of wildtype pathogenic T_H17 cells into IL-17$^-$IFN-γ^+ cells might mask the impact of the loss of Satb1 on the differentiation of T_H1 cells (Damsker et al., 2010; Hirota et al., 2011). Mouse models like LCMV infection, in which T_H1 cells play an important role (Whitmire et al., 1998), might be useful to further elucidate the role of Satb1 in the development of T_H1 cells. Furthermore, it would be interesting to compare how the overexpression of Satb1 in R26-STOP-Satb1/CD4-Cre mice would influence T_H1 cell-mediated disease models. In wildtype cells, *Satb1* is downregulated in T_H1 cells early on. Thus, an overexpression might result in a more defined phenotype *in vivo*. In addition, in mice harboring Satb1-deficient CD4$^+$ T cells especially the early time points during the disease development should be analyzed.

It is already known that Satb1 plays an important role during the development of T_H2 cells. Satb1 is upregulated by IL-4 signaling in a Stat6-dependent manner and subsequently Satb1 directly promotes Gata3 expression and enhances IL-4 expression (Ahlfors et al., 2010; Jargosch et al., 2016; Lund et al., 2003, 2005; Notani et al., 2010). Furthermore, Satb1 rearranges the T_H2 cell-associated cytokine locus and consequently regulates IL-4, IL-5 and IL-13 expression (Cai et al., 2006). Thus, Satb1 is described as a positive regulator of T_H2 cell differentiation.

In line with this, this thesis could show that *in vitro* differentiation of Satb1-deficient cells resulted in a diminished generation of IL-4 and Gata3 positive cells and thus in a reduced differentiation of T_H2 cells. Nevertheless, Yasuda et al. did not observe alterations in the differentiation of Satb1-deficient cells into T_H2 cells *in vitro* (Yasuda et al., 2019). As discussed above, this discrepancy might be the result of different stimulation conditions. This is further supported by the different efficiencies in generation of T_H2 cells between the two protocols, resulting in an increased conversation of naive CD4$^+$ T cells into T_H2 cells when stimulated with CD3 and CD28 antibodies cross-linked to IgG.

Besides Satb1 deficiency, also overexpression of Satb1 resulted in the downregulation of IL-4, while in contrast Gata3 expression was mainly unaffected. However, transfection of human naive CD4$^+$ T cells with plasmid DNA promoting overexpression of Satb1 resulted in

an upregulation of *GATA3* on mRNA level (Notani et al., 2010). This difference might be explained by the fact that Notani et al. analyzed mRNA levels in humans on day three while in this thesis protein levels in mice were analyzed at day five after initiation of T_H2 cell differentiation.

When studying *Satb1* mRNA expression in wildtype cells, a time-dependent regulation of *Satb1* expression was observed. While 12 hours after initiation of differentiation *Satb1* was still on the same level as in naive $CD4^+$ T cells, transient downregulation of *Satb1* mRNA started at day one of T_H2 cell differentiation. Over time *Satb1* expression was restored to a level similar to that of naive $CD4^+$ T cells. Meanwhile, on the protein level, Satb1 was upregulated especially on day three.

Taken together, this indicates that the development of T_H2 cells needs a precise level of Satb1 protein expression, which might explain why both downregulation and overexpression of Satb1 negatively influences T_H2 cell differentiation. Further studies might reveal the exact mechanism how Satb1 controls the differentiation of T_H2 cells. For instance, deletion or overexpression of Satb1 *in vitro* at different time point during the differentiation process might give new insights. Furthermore, T_H2 cell-driven disease models, such as specific allergic airway diseases or food allergies could be used to gain more insights into the role of Satb1 for T_H2 cells *in vivo* (Fallon and Schwartz, 2020; Schülke and Albrecht, 2019). In addition, analyzing animals overexpressing or lacking Satb1 in cells expressing Gata3 might be interesting to better understand the influence of Satb1 on the maintenance of already committed T_H2 cells. These analyses are important as Satb1 induces Gata3 expression in the early steps of T_H2 cell development and thus analyzing effects after the commitment of T_H2 cells might be difficult in CD4-Cre lines.

T_H9 cells are one of the more recently identified subset of T_H cells (Dardalhon et al., 2008; Veldhoen et al., 2008). Very little is known about a link between Satb1 and T_H9 cells. Karim et al. showed that co-stimulating naive $CD4^+$ T cells with Toll like receptor 2 (TLR2) ligands induces the differentiation of T_H9 cells (Karim et al., 2017). Satb1 was one of the top four genes which were upregulated, together with IL-9, in response to TLR2 stimulation (Karim et al., 2017). This indicates a role of Satb1 for the development of T_H9 cells. However, no further experimental evidence has so far linked Satb1 to the differentiation or functionality of T_H9 cells.

When analyzing *Satb1* expression in wildtype $CD4^+$ T cells during the differentiation into T_H9 cells *in vitro*, the expression profile of *Satb1* was reminiscent to that in T_H2 cells. Furthermore, on the protein level, Satb1 was upregulated. Interestingly, T_H2 and T_H9 cells are

closely related as both require IL-4 signaling, express Gata3 and promote a mast cell response (Kaplan, 2013). Thus, T_H9 cells are associated with T_H2 cells and it is still under debate whether T_H9 cells are a distinct T_H subset or are merely a subgroup within the T_H2 cell pool in humans (Micossé et al., 2019). As Satb1 has been described to play a vital role in T_H2 cells, it is likely that Satb1 additionally has a fundamental role in T_H9 cells. Indeed, upon deletion of Satb1 in naive $CD4^+$ T cells, differentiation into T_H9 cells was impaired while overexpression of Satb1 enhanced T_H9 cell differentiation, indicating an essential role of Satb1 for T_H9 cell differentiation. The *Il9* locus is associated with the T_H2 cytokine locus, which is regulated by Satb1 (Cai et al., 2006; Kaplan, 2013). Thus, it would be interesting to investigate whether Satb1 also controls the accessibility of *Il9*. Furthermore, it would be interesting to study the role of Satb1 in mouse models of asthma and oxazolone-induced colitis as well as in antitumor immunity in the context of T_H9 cell development (Chen et al., 2019; Gerlach et al., 2014; Malik and Awasthi, 2018). In addition, the role of Satb1 for the maintenance of T_H9 cells needs to be further studied. However, conditional deletion of Satb1 specifically in already *in vivo* committed T_H9 cells might be difficult. PU.1 as well as IL-9 are not uniquely expressed in T_H9 cells but it is their combined expression in a unique network, together with other transcription factors like Irf4, which defines a T_H9 cell. T_H2, T_H17, Treg, Natural Killer T cells as well as innate lymphoid cells and mast cells can produce IL-9 (Chen et al., 2019; Kaplan, 2013; Tan and Gery, 2012). Furthermore, although PU.1 is especially upregulated in T_H9 cells, it is still expressed in T_H1, T_H2 and T_H17 cells on a low level (Chang et al., 2010). Thus, functional studies on the role of Satb1 in T_H9 cells *in vivo* without altering the expression of Satb1 in other T_H cells will be challenging and would probably require novel mouse models to specifically address this question. Nevertheless, although challenging it is important to further study the specific role of Satb1 in T_H9 cells *in vivo* as it is likely that Satb1 sustains T_H9 cells as suggested already from the *in vitro* data.

It is known that Satb1 has a dual role during the development of Treg cells. While Satb1 is essential during the initial phase of tTreg cell development in the thymus by regulating Treg cell-specific super-enhancers, Satb1 is repressed in Treg cells in the periphery (Beyer et al., 2011; Kitagawa et al., 2017). In $Satb1^{fl/fl}$/CD4-Cre, $Satb1^{fl/fl}$/Vav-Cre as well as $Satb1^{fl/fl}$/Lck-Cre mice the development of pTreg cells is enhanced (Kitagawa et al., 2017; Kondo et al., 2016). This might be a compensatory mechanism due to the loss of tTreg cells and at the same time an attempt to counteract the resulting autoimmune responses, which was observed within these mice 4-16 weeks after birth. However, in our hands $Satb1^{fl/fl}$/CD4-Cre mice did not show any autoimmune symptoms (Sommer, 2018). This discrepancy might be

influenced by the microbial composition of these animals. In addition, analysis of pTreg cells in Satb1$^{fl/fl}$/Thpok-Cre mice revealed that a loss of Satb1 also slightly enhances the development of pTreg cells independent of the tTreg cell development and autoimmunity (Kitagawa et al., 2017). Taken together, these data show that the loss of Satb1 facilitates the differentiation of pTreg cells while having different impact on thymic Treg cell development dependent on the time point of Satb1 deletion.

In this thesis, when assessing the kinetics of *Satb1* expression during the differentiation of iTreg cells, a clear downregulation of *Satb1* was observed in the early phase of the differentiation process. This was mirrored also on the protein level. Furthermore, upon deletion of Satb1 in naive CD4$^+$ T cells, the development of iTreg cells was facilitated resulting in an increased percentage of Foxp3$^+$ cells at day three. This is in line with our current understanding and further underlines the influence of Satb1 on the development of Treg cells. In contrast, Yasuda at al. did not detect an alteration in the differentiation into iTreg cells of Satb1-deficient naive CD4$^+$ T cells of Satb1$^{fl/fl}$/Thpok-Cre mice (Yasuda et al., 2019). Nevertheless, the loss of Satb1 indirectly activates Treg cell-specific super-enhancers in the periphery, which subsequently enables Foxp3 expression in Tconv cells in Satb1$^{fl/fl}$/Thpok-Cre mice (Kitagawa et al., 2017). In line with this, transcriptional analysis of Satb1-deficient naive CD4$^+$ T cells revealed an increased Foxp3 expression in this thesis. This might explain why a deletion of Satb1 improves the development of iTreg cells especially in the early stages of differentiation and that wildtype cells, which shortly after initialization of iTreg cell differentiation start to downregulate Satb1 expression, over time catch up in expression of Foxp3. It would be interesting to further analyze the kinetics of Foxp3 in parallel to Satb1 expression.

Similar as in Tconv cells from Satb1$^{fl/fl}$/Thpok-Cre mice, increased *Foxp3* expression in Satb1-deficient naive CD4$^+$ T cells from Satb1$^{fl/fl}$/CD4-CreERT2 mice was not associated with other Treg cell signature genes and *Foxp3* expression was unstable. In line with this, an increased percentage of CD25$^-$Foxp3$^+$ cells were detected in Satb1$^{fl/fl}$/CD4-CreERT2 mice upon EAE induction. However, when assessing the development of CD25$^+$Foxp3$^+$ pTreg cells, no increased pTreg cells were observed in Satb1$^{fl/fl}$/CD4-CreERT2 mice upon EAE induction and the total number of Treg cells was even diminished in the CNS. Furthermore, the number of pTreg cells was reduced in the adoptive transfer colitis when Satb1-deficient naive CD4$^+$ T cells were injected into Rag2$^{-/-}$ mice compared to injection of Satb1-sufficient naive CD4$^+$ T cells. Thus, no enhanced development of pTreg cells was observed either during colitis or EAE development upon loss of Satb1 in CD4$^+$ T cells. These data lead to the

hypothesis that a downregulation of Satb1 in Tconv cells activates *Foxp3* expression but does not generally results in an enhanced development of fully committed pTreg cells. The development of Treg cells still requires optimal conditions. However, in an optimal microenvironment it is likely that linage commitment into pTreg cells is accelerated upon loss of Satb1.

Beyer et al. showed that downregulation of Satb1 in pTreg cells is essential for the maintenance of the regulatory phenotype both in mice and human. Lentiviral overexpression of Satb1 resulted in a loss of suppressive function (Beyer et al., 2011). Furthermore, Sommer et al. showed that an upregulation of Satb1 in Treg cells results in a partial conversion into exFoxp3 Treg cells (Sommer, 2018). In line with this, overexpression of Satb1 partially diminished the development of iTreg cells. It would be interesting to further study the influence of overexpression of Satb1 in Treg cells as this might be helpful to find novel therapeutic targets, for instance for the treatment of autoimmunity.

Analysis of Satb1 expression as well as functional studies revealed that Satb1 is essential for the differentiation of T_H17 cells. Thus, further detailed experiments were performed to unravel how Satb1 mediates T_H17 cell differentiation as discussed below.

Taken together, these data clearly show an important role of Satb1 in the early phase of T_H cell differentiation and lineage commitment. While in the last years the impact of Satb1 on thymopoiesis has been characterized in great detail, in this thesis the role of Satb1 after thymopoiesis was investigated to understand how Satb1 shapes the differentiation of naive $CD4^+$ T cells towards T_H1, T_H2, T_H9, T_H17 and iTreg cells. In the future, the contribution of Satb1 for the maintenance and plasticity of T_H subsets still needs to be further investigated. In addition, the role of Satb1 in T_{FH} and T_H22 cells should be studied. Furthermore, the individual microenvironment as well as other conditions like the TCR signaling strength might influence the contribution of Satb1 during lineage commitment and thus further *in vivo* studies are needed to fully understand the role of Satb1.

Besides, it is interesting that $CD4^+CD44^+CD62L^-CD25^-$ effector/memory T cells downregulated Satb1 on mRNA as well as protein level and that in both aged $Satb1^{fl/fl}$/CD4-Cre as well as R26-STOP-Satb1/CD4-Cre mice an increase in effector/memory $CD4^+$ T cells was observed, indicating that alterations of Satb1 expression might lead to changes in the $CD4^+$ T cell pool with increasing age. This raises the question how Satb1 influences the formation and maintenance of memory cells.

5.2. Satb1 is essential for the development of T_H17 cells

Although both exhibit distinct functions, it is likely that T_H17 and pTreg cells co-evolved, as a close relationship between these two subsets was observed (Weaver and Hatton, 2009). As Satb1 influences the development of pTreg cells (Beyer et al., 2011; Kitagawa et al., 2017; Kondo et al., 2016), it is reasonable to ask whether Satb1 controls the differentiation of T_H17 cells as well and if so, whether it does so in a similar or contrary manner. In addressing this question, it has been shown in the last years that Satb1 positively influences the development of T_H17 cells in contrast to the differentiation of pTreg cells. Characterization of the T_H17 cell-specific gene network predicted Satb1 as a regulator of T_H17 cells (Ciofani et al., 2012; Yosef et al., 2013). Furthermore, siRNA-mediated knockdown of Satb1 resulted in a loss of IL-17 expression and thus validated these bioinformatics predictions (Ciofani et al., 2012). Analysis of the *Satb1* mRNA profile in this thesis revealed a clear increase of *Satb1* expression over time *in vitro* in wildtype T_H17 cells compared to the other T_H subsets as well as to naive $CD4^+$ T cells, a finding corroborated by Yasuda et al. (Yasuda et al., 2019). In line with this, an enhanced Satb1 protein expression in wildtype T_H17 cells was observed. To address the functional impact of Satb1 on the lineage commitment of T_H17 cells, differentiation of Satb1-deficient as well as -overexpressing naive $CD4^+$ T cells into T_H17 cells was conducted *in vitro*. Similar to the results of the siRNA experiment, a clear reduction in the development of T_H17 cell was observed in the absence of Satb1 expression. Deletion of Satb1 in naive $CD4^+$ T cells nearly completely prevented the *in vitro* generation of IL-17^+ as well as RORγt^+ cells. Furthermore, overexpression of Satb1 during the differentiation process promoted the differentiation of T_H17 cells indicated by an increased percentage of IL-17-producing cells. This was not accompanied by a simultaneous increase in RORγt production. However, this might be due to fluctuations in RORγt expression. In contrast, Yasuda et al. saw no differences in the efficacy of T_H17 cell generation when differentiating naive $CD4^+$ T cells from $Satb1^{fl/fl}$/Thpok-Cre or wildtype control mice (Yasuda et al., 2019). This might be due to differences in the differentiation protocol as both the CD3 antibody coating but also the cytokine cocktails differed between the used protocols. While in this thesis only TGF-β1 and IL-6 were added, Yasuda et al. additionally supplemented their cultures with IL-1β (Yasuda et al., 2019). It has been shown that IL-1β enhances the differentiation as well as maintenance of T_H17 cells (Chung et al., 2009). However, the role of IL-1β in T_H17 cells is primarily characterized in combination with IL-23 and it boosts and maintains the T_H17 cell phenotype especially in the presence of IL-23 (Chang et al., 2013; Chung et al., 2009; Whitley et al., 2018). In humans, IL-1β facilitates the differentiation of

T_H17 cells by inducing a different Foxp3 isoform, whose expression favors the differentiation into T_H17 cells (Mailer et al., 2015). Thus, it would be interesting to investigate to which extend TCR signaling and IL-1β signaling influences the role of Satb1 during the differentiation of T_H17 cells in comparison *in vitro*.

In vivo, a reduced percentage of T_H17 cells within the effector cell pool of Satb1$^{fl/fl}$/CD4-Cre mice and an increased percentage of T_H17 cells in R26-STOP-Satb1/CD4-Cre mice were observed in the spleen. These results mirror the data obtained *in vitro* and confirm that Satb1 has an important role in the differentiation of T_H17 cells not only *in vitro* but also *in vivo*.

When looking in more detail, Satb1 regulated the differentiation of T_H17 cells especially within the first two days after the initialization of differentiation. This indicates that Satb1 functions as a pioneering factor that shapes the epigenetic landscape in the early phase of differentiation. This was confirmed by the observation, that during the differentiation of Satb1-deficient naive CD4$^+$ T cells into T_H17 cells the T_H17-specific gene network was not formed. Transcriptional analysis of T_H17 cell network genes defined by Ciofani et al. as well as Yosef et al. (Ciofani et al., 2012; Yosef et al., 2013) revealed that the expression of the gene module positively associated with T_H17 cell formation was not induced in Satb1-deficient CD4$^+$ T cells. Consequently, this resulted in an almost complete absence of effector cytokine expression. Furthermore, the data support that Satb1 does not control the differentiation of T_H17 cells by upregulating the negative module in the early phase of differentiation.

In wildtype cells an upregulation of *Il21* and *Tgfb1* expression was observed 12 hours after initialization of T_H17 cell differentiation, while the expression of both was downregulated again already 36 hours later. In parallel to these autocrine factors, *Tnfa* displayed a similar expression pattern raising the question whether TNF-α additionally promotes the differentiation of T_H17 cells in an autocrine fashion. This might be interesting to investigate further and could explain one aspect of the successful treatment of autoimmune disorders with anti-TNF-α or TNF-α inhibitor therapies, which reduce the frequency of circulating T_H17 cells and suppressed IL-17-related cytokine production (Chen et al., 2011; Lin et al., 2017).

As the transcriptional analysis of the T_H17 cell gene network indicates that Satb1 is a pioneer factor, further studies were performed to investigate whether Satb1 regulates Stat3 expression, which is a well-known lineage transcription factor of T_H17 cells and is important for the formation of the T_H17 gene network (Durant et al., 2010; Korn et al., 2009). However, phosphorylation of Stat3 was detected both in Satb1-sufficient as well as -deficient cells directly after the initialization of T_H17 cell differentiation. Phosphorylation of Stat3 was even

found to be prolonged in Satb1-deficient cells during *in vitro* T_H17 cell differentiation. This maintenance of Stat3 activation might be a compensatory mechanism to allow for differentiation of T_H17 cells. Nevertheless, the absence of Satb1 prevented the differentiation of T_H17 cells even in the presence of Stat3 activation.

Additionally, the question arose whether Satb1-deficient cells might differentiate into other T_H subsets under T_H17 cell-promoting conditions. However, *in vitro* no differentiation into T_H1, T_H2 or iTreg cells could be observed. This is not unexpected as the necessary microenvironment for the differentiation into another T_H subset is missing. Still, as T_H17 cells and pTreg cells develop from the same precursor cells and both require TGF-β1 signaling, this experiment further supports the finding that Satb1-deletion does not directly result in the development of Treg cells. To fully address this question, further experiments that allow for the simultaneous generation of T_H17 and Treg cells under more optimal conditions should be performed. However, as no increased development of $CD25^+Foxp3^+$ pTreg cells was observed *in vivo* upon deletion of Satb1 as discussed above, it is likely that Satb1 is not the decisive factor which determines the choice between T_H17 or Treg cell commitment of the precursor cells, despite its contrarious expression and exigency for both phenotypes.

Besides forming the T_H17 cell gene network, Satb1 might be involved in regulating the cellular metabolism of T_H17 cells. The metabolic program between T_H subsets differs. Inflammatory effector cells switch to aerobic glycolysis, while Treg cells rely on mitochondrial oxidation as their main energy source both *in vitro* and *in vivo* (Gerriets et al., 2015; Michalek et al., 2011; Shi et al., 2011). In addition, it has been reported that metabolic programming can influence lineage decisions as e.g. the block of glycolysis promotes the development of Treg cells over T_H17 cells (Shi et al., 2011). Furthermore, within the pool of effector cells differences in glycolysis have been observed as T_H2 cells display the highest glycolytic activity followed by T_H17 cells and T_H1 cells (Michalek et al., 2011). When comparing the metabolic program of Satb1-sufficient and -deficient cells three days after initialization of T_H17 cell differentiation, both the ECAR as well as the OCR were reduced upon loss of Satb1. However, upon metabolic challenge of these cells, similar rates of glycolysis as well as mitochondrial respiration were observed. Thus, Satb1-sufficent as well as -deficient cells cultured in a T_H17 cell-polarizing milieu exhibit a comparable metabolic potential upon activation. This indicates that Satb1 does not influence the lineage decision of naive $CD4^+$ T cells into T_H17 cells by regulating cellular metabolism.

As Satb1 is essential in the early phase of T_H17 cell development, the question arose whether Satb1 is also important for the maintenance of T_H17 cells or during restimulation of

pre-committed T_H17 cells. Deletion of Satb1 on day three of T_H17 cell differentiation did not alter IL-17 expression, indicating that Satb1 is dispensable for the maintenance of T_H17 cells. In line with this, a deletion of Satb1 on day five in fully committed T_H17 cells did not alter the phenotype of T_H17 cells after two days under resting conditions. However, when restimulating these cells under T_H17 cell-polarizing conditions, IL-17 expression was not further increased while in wildtype cells an expansion of the percentage of IL-17-producing cells could be observed. This indicates that Satb1 is not important for the maintenance of T_H17 cells in the absence of stimulus but helps to increase T_H17 cell numbers upon restimulation. Further experiments are required to unravel how Satb1 augments IL-17 production during the restimulation of T_H17 cells as the reduced percentage of IL-17-producing Satb1-deficient cells could be explained either by reduced survival or proliferation of already existing T_H17 cells or by a diminished conversion of previously IL-17-non-producing cells into T_H17 cells. Thus, analyzing survival and proliferation of these cells by performing Annexin-V or cell proliferation staining could describe the behavior of these cells in more detail. Furthermore, analysis of gene expression before as well as after restimulation might elucidate how Satb1 controls the behavior of T_H17 cells after lineage commitment. T_H17 cells are long lived cells which exhibit a stem cell-like character (Muranski et al., 2011). This stem cell phenotype is mediated by the activation of the Wnt/β-catenin pathway, which generally plays a role in self-renewal as well as survival during T cell development (Gattinoni et al., 2010; Muranski et al., 2011; Staal and M. Sen, 2008). Satb1 has been associated with the Wnt/β-catenin pathway in T_H2 cells, as it was reported that Satb1 can interact with β-catenin which subsequently results in transcriptional activation of numerous genes required for the differentiation of T_H2 cells (Notani et al., 2010). Regulation of the Wnt/β-catenin pathway in mature T_H17 cells might be one mechanism by which Satb1 controls T_H17 cells after lineage commitment.

In addition, it has been suggested that Satb1 controls the expression levels of PD-1. Downregulation or loss of Satb1 results in an upregulation of PD-1 (Nüssing et al., 2019; Stephen et al., 2017; Yasuda et al., 2019). Upon deletion of Satb1 in T_H17 cells, Yasuda et al. detected an upregulation of PD-1 within the inflamed tissue of EAE mice but not in the periphery (Yasuda et al., 2019). Furthermore, they showed that regulation of PD-1 is one mechanism how Satb1 controls the pathogenicity of T_H17 cell in the EAE model (Yasuda et al., 2019). This further indicates that Satb1 does not control the maintenance of T_H17 cells under homeostasis but shapes the phenotype of T_H17 cells upon stimulation. In line with this, Akiba et al. showed that tamoxifen-induced deletion of Satb1 after onset of EAE development

reduces the clinical score of the disease (Akiba et al., 2018). It would be further interesting to analyze PD-1 expression and the stem cell-character of the remaining T_H17 cell in these mice as the development of pathogenic T_H17 cells should have already occurred at this time point. Taken together, these data show that Satb1 is important for the functionality and pathogenicity of T_H17 cells.

As their plasticity allows T_H17 cells to gain additional pathogenic features and adopt a pathogenic phenotype, the role of Satb1 for T_H cell plasticity was further investigated. Thus, experiments were performed to validate whether T_H1 cells can be converted into T_H17 cells in the absence of Satb1. While Satb1-sufficient cells could be converted, Satb1-deficient cells did not gain characteristics of T_H17 cells and retained their T_H1 cell phenotype. Further experiments are needed to validate whether this is due to a general block of T_H17 cell commitment upon deletion of Satb1 or whether Satb1 generally allows for plasticity between the different T_H subsets. In addition, it would be interesting to analyze the expression levels of Satb1 in wildtype cells during the conversion of T_H1 to T_H17 cells to determine whether Satb1 needs to be upregulated during conversion. Furthermore, it would be interesting to delete Satb1 after the commitment of T_H17 cells and subsequently analyze plasticity of these cells by skewing them into other T_H subsets. One mechanism which allows for plasticity in T_H17 cells is the epigenetic instability of key cytokine and transcription factor genes (Mukasa et al., 2010), raising the question whether Satb1 is involved in the epigenetic modifications of these genes. ChIP analysis of various histone modifications in Satb1-sufficient and -deficient cells before and after T_H subset skewing would help to obtain a more detailed view of the role of Satb1 for the plasticity of T_H subsets.

In summary, these data indicate that the expression of Satb1 is important in the early phase of the development of T_H17 cells and is required for the establishment of the T_H17 cell-specific gene network. Furthermore, Satb1 governs the differentiation of T_H17 cells without directly affecting the metabolic program of the cells. Although the maintenance of T_H17 cells is independent of Satb1, T_H17 cells rely on the expression of Satb1 after rechallenge to increase their inflammatory phenotype. Thus, similar to neurons, in which Satb1 can maintain neuronal plasticity and prevent cellular senescence (Balamotis et al., 2012; Riessland et al., 2019), Satb1 seems to be important in committed T_H17 cells to maintain plasticity and prevent senescence. In the future, it will be important to establish how Satb1 affects the plasticity of T_H17 cells and if Satb1 influences Wnt/β-catenin signaling to allow for the gain of stem cell features.

5.3. Satb1 plays an important role in autoimmunity

The incidence and prevalence of autoimmune diseases have been on the rise over the last years (Bach, 2002). By regulating differentiation and function of T_H17 cells, Satb1 plays an important role in the development of T_H17 cell-driven autoimmune diseases. Mice with Satb1-deficient cells fail to develop colitis in the adoptive transfer colitis model as well as EAE as published by Akiba et al., Sommer et al. as well as Yasuda et al. (Akiba et al., 2018; Sommer, 2018; Yasuda et al., 2019). Complete prevention of both T_H17 cell-driven pathologies was confirmed by this thesis.

When analyzing the development of T_H17 cells, a reduced generation of both non-pathogenic IL-17$^+$IFN-γ^- but especially pathogenic IL-17$^+$IFN-γ^+ T_H17 cells was observed in both models. Pathogenic T_H17 cells are linked to the development of adoptive transfer colitis and EAE in mice and in the absence of these cells, disease development is prevented (Ahern et al., 2010; Lee et al., 2012). Thus, it is likely that the reduced development of pathogenic T_H17 cells in mice harboring Satb1-deficient cells prevents disease development in both models.

Satb1-deficient CD4$^+$ T cells showed reduced proliferation after transfer into Rag2$^{-/-}$ animals, which was also observed by Sommer et al. by assessing Ki-67 expression and Akiba et al. by labeling Satb1-deficient CD4$^+$ T cells with a proliferation dye (Akiba et al., 2018; Sommer, 2018). This raises the questions whether the reduced proliferation was due to a diminished proliferative capacity of Satb1-deficient CD4$^+$ T cells, subsequently resulting in less inflammation and development of pathogenic T_H17 cells or whether, because of the reduced development of pathogenic T_H17 cells and the resulting reduced inflammation, fewer proliferation signals were present. When stimulating Satb1-deficient CD4$^+$ T cells *in vitro*, increased proliferation in comparison to Satb1-sufficient CD4$^+$ T cells was observed, indicating that the lack of Satb1 even improves cell proliferation. Furthermore, although Alvarez et al. showed that CD4$^+$ T cells of Satb1-null mice undergo apoptosis upon stimulation (Alvarez et al., 2000), Akiba et al. observed reduced apoptosis in Satb1-deficient CD4$^+$ T cells isolated from conditional Satb1 knock-out mice after stimulation *in vitro* (Akiba et al., 2018). In line with this, preliminary data from our lab, not shown in this thesis, did not show increased apoptosis upon conditional deletion of Satb1. Thus, loss of cell viability in CD4$^+$ T cells from Satb1-null mice might be the result of problems arising during thymopoiesis. As neither reduced proliferation nor increased apoptosis were observed *in vitro* in conditional Satb1-deficient CD4$^+$ T cells, it is conceivable that the reduced differentiation potential of Satb1-deficient CD4$^+$ T cells prevents disease formation. In line with this, characterization of effector cytokine expression of Satb1-deficient CD4$^+$ T cells in the

adoptive transfer colitis model revealed a clear unidimensionality of the expression profile. Especially in the mLN, Satb1-deficient $CD4^+$ T cells failed to gain polyfunctionality as they preferably expressed none or only a single cytokine. Thus, the expression of Satb1 is required for the development of T_H17 cell and is important for plasticity and polyfunctionality not only *in vitro* but also *in vivo*.

Similar results were observed when characterizing Satb1-sufficient and -deficient $CD4^+$ T cells in the EAE model. Yasuda et al. already showed that Satb1 allows for the expression of GM-CSF in already committed T_H17 cells and thus controls polyfunctionality and disease development (Yasuda et al., 2019). Restoring GM-CSF expression in Satb1-deficient T_H17 cells increased EAE development in $Satb1^{fl/fl}$/IL-17-Cre mice, although diseases symptoms were still reduced compared to wildtype mice (Yasuda et al., 2019). In line with this, reduced GM-CSF expression was observed in this thesis when characterizing Satb1-deficient cells during *in vitro* T_H17 cell differentiation. An overall reduction in GM-CSF expression was detected in Satb1-deficient cells but also in particular in the few IL-17^+ cells which still develop. This confirms the role of Satb1 for GM-CSF expression.

Interestingly, in the previous reports different clinical courses of disease were observed depending on the time point of Satb1 deletion. $Satb1^{fl/fl}$/Vav-Cre mice and $Satb1^{fl/fl}$/Lck-Cre mice as used by Akiba et al. as well as $Satb1^{fl/fl}$/CD4-CreERT2 mice as used in this thesis were completely resistant to EAE (Akiba et al., 2018). There are only very few targets which completely prevent the development of EAE. Master regulators of T_H17 cell differentiation like RORγt, Batf and Stat3 prevent disease development as well as the absence of the cytokine IL-6 (Harris et al., 2007; Ivanov et al., 2006; Korn et al., 2007; Schraml et al., 2009). Furthermore, deleting proteins which regulate the pathogenicity of T_H17 cells like IL-23R, T-bet and Gpr65 abolish EAE development (Awasthi et al., 2009; Gaublomme et al., 2015; Nath et al., 2006; Yang et al., 2009). Now, Satb1 was confirmed as another master regulator. Satb1 has a crucial role like RORγt, Batf and Stat3 in the development of T_H17 cells and with this in T_H17 cell-driven autoimmunity.

In contrast, induction of EAE in $Satb1^{fl/fl}$/IL-17-Cre resulted in reduced but not completely abrogated disease development (Yasuda et al., 2019). Thus, similar to the deletion of network proteins like c-Maf, Sox5, Fosl2 and Irf4 as well as the effector cytokine IL-17 in $CD4^+$ T cells, a deletion of Satb1 in committed T_H17 cells reduces the severity of EAE progression but cannot completely prevent disease development (Ciofani et al., 2012; Gabryšová et al., 2018; Komiyama et al., 2006; Tanaka et al., 2014; Yang et al., 2015a). Additionally, deletion of Satb1 after the onset of disease symptoms suppresses further disease progression (Akiba et

al., 2018). Thus, as indicated from the data generated *in vitro*, this point towards an important role of Satb1 not only in the early phase of T_H17 cell development but Satb1 additionally mediates pathogenicity of already committed T_H17 cells.

Also in humans Satb1 has been associated with T_H17 cell-driven diseases like multiple sclerosis (Beecham et al., 2013). Furthermore, in anaplastic T cell lymphoma the overexpression of Satb1 has been associated with an increased T_H17 cell profile (Sun et al., 2018). Thus, Satb1 or Satb1-induced pathways might be an interesting target in humans suffering from an enhanced T_H17 cell response. Targeting Satb1 would affect both the differentiation but also the effector phase of T_H17 cells. However, the different mechanisms how Satb1 controls T_H17 cells still need to be better understood. Yasuda et al. showed that Satb1 controls the effector phase by regulating GM-CSF and PD-1 expression (Yasuda et al., 2019). However, by studying $Satb1^{fl/fl}$/IL-17-Cre mice they could not investigate the influence of Satb1 in the early differentiation phase. Analysis of the early phase during the differentiation, as presented in this thesis, is important to fully understand the role of Satb1 for T_H17 cells and to discover new downstream genes which can be subsequently used as therapeutic targets to treat T_H17 cell-driven autoimmune diseases.

5.4. Satb1 enables the differentiation of T_H17 cells by repressing the *Il2* gene locus and thus IL-2 signaling

To identify new mechanisms how Satb1 governs the early phase of T_H17 cell development, differences in chromatin accessibility and mRNA expression were analyzed between Satb1-sufficient and deficient naive $CD4^+$ T cells. Satb1-deficient naive $CD4^+$ T cells exhibited a generally more open chromatin state and showed a slightly increased transcription confirming that Satb1 functions mainly as a genomic repressor. As a consequence, Satb1-deficient naive $CD4^+$ T cells exhibited a different activation state, which was predominantly observed on the chromatin level. Increased accessible chromatin did not directly correlate with gene expression in naive $CD4^+$ T cells but rather provided an appropriate genomic framework to allow for an immediate reaction towards activation stimuli. In line with this, upon TCR stimulation, Satb1-deficient cells reacted stronger to the activation, reflected e.g. by increased glycolysis. As a downregulation of Satb1 was observed in the memory pool of $CD4^+$ T cells, one next question to answer is whether downregulation of Satb1 is necessary to keep an activated chromatin state in memory cells allowing direct reaction upon restimulation.

One interesting candidate regulated by Satb1 in naive $CD4^+$ T cells is the *Il2* gene locus. It has been previously reported that both IL-2 and CD25 are regulated by Satb1 (Alvarez et al., 2000; Kumar et al., 2005; Pavan Kumar et al., 2006; Yasui et al., 2002). Binding of Satb1 to the regulatory region of IL-2 has been shown in T lymphoblastoid cell lines and PBMCs (Kumar et al., 2005; Pavan Kumar et al., 2006). In this thesis, ATAC-seq revealed that Satb1-sufficient naive $CD4^+$ T cells displayed a closed chromatin state at the *Il2* gene locus, while in Satb1-deficent cells the locus was accessible. Furthermore, the increased accessibility of the *Il2* gene locus resulted in an increased *Il2* expression already in naive $CD4^+$ T cells. In addition, stimulation of splenocytes from $Satb1^{fl/fl}$/CD4-Cre mice resulted in an increased IL-2 protein expression in naive $CD4^+$ T cells but also in effector/memory cells, while overexpression of Satb1 resulted in a reduced IL-2 expression in effector/memory $CD4^+$ T cells from R26-STOP-Satb1/CD4-Cre mice. Moreover, activation of Satb1-deficient cells with CD3 and CD28 antibody-coated beads resulted in increased cell proliferation supporting that the increased IL-2 expression also results in functional IL-2 signaling. In line with this, the upregulation of Satb1 upon deletion of Foxp1 in Treg cells was accompanied by a reduced CD25 expression and IL-2 responsiveness (Konopacki et al., 2019), further indicating that Satb1 is an important repressor of IL-2 signaling. As Foxp1 represses Satb1 expression in Treg cells (Konopacki et al., 2019), Foxp1 is an interesting candidate to study in terms of Satb1 regulation in other $CD4^+$ T_H subsets. Maybe induced expression of Foxp1 can block Satb1 expression and thus can constrain the development of T_H17 cells. Thus, Foxp1 might be a potentially interesting therapeutic target gene in autoimmune diseases as Foxp1 is important to maintain the suppressive function of Treg cells and its expression positively correlates with non-pathogenic T_H17 cells but not with pathogenic T_H17 cells (Gaublomme et al., 2015; Ren et al., 2019).

IL-2 is a well-known regulator of T_H subset differentiation and known to inhibit the development of T_H17 cells (Boyman and Sprent, 2012; Liao et al., 2013). Thus, the differentiation of T_H17 cells might be promoted by Satb1 through repression of *Il2* transcription in the early phase of development. IL-2 controls the differentiation of T_H17 cells by downregulating IL-6R expression as well as inducing phosphorylation of Stat5 (Laurence et al., 2007; Liao et al., 2011; Yang et al., 2011). Both IL-6Rα expression and Stat5 activation were altered in Satb1-deficient cells when cultured in a T_H17 cell-polarizing milieu (Figure 64). Increased Stat5 phosphorylation was observed starting 12 hours after initialization of T_H17 cell differentiation. It has been reported that the balance of activated Stat proteins influences epigenetic modifications and gene transcription (Peters et al., 2015; Yang et al.,

2011). Stat proteins can form homo- as well as heterodimers as well as -tetramers composed of different Stat proteins and this diversity in composition allows for the transcription of specific genes (Villarino et al., 2015). It is known that pStat5 diminishes the differentiation of T_H17 cells by repressing *IL17a* expression (Laurence et al., 2007). Both pStat5 and pStat3 have binding sites within the *IL17a* promoter reciprocally controlling *Il17a* expression (Yang et al., 2011). Neither IL-2 nor pStat5 impair the phosphorylation of Stat3, but the altered balance of pStat3 and pStat5 diminishes the differentiation of T_H17 cells (Yang et al., 2011). Thus, target genes of pStat5 and pStat3 were further analyzed to determine the dominant Stat signaling. When assessing the impact of elevated Stat5 phosphorylation on Stat5 target genes, increased CD25 expression was observed confirming enhanced Stat5 signaling in Satb1-deficient cells when cultured under T_H17 cell-driving conditions. In contrast, expression of both IL-6Rα as well as IL-17, which are both induced by pStat3 (Durant et al., 2010), was diminished in Satb1-deficient cells. Thus, a reduced Stat3 signaling with simultaneously augmented Stat5 signaling was observed in Satb1-deficient cells during *in vitro* T_H17 cell culture due to the altered balance of Stat proteins. Thus, it can be concluded that Satb1 promotes the differentiation of T_H17 cells by repressing IL-2 expression and impairing phosphorylation of Stat5 (Figure 64).

Interestingly, IL-1α and IL-1β counteract the IL-2-mediated reduction of T_H17 cell differentiation (Basu et al., 2015; Kryczek et al., 2007). Both IL-1α and IL-1β can bind to the IL-1R1, which is upregulated during the differentiation of T_H17 cells (Dinarello, 2018). IL-1β prolongs Stat3 phosphorylation and with this alters the balance of pStat3 and pStat5 preventing dominant Stat5 signaling (Basu et al., 2015; Bhaumik and Basu, 2017). This might explain the differences observed during T_H17 cell differentiation between the work by Yasuda et al. and the differentiation protocol performed in this thesis or Ciofani et al. (Ciofani et al., 2012; Yasuda et al., 2019). In the absence of IL-1β, a clear reduction in T_H17 cell differentiation with concomitantly increased IL-2 signaling was observed, while the presence of IL-1β allowed for normal T_H17 cell differentiation of Satb1-deficient naive $CD4^+$ T cells *in vitro* (Ciofani et al., 2012; Yasuda et al., 2019). This additionally indicates that Satb1 is essential in the early phase of T_H17 cell differentiation by repressing IL-2 expression.

Indeed, when blocking IL-2 signaling by adding anti-IL-2 and CD25-blocking antibodies during *in vitro* T_H17 cell differentiation, Satb1-deficient $CD4^+$ T cells gained a T_H17 cell phenotype and upregulated IL-17 expression similar to Satb1-sufficent cells. Thus, Satb1 regulates the differentiation of T_H17 cells by repressing *Il2* expression (Figure 64).

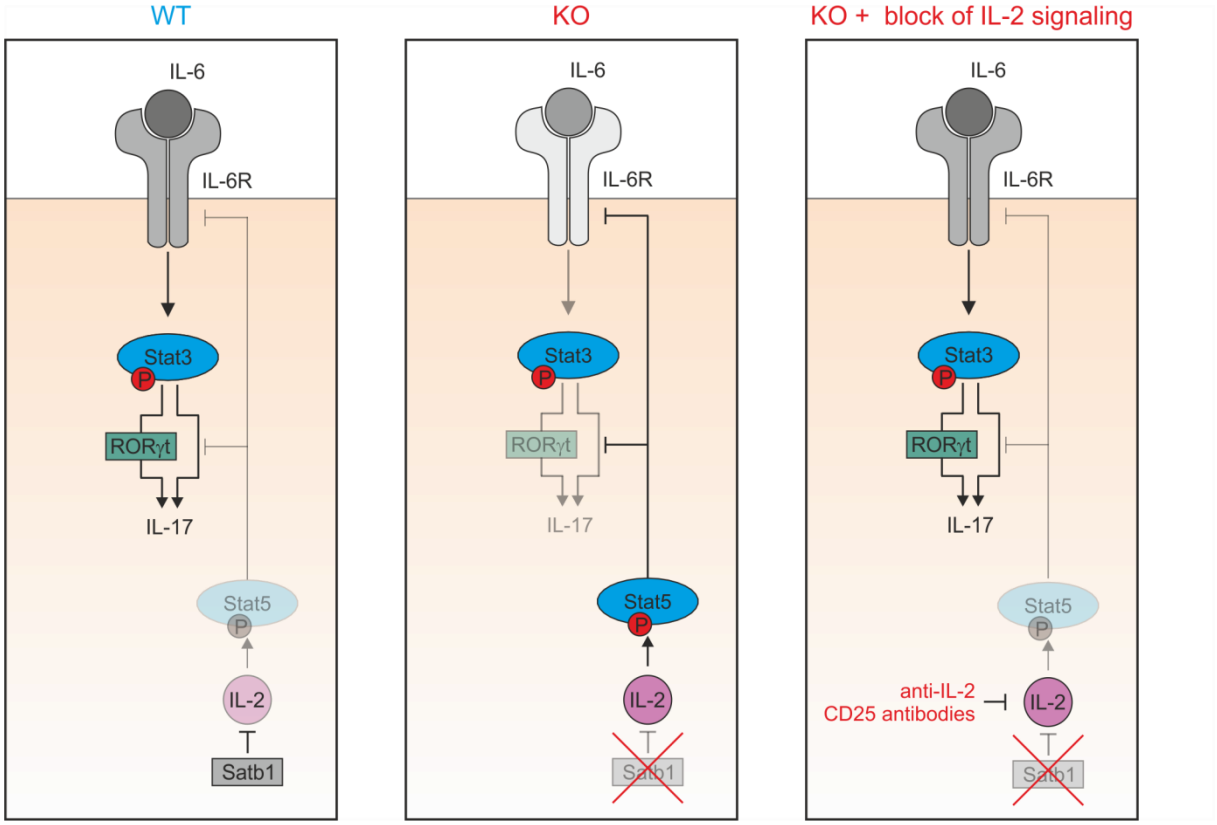

Figure 64: Satb1 controls the development of T_H17 cells by regulating IL-2 expression. Satb1 blocks IL-2 expression in naive $CD4^+$ T cells as well as during the early phase of T_H17 cell differentiation. Loss of Satb1 allows for IL-2 signaling, resulting in an increased Stat5 phosphorylation, reduced IL-6R expression and leading to deficient T_H17 cell differentiation. In line with this, blocking IL-2 signaling rescues the differentiation of T_H17 cells in Satb1-deficient cells. CD, cluster of differentiation; IL, interleukin; P, phosphorylated; IL-6R, interleukin 6 receptor; RORγt, retinoic acid receptor-related orphan receptor-γt; Satb1, special AT-rich sequence-binding protein 1; Stat, Signal transducer and activator of transcription. Figure modified from Boyman and Sprent (Boyman and Sprent, 2012).

In the last years, Kim et al. studied the role of Pten during the differentiation of T_H17 cells showing that Pten is important for *Il2* repression (Kim et al., 2017). Pten deficiency results in a similar phenotype as observed upon deletion of Satb1 further stressing the importance of Satb1 during the differentiation of T_H17 cells through regulation of IL-2 (Kim et al., 2017). Furthermore, deletion of Pten in T_H17 cells results in a decreased *Satb1* expression raising the question whether Pten and Satb1 are mechanically linked and Pten might be upstream of Satb1. In Jurkat cells, which exhibit a defective Pten function (Shan et al., 2000), Satb1 still regulates IL-2 expression (Kumar et al., 2005; Pavan Kumar et al., 2006). However, further studies independent of lymphoblastoid cell lines ought to be conducted. *Pten* expression was not altered in Satb1-deficient naive $CD4^+$ T cells, yet further analysis of *Pten* expression in the early phase of T_H17 cell differentiation should be performed. In addition, inhibition of Pten during T_H17 cell differentiation of Satb1-overexpressing naive $CD4^+$ T cells using the Pten inhibitor SF1670 might indicate whether Pten induces IL-2 repression dependent on

Satb1 regulation. It would be interesting to find upstream mechanisms to understand how Satb1 is regulated in T_H17 cells but also in the other T_H subsets.

Furthermore, assessing how Satb1 mechanistically controls the other T_H subset would be critical to fully understand the role of Satb1 for the differentiation and functionality of T_H cells. This is especially necessary to subsequently validate whether Satb1 or Satb1-induced pathways can be used as therapeutic targets. Although Satb1 regulates the differentiation of T_H17 cells by repressing IL-2 signaling, downregulation of Satb1 in Treg cells can not result in increased IL-2 production as Treg cells are incapable of producing IL-2 (Boyman and Sprent, 2012). Nevertheless, downregulating Satb1 might foster CD25 expression. Thus, it is conceivable that during the differentiation of Treg cells other mechanism shape Satb1-regulated pathways. In contrast, IL-2 regulates the accessibility of the IL-4 and IL-13 gene loci (Cai et al., 2006; Liao et al., 2008) similar as Satb1, which might indicate a regulation of IL-2 by Satb1 in T_H2 cells. Furthermore, downregulation of Satb1 in T_H1 cells might promote IL-2-mediated upregulation of IL-12Rβ2 and T-bet expression, resulting in increased IFN-γ expression (Liao et al., 2011). In addition, IL-2 signaling is necessary for the generation of T_H9 cells. IL-2 expression is important during the early stages of the differentiation of T_H9 cells and induces IL-9 expression (Liao et al., 2014). Interestingly, Satb1 was downregulated during the differentiation of T_H9 cells on day one and two, which subsequently might result in the induction of IL-2 expression. Nevertheless, a complete loss of Satb1 during the differentiation process reduced the development of T_H9 cells, indicating that other mechanisms induced by Satb1 play an important role and that upregulation of Satb1 from day three on might be necessary. Since *Satb1* is differentially expressed during the differentiation into T_H cells not only in a cell type but also time-dependent fashion, it is likely that Satb1 regulates various mechanisms during differentiation. Every T_H subset is characterized by a specific gene network formation, which likely both controls and is controlled by mechanism induced by Satb1. Furthermore, the surrounding cytokine microenvironment, like e.g. the presence of IL-1β, might influence Satb1-induced pathways. Thus, further studies are needed to fully understand the role of Satb1 during the differentiation into T_H subsets. Focusing on the role of Satb1 for IL-2 expression and Stat5 phosphorylation during T_H cell differentiation might help to unravel the influence of Satb1 on T_H1, T_H2, T_H9 and iTreg cells, however additional mechanisms should be considered.

5.5. Model of Satb1-mediated T_H17 cell differentiation and effector function

In summary, new insights about the development of T_H17 cells were obtained. Both, the study of Yasuda et al. as well as this thesis together give a comprehensive view on the role of Satb1

for the differentiation and functionality of T_H17 cells (Figure 65). While Yasuda et al. studied the role of Satb1 during the effector phase (Yasuda et al., 2019), this study concentrated on the role of Satb1 during the commitment of naive $CD4^+$ T cells to T_H17 cells and the resulting consequences in autoimmune disease. New mechanisms were identified as the data support that Satb1 controls the differentiation of T_H17 cells by repressing the *Il2* gene locus. Loss of Satb1 results in increased IL-2 signaling, Stat5 phosphorylation and IL-6Rα downregulation while CD25 is upregulated. The increased phosphorylation of Stat5 results in a loss of pStat3 signaling and consequently prevents the formation of the T_H17 cell gene network. Satb1 is essential during the development but likely not required for the maintenance of T_H17 cells under homeostatic conditions. In contrast, upon stimulation Satb1 is required for the plasticity of T_H17 cells and the formation of pathogenic T_H17 cells. Loss of Satb1 signaling especially in the early but also in the effector phase results in the prevention or reduced severity of T_H17 cell-driven autoimmune diseases, which suggests that Satb1 or Satb1-induced mechanisms may be putative targets for therapeutic treatments.

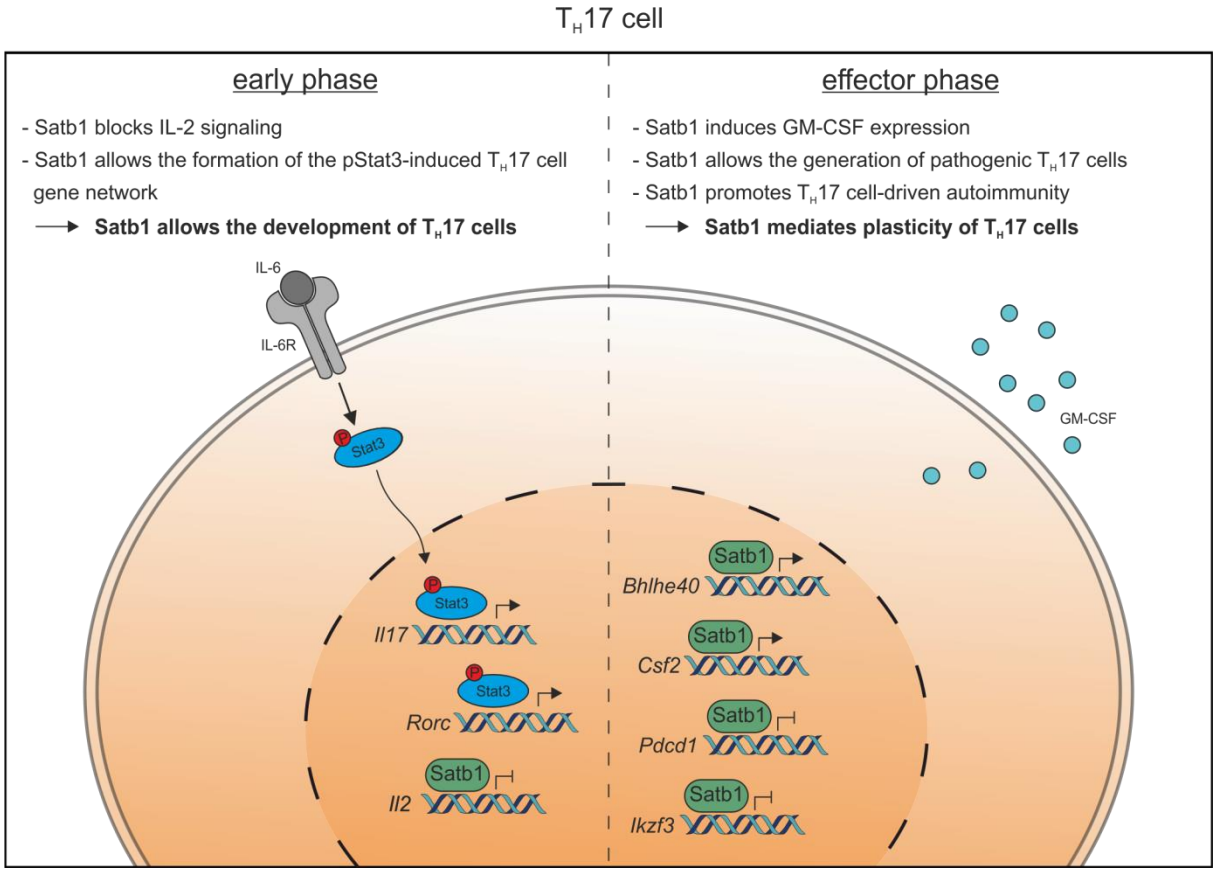

Figure 65: Model for the role of Satb1 in the differentiation and effector function of T_H17 cells.
Satb1 regulates the differentiation as well as the effector function of T_H17 cells. Repression of *Il2* during the development allows Stat3 signaling and the formation of the T_H17 cell gene network. In addition, Satb1 is highly expressed in mature T_H17 cells regulating GM-CSF, PD-1 and Ikzf3 expression. In this way, Satb1 controls the plasticity of T_H17 cells allowing

the generation of pathogenic cells and the development of T_H17 cell-driven autoimmune diseases. Bhlhe40, basic helix-loop-helix family member E40; Csf2, colony stimulating factor 2; GM-CSF, Granulocyte Macrophage-Colony Stimulating Factor; IL, interleukin; Ikzf3, IKAROS family zinc finger 3; P, phosphorylated; Pdcd1, programmed cell death 1; IL-6R, interleukin 6 receptor; Rorc, retinoic acid receptor-related orphan receptor C; Satb1, special AT-rich sequence-binding protein 1; Stat, Signal transducer and activator of transcription.

6. References

Agrelo, R., Souabni, A., Novatchkova, M., Haslinger, C., Leeb, M., Komnenovic, V., Kishimoto, H., Gresh, L., Kohwi-Shigematsu, T., Kenner, L., et al. (2009). SATB1 Defines the Developmental Context for Gene Silencing by Xist in Lymphoma and Embryonic Cells. Dev. Cell *16*, 507–516.

Ahern, P.P., Schiering, C., Buonocore, S., McGeachy, M.J., Cua, D.J., Maloy, K.J., and Powrie, F. (2010). Interleukin-23 Drives Intestinal Inflammation through Direct Activity on T Cells. Immunity *33*, 279–288.

Ahlfors, H., Limaye, A., Elo, L.L., Tuomela, S., Burute, M., Gottimukkala, K.V.P., Notani, D., Rasool, O., Galande, S., and Lahesmaa, R. (2010). SATB1 dictates expression of multiple genes including IL-5 involved in human T helper cell differentiation. Blood *116*, 1443–1453.

Akiba, Y., Kuwabara, T., Mukozu, T., Mikami, T., and Kondo, M. (2018). Special AT-rich sequence binding protein 1 is required for maintenance of T cell receptor responsiveness and development of experimental autoimmune encephalomyelitis. Microbiol. Immunol. *62*, 255–268.

Alvarez, J.D., Yasui, D.H., Niida, H., Joh, T., Loh, D.Y., and Kohwi-Shigematsu, T. (2000). The MAR-binding protein SATB1 orchestrates temporal and spatial expression of multiple genes during T-cell development. Genes Dev. *14*, 521–535.

Annunziato, F., Cosmi, L., Santarlasci, V., Maggi, L., Liotta, F., Mazzinghi, B., Parente, E., Filì, L., Ferri, S., Frosali, F., et al. (2007). Phenotypic and functional features of human Th17 cells. J. Exp. Med. *204*, 1849–1861.

Apetoh, L., Quintana, F.J., Pot, C., Joller, N., Xiao, S., Kumar, D., Burns, E.J., Sherr, D.H., Weiner, H.L., and Kuchroo, V.K. (2010). The aryl hydrocarbon receptor interacts with c-Maf to promote the differentiation of type 1 regulatory T cells induced by IL-27. Nat. Immunol. *11*, 854–861.

Arudchelvan, Y., Nishimura, Y., Tokuda, N., Sawada, T., Shinozaki, F., and Fukumoto, T. (2002). Differential expression of MHC class II antigens and cathepsin L by subtypes of cortical epithelial cells in the rat thymus: an immunoelectron microscopic study. J. Electron Microsc. (Tokyo). *51*, 173–181.

Ashburner, M., Ball, C.A., Blake, J.A., Botstein, D., Butler, H., Cherry, J.M., Davis, A.P.,

Dolinski, K., Dwight, S.S., Eppig, J.T., et al. (2000). Gene Ontology: tool for the unification of biology. Nat. Genet. *25*, 25–29.

Avni, O., and Rao, A. (2000). T cell differentiation: a mechanistic view. Curr. Opin. Immunol. *12*, 654–659.

Awasthi, A., Riol-Blanco, L., Jäger, A., Korn, T., Pot, C., Galileos, G., Bettelli, E., Kuchroo, V.K., and Oukka, M. (2009). Cutting Edge: IL-23 Receptor GFP Reporter Mice Reveal Distinct Populations of IL-17-Producing Cells. J. Immunol. *182*, 5904–5908.

Baaten, B.J.G., Li, C.-R., and Bradley, L.M. (2010). Multifaceted regulation of T cells by CD44. Commun. Integr. Biol. *3*, 508–512.

Bach, J.-F. (2002). The Effect of Infections on Susceptibility to Autoimmune and Allergic Diseases. N. Engl. J. Med. *347*, 911–920.

Balamotis, M.A., Tamberg, N., Woo, Y.J., Li, J., Davy, B., Kohwi-Shigematsu, T., and Kohwi, Y. (2012). Satb1 Ablation Alters Temporal Expression of Immediate Early Genes and Reduces Dendritic Spine Density during Postnatal Brain Development. Mol. Cell. Biol. *32*, 333–347.

Barry, M., and Bleackley, R.C. (2002). Cytotoxic T lymphocytes: all roads lead to death. Nat. Rev. Immunol. *2*, 401–409.

Basu, R., Whitley, S.K., Bhaumik, S., Zindl, C.L., Schoeb, T.R., Benveniste, E.N., Pear, W.S., Hatton, R.D., and Weaver, C.T. (2015). IL-1 signaling modulates activation of STAT transcription factors to antagonize retinoic acid signaling and control the TH17 cell–iTreg cell balance. Nat. Immunol. *16*, 286–295.

Bautista, J.L., Lio, C.-W.J., Lathrop, S.K., Forbush, K., Liang, Y., Luo, J., Rudensky, A.Y., and Hsieh, C.-S. (2009). Intraclonal competition limits the fate determination of regulatory T cells in the thymus. Nat. Immunol. *10*, 610–617.

Bebo, B.F., Dehghani, B., Foster, S., Kurniawan, A., Lopez, F.J., and Sherman, L.S. (2009). Treatment with selective estrogen receptor modulators regulates myelin specific T-cells and suppresses experimental autoimmune encephalomyelitis. Glia *57*, 777–790.

Beecham, A.H., Patsopoulos, N.A., Xifara, D.K., Davis, M.F., Kemppinen, A., Cotsapas, C., Shah, T.S., Spencer, C., Booth, D., Goris, A., et al. (2013). Analysis of immune-related loci identifies 48 new susceptibility variants for multiple sclerosis. Nat. Genet. *45*, 1353–1360.

Beyer, M., Thabet, Y., Müller, R.-U., Sadlon, T., Classen, S., Lahl, K., Basu, S., Zhou, X., Bailey-Bucktrout, S.L., Krebs, W., et al. (2011). Repression of the genome organizer SATB1 in regulatory T cells is required for suppressive function and inhibition of effector differentiation. Nat. Immunol. *12*, 898–907.

Bhaumik, S., and Basu, R. (2017). Cellular and Molecular Dynamics of Th17 Differentiation and its Developmental Plasticity in the Intestinal Immune Response. Front. Immunol. *8*, 254.

Bolger, A.M., Lohse, M., and Usadel, B. (2014). Trimmomatic: a flexible trimmer for Illumina sequence data. Bioinformatics *30*, 2114–2120.

Bosselut, R. (2004). CD4/CD8-lineage differentiation in the thymus: from nuclear effectors to membrane signals. Nat. Rev. Immunol. *4*, 529–540.

Boyman, O., and Sprent, J. (2012). The role of interleukin-2 during homeostasis and activation of the immune system. Nat. Rev. Immunol. *12*, 180–190.

Brand, S. (2009). Crohn's disease: Th1, Th17 or both? The change of a paradigm: new immunological and genetic insights implicate Th17 cells in the pathogenesis of Crohn's disease. Gut *58*, 1152–1167.

Brandstätter, O., Schanz, O., Vorac, J., König, J., Mori, T., Maruyama, T., Korkowski, M., Haarmann-Stemmann, T., von Smolinski, D., Schultze, J.L., et al. (2016). Balancing intestinal and systemic inflammation through cell type-specific expression of the aryl hydrocarbon receptor repressor. Sci. Rep. *6*, 26091.

Brown, C.C., Esterhazy, D., Sarde, A., London, M., Pullabhatla, V., Osma-Garcia, I., Al-Bader, R., Ortiz, C., Elgueta, R., Arno, M., et al. (2015). Retinoic Acid Is Essential for Th1 Cell Lineage Stability and Prevents Transition to a Th17 Cell Program. Immunity *42*, 499–511.

Buenrostro, J.D., Giresi, P.G., Zaba, L.C., Chang, H.Y., and Greenleaf, W.J. (2013). Transposition of native chromatin for fast and sensitive epigenomic profiling of open chromatin, DNA-binding proteins and nucleosome position. Nat. Methods *10*, 1213–1218.

Cai, S., Han, H.-J., and Kohwi-Shigematsu, T. (2003). Tissue-specific nuclear architecture and gene expression regulated by SATB1. Nat. Genet. *34*, 42–51.

Cai, S., Lee, C.C., and Kohwi-Shigematsu, T. (2006). SATB1 packages densely looped, transcriptionally active chromatin for coordinated expression of cytokine genes. Nat. Genet.

38, 1278–1288.

Carbon, S., Douglass, E., Dunn, N., Good, B., Harris, N.L., Lewis, S.E., Mungall, C.J., Basu, S., Chisholm, R.L., Dodson, R.J., et al. (2019). The Gene Ontology Resource: 20 years and still GOing strong. Nucleic Acids Res. *47*, D330–D338.

Chang, D., Nalls, M.A., Hallgrímsdóttir, I.B., Hunkapiller, J., van der Brug, M., Cai, F., Kerchner, G.A., Ayalon, G., Bingol, B., Sheng, M., et al. (2017). A meta-analysis of genome-wide association studies identifies 17 new Parkinson's disease risk loci. Nat. Genet. *49*, 1511–1516.

Chang, H.C., Sehra, S., Goswami, R., Yao, W., Yu, Q., Stritesky, G.L., Jabeen, R., McKinley, C., Ahyi, A.N., Han, L., et al. (2010). The transcription factor PU.1 is required for the development of IL-9-producing T cells and allergic inflammation. Nat. Immunol. *11*, 527–534.

Chang, J., Burkett, P.R., Borges, C.M., Kuchroo, V.K., Turka, L.A., and Chang, C.-H. (2013). MyD88 is essential to sustain mTOR activation necessary to promote T helper 17 cell proliferation by linking IL-1 and IL-23 signaling. Proc. Natl. Acad. Sci. *110*, 2270–2275.

Chen, D.-Y., Chen, Y.-M., Chen, H.-H., Hsieh, C.-W., Lin, C.-C., and Lan, J.-L. (2011). Increasing levels of circulating Th17 cells and interleukin-17 in rheumatoid arthritis patients with an inadequate response to anti-TNF-α therapy. Arthritis Res. Ther. *13*, R126.

Chen, J., Guan, L., Tang, L., Liu, S., Zhou, Y., Chen, C., He, Z., and Xu, L. (2019). T Helper 9 Cells: A New Player in Immune-Related Diseases. DNA Cell Biol. *38*, 1040–1047.

Choi, Y.S., Kageyama, R., Eto, D., Escobar, T.C., Johnston, R.J., Monticelli, L., Lao, C., and Crotty, S. (2011). ICOS Receptor Instructs T Follicular Helper Cell versus Effector Cell Differentiation via Induction of the Transcriptional Repressor Bcl6. Immunity *34*, 932–946.

Chung, Y., Chang, S.H., Martinez, G.J., Yang, X.O., Nurieva, R., Kang, H.S., Ma, L., Watowich, S.S., Jetten, A.M., Tian, Q., et al. (2009). Critical Regulation of Early Th17 Cell Differentiation by Interleukin-1 Signaling. Immunity *30*, 576–587.

Ciofani, M., Madar, A., Galan, C., Sellars, M., Mace, K., Pauli, F., Agarwal, A., Huang, W., Parkurst, C.N., Muratet, M., et al. (2012). A Validated Regulatory Network for Th17 Cell Specification. Cell *151*, 289–303.

Close, J., Xu, H., De Marco Garcia, N., Batista-Brito, R., Rossignol, E., Rudy, B., and Fishell,

G. (2012). Satb1 Is an Activity-Modulated Transcription Factor Required for the Terminal Differentiation and Connectivity of Medial Ganglionic Eminence-Derived Cortical Interneurons. J. Neurosci. *32*, 17690–17705.

Codarri, L., Gyülvészi, G., Tosevski, V., Hesske, L., Fontana, A., Magnenat, L., Suter, T., and Becher, B. (2011). RORγt drives production of the cytokine GM-CSF in helper T cells, which is essential for the effector phase of autoimmune neuroinflammation. Nat. Immunol. *12*, 560–567.

Corthay, A. (2006). A Three-cell Model for Activation of Naïve T Helper Cells. Scand. J. Immunol. *64*, 93–96.

Crotty, S. (2014). T Follicular Helper Cell Differentiation, Function, and Roles in Disease. Immunity *41*, 529–542.

Damsker, J.M., Hansen, A.M., and Caspi, R.R. (2010). Th1 and Th17 cells: adversaries and collaborators. Ann. N. Y. Acad. Sci. *1183*, 211–221.

Dardalhon, V., Awasthi, A., Kwon, H., Galileos, G., Gao, W., Sobel, R.A., Mitsdoerffer, M., Strom, T.B., Elyaman, W., Ho, I.-C., et al. (2008). IL-4 inhibits TGF-β-induced Foxp3+ T cells and, together with TGF-β, generates IL-9+ IL-10+ Foxp3− effector T cells. Nat. Immunol. *9*, 1347–1355.

Dickinson, L.A., Joh, T., Kohwi, Y., and Kohwi-Shigematsu, T. (1992). A tissue-specific MAR/SAR DNA-binding protein with unusual binding site recognition. Cell *70*, 631–645.

Dickinson, L.A., Dickinson, C.D., and Kohwi-Shigematsu, T. (1997). An Atypical Homeodomain in SATB1 Promotes Specific Recognition of the Key Structural Element in a Matrix Attachment Region. J. Biol. Chem. *272*, 11463–11470.

Dinarello, C.A. (2018). Overview of the IL-1 family in innate inflammation and acquired immunity. Immunol. Rev. *281*, 8–27.

DiToro, D., Winstead, C.J., Pham, D., Witte, S., Andargachew, R., Singer, J.R., Wilson, C.G., Zindl, C.L., Luther, R.J., Silberger, D.J., et al. (2018). Differential IL-2 expression defines developmental fates of follicular versus nonfollicular helper T cells. Science (80-.). *361*, eaao2933.

Dobin, A., Davis, C.A., Schlesinger, F., Drenkow, J., Zaleski, C., Jha, S., Batut, P., Chaisson, M., and Gingeras, T.R. (2013). STAR: ultrafast universal RNA-seq aligner. Bioinformatics

29, 15–21.

Doi, Y., Yokota, T., Satoh, Y., Okuzaki, D., Tokunaga, M., Ishibashi, T., Sudo, T., Ueda, T., Shingai, Y., Ichii, M., et al. (2018). Variable SATB1 Levels Regulate Hematopoietic Stem Cell Heterogeneity with Distinct Lineage Fate. Cell Rep. *23*, 3223–3235.

Domingues, H.S., Mues, M., Lassmann, H., Wekerle, H., and Krishnamoorthy, G. (2010). Functional and Pathogenic Differences of Th1 and Th17 Cells in Experimental Autoimmune Encephalomyelitis. PLoS One *5*, e15531.

Duhen, R., Glatigny, S., Arbelaez, C.A., Blair, T.C., Oukka, M., and Bettelli, E. (2013). Cutting edge: the pathogenicity of IFN-γ-producing Th17 cells is independent of T-bet. J. Immunol. *190*, 4478–4482.

DuPage, M., and Bluestone, J.A. (2016). Harnessing the plasticity of CD4+ T cells to treat immune-mediated disease. Nat. Rev. Immunol. *16*, 149–163.

Durant, L., Watford, W.T., Ramos, H.L., Laurence, A., Vahedi, G., Wei, L., Takahashi, H., Sun, H.-W., Kanno, Y., Powrie, F., et al. (2010). Diverse Targets of the Transcription Factor STAT3 Contribute to T Cell Pathogenicity and Homeostasis. Immunity *32*, 605–615.

Eisenstein, E.M., and Williams, C.B. (2009). The Treg/Th17 Cell Balance: A New Paradigm for Autoimmunity. Pediatr. Res. *65*, 26R–31R.

El-Behi, M., Ciric, B., Dai, H., Yan, Y., Cullimore, M., Safavi, F., Zhang, G.-X., Dittel, B.N., and Rostami, A. (2011). The encephalitogenicity of TH17 cells is dependent on IL-1- and IL-23-induced production of the cytokine GM-CSF. Nat. Immunol. *12*, 568–575.

Ellwardt, E., Pramanik, G., Luchtman, D., Novkovic, T., Jubal, E.R., Vogt, J., Arnoux, I., Vogelaar, C.F., Mandal, S., Schmalz, M., et al. (2018). Maladaptive cortical hyperactivity upon recovery from experimental autoimmune encephalomyelitis. Nat. Neurosci. *21*, 1392–1403.

Fallon, P.G., and Schwartz, C. (2020). The high and lows of type 2 asthma and mouse models. J. Allergy Clin. Immunol. *145*, 496–498.

Fessing, M.Y., Mardaryev, A.N., Gdula, M.R., Sharov, A.A., Sharova, T.Y., Rapisarda, V., Gordon, K.B., Smorodchenko, A.D., Poterlowicz, K., Ferone, G., et al. (2011). p63 regulates Satb1 to control tissue-specific chromatin remodeling during development of the epidermis. J. Cell Biol. *194*, 825–839.

Fredholm, S., Willerslev-Olsen, A., Met, Ö., Kubat, L., Gluud, M., Mathiasen, S.L., Friese, C., Blümel, E., Petersen, D.L., Hu, T., et al. (2018). SATB1 in Malignant T Cells. J. Invest. Dermatol. *138*, 1805–1815.

Fujimura, K., Oyamada, A., Iwamoto, Y., Yoshikai, Y., and Yamada, H. (2013). CD4 T cell-intrinsic IL-2 signaling differentially affects Th1 and Th17 development. J. Leukoc. Biol. *94*, 271–279.

Furtado, G.C., de Lafaille, M.A.C., Kutchukhidze, N., and Lafaille, J.J. (2002). Interleukin 2 Signaling Is Required for CD4+ Regulatory T Cell Function. J. Exp. Med. *196*, 851–857.

Gabriel, C.H., Gross, F., Karl, M., Stephanowitz, H., Hennig, A.F., Weber, M., Gryzik, S., Bachmann, I., Hecklau, K., Wienands, J., et al. (2016). Identification of Novel Nuclear Factor of Activated T Cell (NFAT)-associated Proteins in T Cells. J. Biol. Chem. *291*, 24172–24187.

Gabryšová, L., Alvarez-Martinez, M., Luisier, R., Cox, L.S., Sodenkamp, J., Hosking, C., Pérez-Mazliah, D., Whicher, C., Kannan, Y., Potempa, K., et al. (2018). c-Maf controls immune responses by regulating disease-specific gene networks and repressing IL-2 in CD4+ T cells. Nat. Immunol. *19*, 497–507.

Gaffen, S.L. (2008). An overview of IL-17 function and signaling. Cytokine *43*, 402–407.

Galande, S., Dickinson, L.A., Mian, I.S., Sikorska, M., and Kohwi-Shigematsu, T. (2001). SATB1 Cleavage by Caspase 6 Disrupts PDZ Domain-Mediated Dimerization, Causing Detachment from Chromatin Early in T-Cell Apoptosis. Mol. Cell. Biol. *21*, 5591–5604.

Gattinoni, L., Ji, Y., and Restifo, N.P. (2010). Wnt/beta-catenin signaling in T-cell immunity and cancer immunotherapy. Clin. Cancer Res. *16*, 4695–4701.

Gaublomme, J.T., Yosef, N., Lee, Y., Gertner, R.S., Yang, L. V., Wu, C., Pandolfi, P.P., Mak, T., Satija, R., Shalek, A.K., et al. (2015). Single-Cell Genomics Unveils Critical Regulators of Th17 Cell Pathogenicity. Cell *163*, 1400–1412.

Georgiev, H., Ravens, I., Papadogianni, G., Halle, S., Malissen, B., Loots, G.G., Förster, R., and Bernhardt, G. (2018). Shared and Unique Features Distinguishing Follicular T Helper and Regulatory Cells of Peripheral Lymph Node and Peyer's Patches. Front. Immunol. *9*, 714.

Gerlach, K., Hwang, Y., Nikolaev, A., Atreya, R., Dornhoff, H., Steiner, S., Lehr, H.-A., Wirtz, S., Vieth, M., Waisman, A., et al. (2014). TH9 cells that express the transcription factor PU.1 drive T cell–mediated colitis via IL-9 receptor signaling in intestinal epithelial

cells. Nat. Immunol. *15*, 676–686.

Germain, R.N. (2002). T-cell development and the CD4–CD8 lineage decision. Nat. Rev. Immunol. *2*, 309–322.

Gerriets, V.A., Kishton, R.J., Nichols, A.G., Macintyre, A.N., Inoue, M., Ilkayeva, O., Winter, P.S., Liu, X., Priyadharshini, B., Slawinska, M.E., et al. (2015). Metabolic programming and PDHK1 control CD4+ T cell subsets and inflammation. J. Clin. Invest. *125*, 194–207.

Gong, F., Sun, L., Wang, Z., Shi, J., Li, W., Wang, S., Han, X., and Sun, Y. (2011). The BCL2 gene is regulated by a special AT-rich sequence binding protein 1-mediated long range chromosomal interaction between the promoter and the distal element located within the 3′-UTR. Nucleic Acids Res. *39*, 4640–4652.

Gottimukkala, K.P., Jangid, R., Patta, I., Sultana, D.A., Sharma, A., Misra-Sen, J., and Galande, S. (2016). Regulation of SATB1 during thymocyte development by TCR signaling. Mol. Immunol. *77*, 34–43.

Gotzmann, J., Meissner, M., and Gerner, C. (2000). The fate of the nuclear matrix-associated-region-binding protein SATB1 during apoptosis. Cell Death Differ. *7*, 425–438.

Guermonprez, P., Valladeau, J., Zitvogel, L., Théry, C., and Amigorena, S. (2002). Antigen presentation and T cell stimulation by dendritic cells. Annu. Rev. Immunol. *20*, 621–667.

Gutcher, I., Donkor, M.K., Ma, Q., Rudensky, A.Y., Flavell, R.A., and Li, M.O. (2011). Autocrine Transforming Growth Factor-β1 Promotes In Vivo Th17 Cell Differentiation. Immunity *34*, 396–408.

Haas, S., Trumpp, A., and Milsom, M.D. (2018). Causes and Consequences of Hematopoietic Stem Cell Heterogeneity. Cell Stem Cell *22*, 627–638.

Hao, B., Naik, A.K., Watanabe, A., Tanaka, H., Chen, L., Richards, H.W., Kondo, M., Taniuchi, I., Kohwi, Y., Kohwi-Shigematsu, T., et al. (2015). An anti-silencer– and SATB1-dependent chromatin hub regulates Rag1 and Rag2 gene expression during thymocyte development. J. Exp. Med. *212*, 809–824.

Harrington, L.E., Hatton, R.D., Mangan, P.R., Turner, H., Murphy, T.L., Murphy, K.M., and Weaver, C.T. (2005). Interleukin 17–producing CD4+ effector T cells develop via a lineage distinct from the T helper type 1 and 2 lineages. Nat. Immunol. *6*, 1123–1132.

Harris, T.J., Grosso, J.F., Yen, H.-R., Xin, H., Kortylewski, M., Albesiano, E., Hipkiss, E.L., Getnet, D., Goldberg, M. V., Maris, C.H., et al. (2007). Cutting Edge: An In Vivo Requirement for STAT3 Signaling in TH17 Development and TH17-Dependent Autoimmunity. J. Immunol. *179*, 4313–4317.

Hasbold, J., Hong, J.S.-Y., Kehry, M.R., and Hodgkin, P.D. (1999). Integrating Signals From IFN-gamma and IL-4 by B Cells: Positive and Negative Effects on CD40 Ligand-Induced Proliferation, Survival, and Division-Linked Isotype Switching to IgG1, IgE, and IgG2a. J. Immunol. *163*, 4175–4181.

Henriksson, J., Chen, X., Gomes, T., Ullah, U., Meyer, K.B., Miragaia, R., Duddy, G., Pramanik, J., Yusa, K., Lahesmaa, R., et al. (2019). Genome-wide CRISPR Screens in T Helper Cells Reveal Pervasive Crosstalk between Activation and Differentiation. Cell *176*, 882–896.e18.

Hirota, K., Duarte, J.H., Veldhoen, M., Hornsby, E., Li, Y., Cua, D.J., Ahlfors, H., Wilhelm, C., Tolaini, M., Menzel, U., et al. (2011). Fate mapping of IL-17-producing T cells in inflammatory responses. Nat. Immunol. *12*, 255–263.

ten Hove, T., van den Blink, B., Pronk, I., Drillenburg, P., Peppelenbosch, M.P., and van Deventer, S.J.H. (2002). Dichotomal role of inhibition of p38 MAPK with SB 203580 in experimental colitis. Gut *50*, 507–512.

Hsieh, C.S., Lee, H.M., and Lio, C.W.J. (2012). Selection of regulatory T cells in the thymus. Nat. Rev. Immunol. *12*, 157–167.

Huber, M., and Lohoff, M. (2014). IRF4 at the crossroads of effector T-cell fate decision. Eur. J. Immunol. *44*, 1886–1895.

Ignatiadis, N., Klaus, B., Zaugg, J.B., and Huber, W. (2016). Data-driven hypothesis weighting increases detection power in genome-scale multiple testing. Nat. Methods *13*, 577–580.

Ivanov, I.I., McKenzie, B.S., Zhou, L., Tadokoro, C.E., Lepelley, A., Lafaille, J.J., Cua, D.J., and Littman, D.R. (2006). The Orphan Nuclear Receptor RORγt Directs the Differentiation Program of Proinflammatory IL-17+ T Helper Cells. Cell *126*, 1121–1133.

Ivanova, E.A., and Orekhov, A.N. (2015). T Helper Lymphocyte Subsets and Plasticity in Autoimmunity and Cancer: An Overview. Biomed Res. Int. *2015*, 327470.

Jain, A., and Pasare, C. (2017). Innate Control of Adaptive Immunity: Beyond the Three-Signal Paradigm. J. Immunol. *198*, 3791–3800.

Jargosch, M., Kröger, S., Gralinska, E., Klotz, U., Fang, Z., Chen, W., Leser, U., Selbig, J., Groth, D., and Baumgrass, R. (2016). Data integration for identification of important transcription factors of STAT6-mediated cell fate decisions. Genet. Mol. Res. *15*.

Johnston, R.J., Choi, Y.S., Diamond, J.A., Yang, J.A., and Crotty, S. (2012). STAT5 is a potent negative regulator of TFH cell differentiation. J. Exp. Med. *209*, 243–250.

Josefowicz, S.Z., Lu, L.-F., and Rudensky, A.Y. (2012). Regulatory T Cells: Mechanisms of Differentiation and Function. Annu. Rev. Immunol. *30*, 531–564.

Kakugawa, K., Kojo, S., Tanaka, H., Seo, W., Endo, T.A., Kitagawa, Y., Muroi, S., Tenno, M., Yasmin, N., Kohwi, Y., et al. (2017). Essential Roles of SATB1 in Specifying T Lymphocyte Subsets. Cell Rep. *19*, 1176–1188.

Kaplan, M.H. (2013). Th9 cells: differentiation and disease. Immunol. Rev. *252*, 104–115.

Kaplan, M.H. (2017). The transcription factor network in Th9 cells. Semin. Immunopathol. *39*, 11–20.

Karim, A.F., Reba, S.M., Li, Q., Boom, W.H., and Rojas, R.E. (2017). Toll like Receptor 2 engagement on CD4+ T cells promotes TH9 differentiation and function. Eur. J. Immunol. *47*, 1513–1524.

Katzman, S.D., Hoyer, K.K., Dooms, H., Gratz, I.K., Rosenblum, M.D., Paw, J.S., Isakson, S.H., and Abbas, A.K. (2011). Opposing functions of IL-2 and IL-7 in the regulation of immune responses. Cytokine *56*, 116–121.

Kaur, S., Coulombe, Y., Ramdzan, Z.M., Leduy, L., Masson, J.-Y., and Nepveu, A. (2016). Special AT-rich Sequence-binding Protein 1 (SATB1) Functions as an Accessory Factor in Base Excision Repair. J. Biol. Chem. *291*, 22769–22780.

Kebir, H., Ifergan, I., Alvarez, J.I., Bernard, M., Poirier, J., Arbour, N., Duquette, P., and Prat, A. (2009). Preferential recruitment of interferon-γ-expressing TH17 cells in multiple sclerosis. Ann. Neurol. *66*, 390–402.

Kim, H.S., Jang, S.W., Lee, W., Kim, K., Sohn, H., Hwang, S.S., and Lee, G.R. (2017). PTEN drives Th17 cell differentiation by preventing IL-2 production. J. Exp. Med. *214*,

3381–3398.

Kitagawa, Y., Ohkura, N., Kidani, Y., Vandenbon, A., Hirota, K., Kawakami, R., Yasuda, K., Motooka, D., Nakamura, S., Kondo, M., et al. (2017). Guidance of regulatory T cell development by Satb1-dependent super-enhancer establishment. Nat. Immunol. *18*, 173–183.

Kohwi-Shigematsu, T., Maass, K., and Bode, J. (1997). A Thymocyte Factor SATB1 Suppresses Transcription of Stably Integrated Matrix-Attachment Region-Linked Reporter Genes †. Biochemistry *36*, 12005–12010.

Komiyama, Y., Nakae, S., Matsuki, T., Nambu, A., Ishigame, H., Kakuta, S., Sudo, K., and Iwakura, Y. (2006). IL-17 Plays an Important Role in the Development of Experimental Autoimmune Encephalomyelitis. J. Immunol. *177*, 566–573.

Kondo, M., Tanaka, Y., Kuwabara, T., Naito, T., Kohwi-Shigematsu, T., and Watanabe, A. (2016). SATB1 Plays a Critical Role in Establishment of Immune Tolerance. J. Immunol. *196*, 563–572.

Konopacki, C., Pritykin, Y., Rubtsov, Y., Leslie, C.S., and Rudensky, A.Y. (2019). Transcription factor Foxp1 regulates Foxp3 chromatin binding and coordinates regulatory T cell function. Nat. Immunol. *20*, 232–242.

Korn, T., Bettelli, E., Gao, W., Awasthi, A., Jäger, A., Strom, T.B., Oukka, M., and Kuchroo, V.K. (2007). IL-21 initiates an alternative pathway to induce proinflammatory TH17 cells. Nature *448*, 484–487.

Korn, T., Bettelli, E., Oukka, M., and Kuchroo, V.K. (2009). IL-17 and Th17 Cells. Annu. Rev. Immunol. *27*, 485–517.

Kovanen, P.E., Young, L., Al-Shami, A., Rovella, V., Pise-Masison, C.A., Radonovich, M.F., Powell, J., Fu, J., Brady, J.N., Munson, P.J., et al. (2005). Global analysis of IL-2 target genes: Identification of chromosomal clusters of expressed genes. Int. Immunol. *17*, 1009–1021.

Kryczek, I., Wei, S., Vatan, L., Escara-Wilke, J., Szeliga, W., Keller, E.T., and Zou, W. (2007). Cutting Edge: Opposite Effects of IL-1 and IL-2 on the Regulation of IL-17+ T Cell Pool IL-1 Subverts IL-2-Mediated Suppression. J. Immunol. *179*, 1423–1426.

Kumar, P.P., Purbey, P.K., Ravi, D.S., Mitra, D., and Galande, S. (2005). Displacement of SATB1-Bound Histone Deacetylase 1 Corepressor by the Human Immunodeficiency Virus

Type 1 Transactivator Induces Expression of Interleukin-2 and Its Receptor in T Cells. Mol. Cell. Biol. *25*, 1620–1633.

van Langelaar, J., van der Vuurst de Vries, R.M., Janssen, M., Wierenga-Wolf, A.F., Spilt, I.M., Siepman, T.A., Dankers, W., Verjans, G.M.G.M., de Vries, H.E., Lubberts, E., et al. (2018). T helper 17.1 cells associate with multiple sclerosis disease activity: perspectives for early intervention. Brain *141*, 1334–1349.

Langmead, B., and Salzberg, S.L. (2012). Fast gapped-read alignment with Bowtie 2. Nat. Methods *9*, 357–359.

Langrish, C.L., Chen, Y., Blumenschein, W.M., Mattson, J., Basham, B., Sedgwick, J.D., McClanahan, T., Kastelein, R.A., and Cua, D.J. (2005). IL-23 drives a pathogenic T cell population that induces autoimmune inflammation. J. Exp. Med. *201*, 233–240.

Laurence, A., Tato, C.M., Davidson, T.S., Kanno, Y., Chen, Z., Yao, Z., Blank, R.B., Meylan, F., Siegel, R., Hennighausen, L., et al. (2007). Interleukin-2 Signaling via STAT5 Constrains T Helper 17 Cell Generation. Immunity *26*, 371–381.

Lawrence, M., Huber, W., Pagès, H., Aboyoun, P., Carlson, M., Gentleman, R., Morgan, M.T., and Carey, V.J. (2013). Software for Computing and Annotating Genomic Ranges. PLoS Comput. Biol. *9*, e1003118.

Lee, H.M., and Hsieh, C.-S. (2009). Rare Development of Foxp3+ Thymocytes in the CD4+ CD8+ Subset. J. Immunol. *183*, 2261–2266.

Lee, P.P., Fitzpatrick, D.R., Beard, C., Jessup, H.K., Lehar, S., Makar, K.W., Pérez-Melgosa, M., Sweetser, M.T., Schlissel, M.S., Nguyen, S., et al. (2001). A Critical Role for Dnmt1 and DNA Methylation in T Cell Development, Function, and Survival. Immunity *15*, 763–774.

Lee, Y., Awasthi, A., Yosef, N., Quintana, F.J., Xiao, S., Peters, A., Wu, C., Kleinewietfeld, M., Kunder, S., Hafler, D.A., et al. (2012). Induction and molecular signature of pathogenic TH17 cells. Nat. Immunol. *13*, 991–999.

Lee, Y.K., Turner, H., Maynard, C.L., Oliver, J.R., Chen, D., Elson, C.O., and Weaver, C.T. (2009). Late Developmental Plasticity in the T Helper 17 Lineage. Immunity *30*, 92–107.

Leppkes, M., Becker, C., Ivanov, I.I., Hirth, S., Wirtz, S., Neufert, C., Pouly, S., Murphy, A.J., Valenzuela, D.M., Yancopoulos, G.D., et al. (2009). RORγ-Expressing Th17 Cells Induce Murine Chronic Intestinal Inflammation via Redundant Effects of IL-17A and IL-17F.

Gastroenterology *136*, 257–267.

Létourneau, S., Krieg, C., Pantaleo, G., and Boyman, O. (2009). IL-2– and CD25-dependent immunoregulatory mechanisms in the homeostasis of T-cell subsets. J. Allergy Clin. Immunol. *123*, 758–762.

Leung, M.W.L., Shen, S., and Lafaille, J.J. (2009). TCR-dependent differentiation of thymic Foxp3+ cells is limited to small clonal sizes. J. Exp. Med. *206*, 2121–2130.

Li, H., Handsaker, B., Wysoker, A., Fennell, T., Ruan, J., Homer, N., Marth, G., Abecasis, G., and Durbin, R. (2009). The Sequence Alignment/Map format and SAMtools. Bioinformatics *25*, 2078–2079.

Li, J., Chen, S., Xiao, X., Zhao, Y., Ding, W., and Li, X.C. (2017). IL-9 and Th9 cells in health and diseases—From tolerance to immunopathology. Cytokine Growth Factor Rev. *37*, 47–55.

Liao, W., Schones, D.E., Oh, J., Cui, Y., Cui, K., Roh, T.-Y., Zhao, K., and Leonard, W.J. (2008). Priming for T helper type 2 differentiation by interleukin 2–mediated induction of interleukin 4 receptor α-chain expression. Nat. Immunol. *9*, 1288–1296.

Liao, W., Lin, J.-X., Wang, L., Li, P., and Leonard, W.J. (2011). Modulation of cytokine receptors by IL-2 broadly regulates differentiation into helper T cell lineages. Nat. Immunol. *12*, 551–559.

Liao, W., Lin, J.-X., and Leonard, W.J. (2013). Interleukin-2 at the Crossroads of Effector Responses, Tolerance, and Immunotherapy. Immunity *38*, 13–25.

Liao, W., Spolski, R., Li, P., Du, N., West, E.E., Ren, M., Mitra, S., and Leonard, W.J. (2014). Opposing actions of IL-2 and IL-21 on Th9 differentiation correlate with their differential regulation of BCL6 expression. Proc. Natl. Acad. Sci. *111*, 3508–3513.

Liberzon, A., Birger, C., Thorvaldsdóttir, H., Ghandi, M., Mesirov, J.P., and Tamayo, P. (2015). The Molecular Signatures Database (MSigDB) hallmark gene set collection. Cell Syst. *1*, 417–425.

Lin, Y.-C., Lin, Y.-C., Wu, C.-C., Huang, M.-Y., Tsai, W.-C., Hung, C.-H., and Kuo, P.-L. (2017). The immunomodulatory effects of TNF-α inhibitors on human Th17 cells via RORγt histone acetylation. Oncotarget *8*, 7559–7571.

Love, M.I., Huber, W., and Anders, S. (2014). Moderated estimation of fold change and dispersion for RNA-seq data with DESeq2. Genome Biol. *15*, 550.

Lund, R., Aittokallio, T., Nevalainen, O., and Lahesmaa, R. (2003). Identification of Novel Genes Regulated by IL-12, IL-4, or TGF-β during the Early Polarization of CD4 + Lymphocytes. J. Immunol. *171*, 5328–5336.

Lund, R., Ahlfors, H., Kainonen, E., Lahesmaa, A.-M., Dixon, C., and Lahesmaa, R. (2005). Identification of genes involved in the initiation of human Th1 or Th2 cell commitment. Eur. J. Immunol. *35*, 3307–3319.

Mailer, R.K.W., Joly, A.-L., Liu, S., Elias, S., Tegner, J., and Andersson, J. (2015). IL-1β promotes Th17 differentiation by inducing alternative splicing of FOXP3. Sci. Rep. *5*, 14674.

Malek, T.R. (2008). The Biology of Interleukin-2. Annu. Rev. Immunol. *26*, 453–479.

Malhotra, D., Fletcher, A.L., Astarita, J., Lukacs-Kornek, V., Tayalia, P., Gonzalez, S.F., Elpek, K.G., Chang, S.K., Knoblich, K., Hemler, M.E., et al. (2012). Transcriptional profiling of stroma from inflamed and resting lymph nodes defines immunological hallmarks. Nat. Immunol. *13*, 499–510.

Malik, S., and Awasthi, A. (2018). Transcriptional Control of Th9 Cells: Role of Foxo1 in Interleukin-9 Induction. Front. Immunol. *9*, 995.

Mangan, P.R., Harrington, L.E., O'Quinn, D.B., Helms, W.S., Bullard, D.C., Elson, C.O., Hatton, R.D., Wahl, S.M., Schoeb, T.R., and Weaver, C.T. (2006). Transforming growth factor-β induces development of the TH17 lineage. Nature *441*, 231–234.

Martins, G.A., Cimmino, L., Liao, J., Magnusdottir, E., and Calame, K. (2008). Blimp-1 directly represses Il2 and the Il2 activator Fos, attenuating T cell proliferation and survival. J. Exp. Med. *205*, 1959–1965.

McGeachy, M.J., Chen, Y., Tato, C.M., Laurence, A., Joyce-Shaikh, B., Blumenschein, W.M., McClanahan, T.K., O'Shea, J.J., and Cua, D.J. (2009). The interleukin 23 receptor is essential for the terminal differentiation of interleukin 17–producing effector T helper cells in vivo. Nat. Immunol. *10*, 314–324.

Medzhitov, R., and Janeway, C.J. (2000). Innate immune recognition: mechanisms and pathways. Immunol. Rev. *173*, 89–97.

Menk, A. V., Scharping, N.E., Moreci, R.S., Zeng, X., Guy, C., Salvatore, S., Bae, H., Xie, J., Young, H.A., Wendell, S.G., et al. (2018). Early TCR Signaling Induces Rapid Aerobic Glycolysis Enabling Distinct Acute T Cell Effector Functions. Cell Rep. *22*, 1509–1521.

Michalek, R.D., Gerriets, V.A., Jacobs, S.R., Macintyre, A.N., MacIver, N.J., Mason, E.F., Sullivan, S.A., Nichols, A.G., and Rathmell, J.C. (2011). Cutting Edge: Distinct Glycolytic and Lipid Oxidative Metabolic Programs Are Essential for Effector and Regulatory CD4+ T Cell Subsets. J. Immunol. *186*, 3299–3303.

Micossé, C., von Meyenn, L., Steck, O., Kipfer, E., Adam, C., Simillion, C., Seyed Jafari, S.M., Olah, P., Yawlkar, N., Simon, D., et al. (2019). Human "TH9" cells are a subpopulation of PPAR-γ+ TH2 cells. Sci. Immunol. *4*, eaat5943.

Miller, S.D., and Karpus, W.J. (2007). Experimental Autoimmune Encephalomyelitis in the Mouse. Curr. Protoc. Immunol. *77*, Unit 15.1.

Mogensen, T.H. (2009). Pathogen Recognition and Inflammatory Signaling in Innate Immune Defenses. Clin. Microbiol. Rev. *22*, 240–273.

Moran, A.E., and Hogquist, K.A. (2012). T-cell receptor affinity in thymic development. Immunology *135*, 261–267.

Morel, P.A. (2018). Differential T-cell receptor signals for T helper cell programming. Immunology *155*, 63–71.

Mukasa, R., Balasubramani, A., Lee, Y.K., Whitley, S.K., Weaver, B.T., Shibata, Y., Crawford, G.E., Hatton, R.D., and Weaver, C.T. (2010). Epigenetic Instability of Cytokine and Transcription Factor Gene Loci Underlies Plasticity of the T Helper 17 Cell Lineage. Immunity *32*, 616–627.

Muranski, P., Borman, Z.A., Kerkar, S.P., Klebanoff, C.A., Ji, Y., Sanchez-Perez, L., Sukumar, M., Reger, R.N., Yu, Z., Kern, S.J., et al. (2011). Th17 Cells Are Long Lived and Retain a Stem Cell-like Molecular Signature. Immunity *35*, 972–985.

Murphy, K.M., and Reiner, S.L. (2002). The lineage decisions of helper T cells. Nat. Rev. Immunol. *2*, 933–944.

Naik, R., and Galande, S. (2019). SATB family chromatin organizers as master regulators of tumor progression. Oncogene *38*, 1989–2004.

Nath, N., Prasad, R., Giri, S., Singh, A.K., and Singh, I. (2006). T-bet is essential for the progression of experimental autoimmune encephalomyelitis. Immunology *118*, 384–391.

Neefjes, J., Jongsma, M.L.M., Paul, P., and Bakke, O. (2011). Towards a systems understanding of MHC class I and MHC class II antigen presentation. Nat. Rev. Immunol. *11*, 823–836.

Netea, M.G., Schlitzer, A., Placek, K., Joosten, L.A.B., and Schultze, J.L. (2019). Innate and Adaptive Immune Memory: an Evolutionary Continuum in the Host's Response to Pathogens. Cell Host Microbe *25*, 13–26.

Neufert, C., Becker, C., Wirtz, S., Fantini, M.C., Weigmann, B., Galle, P.R., and Neurath, M.F. (2007). IL-27 controls the development of inducible regulatory T cells and Th17 cells via differential effects on STAT1. Eur. J. Immunol. *37*, 1809–1816.

Ng, C.T., Nayak, B.P., Schmedt, C., and Oldstone, M.B.A. (2012). Immortalized clones of fibroblastic reticular cells activate virus-specific T cells during virus infection. Proc. Natl. Acad. Sci. *109*, 7823–7828.

Nie, H., Maika, S.D., Tucker, P.W., and Gottlieb, P.D. (2005). A Role for SATB1, a Nuclear Matrix Association Region-Binding Protein, in the Development of CD8SP Thymocytes and Peripheral T Lymphocytes. J. Immunol. *174*, 4745–4752.

NIH (2011). Guide for the Care and Use of Laboratory Animals (National Academies Press (US)).

Notani, D., Gottimukkala, K.P., Jayani, R.S., Limaye, A.S., Damle, M. V, Mehta, S., Purbey, P.K., Joseph, J., and Galande, S. (2010). Global Regulator SATB1 Recruits β-Catenin and Regulates TH2 Differentiation in Wnt-Dependent Manner. PLoS Biol. *8*, e1000296.

Nüssing, S., Koay, H., Sant, S., Loudovaris, T., Mannering, S.I., Lappas, M., D Udekem, Y., Konstantinov, I.E., Berzins, S.P., Rimmelzwaan, G.F., et al. (2019). Divergent SATB1 expression across human life span and tissue compartments. Immunol. Cell Biol. *97*, 498–511.

O'Shea, J.J., Lahesmaa, R., Vahedi, G., Laurence, A., and Kanno, Y. (2011). Genomic views of STAT function in CD4+ T helper cell differentiation. Nat. Rev. Immunol. *11*, 239–250.

Oh-hora, M., Komatsu, N., Pishyareh, M., Feske, S., Hori, S., Taniguchi, M., Rao, A., and Takayanagi, H. (2013). Agonist-Selected T Cell Development Requires Strong T Cell

Receptor Signaling and Store-Operated Calcium Entry. Immunity *38*, 881–895.

Olson, N.E., Graves, J.D., Shu, G.L., Ryan, E.J., and Clark, E.A. (2003). Caspase Activity Is Required for Stimulated B Lymphocytes to Enter the Cell Cycle. J. Immunol. *170*, 6065–6072.

Ostanin, D. V, Bao, J., Koboziev, I., Gray, L., Robinson-Jackson, S.A., Kosloski-Davidson, M., Price, V.H., and Grisham, M.B. (2009). T cell transfer model of chronic colitis: concepts, considerations, and tricks of the trade. Am. J. Physiol. Liver Physiol. *296*, G135–G146.

Owen, D.L., and Farrar, M.A. (2017). STAT5 and CD4+ T Cell Immunity. F1000Research *6*, 32.

Panagoulias, I., Georgakopoulos, T., Aggeletopoulou, I., Agelopoulos, M., Thanos, D., and Mouzaki, A. (2016). Transcription Factor Ets-2 Acts as a Preinduction Repressor of Interleukin-2 (IL-2) Transcription in Naive T Helper Lymphocytes. J. Biol. Chem. *291*, 26707–26721.

Park, H., Li, Z., Yang, X.O., Chang, S.H., Nurieva, R., Wang, Y.-H., Wang, Y., Hood, L., Zhu, Z., Tian, Q., et al. (2005). A distinct lineage of CD4 T cells regulates tissue inflammation by producing interleukin 17. Nat. Immunol. *6*, 1133–1141.

Parkin, J., and Cohen, B. (2001). An overview of the immune system. Lancet *357*, 1777–1789.

Pavan Kumar, P., Purbey, P.K., Sinha, C.K., Notani, D., Limaye, A., Jayani, R.S., and Galande, S. (2006). Phosphorylation of SATB1, a Global Gene Regulator, Acts as a Molecular Switch Regulating Its Transcriptional Activity In Vivo. Mol. Cell *22*, 231–243.

Pedicini, M., Barrenäs, F., Clancy, T., Castiglione, F., Hovig, E., Kanduri, K., Santoni, D., and Benson, M. (2010). Combining Network Modeling and Gene Expression Microarray Analysis to Explore the Dynamics of Th1 and Th2 Cell Regulation. PLoS Comput. Biol. *6*, e1001032.

Pennock, N.D., White, J.T., Cross, E.W., Cheney, E.E., Tamburini, B.A., and Kedl, R.M. (2013). T cell responses: naïve to memory and everything in between. Adv. Physiol. Educ. *37*, 273–283.

Pepper, M., Pagán, A.J., Igyártó, B.Z., Taylor, J.J., and Jenkins, M.K. (2011). Opposing Signals from the Bcl6 Transcription Factor and the Interleukin-2 Receptor Generate T Helper

1 Central and Effector Memory Cells. Immunity *35*, 583–595.

Perry, J.S.A., and Hsieh, C.-S. (2016). Development of T-cell tolerance utilizes both cell-autonomous and cooperative presentation of self-antigen. Immunol. Rev. *271*, 141–155.

Peters, A., Fowler, K.D., Chalmin, F., Merkler, D., Kuchroo, V.K., and Pot, C. (2015). IL-27 Induces Th17 Differentiation in the Absence of STAT1 Signaling. J. Immunol. *195*, 4144–4153.

Picelli, S., Björklund, Å.K., Reinius, B., Sagasser, S., Winberg, G., and Sandberg, R. (2014). Tn5 transposase and tagmentation procedures for massively scaled sequencing projects. Genome Res. *24*, 2033–2040.

Placek, K., Coffre, M., Maiella, S., Bianchi, E., and Rogge, L. (2009). Genetic and epigenetic networks controlling T helper 1 cell differentiation. Immunology *127*, 155–162.

Plank, M.W., Kaiko, G.E., Maltby, S., Weaver, J., Tay, H.L., Shen, W., Wilson, M.S., Durum, S.K., and Foster, P.S. (2017). Th22 Cells Form a Distinct Th Lineage from Th17 Cells In Vitro with Unique Transcriptional Properties and Tbet-Dependent Th1 Plasticity. J. Immunol. *198*, 2182–2190.

Pohar, J., Simon, Q., and Fillatreau, S. (2018). Antigen-Specificity in the Thymic Development and Peripheral Activity of CD4+FOXP3+ T Regulatory Cells. Front. Immunol. *9*, 1701.

Poppensieker, K., Otte, D.-M., Schurmann, B., Limmer, A., Dresing, P., Drews, E., Schumak, B., Klotz, L., Raasch, J., Mildner, A., et al. (2012). CC chemokine receptor 4 is required for experimental autoimmune encephalomyelitis by regulating GM-CSF and IL-23 production in dendritic cells. Proc. Natl. Acad. Sci. *109*, 3897–3902.

Powrie, F., Leach, M.W., Mauze, S., Caddle, L.B., and Coffman, R.L. (1993). Phenotypically distinct subsets of CD4+ T cells induce or protect from chronic intestinal inflammation in C. B-17 scid mice. Int. Immunol. *5*, 1461–1471.

Purbey, P.K., Singh, S., Notani, D., Kumar, P.P., Limaye, A.S., and Galande, S. (2009). Acetylation-Dependent Interaction of SATB1 and CtBP1 Mediates Transcriptional Repression by SATB1. Mol. Cell. Biol. *29*, 1321–1337.

Ramírez, F., Ryan, D.P., Grüning, B., Bhardwaj, V., Kilpert, F., Richter, A.S., Heyne, S., Dündar, F., and Manke, T. (2016). deepTools2: a next generation web server for deep-

sequencing data analysis. Nucleic Acids Res. *44*, W160–W165.

Ren, J., Han, L., Tang, J., Liu, Y., Deng, X., Liu, Q., Hao, P., Feng, X., Li, B., Hu, H., et al. (2019). Foxp1 is critical for the maintenance of regulatory T-cell homeostasis and suppressive function. PLOS Biol. *17*, e3000270.

Ricklin, D., Hajishengallis, G., Yang, K., and Lambris, J.D. (2010). Complement: a key system for immune surveillance and homeostasis. Nat. Immunol. *11*, 785–797.

Riessland, M., Kolisnyk, B., Kim, T.W., Cheng, J., Ni, J., Pearson, J.A., Park, E.J., Dam, K., Acehan, D., Ramos-Espiritu, L.S., et al. (2019). Loss of SATB1 Induces p21-Dependent Cellular Senescence in Post-mitotic Dopaminergic Neurons. Cell Stem Cell *25*, 514–530.e8.

Sadlack, B., Löhler, J., Schorle, H., Klebb, G., Haber, H., Sickel, E., Noelle, R.J., and Horak, I. (1995). Generalized autoimmune disease in interleukin-2-deficient mice is triggered by an uncontrolled activation and proliferation of CD4+ T cells. Eur. J. Immunol. *25*, 3053–3059.

Satoh, Y., Yokota, T., Sudo, T., Kondo, M., Lai, A., Kincade, P.W., Kouro, T., Iida, R., Kokame, K., Miyata, T., et al. (2013). The Satb1 Protein Directs Hematopoietic Stem Cell Differentiation toward Lymphoid Lineages. Immunity *38*, 1105–1115.

Sawai, C.M., Babovic, S., Upadhaya, S., Knapp, D.J.H.F., Lavin, Y., Lau, C.M., Goloborodko, A., Feng, J., Fujisaki, J., Ding, L., et al. (2016). Hematopoietic Stem Cells Are the Major Source of Multilineage Hematopoiesis in Adult Animals. Immunity *45*, 597–609.

Schenten, D., and Medzhitov, R. (2011). The Control of Adaptive Immune Responses by the Innate Immune System. In Advances in Immunology, pp. 87–124.

Schraml, B.U., Hildner, K., Ise, W., Lee, W.-L., Smith, W.A.-E., Solomon, B., Sahota, G., Sim, J., Mukasa, R., Cemerski, S., et al. (2009). The AP-1 transcription factor Batf controls TH17 differentiation. Nature *460*, 405–409.

Schülke, S., and Albrecht, M. (2019). Mouse Models for Food Allergies: Where Do We Stand? Cells *8*, 546.

Seo, J., Lozano, M.M., and Dudley, J.P. (2005). Nuclear Matrix Binding Regulates SATB1-mediated Transcriptional Repression. J. Biol. Chem. *280*, 24600–24609.

Sha, Y., and Markovic-Plese, S. (2011). A role of IL-1R1 signaling in the differentiation of Th17 cells and the development of autoimmune diseases. Self. Nonself. *2*, 35–42.

Shan, X., Czar, M.J., Bunnell, S.C., Liu, P., Liu, Y., Schwartzberg, P.L., and Wange, R.L. (2000). Deficiency of PTEN in Jurkat T Cells Causes Constitutive Localization of Itk to the Plasma Membrane and Hyperresponsiveness to CD3 Stimulation. Mol. Cell. Biol. *20*, 6945–6957.

Shanker, A. (2010). Adaptive control of innate immunity. Immunol. Lett. *131*, 107–112.

Shannon, M.F. (2003). A nuclear address with influence. Nat. Genet. *34*, 4–6.

Shi, L.Z., Wang, R., Huang, G., Vogel, P., Neale, G., Green, D.R., and Chi, H. (2011). HIF1α–dependent glycolytic pathway orchestrates a metabolic checkpoint for the differentiation of TH17 and Treg cells. J. Exp. Med. *208*, 1367–1376.

Shih, H.-Y., Sciumè, G., Poholek, A.C., Vahedi, G., Hirahara, K., Villarino, A. V., Bonelli, M., Bosselut, R., Kanno, Y., Muljo, S.A., et al. (2014). Transcriptional and epigenetic networks of helper T and innate lymphoid cells. Immunol. Rev. *261*, 23–49.

Shinkai, Y., Rathbun, G., Lam, K.-P., Oltz, E.M., Stewart, V., Mendelsohn, M., Charron, J., Datta, M., Young, F., Stall, A.M., et al. (1992). RAG-2-deficient mice lack mature lymphocytes owing to inability to initiate V(D)J rearrangement. Cell *68*, 855–867.

Skowronska-Krawczyk, D., Ma, Q., Schwartz, M., Scully, K., Li, W., Liu, Z., Taylor, H., Tollkuhn, J., Ohgi, K.A., Notani, D., et al. (2014). Required enhancer–matrin-3 network interactions for a homeodomain transcription program. Nature *514*, 257–261.

Śledzińska, A., Hemmers, S., Mair, F., Gorka, O., Ruland, J., Fairbairn, L., Nissler, A., Müller, W., Waisman, A., Becher, B., et al. (2013). TGF-β Signalling Is Required for CD4+ T Cell Homeostasis But Dispensable for Regulatory T Cell Function. PLoS Biol. *11*, e1001674.

Sommer, D. (2018). Understanding the role of SATB1 in CD4+ T cells by analysis of conditionally targeted mice generated by genetic engineering. urn:nbn:de:hbz:5n-52778.

Sommer, D., Peters, A.E., Wirtz, T., Mai, M., Ackermann, J., Thabet, Y., Schmidt, J., Weighardt, H., Wunderlich, F.T., Degen, J., et al. (2014). Efficient genome engineering by targeted homologous recombination in mouse embryos using transcription activator-like effector nucleases. Nat. Commun. *5*, 3045.

Staal, F.J.T., and M. Sen, J. (2008). The canonical Wnt signaling pathway plays an important role in lymphopoiesis and hematopoiesis. Eur. J. Immunol. *38*, 1788–1794.

Stephen, T.L., Payne, K.K., Chaurio, R.A., Allegrezza, M.J., Zhu, H., Perez-Sanz, J., Perales-Puchalt, A., Nguyen, J.M., Vara-Ailor, A.E., Eruslanov, E.B., et al. (2017). SATB1 Expression Governs Epigenetic Repression of PD-1 in Tumor-Reactive T Cells. Immunity *46*, 51–64.

Strutt, T.M., McKinstry, K.K., and Swain, S.L. (2011). Control of Innate Immunity by Memory CD4 T Cells. In Advances in Experimental Medicine and Biology, pp. 57–68.

Sun, J., Yi, S., Qiu, L., Fu, W., Wang, A., Liu, F., Wang, L., Wang, T., Chen, H., Wang, L., et al. (2018). SATB1 Defines a Subtype of Cutaneous CD30+ Lymphoproliferative Disorders Associated with a T-Helper 17 Cytokine Profile. J. Invest. Dermatol. *138*, 1795–1804.

Sun, L., Fu, J., and Zhou, Y. (2017). Metabolism Controls the Balance of Th17/T-Regulatory Cells. Front. Immunol. *8*, 1632.

Swain, S.L., Croft, M., Dubey, C., Haynes, L., Rogers, P., Zhang, X., and Bradley, L.M. (1996). From Naive to Memory T Cells. Immunol. Rev. *150*, 143–167.

Swain, S.L., McKinstry, K.K., and Strutt, T.M. (2012). Expanding roles for CD4+ T cells in immunity to viruses. Nat. Rev. Immunol. *12*, 136–148.

Tan, C., and Gery, I. (2012). The Unique Features of Th9 Cells and their Products. Crit. Rev. Immunol. *32*, 1–10.

Tan, J.-A.T., Sun, Y., Song, J., Chen, Y., Krontiris, T.G., and Durrin, L.K. (2008). SUMO Conjugation to the Matrix Attachment Region-binding Protein, Special AT-rich Sequence-binding Protein-1 (SATB1), Targets SATB1 to Promyelocytic Nuclear Bodies Where It Undergoes Caspase Cleavage. J. Biol. Chem. *283*, 18124–18134.

Tan, J.-A.T., Song, J., Chen, Y., and Durrin, L.K. (2010). Phosphorylation-Dependent Interaction of SATB1 and PIAS1 Directs SUMO-Regulated Caspase Cleavage of SATB1. Mol. Cell. Biol. *30*, 2823–2836.

Tanaka, S., Suto, A., Iwamoto, T., Kashiwakuma, D., Kagami, S., Suzuki, K., Takatori, H., Tamachi, T., Hirose, K., Onodera, A., et al. (2014). Sox5 and c-Maf cooperatively induce Th17 cell differentiation via RORγt induction as downstream targets of Stat3. J. Exp. Med. *211*, 1857–1874.

Tanaka, Y., Sotome, T., Inoue, A., Mukozu, T., Kuwabara, T., Mikami, T., Kowhi-Shigematsu, T., and Kondo, M. (2017). SATB1 Conditional Knockout Results in Sjögren's

Syndrome in Mice. J. Immunol. *199*, 4016–4022.

Taniuchi, I. (2009). Transcriptional regulation in helper versus cytotoxic-lineage decision. Curr. Opin. Immunol. *21*, 127–132.

Tesone, A.J., Rutkowski, M.R., Brencicova, E., Svoronos, N., Perales-Puchalt, A., Stephen, T.L., Allegrezza, M.J., Payne, K.K., Nguyen, J.M., Wickramasinghe, J., et al. (2016). Satb1 Overexpression Drives Tumor-Promoting Activities in Cancer-Associated Dendritic Cells. Cell Rep. *14*, 1774–1786.

Tomura, M., Itoh, K., and Kanagawa, O. (2010). Naive CD4+ T Lymphocytes Circulate through Lymphoid Organs To Interact with Endogenous Antigens and Upregulate Their Function. J. Immunol. *184*, 4646–4653.

Vahedi, G., Takahashi, H., Nakayamada, S., Sun, H., Sartorelli, V., Kanno, Y., and O'Shea, J.J. (2012). STATs Shape the Active Enhancer Landscape of T Cell Populations. Cell *151*, 981–993.

Veldhoen, M., Hocking, R.J., Atkins, C.J., Locksley, R.M., and Stockinger, B. (2006). TGFβ in the Context of an Inflammatory Cytokine Milieu Supports De Novo Differentiation of IL-17-Producing T Cells. Immunity *24*, 179–189.

Veldhoen, M., Uyttenhove, C., van Snick, J., Helmby, H., Westendorf, A., Buer, J., Martin, B., Wilhelm, C., and Stockinger, B. (2008). Transforming growth factor-β "reprograms" the differentiation of T helper 2 cells and promotes an interleukin 9–producing subset. Nat. Immunol. *9*, 1341–1346.

Vignali, D.A.A., Collison, L.W., and Workman, C.J. (2008). How regulatory T cells work. Nat. Rev. Immunol. *8*, 523–532.

Villarino, A. V., Kanno, Y., Ferdinand, J.R., and O'Shea, J.J. (2015). Mechanisms of Jak/STAT Signaling in Immunity and Disease. J. Immunol. *194*, 21–27.

Villarino, A. V., Kanno, Y., and O'Shea, J.J. (2017). Mechanisms and consequences of Jak-STAT signaling in the immune system. Nat. Immunol. *18*, 374–384.

Walker, J.A., and McKenzie, A.N.J. (2018). TH2 cell development and function. Nat. Rev. Immunol. *18*, 121–133.

Wan, Y.Y., and Flavell, R.A. (2005). Identifying Foxp3-expressing suppressor T cells with a

bicistronic reporter. Proc. Natl. Acad. Sci. *102*, 5126–5131.

Wang, C., Yosef, N., Gaublomme, J., Wu, C., Lee, Y., Clish, C.B., Kaminski, J., Xiao, S., Zu Horste, G.M., Pawlak, M., et al. (2015). CD5L/AIM Regulates Lipid Biosynthesis and Restrains Th17 Cell Pathogenicity. Cell *163*, 1413–1427.

Wang, Y., Godec, J., Ben-Aissa, K., Cui, K., Zhao, K., Pucsek, A.B., Lee, Y.K., Weaver, C.T., Yagi, R., and Lazarevic, V. (2014a). The Transcription Factors T-bet and Runx Are Required for the Ontogeny of Pathogenic Interferon-γ-Producing T Helper 17 Cells. Immunity *40*, 355–366.

Wang, Y., Li, X., Kong, H., Zhu, Q., Dong, Y., Liu, X., and Chen, Y. (2017). Overexpression of SATB1 gene inhibits the immunosuppressive function of regulatory T cells in chronic hepatitis B. Ann. Clin. Lab. Sci. *47*, 403–408.

Wang, Z., Yang, X., Chu, X., Zhang, J., Zhou, H., Shen, Y., and Long, J. (2012). The structural basis for the oligomerization of the N-terminal domain of SATB1. Nucleic Acids Res. *40*, 4193–4202.

Wang, Z., Yang, X., Guo, S., Yang, Y., Su, X.C., Shen, Y., and Long, J. (2014b). Crystal structure of the ubiquitin-like domain-cut repeat-like tandem of special AT-rich sequence binding protein 1 (SATAB1) reveals a coordinating DNA-binding mechanism. J. Biol. Chem. *289*, 27376–27385.

Weaver, C.T., and Hatton, R.D. (2009). Interplay between the TH17 and TReg cell lineages: a (co-)evolutionary perspective. Nat. Rev. Immunol. *9*, 883–889.

Wei, L., Laurence, A., Elias, K.M., and O'Shea, J.J. (2007). IL-21 Is Produced by Th17 Cells and Drives IL-17 Production in a STAT3-dependent Manner. J. Biol. Chem. *282*, 34605–34610.

Wen, J., Huang, S., Rogers, H., Dickinson, L.A., Kohwi-Shigematsu, T., and Noguchi, C.T. (2005). SATB1 family protein expressed during early erythroid differentiation modifies globin gene expression. Blood *105*, 3330–3339.

Whitley, S.K., Balasubramani, A., Zindl, C.L., Sen, R., Shibata, Y., Crawford, G.E., Weathington, N.M., Hatton, R.D., and Weaver, C.T. (2018). IL-1R signaling promotes STAT3 and NF-κB factor recruitment to distal cis -regulatory elements that regulate Il17a/f transcription. J. Biol. Chem. *293*, 15790–15800.

Whitmire, J.K., Asano, M.S., Murali-Krishna, K., Suresh, M., and Ahmed, R. (1998). Long-Term CD4 Th1 and Th2 Memory following Acute Lymphocytic Choriomeningitis Virus Infection. J. Virol. *72*, 8281–8288.

Willerford, D.M., Chen, J., Ferry, J.A., Davidson, L., Ma, A., and Alt, F.W. (1995). Interleukin-2 receptor α chain regulates the size and content of the peripheral lymphoid compartment. Immunity *3*, 521–530.

Wu, H., Deng, Y., Zhao, M., Zhang, J., Zheng, M., Chen, G., Li, L., He, Z., and Lu, Q. (2018). Molecular Control of Follicular Helper T cell Development and Differentiation. Front. Immunol. *9*, 2470.

Yamasaki, K., Akiba, T., Yamasaki, T., and Harata, K. (2007). Structural basis for recognition of the matrix attachment region of DNA by transcription factor SATB1. Nucleic Acids Res. *35*, 5073–5084.

Yang, C., He, D., Yin, C., and Tan, J. (2015a). Inhibition of Interferon Regulatory Factor 4 Suppresses Th1 and Th17 Cell Differentiation and Ameliorates Experimental Autoimmune Encephalomyelitis. Scand. J. Immunol. *82*, 345–351.

Yang, X.-P., Ghoreschi, K., Steward-Tharp, S.M., Rodriguez-Canales, J., Zhu, J., Grainger, J.R., Hirahara, K., Sun, H.-W., Wei, L., Vahedi, G., et al. (2011). Opposing regulation of the locus encoding IL-17 through direct, reciprocal actions of STAT3 and STAT5. Nat. Immunol. *12*, 247–254.

Yang, X.O., Panopoulos, A.D., Nurieva, R., Chang, S.H., Wang, D., Watowich, S.S., and Dong, C. (2007). STAT3 Regulates Cytokine-mediated Generation of Inflammatory Helper T Cells. J. Biol. Chem. *282*, 9358–9363.

Yang, Y., Weiner, J., Liu, Y., Smith, A.J., Huss, D.J., Winger, R., Peng, H., Cravens, P.D., Racke, M.K., and Lovett-Racke, A.E. (2009). T-bet is essential for encephalitogenicity of both Th1 and Th17 cells. J. Exp. Med. *206*, 1549–1564.

Yang, Y., Wang, Z., Sun, L., Shao, L., Yang, N., Yu, D., Zhang, X., Han, X., and Sun, Y. (2015b). SATB1 mediates long-range chromatin interactions: A dual regulator of anti-apoptotic BCL2 and pro-apoptotic NOXA genes. PLoS One *10*, e0139170.

Yasuda, K., Kitagawa, Y., Kawakami, R., Isaka, Y., Watanabe, H., Kondoh, G., Kohwi-Shigematsu, T., Sakaguchi, S., and Hirota, K. (2019). Satb1 regulates the effector program of

encephalitogenic tissue Th17 cells in chronic inflammation. Nat. Commun. *10*, 549.

Yasui, D., Miyano, M., Cai, S., Varga-Weisz, P., and Kohwi-Shigematsu, T. (2002). SATB1 targets chromatin remodelling to regulate genes over long distances. Nature *419*, 641–645.

Yen, D., Cheung, J., Scheerens, H., Poulet, F., McClanahan, T., Mckenzie, B., Kleinschek, M.A., Owyang, A., Mattson, J., Blumenschein, W., et al. (2006). IL-23 is essential for T cell–mediated colitis and promotes inflammation via IL-17 and IL-6. J. Clin. Invest. *116*, 1310–1316.

Yosef, N., Shalek, A.K., Gaublomme, J.T., Jin, H., Lee, Y., Awasthi, A., Wu, C., Karwacz, K., Xiao, S., Jorgolli, M., et al. (2013). Dynamic regulatory network controlling TH17 cell differentiation. Nature *496*, 461–468.

Yu, G., Wang, L.-G., Han, Y., and He, Q.-Y. (2012). clusterProfiler: an R Package for Comparing Biological Themes Among Gene Clusters. Omi. A J. Integr. Biol. *16*, 284–287.

Yu, G., Wang, L.-G., and He, Q.-Y. (2015). ChIPseeker: an R/Bioconductor package for ChIP peak annotation, comparison and visualization. Bioinformatics *31*, 2382–2383.

Zambrano-Zaragoza, J.F., Romo-Martínez, E.J., Durán-Avelar, M.D.J., García-Magallanes, N., and Vibanco-Pérez, N. (2014). Th17 Cells in Autoimmune and Infectious Diseases. Int. J. Inflam. *2014*, 651503.

Zhang, Y., Liu, T., Meyer, C.A., Eeckhoute, J., Johnson, D.S., Bernstein, B.E., Nussbaum, C., Myers, R.M., Brown, M., Li, W., et al. (2008). Model-based Analysis of ChIP-Seq (MACS). Genome Biol. *9*, R137.

Zhou, L., Lopes, J.E., Chong, M.M.W., Ivanov, I.I., Min, R., Victora, G.D., Shen, Y., Du, J., Rubtsov, Y.P., Rudensky, A.Y., et al. (2008). TGF-β-induced Foxp3 inhibits TH17 cell differentiation by antagonizing RORγt function. Nature *453*, 236–240.

Zhu, J., Yamane, H., and Paul, W.E. (2010). Differentiation of Effector CD4 T Cell Populations. Annu. Rev. Immunol. *28*, 445–489.

Zlotoff, D.A., and Bhandoola, A. (2011). Hematopoietic progenitor migration to the adult thymus. Ann. N. Y. Acad. Sci. *1217*, 122–138.

7. Appendix

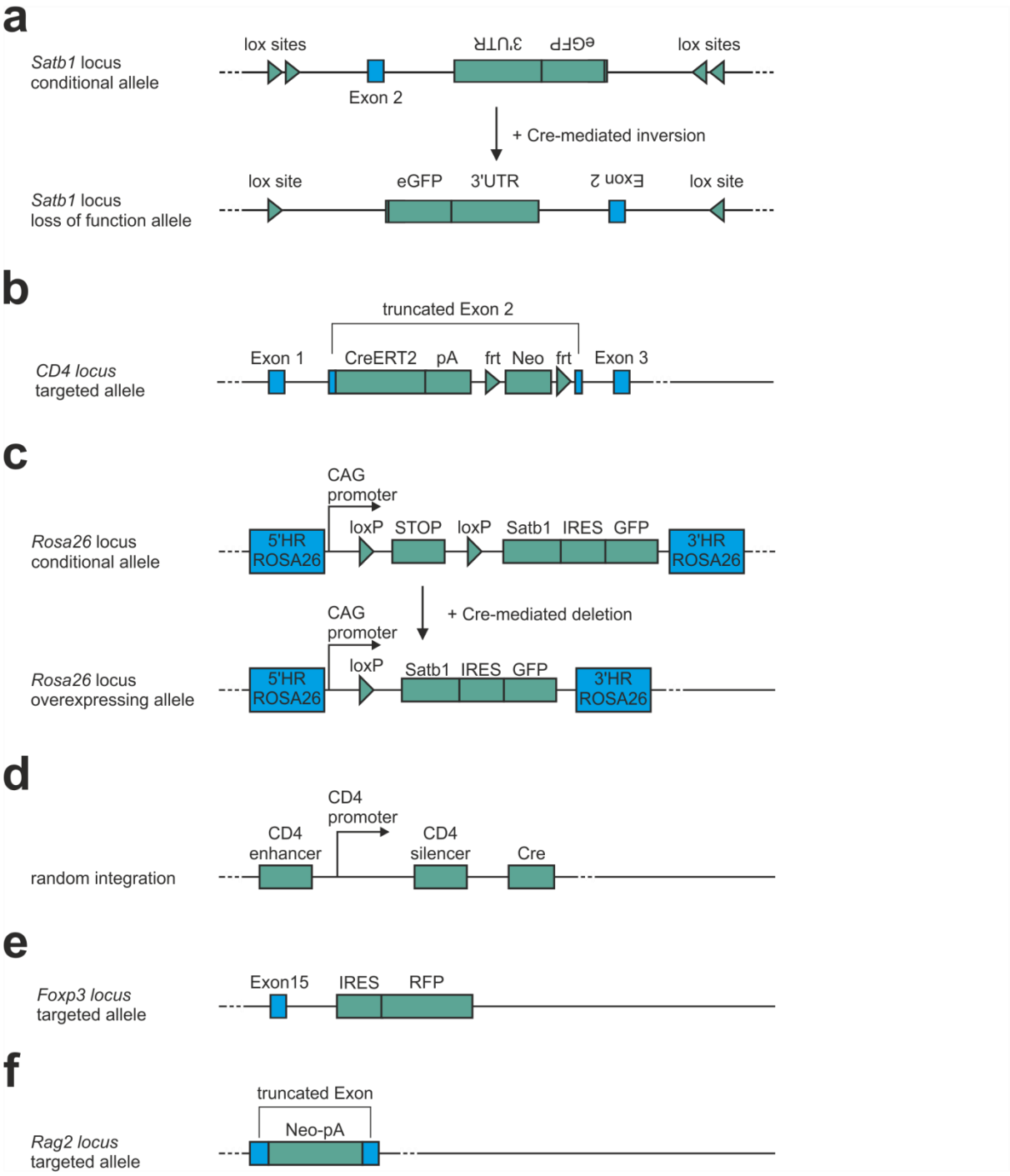

Figure 66: Gene loci of the targeted mouse alleles.

(a) Conditional *Satb1*$^{fl/fl}$ locus before and after recombination: Targeting of the *Satb1* locus allows deletion of Satb1 and expression of eGFP upon Cre-mediated recombination (Sommer et al., 2014). **(b)** Targeted *CD4* locus of CD4-CreERT2 mice enables CreERT2 expression in CD4^{+} T cells (Śledzińska et al., 2013). **(c)** Conditional *R26-STOP-Satb1* locus before and after recombination: Integration of a Satb1 gene cassette in the *Rosa26* locus allows for the generation of a conditional Satb1 KI mouse (Sommer, 2018). **(d)** Randomly integrated construct in CD4-Cre mice results in the expression of a Cre recombinase under control of CD4-regulatory elements in CD4-expressing cells (Lee et al., 2001). **(e)** Integration of an IRES-RFP reporter construct at the Foxp3 locus allows detection of Foxp3-expressing cells via the expression of a fluorescent reporter (Wan and Flavell, 2005). **(f)** Targeting of the *Rag2*

locus of Rag2$^{-/-}$ mice results in a disruption of the gene and loss of B and T cells (Shinkai et al., 1992). (a-f) Blue elements display endogenous gene cassettes, while new integrated constructs are marked in turquoise. CD, cluster of differentiation; Cre, causes recombination; CreERT2, causes recombination mutant estrogen receptor 2; eGFP, enhanced green fluorescent protein; frt, recombination sites for Flp recombinase; HR, homology region; IRES, internal ribosomal entry site; Neo, neomycin cassette; loxP, locus of X-over in P1; pA, polyadenylation site; RFP, red fluorescent protein; Satb1, special AT-rich sequence-binding protein 1; UTR, untranslated region.